PROBING THE SENSITIVITY OF AUTOANTIBODY PRODUCTION TO B CELL DEPLETION BY RITUXIMAB

BY

DR ALASTAIR JAMES FERRARO

A thesis submitted to
The University of Birmingham
for the degree of
Doctor of Philosophy

School of Immunity and Infection
College of Medical and Dental Sciences
The University of Birmingham
March 2010

Abstract

Rituximab, a monoclonal antibody directed against the human CD20 antigen, causes profound depletion of all B cells. When used in patients with autoimmune disease, IgG autoantibody titres often fall whilst serum IgG anti-tetanus toxoid antibody titres are unaffected. Antibodies of both these antibody specificities have features associated with production by long-lived $CD20^-$ plasma cells that should be resistant to Rituximab. Reasons for the differential loss of these apparently similar types of antibody were investigated.

Initial experiments established multiplexed bead assays to measure, in parallel, serum titres of multiple antibody specificities. Paired acute and convalescent sera, from 11 patients treated with Rituximab for Wegener's granulomatosis, were then studied. During 5 months after treatment, and following clinical remission, IgG anti-Proteinase 3 autoantibody titres fell gradually. All other measured antibody titres remained little changed. These findings favour the hypothesis that autoantibody producing plasma cells are sustained by disease related inflammation.

Subsequent experimental studies support a wider hypothesis - that inflamed sites can support increased plasma cell numbers. In the prolific humoral response of QM mice to immunisation with NP-Ficoll, concurrent infection with attenuated *Salmonella enterica* serovar Typhimurium increases splenic capacity to support plasma cells. The enhanced support may reflect locally increased IL-6 production.

Dedication

To Dan and James – may they grow up with a love of learning, and an appreciation of the wonders of nature.

Acknowledgments

I would like to thank my supervisors, Professor MacLennan and Professor Savage, for their guidance and wisdom, and for teaching me skills that apply far beyond the work in this thesis. I am also grateful to Dr Khan, Dr Mohr, Dr Serre, Dr Hardie, and Dr Cunningham and Ms Marshall (all at the Institute of BioMedical Research, University of Birmingham), and to Dr Ashton (Institute of Child Health, London) for their patient technical help and advice to a clinician that invaded their laboratory.

Thanks also to the Medical Research Council for their generous funding, without which I could not have taken the opportunities available, and to the patients with ANCA-associated vasculitis who have generously supported this work with their time, and their tissues.

Lastly, and by no means least, I would like to thank my wife Sue. I am very grateful for her unstinting support, encouragement, and perceptive comments in an unfamiliar scientific field – before, during, and after, my research fellowship.

Table of Contents

List of figures

List of tables

Common Abbreviations

@	Anti- (in context of antibody specificities)
bt	Biotin
autoAFC	Autoantibody forming cell
ADCC	Antibody–dependent cell-mediated cytotoxicity
AFC	Antibody forming cell
AMCA	7-amino-4-methylcoumarin-3- acetic acid
ANCA	Anti-neutrophil cytoplasm antibody
APC	Allophycocyanin
APRIL	A proliferation inducing ligand
BAFF	B cell activating factor
BAFF-R	BAFF receptor
BCMA	B cell maturation antigen
BCR	B cell receptor
Blimp-1	B-lymphocyte induced maturation protein-1
BMSU	BioMedical Services Unit
BrdU	5-Bromo 2´-deoxyuridine
BSA	Bovine serum albumin
BVAS	Birmingham vasculitis activity score
CWPS	Pneumococcal cell wall polysaccharide
DAB	3,3'Diaminobenzidine tetrahydrochloride
Dk	Donkey
DNA	Deoxyribonucleic acid
EBV-CA	Epstein-Barr virus capsid antigen
EDTA	Ethylenediaminetetraacetic acid
ELISA	Enzyme linked immunospecific assay
EUVAS	European Vasculitis Study Group
FACS	Flow-assisted cytometric sorting
FAM	6-carboxyfluoroscein
FCS	Fetal calf serum
FITC	Fluorescein-isothiocyanate
GC	Germinal centre
G-CSF	Granulocyte-Colony Stimulating Factor
GM-CSF	Granulocyte Macrophage -Colony Stimulating Factor
Gt	Goat
HLA	Human leucocyte antigen
Hs	Hamster
i.v.	Intravenous
IFN	Interferon
Ig	Immunoglobulin
IL	Interleukin
int	Intermediate
IP-10	Interferon gamma inducing protein-10

ITAC	Interferon–inducible T Cell Alpha Chemoattractant
kDa	Kilo-dalton
LFA-1	Lymphocyte function-associated antigen-1
LN	Lymph node
LPS	Lipopolysaccharide
MCP-1	Macrophage Chemotaxis protein 1
MFI	Median fluorescence intensity
MIG	Monokine induced by gamma interferon
MIP-1α or β	Macrophage inflammatory protein -1 α or β
MPO	Myeloperoxidase
mRNA	Messenger ribonucleic acid
MZ	Marginal zone
NK	Natural Killer
NGS	Normal goat serum
NMS	Normal mouse serum
NP	4-hydroxy-3-nitrophenyl acetyl
NP-CGG	4-hydroxy-3-nitrophenyl acetyl-Chicken Gamma Globulin
OVA	Ovalbumin
PBS	Phosphate buffered saline
PC	Phosphorylcholine
PCR	Polymerase chain reaction
PDGF	Platelet Derived Growth Factor
PE	Phycoerythrin
PnCP	Pneumococcal capsular polysaccharides
pNPP	p-Nitrophenyl Phosphate
PR3	Proteinase 3
QM	Quasi-monoclonal
Rb	Rabbit
Rabbit PAP	Rabbit Peroxidase / Antiperoxidase complex
RBC	Red blood cells
RNA	Ribonucleic acid
Rt	Rat
RT_2-PCR	Real time reverse transcriptase polymerase chain reaction assays
Sal.	*Salmonella enterica* serovar Typhimurium
SCID	Severe combined immunodeficiency
SDF-1	Stromal derived factor-1
Sh	Sheep
Strept AP	Steptavidin-Biotin Alkaline Phosphatase complex
TACI	Transmembrane activator and calcium modulator and cyclophilin ligand interactor
TD	T cell-dependent
TdT	terminal deoxynucleotide transferase
T_H-1	T-helper type 1
TI-1	T cell-independent type 1
TI-2	T cell-independent type 2

TLR	Toll Like Receptor
TNF-α	Tumour necrosis factor alpha
Tris	Tris(hydroxymethyl)aminomethane
UHB	University Hospital Birmingham
VCAM-1	Vascular cell adhesion molecule-1
VEGF	Vascular endothelium derived growth factor
VIC	A proprietary dye from Applied Biosystems
VLA-4	Very late antigen-4
V-region	Variable region (of immunoglobulin)
WG	Wegener's granulomatosis
WHO	World Health Organization

1 CLINICAL OBSERVATIONS LEADING TO THIS WORK, AND OUTLINE OF THE THESIS

Rituximab is a monoclonal antibody directed against the human CD20 antigen, which is expressed on the surface of B cells but not expressed on terminally differentiated plasma cells [1]. This antibody, which was developed for the treatment of B cell neoplasms, causes profound depletion of $CD20^+$ cell populations [2].

A formal randomised trial has also confirmed its therapeutic efficacy in rheumatoid arthritis [3]. To date evidence of efficacy in other autoimmune diseases is from case reports and case series [4-8], but further randomized controlled trials are currently underway [9;10].

Some of these publications report the preservation, during Rituximab therapy, of levels of serum immunoglobulin and of serum titres of some antibody specificities including IgG against the protein antigen tetanus toxoid [3;11-13]. This is not surprising as the plasma cells that produce antibody in the blood and tissue fluids are not $CD20^+$ [1], and so should not be affected directly by Rituximab. These same publications [3;11-13], and others [4;5] report that in contrast to the stability of total serum IgG levels following Rituximab treatment there is a selective decline in titres of IgG autoantibodies. The relevant autoantigens in these publications – immunoglobulins and proteinase-3 (PR3) – are also proteins. Thus, prior to these observations, it was tempting to assume that the production of corresponding autoantibodies was by a pathway analogous to that producing antibody against tetanus toxoid. The effect of Rituximab on autoantibody production was therefore unexpected. This thesis seeks to address this paradox.

Our first aim was to assess whether Rituximab therapy affected serum levels of a large number of antibodies specific for extrinsic antigens. The range of antibodies studied was chosen to reflect responses that are a) generated via the known different antibody production pathways, and b) generated from the whole spectrum of B cell subtypes. Tests were performed on paired sera from patients before and after treatment with Rituximab.

All patients had Wegener's granulomatosis, and detectable levels of the associated autoantibody IgG anti-PR3. This autoantibody is one of those previously noted to decline after Rituximab therapy [4;5;12].

The background to this work is discussed in detail in Chapter 2. Previously established methods that were used in studies reported in this thesis are reported in Chapter 3. Before the serological studies themselves could be performed it was necessary to develop the technology to assay some of the antibodies of interest – particularly those specific for pneumococcal capsular polysaccharides (PnCP). The development of these assays is described in Chapter 4. Findings from serological studies of human sera are reported in Chapter 5.

The results of our human studies do not support the concept that the vulnerability of autoantibody production to Rituximab therapy was a feature of either i) a particular B cell subset or ii) a particular antibody production pathway. Furthermore the findings do not suggest that autoantibody forming cells (autoAFC) are predominantly short lived. We therefore sought other hypotheses to explain the paradoxical clinical observations.

The most plausible alternative hypothesis appears to be that autoAFC are sustained in niches that are closely associated with disease-related inflammation. Treating the disease – and reducing the associated inflammation – would then be expected to reduce the

numbers of supported autoAFC, and so reduce circulating titres of autoantibody. In support of this hypothesis Muehlinghaus et al [14] have shown that in certain conditions antibody forming cells express the chemokine receptor CXCR3 and that this enables them to migrate to CXCL9, a chemokine found at sites of inflammation. A mouse model was used to test the hypothesis that 'inflammatory niches' can support the extended survival of plasma cells. The results of this experiment are reported in chapter 6.

Lastly the overall conclusions of this thesis, and the implications for further research into human health and disease, are discussed in chapter 7.

2 INTRODUCTION

2.1 Wegener's granulomatosis, and anti-Proteinase 3 antibodies.

Wegener's granulomatosis (WG) is one of the anti-neutrophil cytoplasm antibody (ANCA) associated vasculitides. These are rare systemic diseases typically associated with autoantibodies to antigens within cytoplasmic granules of neutrophils and monocytes. Disease manifestations can include necrotising inflammation in small vessels (arterioles, capillaries, and venules) of various tissues, granulomatous inflammation, and constitutional symptoms (including fever, malaise, weight loss, and arthralgias) [15]. Vasculitis within the kidney typically results in a glomerulonephritis that can result in acute renal failure. Capillaritis in the lung can cause life threatening pulmonary haemorrhage. The combined incidence of these vasculitides is 18.9 per million per year in the UK [16]. Disease activity is reported using the Birmingham Vasculitis Activity Scores (BVAS) (see Appendix 1) [17]. The aetiology of Wegner's granulomatosis remains obscure although its inflammatory nature and the presence of autoantibodies have led to it being classified among the autoimmune diseases.

The ANCA in WG are usually specific for the neutrophil lysosomal enzyme - proteinase 3 (PR3). Other ANCA that are specific for myeloperoxidase (MPO), which is also a lysosomal enzyme, are more closely linked with two other ANCA-associated vasculitides (microscopic polyangiitis, and Churg Strauss Syndrome). Combined serological testing by immunofluorescence (detecting any ANCA) and ELISA (detecting ANCA specific for PR3 or MPO) has a specificity for ANCA-associated disease of nearly 100% [18]. Bosch et al have recently written a comprehensive review of ANCA antibodies [19]. The

implications of the immunoglobulin V-region (Variable-region) somatic mutations identified in ANCA-producing antibody forming cells (AFC) are discussed below (section 2.2).

In many patients with ANCA associated vasculitides, ANCA levels correlate with disease activity and severity, and changes in titres can reflect disease activity (see review by Harper and Savage [20]). ANCA antibodies are likely to contribute to disease pathogenesis [21]. Conventional therapy for induction of remission in ANCA-associated vasculitis involves substantial doses of the cytotoxic drug cyclophosphamide. Cyclophosphamide is toxic to plasma cells but also affects a wide range of other cell types, and the mechanism of its therapeutic action has not been confirmed.

Toxicity can limit the therapeutic use of cyclophosphamide. Furthermore, relapses are common in WG - so further courses of cyclophosphamide are often needed and the risk of subsequent malignancy is related to cumulative exposure to the drug. As a result there has been much clinical interest in the potential for Rituximab to be used as an alternative therapeutic in ANCA-associated vasculitis.

Professor Savage, one of my supervisors for the research undertaken here, has developed substantial clinical experience in the use of Rituximab in this setting. She runs a research-orientated vasculitis clinic at the Wellcome Clinical Research Facility within the University Hospital Birmingham (UHB). The existence of this clinic not only provides a centre of excellence for the diagnosis and management of patients with WG but also facilitates both the recruitment of patients for research into therapies in vasculitis, and the collection of research samples from such patients.

2.2 The production of IgG Rheumatoid factor, and IgG PR3-ANCA autoantibody, is vulnerable to Rituximab.

Serum levels of IgG anti-PR3 ANCA (PR3-ANCA) – and IgG rheumatoid factor – typically fall after Rituximab therapy [3-5;11;12] although not all autoantibody production appears similarly vulnerable [22;23].

Isotype switched PR3-ANCA and rheumatoid factor can exhibit variable (V)-region somatic mutations [24-26]. Others have identified V-region somatic mutations in IgM anti-PR3 from a patient with Wegener's Granulomatosis [27]. This later report includes a conformational model of the antibody-antigen interaction, and concluded that the acquired mutations were predominantly within the PR3 binding region [27]. This is consistent with a process of affinity maturation, as discussed in section 2.4.1 below, and is analogous to that seen in the response to tetanus toxoid [28].

2.3 Rituximab and CD20.

Rituximab is an IgG_1 chimeric, human-mouse, monoclonal antibody specific for an extra-cellular epitope on human CD20 [29]. CD20 is a 33-35 kDa surface antigen that is first expressed in large pre-B cells during primary B lymphopoiesis. It remains expressed throughout the B cell differentiation pathway, until B cells differentiate into plasma cells [1]. Surface CD20 is also detectable, at lower levels, in a small proportion of peripheral T cells from healthy controls and patients [30-32]. $CD3^{+}CD20^{dim}$ cells are reported to be predominantly $CD8^{+}CD45RO^{+}CD28^{+}HLA\text{-}DR^{-}$ [33], but their functional role – if any – is unclear.

The B cell surface protein, CD20, sits in the plasma membrane of B cells and crosses the plasma membrane 4 times. Both the amino and carboxylic ends of the molecule are in the cytosol. This molecular structure and other largely indirect evidence has led to the suggestion that it acts as a calcium ion channel [34;35]. Although its function has been difficult to pin down, evidence supports a role for CD20 in B cell activation [34;35]. CD20 knockout mice have been developed, but have only mild phenotypic changes [36]. The role of CD20, if any, in other cell populations is unclear.

High affinity binding of the drug results in the rapid and profound loss of virtually all B cells from peripheral blood [2]. This depletion lasts for several months. As the B cell progenitors – haemopoietic stem cells and pro-B cells – do not express CD20, peripheral B cell repopulation occurs once therapeutic drug levels fall sufficiently. This usually takes place between 6 and 12 months after administration. Where studied, CD20dim non-B cell populations were not detected in peripheral blood after Rituximab [31].

Rituximab-induced B cell depletion appears primarily to be due to antibody–dependent cell-mediated cytotoxicity (ADCC) [37]. Consistent with this, its efficacy may be influenced by polymorphisms in FcγRIIIa [38;39], a receptor involved in ADCC. In mice transgenic for human CD20, complement-mediated lysis appears to be the dominant mechanism in some anatomical locations [40]. This may be because ADCC is less effective in mice than humans or rats [41]. There is also evidence of a role for complement-mediated lysis in the action of Rituximab in certain human diseases [42]. Other reports indicate that Rituximab can also act, at least *in vitro*, by inducting apoptotic cell death [43].

2.4 Follicular and extra-follicular pathways of AFC production.

The B cell response to antigen can result in AFC production via one or both of two pathways: i) follicular responses associated with germinal centre formation or ii) extra-follicular responses. Productive germinal centre (GC) responses only appear to be evoked by antigens that can elicit cognate interaction between T cells and B cells [44]. In most instances this means the antigen must have a peptide component. Extra-follicular antibody responses can be evoked both by T-dependent and T-independent antigens [45]. There is evidence that these are heterogeneous. Thus extrafollicular responses resulting from B2 cell activation are generally short-lived [45] while B1 cells can give rise to protracted extrafollicular responses with T independent memory B cell formation [46;47].

The systemic B cell response to antigen mainly occurs in the secondary lymphoid tissues – the spleen and the lymph nodes. Mucosal responses are not considered here. At sites of chronic inflammation, tertiary lymphoid structures can be formed [48-50]. These share features with but may not always be directly analogous to the secondary lymphoid tissues (which include the lymph nodes, splenic white pulp and Peyer's patches) [51;52]. Recent evidence indicates that, at least in Rheumatoid Arthritis, these structures do not have a direct role in autoantibody production [53].

Antibody production can occur in the absence of antigenic stimulation. Thus germ-free mice fed on a chemically defined diet in stainless steel cages have normal IgM levels and secrete some IgA from the gut. These so-called natural antibodies are produced by B1 cells [54;55]. These B1 cells can also participate in antigen-driven responses [46;56]. This is discussed further in section 2.5.2.

2.4.1 Follicular responses generate affinity matured antibody and CD20 - plasma cells that can be long lived.

In responses to T-dependent antigens follicular and extrafollicular responses usually develop in parallel, although these can occur independently of each other (see, for example, work by Cunningham et al [57]). Cells producing high affinity, isotype switched, antibody are produced in germinal centres through cycles of proliferation and somatic hypermutation, followed by selection involving antigen uptake and cognate interaction with CD4 T cells [44]. Germinal centre responses give rise to plasma cells that have the capacity to be long lived [58;59] and this longevity does not require continued antigenic stimulation [59]. However, it should be intuitively obvious that not all AFC survive indefinitely as new antibody responses are generated throughout adult life while levels of serum immunoglobulin remain relatively stable in healthy adults. Thus the concept of plasma cell longevity evolved to include an understanding that plasma cells require extrinsic support in 'niches' and that the number of these niches together with the number of plasma cells they can support is limited. Experimental evidence supports this at the level of whole organs. This was shown by studying responses where the number of antigen-specific B cells was varied. This resulted in peak plasma cell numbers which were roughly proportional to the number of specific B cells. Nevertheless, the number of splenic plasma cells present after 10 days had fallen so that these were more or less comparable in all groups [60]. Subsequently, studies have identified some of the local factors likely to contribute to plasma cell survival in niches. These are considered further in the introduction to Chapter 6.

As plasma cells do not express CD20 [1] one would not expect B cell depletion by anti-CD20 antibodies to shorten their natural lifespan. This has recently been confirmed in experimental mice [61]. On the contrary if Rituximab prevents the new formation of plasma cells, B cell depletion might actually prolong natural plasma cell lifespan by removing competition for niches that secure plasma cell survival. The functional correlate of AFC sparing during B cell depletion therapy – preservation of serum immunoglobulin levels, and specific antibody titres including as anti-tetanus toxoid antibodies – has been reported in humans [3;11-13], and more recently in mice [62].

2.4.1.1 Germinal centres generate $CD20^+$ memory B cells as well as plasma cells.

Germinal centre responses generate memory B cells as well as plasma cells [44;63]. Memory B cells, which have also acquired somatic mutations, and which are isotype switched, are found in the blood [64], and in the marginal zone (MZ) of the spleen [65]. Such cells can be recruited into subsequent extrafollicular responses which can generate further antibody. Memory B cells are $CD20^+$ [66]. In animal models anti-CD20 monoclonal antibodies deplete memory B cells [61], and abolish the recall response to T-dependent antigens [62]. Evidence in humans is more difficult to obtain for ethical reasons, but recall responses to antigens are reduced (though not absent) after Rituximab [67;68]. Thus Rituximab should greatly reduce, if not absolutely prevent, further production of new plasma cells from memory B cells.

In the response to a widespread, and persistent, antigen – such as a blood-borne autoantigen – ongoing activation of memory B cells could result in production of massive numbers of plasmablasts and unsupported plasma cells. Importantly, both these cell types

can secrete antibody. As the memory B cells entering the extra-follicular response, and plasmablasts produced by it, are all $CD20^+$, the production of new plasma cells from memory B cells should wane rapidly after Rituximab therapy. Unsupported AFC would die by apoptosis within days [60], and so this process would be swiftly followed by a decline in any antibody production. The indirect evidence that immunoglobulin levels are stable after B cell depletion by Rituximab indicates that the contribution of short-lived plasma cells to total serum antibody levels is probably small, although their contribution may be critical to countering specific infections. This thesis considers if autoantibody-producing cells are shorter lived than those generated in response to extrinsic antigens. It will also consider whether Rituximab treatment can alter the number of niches that sustain autoantibody-producing cells.

While memory B cells are likely to be Rituximab sensitive, germinal centre responses which generate memory B cells are also likely to form substantial numbers of plasma cells that have the capacity to find and compete for niches that can secure their own long-term survival. It has previously been proposed that a chronic process of memory B cell activation is required to renew and maintain the 'stable' plasma cell pool [69]. Such renewal of the pool from $CD20^+$ cells would be expected to be Rituximab sensitive. If this was a process necessary for sustaining autoantibody levels, it too could explain the decline in autoantibody levels following Rituximab. The relative preservation of anti-tetanus toxoid titres suggests that these are not being sustained by chronic memory B cell activation, a conclusion supported by long-term analysis of specific serum antibody titres in man [70]. The numbers of plasma cells in the spleen and bone marrow of mice are unaffected by B cell depletion therapy that results in prolonged depletion of memory B

cells [71]. This has been taken as evidence against the argument that ongoing renewal of the plasma cell pool is biologically significant. A more likely interpretation of the available data is that AFC will continue to occupy niches unless there is competition from newly-formed AFC. If this is the case it follows that plasma cells present in niches before Rituximab administration are likely to have an extended lifespan, when the treatment stops the formation of new AFC.

2.4.2 Extra-follicular antibody responses.

Extrafollicular antibody response can be induced by all classes of antigen – T-independent type I (TI-1) [72], TI-2 antigens [56;73] or T-dependent (TD) antigens [60]. Antigens based on pure polysaccharide cores evoke a pure extrafollicular antibody response and do not form productive GC. Most commonly these responses have been studied using synthetic antigens such as haptenated polysaccharides such as Ficoll and hydroxyl ethyl starch [45]. Although less well studied, it is likely that responses against bacterial capsular polysaccharides, such those of pneumococci, behave in the same way.

Many of the antibody forming cells produced in extrafollicular responses are short-lived [74;75]. This is likely to be because not all AFC produced in such an extra-follicular response find supportive niches required for long time survival [60].

In the same way that ongoing stimulation of the memory B cells population could result in substantial Rituximab-sensitive antibody production by unsupported plasmablasts and plasma cells (see section 2.4.1.1), ongoing stimulation of naïve B cells could also generate substantial antibody production. However, evidence discussed in section 2.2 indicates that the autoantibodies of interest are likely to be the product of a process of affinity maturation. Therefore this pathway is only a plausible candidate for Rituximab

sensitive autoantibody production if extra-follicular responses can generate somatically mutations.

2.4.2.1 Extra-follicular responses can generate somatic mutations in V-region genes.

Extrafollicular responses, both to TI and TD antigens, are associated with isotype switching, but have not conventionally been associated with the somatic hypermutation and affinity maturation seen in the TD follicular response. Nevertheless, published evidence shows that low level mutation can occur in TI responses [76], including autoantibody responses [77], and also in patients unable to develop GCs due to defective CD40-CD40L signalling [78]. Indeed, extra-follicular responses against a protein autoantigen have been demonstrated, which include accumulation of somatic mutations in immunoglobulin genes, and lead to affinity maturation of the corresponding autoantibody response [79;80] (Figure 2-1).

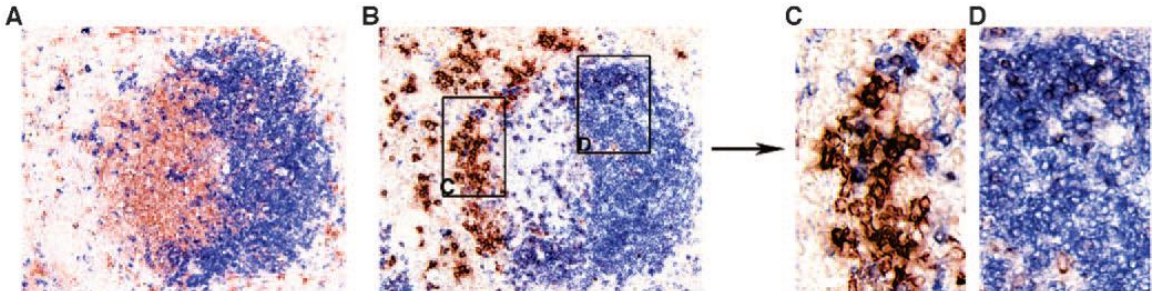

Figure 2-1 shows that autoantibody producing cells can accumulate at the border of the T zone and red pulp. Image taken from William et al. [79].
Panel A. Antibodies against Thy1.1 (brown) and CD22 (blue) identify the splenic T zone and B cell follicle respectively. In **Panels B, C, and D,** anti-idiotype antibody (4.44) (brown) identifies rheumatoid factor producing AFC, and CD22 (blue) identifies B cells. Boxes in panel B indicate areas enlarged in panel C (extra-follicular focus) and panel D (B cell follicle). **Panel C** shows $Id4.44^{+}CD22^{variable}$ cells of plasma cell morphology in extra-follicular foci. **Panel D** shows smaller $Id4.44^{+}CD22^{+}$ B cells in the B cell follicle.

The affinity maturation occurring within an extrafollicular response justifies reconsideration of the possibility that human autoantibody production can occur by an

extrafollicular pathway. Furthermore this pathway appears able to recruit a range of B cell subtypes (see below). If this pathway produced plasma cells that were only (or predominantly) short lived, this could offer one explanation for the observations relating to Rituximab therapy.

2.5 Subsets of B cells.

In addition to the existence of more than one pathway to antibody production, the presence of several B cell subsets adds further complexity to the field. B cells have been categorised into B1 and B2 subtypes on the basis of differences in the process of primary B lymphopoiesis, their capacity to self renew as mature cells and their phenotype. These subtypes of B cell also show distinct functional differences and to some extent, anatomical segregation. Although the concept of B1 and B2 cells is well established and the cells of these lineages have characteristic phenotypes in mice it is often not possible to be confident on the basis of phenotype alone that a B cell belongs to the B1 or B2 lineages. Importantly, this ambiguity is greater in humans than in mice [81;82].

2.5.1 B2 cells.

Naïve B2 cells are divided into a majority population of naïve recirculating cells ($sIgM^{+}sIgD^{+}B220^{hi}CD21^{+}CD23^{+}$), and cells typified by the fraction of splenic MZ B cells that are naïve ($sIgM^{hi}sIgD^{lo}B220^{hi}CD21^{+/hi}CD23^{-}$). The recirculating B cells in adult rats were found to have an average lifespan of about 6 weeks and MZ B cells probably somewhat less [83-85]. Their survival is governed by the rate at which immature B cells are induced to mature into recirculating or MZ cells, and by signals such as those delivered by BAFF (the tumour necrosis factor alpha (TNF-α) family member B cell

Activating Factor) [86], and APRIL (A proliferation inducing ligand) [87]. In the absence of competition from immature B cells recently produced in the marrow (e.g. when transferred into severe combined immunodeficiency, SCID, mice), mature B cells can survive indefinitely and many maintain a virgin phenotype [88]. Immature B cells, by contrast, only live around 3 days and will die by apoptosis within days, unless they manage to secure a signal that induces them to differentiate either into a recirculating B cell or a MZ B cell [83], or they are recruited to enter an immune response by antigen [89].

If B2 cells encounter antigen, and receive antigen-specific T-cell help, recirculating B2 cells can be recruited into both follicular and extrafollicular responses [90;91]. Unlike naïve recirculating B cells, MZ B cells (both naïve and memory) can respond to TI-2 antigens as well as TD antigens [92;93]. The fate of self-reactive B cells depends primarily on the degree of antigen receptor engagement [94] and availability of T cell help [89].

2.5.2 B1 cells.

In mice, B1 cells are $sIgM^{hi}sIgD^{lo}CD11b^{+}B220^{intermediate}CD21^{lo}CD23^{lo}$, and are further subdivided into B1a cells that express CD5, and B1b cells that do not [95]. B1 cell production is dominant over B2 production during fetal life and first occurs in the fetal liver [96] before moving to the splenic red pulp and bone marrow. Recently, a distinct phenotype for B1 cell progenitor has been characterised [97]. Postnatal B cell production is dominated by B2 lymphopoiesis. The B1 cell repertoire is limited as fetal pre-B cells do not express terminal deoxynucleotide transferase (TdT), preventing N nucleotide insertions during VDJ rearrangements. However, evidence has been presented suggesting

that 60% of adult mouse peritoneal B1 cells contain N insertions [98], which supports the concept that B1 lymphopoiesis also occurs in adult mice. V-region somatic mutations are not found in peritoneal B1 cells [99]. This is taken as evidence that B1 cells do not form GC.

B1 cells can produce 'natural' IgM and some IgA antibody in the absence of antigenic stimulation [54;55]. Its limited repertoire intrinsically provides protection against a number of pathogens, and includes specificities for phosphorylcholine (PC) (a constituent of cell wall carbohydrate of bacteria including pneumococci) [100]. Serotype-specific responses to type 3 pneumococci may also be included in the B1 repertoire in mice [101]. Evidence for this applying in humans is limited but it is consistent with the findings that vaccine responses to this serotype can be seen at an age when conventional extra-follicular responses are not established [102].

Isohaemagglutinins, human natural antibodies against A and B blood group antigens [103], are taken to be produced by B1 cells. Direct evidence for this has been limited, but relatively recently Zhou et al have reported that human IgM^+ B cells which bind the blood group A antigen are $CD11b^+CD5^+$, consistent with a B1a phenotype [104].

Many studies have shown that immature high affinity autoreactive B cells are deleted or rendered anergic [105-108]. Clearly this is not absolute and low affinity autoreactive B cells can be positively recruited into the MZ and B1 pools [109-111]. For example, NZB mice develop spontaneous auto-immune haemolytic anaemia. This can be prevented by intra-peritoneal injection of water - a treatment that results in apoptosis of local B1 cells but not circulating B2 cells [112]. Early evidence indicated that some human autoantibody producing cells are derived from putative B1 cells ($CD5^+$ B cells) [113]

though another, more recent, report indicates that anti-DNA antibodies [114] arise from $CD5^-$ B cells.

In addition to natural antibody production, B1 cells (including B cells which can generate isohaemagglutinin responses) have capacity for antigen dependent responses [46;101;115]. These are probably B1b responses [46;101;105;116], and may be very persistent [46]. Isotype switching of B1 responses has been described in mice [46], and natural human IgG against blood group antigens are also described [117;118].

It is not clear if B1 cells can undergo conventional TD responses to protein antigens [119]. However, Ferry et al have reported intriguing findings from a model in which mice have widespread intracellular expression of a protein antigen (mHEL-KK), and in which their B cells express a transgenic anti-HEL B cell receptor (BCR) [120]. The mice have greatly increased numbers of antigen-specific B1b cells in the peritoneum. They also describe greatly increased numbers of HEL–specific AFCs in the spleen, and T-independent production of anti-HEL antibody. The wider implications of this complex transgenic system are not clear, but it is interesting to note that many autoantigens are intracellular. The autoantigen of greatest interest here – PR3 – is a protein of cytoplasmic granules of macrophages and neutrophils, but it is externalized upon phagocyte activation.

2.6 Extra-follicular immune responses in the spleen.

Much of our understanding of immune responses has emerged from the study of splenic responses to antigen in experimental mice. Two examples, which are pertinent to the animal studies reported in chapter 6, are described below after an outline of the structure

of the mouse spleen. These are followed by a more detailed discussion of the splenic extra-follicular responses to antigen. Splenic follicular responses, which are not a feature of the antibody responses studied in chapter 6, are not discussed further here.

2.6.1 The structure of the spleen.

The spleen is the largest secondary lymphoid organ in mammals. It is the predominant site of immune responses to blood borne antigens (and peritoneal antigens). The spleen consists of distinct areas of white and red pulp. The red pulp consists largely of vascular sinusoids containing erythrocytes and macrophages. Scattered through the red pulp are fibrous collagen bundles, or trabeculae, which run between the major red pulp blood vessels and the splenic capsule [45].

Lymphoid white pulp areas are scattered throughout the red pulp, and are divided into T zones and B cell areas (follicles) according to the dominant lymphocyte subtype present in the non-immunised state. In the resting state, B cell areas can be further subdivided into primary follicles, through which naïve recirculating $IgM^{+}IgD^{+}$ B2 cells pass, and the outer MZ which contains naïve $IgM^{+}IgD^{low/-}$ B cells and can also contain memory B cells [45;121].

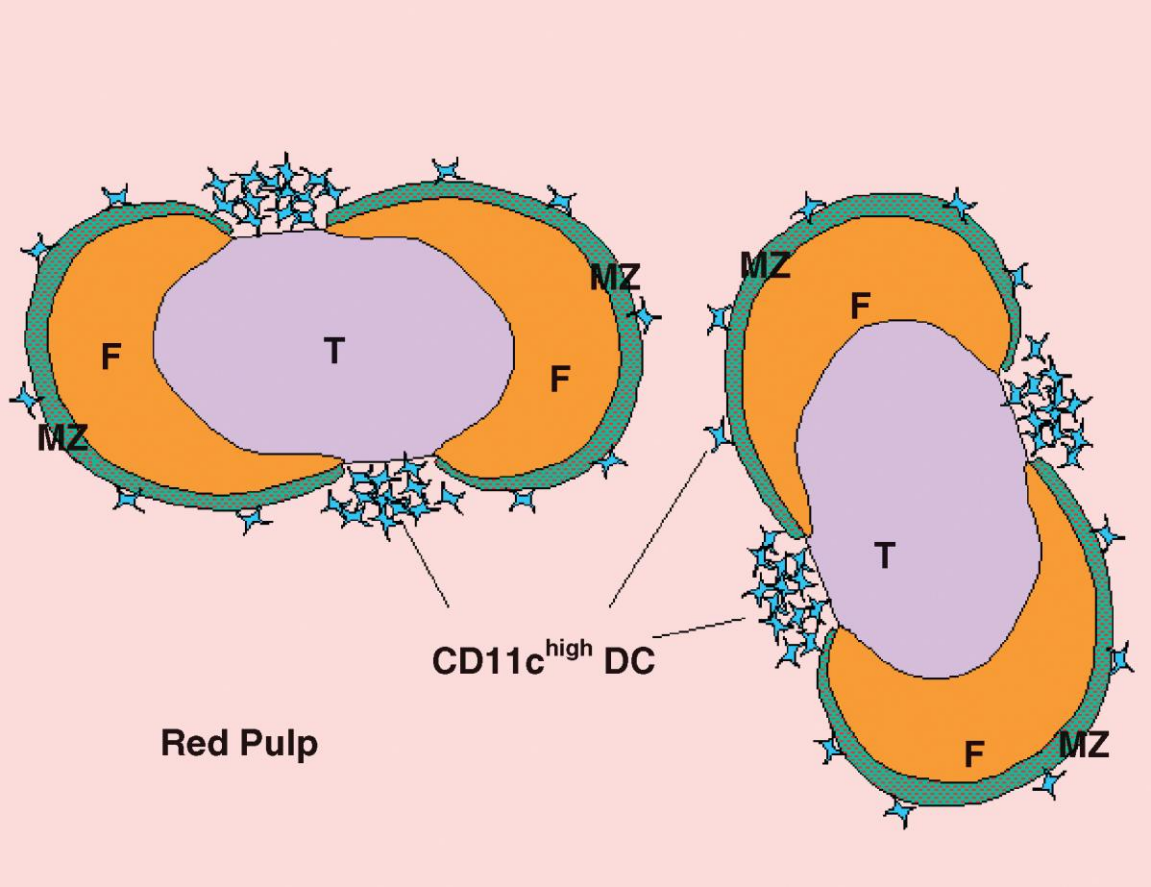

Figure 2-2 is a schematic diagram of areas within the splenic white pulp. T: T zone. F: B cell follicle. MZ: marginal zone. Taken from MacLennan et al. 2003 [45].

In the resting state, the MZ can thus be identified by the presence of $IgM^{+}IgD^{low/-}$cells. The marginal sinus that separates the more peripheral MZ from the B cell follicle can be identified by the presence of "marginal zone metalophillic macrophages". These cells express the MOMA-1 antibody, also known as CD169 [122].

2.6.2 Two informative animal models of the immune response.

2.6.2.1 The Quasi-monoclonal (QM) mouse.

Cascalho et al reported the development of the QM mouse in 1996 [123], and it has subsequently been widely used in the study of the response to the hapten NP (4-hydroxy-

3-nitrophenyl acetyl). Conjugation of NP to the neutral polysaccharide Ficoll results in the formation of the TI-2 antigen NP-Ficoll.

The QM mouse has one transgenic immunoglobulin heavy chain gene – μ_H 17.2.25 – and can neither express genes that encode for germline heavy chains nor those that encode for κ light chains. Thus the transgenic heavy chain can only combine with a λ light chain. Any such combination results in a primary antibody specificity for NP. In practice subsequent somatic mutation and secondary rearrangements result in a naïve B cell repertoire that is 80% specific for NP [123].

When such mice are immunised with NP-Ficoll a massive extra-follicular response is generated, filling the splenic red pulp with NP-specific AFC [60] by day 3. AFC numbers then decline precipitately, with steady state numbers reached by day 8 to 10 which are the comparable to the number present pre-immunisation. This is consistent with an extrinsic (tissue related) limit to the number of AFC that can be supported by the tissues [60].

"QMxB6 mice" are generated locally by crossing QM mice with C57/BL6 mice for 10 generations, selecting for the NP heavy chain each time. In these mice approximately 5% of naïve B cells are specific for NP. Intraperitoneal immunisation of such mice with NP-Ficoll still results in a very substantial, and reproducible, T-independent extra-follicular response; and generates numbers of NP-specific AFC far in excess of those that can be supported by the spleen in the longer term.

2.6.2.2 The splenic immune response to attenuated *Salmonella enterica* serovar Typhimurium.

After intraperitoneal injection of 10^5 viable *S.* Typhimurium (strain SL3261), susceptible C57/BL6 develop clinical infection which lasts more than 1 month [57]. This infection is characterised by progressive splenomegally which typically reaches 10 times its original size by 3 weeks, before gradually resolving. This is accompanied by a massive TD extra-follicular immune response which results in relative increases in numbers of splenic IgM- and IgG2c- (equivalent to IgG2a- in other strains of mice) AFC that are even greater than the concurrent increases in splenic size. TD follicular responses only emerge as the bacteria are largely cleared during the second month of infection.

By day 7 post infection, few of the AFC generated from extra-follicular responses are dividing (as assessed by $Ki67^+$ staining) yet their numbers decline only slowly and remain well above baseline values through to 1 month. This is consistent with an increased capacity for the infected spleen to support non-dividing plasma cells.

2.6.3 The splenic extrafollicular response to antigen.

If naïve recirculating B cells or MZ B cells encounter protein antigen within the circulation they exit the splenic vasculature and migrate to the outer splenic T zone [72]. These antigen-activated B cells acquire the ability to find and make cognate interaction with primed T cells, which also accumulate in the outer T zone. After interaction with appropriate, primed, T cells the B cells begin to proliferate and after 2 to 3 days either enter follicles and form GC or become migrate to extrafollicular foci and become plasmablasts as part of an extra-follicular response [45]. Available evidence indicates that recirculating B2 cells do not generally respond to TI-2 antigens [92;93].

MZ B cells, which do not recirculate through the blood [124], but migrate back and forth between local follicles [125], are capable of responding to TI-2 antigens as well as TD and TI-1 antigens [93]. TI-2 antigens include haptenated Ficoll [92]. The extra-follicular response to NP-Ficoll has been extensively studied, including in our laboratory. Upon activation via their B cell receptor, NP-specific B cells migrate into the outer T zone within 8 hours [126]. Towards the end of the second day after immunization, these cells start to upregulate CD138 - a surface and cytoplasmic marker associated with plasma cells [1]. These cells then upregulate Blimp-1 (B-lymphocyte induced maturation protein-1) – a transcription regulator required for further differentiation into plasma cells [127]. By 48 hours after B cell activation by NP-Ficoll, the B cells have undergone three divisions.

As the proliferating B cells (B-blasts) differentiate into plasmablasts, they migrate to extra-follicular foci at the margin between the T zone and the red pulp [45;128], and on into the red pulp itself [128]. Not all of these plasmablasts survive, and most are short lived [60;74;75].

In mice with a high proportion of B cells that are specific for NP, the plasmablasts generated following immunisation fill the red pulp by day 3 [60;128]. In the response to NP-Ficoll in QM mice [60], mass apoptosis of plasmablasts is seen between 4 & 6 days, such that only about 5% of AFC remain by day 8. Our group has reported that AFC contact with, or at least proximity to, $CD11c^{hi}$ dendritic cells contributes to subsequent AFC survival [128]. These $CD11c^{hi}$ cells are usually confined to the interface between the red pulp and T zone [128]. However, others have presented evidence that AFC numbers at day 6 post immunization are unaffected by the absence of $CD11c^{hi}$ cells

[129]. Recently Mohr et al [130] have shown that $CD11c^+$ dendritic cells, associated with plasmablasts in lymph nodes (LN), are the main source of IL-6 in LN during T-dependent antibody responses.

Those plasmablasts that do survive differentiate into plasma cells. Whilst both plasmablasts and plasma cells secrete antibody, plasma cells are probably more productive of antibody on a per cell basis [131;132]. As already mentioned plasma cells are terminally differentiated antibody secreting cells, that have the potential to be very long lived [58;59;70]. Longevity appears to depend upon the plasma cells finding extrinsic support (see section 2.8). Importantly, it appears that tissues have only limited capacity to provide such support [60]. In the steady state, splenic plasma cells are predominantly found clustered around large collagen fibres in the red pulp [45;133].

2.7 Chemokines mediate co-ordinated migration of AFCs.

Migration of AFCs from extra-follicular foci of the spleen, to their final site of retention is co-ordinated by chemokines, and occurs at the plasmablast stage [133;134]. Chemokines are chemotactic cytokines; small (8-15 kDa) structurally related molecules with diverse roles in cell trafficking. The CXC subfamily of chemokines, so called because they all have one intervening amino acid between their two N-terminal cysteine residues, includes CXCL9, CXCL10, CXCL11, and CXCL12 [135].

2.7.1 Four CXC chemokines: CXCL9, CXCL10, CXCL11 and CXCL12.

The chemokines CXCL9, CXCL10, and CXCL11 are also known as Monokine induced by gamma interferon (MIG), Interferon gamma inducing protein-10 (IP-10) and Interferon–inducible T Cell Alpha Chemoattractant (ITAC), respectively. All are ligands

for the receptor CXCR3 which is expressed on T cells, NK cells, and some AFC, but not monocytes or neutrophils [136]. CXCL11 has the highest affinity interaction with CXCR3, and CXCL9 has the least [137]. As implied by their names, γ-Interferon (γ-IFN) induces expression of all three chemokines in macrophages [138;139]. However γ-IFN, often alternatively IFN-α, and sometimes also TNF-α, can induce expression from a range of other cell types including endothelial cells [140;141], fibroblasts [141-143], and eosinophils [144]. Constitutive CXCL9 mRNA expression has been found in splenic $CD11c^+$ dendritic cells and splenic $B220^+$ cells in mice, though in both these cell types levels of CXCL9 mRNA are also enhanced by γ-IFN stimulation [145]. CXCL10 is reported to be constitutively expressed in spleen stromal cells [146]. Lipopolysaccharide can induce expression of CXCL10 and CXCL11 in macrophages by an γ-IFN independent pathway [147;148].

CXCL12 (Stromal derived factor-1; SDF-1) is constitutively expressed at high levels on bone marrow stromal cells (at the level of mRNA), and at lower levels in stromal cells from the LN or spleen [149]. It is also found in high concentrations in the inflamed rheumatoid joint, where it produced by synoviocytes [150]. *In vitro,* CXCL12 is chemotactic for B cells, T cells and macrophages [151] and plasmablasts [133]. All these cell types express CXCR4, the main receptor for CXCL12 [133;135;152]. The *in vivo* role of CXCL12 in guiding plasmablast chemotaxis is further discussed in section 2.8. CXCR4 is also widely expressed on many other cell types including neutrophils [153] and plasma cells [134]. Its possible role as a receptor that enhances plasma cell survival factor is discussed in section 2.8.1.3.

2.7.2 CXCR4 mediated AFC migration.

At least in secondary responses to protein antigens, most AFC express CXCR4, the receptor for CXCL12 [14;134]. The absence of CXCR4 greatly reduces, but does not abolish, the accumulation of AFC in the bone marrow after a secondary immune response, thus other mechanisms for guiding migration to bone marrow are likely to co-exist [133].

In the primary response to intra-peritoneal NP-Chicken Gamma Globulin (NP-CGG), splenic AFC are more frequent than bone marrow AFC [133]. Six days after immunization with NP-CGG, most of these AFC appear to cluster near fibres or vessels in the splenic red pulp [133]. In contrast, six days after similar immunization of $CXCR4^{-/-}$ mice the AFC are aberrantly located within the spleen – residing largely in the MZ though some are scattered through the red pulp. However in elegant studies of the response to NP-CGG in chimeric mice, at day 14 after immunization, splenic numbers of IgG_1 $CXCR4^{-}$ NP-specific AFC and IgM $CXCR4^{-}$ NP-specific AFC are little affected by the co-existence of $CXCR4^{+}$ NP-specific AFC [133]. From these studies one can conclude that i) CXCR4 is normally expressed by most AFC emerging from a primary splenic TD response, that ii) CXCR4 expression on AFC influences their migration within the spleen, but that iii) the absence of CXCR4 does not impair splenic AFC survival, at least in that model, and that iv) some AFC migrate into the splenic red pulp without CXCR4 [133]. Equivalent, detailed studies of the splenic T-independent extra-follicular response to antigen have not been reported.

2.7.3 CXCR3 mediated AFC migration.

A proportion of plasmablasts migrate towards CXCL9 and CXCL10 and CXCL11 in secondary responses *in vitro* [134]. The proportion of memory B cell derived AFC that express CXCR3, and the proportion that migrate to CXCL9 and CXCL10 and CXCL11 is increased by *in vitro* incubation of the precursor memory B cells with γ-IFN [14]. Most T cells present at sites of inflammation express CXCR3 [136]. It is tempting to assume that CXCR3 expression on AFC accounts for the observed accumulation of some AFC at sites of inflammation, but it has yet to be formally demonstrated, in mice or humans, that a high proportion of AFC at these sites express CXCR3. CXCR3 expression on AFC from primary responses is yet to be reported. Conversely CXCL12 expression is present at some inflamed sites [154], and so CXCR4 mediated AFC migration to sites of inflammation is also possible.

2.8 Niches that allow plasma cell survival.

It is inherently probable that there is likely to be finite capacity to the number of AFC an organism can support. As individual plasma cells can be very long lived [58;59], and antigenic stimulation continues throughout life, a virtually limitless capacity for support of AFC would result in a steady rise in immunoglobulin titres throughout life. This is not the case [155].

By extension, the capacity of an individual organ to accommodate plasma cells is likely to be limited. Evidence to support of this concept, with respect to the spleen, has previously been published by our group [60]. They found that the number of AFC persisting in the spleen 10 days or more after an immunization is constant, even where a

huge excess of plasma cells is generated early in the response. AFC numbers were comparable in both T-dependent, and T-independent responses. This is consistent with a fixed number of niches available to accommodate AFC generated from any type of response.

It follows that if an organism's capacity is constant, new AFC can only acquire niches by displacing in-situ AFC. Odendahl et al have offered evidence to support this [156]; six days after immunization of humans with tetanus toxoid, relatively immature blood-borne AFC were largely specific for tetanus toxoid, while co-existent mature AFC in the blood were not.

2.8.1 Extrinsic factors that may contribute to plasma cell survival.

As discussed above, only a small proportion of plasma cells generated in a splenic immune response achieve longevity [60;74;75] but, at least in the bone marrow, plasma cells can be very long lived [58;157]. *In vitro* and in *vivo* studies have identified multiple extrinsic factors that may contribute to this survival.

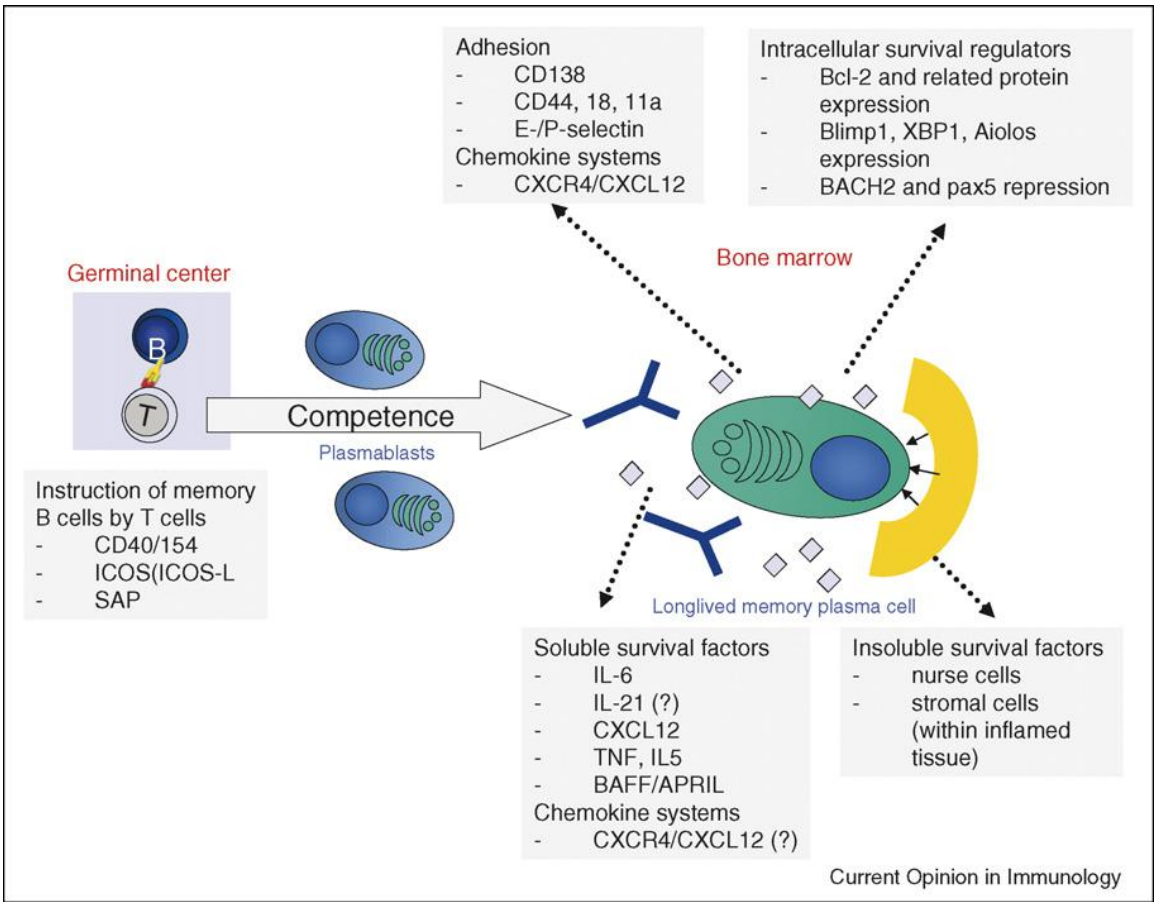

Figure 2-3 shows some putative factors associated with plasma cell survival in niches. Taken from Tarlinton et al. 2008 [158].

2.8.1.1 Interleukin-6.

Interleukin-6 (IL-6) can be produced by a wide range of cell types including fibroblasts, macrophages, B cells, T cells, and synovial 'nurse-like cells' [159-161] and $CD11c^{+}$ dendritic cells [130]. Whilst plasma cell numbers decline precipitately if cultured *in vitro* with medium alone [160;162], the addition of IL-6 to such cultures greatly increases the proportion of cells surviving, at least to 3 days [162]. Others have offered evidence that, in co-culture, bone marrow stromal cells can similarly prolong plasma cell survival; an effect dependent in part on stromal cell production of IL-6 [160]. However the same group have subsequently demonstrated that even though splenic stromal cells generate

more IL-6 than bone marrow stromal cells, it is the latter cell type that has greater efficacy at ensuring plasma cell survival [149].

Results from *in vivo* studies are also superficially conflicting. Twenty-one weeks after immunization of IL-6 deficient mice with alum-precipitated ovalbumin (OVA), serum levels of IgG anti-OVA, and numbers of OVA-specific AFC in the bone marrow are no different to wild type animals [162]. In contrast an earlier report demonstrated that excess IL-6 results in greatly increased numbers of plasma cells in multiple lymphoid tissues, and greatly increased serum levels of IgG_1, but only modest increases in serum levels other IgG subclasses or IgM [163]. The plasma cells in this latter study did not have neoplastic features, but the findings could be due to increased proliferation of AFC precursors, rather than increased plasma cell survival. Recently published evidence indicates that IL-6 dependent effects on serum levels of IgG_1 after immunization are mediated by IL-21 [164] (see section 2.8.1.5 below). Nevertheless, collectively, these results are compatible with two conclusions: i) that increased levels of IL-6 may enhance plasma cell survival and ii) that there is functional redundancy between IL-6 and other factors that support *in vivo* plasma cell survival.

At least *in vitro*, IL-6 demonstrates marked synergy with other factors that can enhance plasma cell survival. These include BAFF [165], and ligands for CD44 [162] (see sections 2.8.1.2.2 and 2.8.1.7).

2.8.1.2 Members of the Tumour Necrosis Factor α superfamily.

2.8.1.2.1 Tumour Necrosis Factor-α.

TNF-α is predominantly produced by macrophages and T cells [166], though secretion from activated B cells also occurs [167;168]. TNF-α significantly enhances plasma cell survival in vitro [162]. In a direct comparison with IL-6, the supportive effect of TNF-α is less marked, at least at the concentrations used [162]. Limited data in humans come from reports regarding therapeutic administration of anti-TNF therapy (Etanercept). This therapy does not appear to result in a fall in total serum immunoglobulin levels [169]. The possibility that TNF-α may have synergistic effects with other plasma cell survival factors has not been reported.

2.8.1.2.2 B cell activating factor (BAFF) and A proliferation inducing ligand (APRIL).

BAFF and APRIL are also members of the TNF-α superfamily [170]. Both exist in a secreted form, though BAFF can also be expressed in a transmembrane form [170]. BAFF and APRIL are both expressed by monocytes, macrophages, cells of dendritic morphology, and T cells [170;171]. Expression of BAFF has also been reported in a range of other cell types, including synoviocytes [172], Vascular cell adhesion molecule-1^+ (VCAM-1^+) bone marrow stromal cells [173], and neutrophils [174;175]. More recently expression of BAFF and APRIL (at the level of both mRNA and protein) has been reported in the B-lymphocyte lineage [176]. Interestingly, the same report presented data to indicate that splenic plasma cells in autoimmune-prone NZB/NZW F_1 mice express both BAFF and APRIL.

Three recognised receptors can interact with either BAFF or APRIL, or both. These are the BAFF receptor (BAFF-R), transmembrane activator and calcium modulator and cyclophilin ligand interactor (TACI), and B cell maturation antigen (BCMA). Only BAFF can interact with the BAFF-R. TACI and BCMA can be activated by either APRIL or BAFF [170]. Syndecan-1 (CD138) has also been reported to bind APRIL though downstream effects mediated through this interaction have not been confirmed [177].

BAFF-R and TACI are expressed on B cells [170]. TACI is also expressed on macrophages [170], whilst BAFF-R is expressed on some T cells [170;178]. As B cells differentiate into plasma cells BAFF-R is down-regulated TACI is little changed and BCMA is massively up-regulated [130]. This implies a stronger role for APRIL in securing plasma cell survival. Recently $GR1^{+}$ macrophages in the medullary cords of LN that are surrounded by clusters of plasma cells have been found to be potent producers of APRIL [130]. Downstream effects mediated by ligation of BAFF-R or TACI are not further discussed here.

BCMA is also expressed on bone marrow plasma cells [165]. Ligation of this receptor greatly enhances *in vitro* survival of bone marrow derived plasma cells and, as mentioned above, their survival is further augmented by the additional presence of IL-6 [165]. *In vivo* studies support this; in $BCMA^{-/-}$ mice numbers of bone marrow PCs are greatly reduced (but remain detectable) several weeks after immunisation [165]. In keeping with previous studies [177], recent evidence from transfer experiments [179] appears to indicate that the presence of APRIL, but not BAFF, in the recipient bone marrow enhances survival of engrafted AFC up to 48 hours after transfer.

2.8.1.3 CXCL12.

During early *in vitro* studies CXCL12 – the ligand for CXCR4 – was reported to enhance plasma cell survival [162]. VCAM-1^+ bone marrow stromal cells express CXCL12 [173], and it appears that *in vivo* most bone marrow plasma cells are in proximity to these cells [180]. However, as discussed above (section 2.7.2), experimental data indicates that $CXCR4^-$ AFC are at little or no survival disadvantage, within the spleen, compared to $CXCR4^+$ AFC [133]. Furthermore, although at 14 days after an immunization numbers of $CXCR4^-$ AFC in the bone marrow are reduced when in competition with $CXCR4^+$ AFC [134], separate studies indicate that at 90 days after immunisation the numbers of bone marrow AFC are comparable in mice with $CXCR4^-$ AFC and those with $CXCR4^+$ AFC [181]. More recently, and in contrast to earlier work [162], Minges-Wols et al have found that plasma cell survival during *in vitro* co-culture with stromal cells is not affected by the addition of neutralising anti-CXCL12 antibody [149].

Thus whilst there is strong evidence that CXCR4 is a significant chemotactic factor for plasma cell precursors is strong (see section 2.7.2), the evidence that CXCR4 is also an *in vivo* survival factor for plasma cells themselves is less convincing.

2.8.1.4 Interleukin-5.

Interleukin-5 was amongst the extensive range of cytokines investigated by Cassese et al for capacity to support plasma cell *in vitro* [162]. At the concentrations used, it substantially enhanced plasma cell survival to 3 days, though to a lesser extent than IL-6 or CXCL12.

However, the same report noted that bone marrow supernatants from IL-$5^{-/-}$ mice were no less effective than supernatants from wild type mice in supporting plasma cell survival *in vitro* - consistent with significant functional redundancy, and a therefore lesser role for IL-5 *in vivo.*

2.8.1.5 Interleukin-21.

Interleukin-21 has been described only relatively recently [182]. It is secreted by $CD4^+$ T cells, and has homology to several other cytokines including IL-2, IL-4 and IL-7 [183]. The receptors for these various cytokines all share a common γ_c chain [183].

IL-21 has many known functions, affecting a range of immunological cell types [183]. Excess production of IL-21 by transgenic mice results in increased plasma cell numbers [184] in part, at least, through upregulating Blimp-1 [184]. Other actions of IL-21 on cells of the B-cell lineage are complex and are discussed below:

IL-21 receptor knockout mice have impaired antigen specific IgG_1 responses, whilst corresponding antigen specific IgM responses are relatively spared [185]. Furthermore, recently published data indicates that IL-21 mediates the increased *in vivo* production of antigen specific IgG_1 that occurs when antigen is co-administered with IL-6 (but without any other adjuvant) [164]. The IgM response to antigen is not enhanced in the same way [164].

It appears that when B cell IL-21 receptor ligation occurs concurrently with BCR activation, then B cell proliferation is induced [186]. In contrast in the absence of BCR activation, IL-21 receptor ligation results in induction of apoptosis – even if Toll Like Receptor (TLR)-mediated B cell signalling is available [186].

IL-21 has also been proposed as a putative plasma cell survival factor [158].

2.8.1.6 Cells that may support plasma cell survival.

Although many molecules that are putatively supportive of plasma cells have been identified, the cells that comprise plasma cell niches have been relatively less well characterised.

Some cells types that may support plasma cell development or survival have already been discussed above. These include $CD11c^{hi}$ dendritic cells in the spleen (section 2.6.3), and $VCAM\text{-}1^{+}$ bone marrow stromal cells that express CXCL12 (section 2.8.1.3), and/or BAFF (section 2.8.1.2.2). Markers that identify putative niche-forming cells in the spleen are less well investigated. As VCAM-1 is very widely expressed in the splenic red pulp [187] it is unlikely, on its own, to define a cell type that supports plasma cells.

BP3 (CD157) was identified as a surface antigen on bone marrow stromal cells [188], whilst the same antigen had already been identified on cells in the spleen [189]. $BP3^{-/-}$ mice exhibit defects in the immune response to TI-2 antigens [190]. The mechanism underlying this is not clear, and it was considered plausible that BP3 cells contribute to splenic plasma cell niches.

Mice deficient in CD169 (sialoadhesin) are reported to have lower levels of IgM [191]. More recently Mohr et al [130] have reported that $CD169^{+}$ cells are present at several sites within the LN, and that some subsets of these $CD169^{+}$ cells, identified according to expression of CD11b and F4/80, are associated with AFC in the LN outer T zone and medullary cords. Some of these cells expressed CXCL12 and adhesion molecules that

may assist interaction with AFC. It therefore appeared plausible that $CD169^+$ cells could contribute to the formation of splenic plasma cell niches.

2.8.1.7 Other factors that may contribute to plasma cell survival.

Plasma cells express CD44. Cassese et al have also demonstrated that CD44 mediated signalling, whether induced by activating antibodies or by hyaluroniuc acid, can significantly enhance plasma cell survival in vitro [162]. Interestingly this effect appears to be synergistic with the effects of IL-6.

Others have demonstrated that VLA-4 (Very late antigen-4) mediated signals may promote plasma cell survival at least *in vitro*, though this does not appear to be via interaction with VCAM-1 [160]. More recently DiLillo et al have reported *in vivo* findings that may support this, or at least support a permissive role for VLA-4 in ensuring plasma cell survival in supportive niches [62]. In experimentally immunised mice that are unable to regenerate their plasma cell pool (due to depletion of plasma cell precursors), co-blockade of LFA-1 (Lymphocyte function-associated antigen-1) and VLA-4 results in a significant fall in both a) numbers of antigen specific AFC in the bone marrow and b) levels of antigen-specific serum IgG.

2.9 Outline of human serological work.

It should be clear from the evidence discussed above, that the conventional pathway for production of most affinity-matured, isotype-switched, antibody specific for protein antigens – namely the GC pathway – should not be sensitive to Rituximab. Available evidence regarding most antibody production still supports this concept. B cell depletion by Rituximab does not significantly affect titres of neutralising antibodies against tetanus

toxoid [3;11;12]. Falls in serum immunoglobulins are also generally modest, although falls in serum IgM have been seen after repeated cycles of treatment [192]. This makes the Rituximab-related falls in titres of certain autoantibodies, which otherwise exhibit features similar to anti-tetanus antibody, all the more striking. The wider literature introduced above raises the possibility that other pathways – and other B cell subtypes – could generate IgG anti-PR3 autoantibodies and IgG rheumatoid factor.

We initially considered three possible explanations for the observations that production of some autoantibody species appears sensitive to Rituximab therapy. Based on the results set out in Chapter 5, a fourth possibility has emerged that seems consistent with available data. These explanations are not mutually exclusive:

1. Autoreactive B cells which differentiate into autoAFC could be contained in a different B cell subset to those containing specificities for other protein antigens.
2. autoAFC could be generated via a different antibody production pathway to that used for conventional protein antigens.
3. autoAFC could be intrinsically short lived, with ongoing production of autoantibody dependent on constant renewal of the autoAFC population by differentiation of new B cells.
4. autoAFC may selectively occupy sites in inflammatory tissues that maintain their survival, but these sites are vulnerable to Rituximab treatment.

The primary aim of the first phase of my research fellowship was to determine whether established antibody production derived from these other pathways and from other B cell

subtypes is also sensitive to disruption by Rituximab. To achieve this, it was initially necessary to develop the technology to assay antibodies to multiple PnCP in parallel.

3 METHODS

3.1 Commonly used reagents.

Protocols for the preparation of some standard laboratory reagents, used widely in this research, are reported below:

Carbonate Coating Buffer: Dissolve 0.8g Na_2CO_3, and 1.47g $NaHCO_3$ in 500ml distilled water, then add Sodium Azide to a final concentration of 0.02%.

Trisma Base solution: Dissolve 121.14g tris(hydroxymethyl)aminomethane in 5L distilled water.

Tris pH 7.4: Made by mixing 2 parts Trisma base solution in distilled water (0.2M), 3 parts stock NaCl solution in water (42.5g per 5L), and 3 parts dilute hydrochloric acid (0.1N).

Tris pH 9.2: Trisma base solution was pH adjusted to 9.2 using concentrated NaOH, and before distilled water was added to make up to twice the original volume.

Phosphate buffered saline (PBS): Consists of distilled water containing 150mM Sodium Chloride and 150mM Sodium Phosphate, adjusted to pH 7.2.

3.2 Methods used in human studies.

3.2.1 Ethical approval for human studies, recruitment of subjects, and details of process for obtaining consent.

The research protocol, and the relevant patient information sheets and consent forms, for the human research undertaken for this thesis were approved by the Oxfordshire South Research Ethics Committee (B) (REC application number 06/Q1605/49).

Patients with ANCA-associated vasculitis attending UHB, and considered as potentially suitable for participation in this research, were first identified by their clinicians. Such patients were provided with written information about the proposed research and their potential role in it, and were given an opportunity to ask questions before written consent was obtained.

3.2.2 Patients and samples.

Samples were collected from 11 patients with disease that fulfilled the ACR classification criteria for Wegener's Granulomatosis [15] and had detectable serum anti-PR3 antibody before treatment. All were under follow up at Queen Elizabeth Hospital, UHB NHS Foundation Trust. Nine patients received Rituximab for induction of remission after a disease relapse. Two received Rituximab for newly diagnosed disease. Patients received 2g to 3.2g intravenous (i.v.) Rituximab in divided doses. Eight patients received concurrent i.v. cyclophosphamide in two divided doses (median total dose 1.25g, range 0.9 – 2.4g). Two patients also received i.v. methylprednisolone (1g and 1.5g). All i.v. therapy was completed within four weeks, and thereafter patients continued a reducing course of oral prednisolone. Six patients continued previous immnunosuppresive medications (Mycophenolate mofetil, Azathioprine, or Methotrexate) at doses unchanged throughout the study period. No patients had previously received Rituximab. All patients gave written informed consent for research participation.

3.2.3 Collation of clinical data on consenting patients.

Demographic data, disease activity scores (BVAS) (see Appendix 1, page 183) [17], serum autoantibody titres, levels of serum immunoglobulins, and serum levels of C-

reactive protein were obtained from clinical laboratory results, patient notes, and hospital databases.

3.2.3.1 Estimation of absolute B cell counts in patients' peripheral blood.

An estimate of the absolute number of $CD19^+$ B cells per μl of patient's whole blood was derived the combination of from two sources:

1. The proportion of blood lymphocytes that were $CD19^+$ was estimated by flow cytometric analysis of fresh whole blood samples, after lysis of red cells by the addition of FACS lysis solution (Becton Dickenson). At least 10,000 flow cytometric events were counted per sample. This is routinely performed by the University of Birmingham Clinical Immunology service on Ethylenediaminetetraacetic acid (EDTA)-anticoagulated samples of peripheral blood taken from those patients attending the UHB Vasculitis clinic that were likely to receive Rituximab, or had previously received Rituximab.
2. Contemporary samples were also sent for semi-automated estimation of various haematological indices including absolute lymphocyte counts per μl of whole blood, by the UHB Hematology Laboratory service.

Measurements were performed before Rituximab treatment (except in one patient), and at intervals during the subsequent 4-5 months (in all patients).

3.2.3.2 Measurement of anti-PR3 antibody titres in patients' serum.

Levels of anti-PR3 antibodies in fresh serum samples were routinely analysed, by the University of Birmingham Clinical Immunology service, for all patients attending the UHB Vasculitis clinic. Assays were performed using a commercially available Enzyme

linked immunospecific assay (ELISA) detection kit (The Binding Site, Birmingham, UK), according to the manufacturers instructions.

3.2.3.3 Measurement of levels of serum immunoglobulins and C-reactive protein in patients' serum.

Total serum IgG and IgM were measured by the University of Birmingham Clinical Immunology service using a routine turbidometric assay (Modular P800, Roche Diagnostics).

Highly sensitive assays for C-reactive protein were performed by the University of Birmingham Clinical Immunology service using a routine turbidometric assay (Hitachi P-module, Dako).

3.2.4 Collection of research blood samples from consenting patients.

Serum samples, and whole blood samples, for research were obtained from consenting patients at the same time as clinical blood samples – usually during routine inpatient phlebotomy rounds or at the time of outpatient appointments.

Serum samples were obtained from clotted blood samples as follows: half an hour after venesection, filled vacutainer tubes were centrifuged at 2000g for 10 minutes. Serum was then removed by pipetting and aliquotted into approximately 500µl quantities for freezing at -20˚C or below. Serum samples were moved to -70˚C within 1 month of collection.

Whole blood samples for flow cytometric analysis were collected into EDTA-containing vacutainer tubes and kept at room temperature until use within 18 hours.

3.2.5 Customized microsphere-based assays of serum antibody concentration.

IgM, IgG_1 or IgG_2 antibody each specific for tetanus toxoid, PnCP 1, 3, 6b, 9v, 14, 19, and 23f, PC, and purified pneumococcal cell wall polysaccharide (CWPS) (Serum Statens Institute, Denmark) were measured by customized multiplexed assays using antigen-coated fluorescent microspheres after Lal et al [193]. The local development, and validation, of these assays is described in chapter 4.

3.2.5.1 Conjugation of antigens to microspheres.

3.2.5.1.1 Carbohydrate conjugation to linker protein (poly-L-Lysine).

Each of the seven pneumococcal capsular polysaccharides (PnCP) (LGC Prochem / ATCC, UK) (5mg/ml in sterile water), and CWPS (1mg/ml in sterile water) were separately added to equal volumes of dilute NaOH (0.01%). The alkalinized solutions were separately added to cyanuric chloride (5mg/ml) (Sigma), vortexed briefly, and 100μL poly-L-lysine (Sigma) (0.1%) was added to each. After further vortexing, the mixtures were incubated overnight in the dark at 4°C, with agitation. Coupled polysaccharides were purified with separate PD-10 desalting columns (Amersham Biosciences) by elution with 3.5ml PBS, and aliquots of each frozen at -80°C.

3.2.5.1.2 Protein conjugation to microspheres.

Subsequently, each of the poly-L-lysine-coupled polysaccharides, tetanus toxoid (48μg/ml) (List Biological Labs) and Bovine Serum Albumin- (BSA)-conjugated Phosphorylcholine (PC) (200μg/ml) (BioSearch, CA, USA) were separately conjugated to carboxylated microspheres (BioRad Labs, UK). Microspheres were first washed (PBS-

Tween 0.05%), and activated with N-(3-Dimethylaminopropyl)-N′-ethylcarbodiimide hydrochloride (Sigma, UK) (5mg/ml) and N-hydroxysulfosuccinimide sodium salt (Sigma, UK) (5mg/ml) in distilled water containing 1.06g NaH2PO4 and 0.32g Na2HPO4 per 100ml (pH 7.3). After 2 further washes (PBS), activated microspheres were separately incubated with solutions of each required antigen (300μl) for 2 hours or overnight, at room temperature in the dark, with agitation. Antigen-conjugated beads were then washed twice in PBS containing 0.1% bovine serum albumin, and 0.05% NaN3, and stored in the dark until use.

3.2.5.2 Performing microsphere based assays of serum antibodies.

Serum antibody levels against PnCP 1, 3, 6b, 9v, 14, 19, & 23f were measured in patient samples and the standard reference serum (Serum 89SF, Food and Drug Administration, Maryland, USA). Seven 4-fold dilutions (1/20-1/81920) of each sample and standard were prepared in diluent buffer consisting of PBS containing 1% BSA (Sigma), 0.05% Tween, and CWPS (2μg/ml). PnCP 22f (5μg/ml) was also added to diluent buffer for samples, in accordance with the WHO (World Health Organization) protocol for ELISA detection of PnCP antibodies [194].

Diluted samples and standards were incubated in 96 well MultiScreenHTS microfilter plates (Milipore, UK) with a mixture of the relevant antigen-coated beads (2500 per bead type) for 1 hour at room temperature, in the dark with shaking, and then washed twice in wash buffer (PBS-Tween 0.05%). Beads were then incubated with phycoerythrin (PE)-conjugated mouse anti-human immunoglobulins (Ig) (specific for IgM, IgG1 or IgG2) (1/200 dilution in wash buffer) (Southern biotech, AL, USA) for 30 minutes at room temperature, in the dark with shaking. After a further wash, beads were re-suspended in

wash buffer (130μl), and median fluorescence intensities (MFI) for each bead/sample combination were obtained by Luminex 100 machine (Luminex Corp, TX, USA). IgM, IgG1 and IgG2 antibodies against tetanus toxoid, CWPS, and PC were separately tested in an analogous fashion, except that samples and standard were diluted in buffer without CWPS or PnCP 22f.

3.2.5.3 Data analysis of microsphere-based assays of serum samples

Standard curves of MFI obtained with Luminex were computed by BioPlex Manager software (version 4, BioRad Labs, CA, USA). Standard curves were generated for each antibody specificity and for each immunoglobulin subclass, for each sample and for the standard serum 89SF. Hypothetical dilutions of samples and standard predicted to result in an equal MFI of 4 x background were obtained from standard curves, and thus relative concentrations of each antibody (compared to the standard) were obtained for each immunoglobulin subclass within each sample.

The limit of detection for each antibody was inferred by the ratio between the dilution of standard serum that generated a MFI equal to 4x background, and the least diluted standard (1 in 20).

3.2.6 Microsphere-based assays of serum cytokine levels

Serum samples from patients of interest were collected and stored as described in section 3.2.4. The cytokine assay kit (BioRad Labs) was used according to the manufacturer's instructions. In summary:

When needed, sample aliquots were thawed on ice, and diluted 1:3 with the sample diluent. The cytokine standard was reconstituted with 500 μL serum standard diluent and

left on ice for 30 minutes. Serial dilutions of the standard were then prepared – the top dilution consisted of 128 µL of reconstituted standard diluted with 72 µL serum standard diluent. Thereafter 7 further dilutions were created using 1:3 fold dilutions. Fifty µl of diluent was kept aside for use as a 'blank' (0 U/ml). All diluted standards were then kept on ice.

96 well filter plates (Millipore) were pre-wet with assay buffer, 50 µL of the multiplex bead working suspension was added to each well, and the beads were washed with 100 µl wash buffer; with each vacuum filtration of excess fluid between each step. Fifty µl of relevant standards or sample were then added to the appropriate wells, and the plate was incubated at room temperature in the dark with shaking. Three further washes were performed before 25µl of biotinylated detection antibody was added to each well. The plate was then reincubated in similar conditions to previously for 30 minutes. After three further washes, 50µl strepavidin-PE was added to each well and the plate re-incubated under similar conditions for 10 minutes. After 3 further washes, the beads were resuspended in 125 µl assay buffer, and MFI associated with each bead region, in each well, were read on the previously calibrated Bioplex 100 platform (BioRad).

Relative concentrations of cytokines in the samples were calculated by BioPlex Manager software (version 4, BioRad Labs, CA, USA) using 5 parameter logistic regression algorithms, with reference to the MFI values obtained for the serial dilutions for the standards.

3.2.7 Enzyme Linked ImmunoSpecfic Assay (ELISA) of IgG anti-Epstein-Barr Virus Capsid Antigen in human serum samples.

Human serum samples had previously been collected and stored as described in section 3.2.4. ELISA assays for levels of serum IgG against Epstein-Barr Virus Capsid Antigen (EBV-CA) were performed according to the manufacturer's instructions (DiaPro). Briefly, 100µl of each diluted sample (101-fold dilution in sample buffer), and control serum, and pre-diluted calibration samples were placed in separate wells pre-coated with EBV-CA, and incubated at 37˚C for 60 minutes. Wells were then washed with 300µl wash buffer and shaken dry, with this cycle being repeated 4 times. One hundred microlitres of pre-prepared enzyme conjugate was then added to each well, and the plate incubated for another 1 hours at 37˚C. After further washes (as before) 100µl chromogen substrate was added to each well, and the plate incubated at room temperature for 20 minutes. The reaction was stopped by the addition of 100µl sulphuric acid (provided by manufacturer) and the wells read on an 'Emax' plate reader (Molecular Devices) using a 450nM filter. After confirming test validity according to the manufacturer's predetermined criteria, serum anti-EBV-CA IgG levels were inferred from the standard curve derived from calibration samples. One patient's samples were found to have levels above the limit of accurate detection (100 Arbitrary units/ml) whereupon both assays of both pre-and post-Rituximab samples were repeated using 1 in 300 and 1 in 1000 dilutions, in parallel with a new standard curve. The lower limit of detection for the assay was reported by the manufacturers.

3.2.8 Measurement of levels of isohaemagglutinins in patients' serum samples.

IgM isohemagglutinins were measured by hemagglutination. Twofold serial dilutions of serum were incubated separately with standard red blood cells (RBC) (blood groups A and B) in Allsevers (National Blood Service, Liverpool, UK), at room temperature. The greatest dilution causing agglutination after 45 min was recorded. Where both anti-A and anti-B antibodies were present in the pretreatment sample, the antigen giving the higher antibody titer in the pretreatment sample was used throughout the study.

3.3 Methods used for mouse studies.

3.3.1 Animal Licence.

All procedures were performed under a Home Office licence to Dr Adam Cunningham, licence number 40/2904, and were approved by the University of Birmingham Ethics Committee.

3.3.2 Animals and animal husbandry.

"QMxB6 mice" were raised by crossing Quasi-monoclonal (QM) mice [123] with C57/BL6 mice for ≥ 6 generations, selecting for the presence of the QM-related transgene each time. Mice were bred and maintained in specific pathogen free conditions in the University of Birmingham BioMedical Services Unit (BMSU). They were provided with unlimited amounts of standard feed, and water.

Where used, 5-Bromo 2′-deoxyuridine (BrdU) was provided *ab libitum* at 1mg/ml in animal's drinking water between 24 hours and 120 hours after inoculations.

3.3.3 *S.* Typhimurium – culture and preparation for inoculation.

The bacteria used for the experiments were kindly cultured and prepared by Ms Saeda Bobat. An attenuated strain of *Salmonella* – *Salmonella enterica* serovar Typhimurium (*S.* Typhimurium) (SL3261 strain) [195] – was cultured overnight in LB media at 37˚C, with aeration. Prior experiments had established the relationship between the cell density of *S.* Typhimurium in exponential phase culture, and the optical density (OD) of the bacterial suspension, measured at 600nm. Once an OD between 0.8 and 1.2 was reached, bacteria were harvested by centrifugation (6000g for 5 minutes). Pelleted cells were then washed twice in PBS (with further centrifugation at 6000g for 5 minutes after each), before being resuspended in 1ml PBS. This was then diluted, as necessary, to give a predicted final concentration of 10^5 cells per 200µl for use in immunisations.

3.3.4 Animal inoculations.

Mice aged between 6 and 8 weeks each received one intra-peritoneal injection of 200µL phosphate buffered saline, to which had previously been added either a) 30µg NP-Ficoll (Biosearch Technologies, Novato, CA), or b) 10^5 live *S.* Typhimurium or c) both. Control (non-immunised) mice did not receive sham injections. Injections were kindly performed by Ms Jennifer Marshall, Dr Elodie Mohr, and the staff of BMSU.

3.3.5 Animal sacrifice and the obtaining of samples.

Animals were sacrificed at differing timepoints from 4 to 35 days after inoculation, by cardiac puncture under terminal anaesthesia. Control mice were sacrificed at the end of the experiment (day 35). Procedures were kindly performed by Ms Jennifer Marshall, Dr Elodie Mohr, and the staff of BMSU.

3.3.5.1 Preparation and storage of serum from mouse blood samples.

Blood samples obtained by cardiac puncture under terminal anaesthesia were allowed to clot at room temperature, and then centrifuged at 16,060g for 10 minutes before extraction of serum by pipetting. Serum samples were then aliquotted and frozen at -20˚C or below before use.

3.3.5.2 Preparation and storage of spleens from sacrificed mice.

Spleens obtained after mouse sacrifice were divided, and both segments weighed. In each case, the larger part was stored for subsequent use in histology (section 3.3.8). The smaller part was used immediately in flow cytometric studies (section 3.3.7).

3.3.6 ELISA-based assay for measurement of isotype specific anti-NP antibody levels in mouse serum samples.

Samples were prepared as described in section 3.3.5.1. Nunc Maxisorb 96 well plates were coated with antigen by overnight incubation, in a dampened box at 4˚C, with 100µl per well of coating buffer (see section 3.1) containing 5mg/ml NP_2-BSA. Sufficient plates were coated for the contemporary measurement of all samples to be compared.

Plates were prepared for use by first being washed three times in PBS (by immersion), and being dried between each by shaking and by banging on dry paper. Plates were then blocked by incubation at 37˚C for 1 hour with 100µl per well of PBS containing 1% BSA, and then washed once again in PBS with shaking and banging to dry.

Meanwhile, samples were prepared for analysis by preparing serial dilutions in PBS containing 1% BSA and 0.05% Tween-20, in a separate non-absorbent 96 well plate. For

assays of IgM anti-NP samples were diluted 1 in 10, and 4-fold thereafter. For assays of other isotypes, starting dilutions of 1 in 100 were used.

One hundred microlitres of all samples' dilutions to be tested were then transferred to the pre-coated, blocked and washed ELISA-plates, and incubated at 37˚C for 1 hour, after which plates were washed and dried three times, as described previously. Plates were left with wells filled with additional PBS, until washing of all concurrently incubated plates was completed. Control (blank) wells, were loaded with diluent alone.

Secondary antibodies used were alkaline-phosphatase conjugated polyclonal goat antibodies against specific mouse immunoglobulin isotypes (all from Southern BioTech). Anti-IgM was used at 1 in 2000 dilution, whilst others were used at 1 in 1000 dilution, in PBS containing 1% BSA, and 0.05% Tween-20. One hundred µl of the relevant antibody was added to each sample well, and to blank wells, and the plates re-incubated for 1 hour at 37˚C, before being washed as described previously.

Meanwhile the buffer for use with enzyme substrate was prepared by dissolving 1 Tris tablet (Sigma) into 20ml distilled water. One p-Nitrophenyl Phosphate (pNPP) Fast^{TM} tab (Sigma) was then added, per 20ml Tris buffer, to be fully dissolved just before use.

One hundred microlitres of pNPP Fast^{TM} solution was then added to each sample and control well and the plate then incubated at 37˚C until sufficient colour had developed for reading at 405nM by plate reader.

Within sets of samples assayed for the same isotype of anti-NP antibody, changes in 405nM absorbance were plotted against each sample's dilution (log scale), and a cut-off absorbance threshold was determined. Relative titres of measured antibody in each

sample were considered to be the inverse of the hypothetical concentration which generated the threshold optical density.

3.3.7 Flow cytometric studies of mouse spleen cell suspensions.

3.3.7.1 Estimation of splenic CD138$^+$ cell counts by flow cytometry.

This work was kindly performed by Ms Jennifer Marshall.

Segments of freshly obtained mouse spleen were pulped, suspended in 5ml RPMI supplemented with 10% fetal calf serum (FCS) and sieved through a 70mm nylon mesh, before being incubated with appropriate antibodies (Table 3-1) suspended in PBS with 1% FCS at predetermined optimal concentrations for 20 minutes at 4˚C.

	FL-1	FL-2	FL-3	FL-4
Reagent	anti-B220-FITC	NP-PE	-	anti CD138-Biotin and steptavidin APC
Source	eBiosciences	Dr P. Lane		Beckton Dickinson

Table 3-1 shows reagents used for the estimation of CD138$^+$ cell numbers by flow cytometry.
FITC: Fluorescein-isothiocyanate. PE: Phycoerythrin. APC: Allophycocyanin.

Samples were then immediately analysed on a Facscalibur (Becton Dickenson) flow cytometer using CellQuest Software. Off-line analysis was achieved with FlowJo software for Mac (Version 6.3.2). Apoptotic cells were excluded by their forward / side scatter characteristics. Amongst the remaining cells, the proportion that were CD138$^+$, and the proportion of these that were also NP-specific, was calculated.

An estimate of the total cell count per spleen was obtained by counting with an improved Neubauer haemocytometer using Trypan blue exclusion.

3.3.7.2 Other flow cytometric studies of mouse spleen cell suspensions.

This work was kindly performed by Dr Elodie Mohr.

One third of the spleen was mashed between two glass slides in RPMI containing 5% FCS, 1 mg/ml of collagenase type II (Lorne Laboratories Ltd) and 0.15mg/ml DNase I (Sigma-Aldrich). The cell suspension was prepared by repeated pipetting for 20 min through a fine tip pastette (alphaLaboratories). It was then treated for 5min with 10mM EDTA (Sigma-Aldrich), before being filtered through a nylon mesh, and centrifuged for 5 min at 1500 rpm. Cells were resuspended in Flow-assisted cytometric sorting (FACS) buffer containing 5% normal mouse serum and 20% v/v of supernatant from 2.4G2 hybridoma culture and incubated for 10 minutes on ice. Cells were then re-centrifuged for 5 min at 1500 rpm and resuspended in FACS buffer. A proportion of the prepared cells were recentrifuged and stored as a dry pellet at -20˚C until needed for RNA extraction (see section 3.3.14.1).

Samples were then incubated with the appropriate antibodies (which were either directly conjugated to fluorochromes or to biotin) for 30 minutes on ice (see Table 3-2, Table 3-3, Table 3-4, and Table 3-5). Where biotinylated secondary antibodies were used, an additional wash step was first performed (using 150 µl PBS containing 2mM EDTA, and 0.1% FCS). Samples were then incubated with the appropriate streptavidin conjugated fluorochrome for 30 minutes on ice, before the final 2 washes.

	FL-1	FL-2	FL-3	FL-4
Reagent	anti-CD169 FITC	anti F4/80 PE	anti-CD11b PerCP-Cy5.5	anti Gr1 biotin + Strept APC
Source (company)	Serotec	e-Bioscience	BD Pharmingen	e-Bioscience, BD Pharmingen

Table 3-2 shows reagents used for the estimation of splenic granulocyte numbers by flow cytometry.

	FL-1	FL-2	FL-3	FL-4
Reagent	anti F4/80 FITC	anti-CD11c PE	anti-CD8 PerCP	anti-CD4 APC
Source (company)	Sertotec	BD Pharmingen	BD Pharmingen	e-Bioscience

Table 3-3 shows reagents used for the characterization of splenic granulocytes with antibodies to CD11c, CD8α, CD4 and F4/80, by flow cytometry.

	FL-1	FL-2	FL-3	FL-4
Reagent	anti IgM FITC	NP-PE	anti-B220 PerCP-Cy5.5	anti-CXCR3 APC
Source (company)	Southern Biotech	Dr Elodie Mohr	BD Pharmingen	Both BD Pharmingen

Table 3-4 shows reagents used to assess expression of the chemokine receptor CXCR3 on putative NP-specific AFC, by flow cytometry.

	FL-1	FL-2	FL-3	FL-4
Reagent	anti IgM FITC	NP-PE	anti-B220 PerCP-Cy5.5	anti-CXCR4 biotin, and steptavidin APC
Source (company)	Southern Biotech	Dr Elodie Mohr	BD Pharmingen	R&D Systems

Table 3-5 shows reagents used to assess expression of the chemokine receptor CXCR4 on putative NP-specific AFC, by flow cytometry.

Where needed, intracellular staining for flow-cytometry was performed using Cytoifx/Cytoperm kit (BD Biosciences), and the BrdU APC flow kit (BD Biosciences), according to the manufacturers instructions (see also Table 3-6).

	FL-1	FL-2	FL-3	FL-4
Reagent	anti-BrdU FITC	NP-PE	anti-B220 PerCP-Cy5.5	anti-CD138 APC
Source	BD Pharmingen	Dr Elodie Mohr	BD Pharmingen	BD Pharmingen

Table 3-6 shows reagents used for the estimation of splenic numbers of NP-specific AFC, including those that have incorporated BrdU, by flow cytometry.

Samples were then analysed on a Facscalibur (Becton Dickenson) flow cytometer using CellQuest Software. Off-line analysis of flow cytometric data was performed with FlowJo software for Mac (Version 6.3.2).

3.3.8 Preparation of tissues for histology.

Part of each spleen obtained after mouse sacrifice was dip frozen in liquid nitrogen and stored at -70 until use.

6µm spleen sections were cut by cryostat (Bright) and placed on multispot glass slides (Hendley), air dried for at least 40 minutes, and fixed in acetone (Baker) (for 20 minutes at 4˚C). Sections were then briefly air dried, and stored at -20˚C or below until required.

3.3.9 Immunohistochemistry.

3.3.9.1 Incubation of tissues with antibodies.

Tissue sections were prepared in advance as described in section 3.3.8. Slides were brought to room temperature and placed under a fan, for at least 15 minutes, before being rehydrated in Tris pH 7.4 (see section 3.1) for at least 10 minutes at room temperature.

Primary antibodies were mixed as necessary, and diluted to the pre-determined optimal concentrations in Tris pH 7.4. Antibody combinations used are listed in Table 3-7, Table 3-8, Table 3-9, Table 3-10, Table 3-11, and Table 3-12. Seventy five microlitres of the antibody mix was added to each tissue section, which was then incubated for 45 minutes. During this, and subsequent, incubations slides were kept at room temperature in a moist cabinet. Slides were washed for at least 5 minutes in Tris pH 7.4, with stirring, between incubation steps.

Secondary antibodies were mixed as necessary and then pre-absorbed with normal mouse serum (NMS) for 30 minutes before use - 1µl NMS being added per 10ul of mixed undiluted antibody. Secondary antibodies were then diluted to pre-determined

concentrations in Tris pH 7.4 for use. Again, 75µl of diluted antibody was added to each section, and the slides incubated for 45 minutes.

	Alkaline Phosphatase		Peroxidase	
Incubation phase 1	Rt @ CD3	BD Pharmingen	IgD – Sh Ig	Dr Khan
Incubation phase 2 (With NMS)	Rb @ Rt bt	Dako	Dk @ Sh Peroxidase	The Binding Site
Incubation phase 3	Strept AP	Vector		

Table 3-7 shows the protocol for immunohistochemical staining of mouse tissue sections for $CD3^+$ cells and IgD^+ cells.
Rt: Rat. Sh: Sheep. Rb: Rabbit. Dk : Donkey.

	Alkaline Phosphatase		Peroxidase	
Incubation phase 1	NP – Sh Ig	Dr Khan	Rat @ IgD	BD Pharmingen
Incubation phase 2 (With NMS)	Dk @ Sh bt	The Binding Site	Rb @ Rt Peroxidase	The Binding Site
Incubation phase 3	Strept AP	Vector		

Table 3-8 shows the protocol for immunohistochemical staining of mouse tissue sections for cells with anti-NP Ig, and for IgD^+ cells.

Where used, Steptavidin-Biotin Alkaline Phosphatase complex (Strept AP) was prepared from component solutions 'A' and 'B' (Vector). Specifically, 10µl of each solution was added to 1ml Tris pH 7.4 and incubated for 30 minutes at room temperature prior to use. When Rabbit Peroxidase / Antiperoxidase complex (Rabbit PAP) was also used for two colour staining, this was added to the Strept AP just before use at a final concentration of 1/100. Seventy five microlitres of the required, diluted, solution was added to each section, and the slides incubated for 30 minutes.

	Alkaline Phosphatase		Peroxidase	
Incubation phase 1	NP – Sh Ig	Dr Khan	Rb @ Ki67	Dako
Incubation phase 2 (With NMS)	Dk @ Sh bt	The Binding Site	Sw @ Rb Ig	Dako
Incubation phase 3	Strept AP	Vector	Rb PAP	Dako

Table 3-9 shows the protocol for immunohistochemical staining of mouse tissue sections for cells with anti-NP IgG. and for cells expressing the nuclear marker for proliferation – Ki67.

	Alkaline Phosphatase		Peroxidase	
Incubation phase 1	Gt @ human Collagen III	Southern BioTech	NP – Rb Ig	Dr Khan
Incubation phase 2 (With NMS)	Dk @ Sheep Bt	The Binding Site	Sw @ Rb Ig	Dako
Incubation phase 3	Strept AP	Vector	Rb PAP	Dako

Table 3-10 shows the protocol for immunohistochemical staining of mouse tissue sections for structures that bind antibodies against human Collagen III, and for cells with anti-NP Ig.

	Alkaline Phosphatase		Peroxidase	
Incubation phase 1	Rt @ BP3 (CD157)	Accurate Chemical and Scientific	NP – Sh Ig	Dr Khan
Incubation phase 2 (With NMS)	Rb @ Rt Bt	Dako	Dk @ Sh Peroxidase	The Binding Site
Incubation phase 3	Strept AP	Vector		

Table 3-11 shows the protocol for immunohistochemical staining of mouse tissue sections with anti-BP3 antibody and for cells with anti-NP Abs.

	Alkaline Phosphatase		Peroxidase	
Incubation phase 1	Rat @ ER-TR7	BMA Biomedicals	NP – Sh Ig	Dr Khan
Incubation phase 2 (With NMS)	Rt @ Rat Bt	Dako	Dk @ Sh - Peroxiadse	The Binding Site
Incubation phase 3	Strept AP	Vector		

Table 3-12 shows the protocol for immunohistochemical staining of mouse tissue sections with anti-ER-TR7 antibody, and for cells with anti-NP Abs.

3.3.9.2 Enzymatic development of coloured substrates.

3.3.9.2.1 Visualisation of peroxidase associated antibodies with 3,3'Diaminobenzidine tetrahydrochloride.

One tablet (10mg) 3,3'Diaminobenzidine tetrahydrochloride (DAB) (Sigma) was brought to room temperature before being dissolved in 15ml Tris pH 7.4, and then filtered. Approximately 100µl Hydrogen peroxide (30% w/v) (Sigma) was then added to 10ml DAB solution immediately prior to use.

Approximately 100 µl of the resulting mixture was added to each slide, and the sample observed by light microscopy to asses the progression of colour development. Once optimal development was achieved, the reaction was stopped by washing in Tris pH 7.4.

3.3.9.2.2 Visualisation of Alkaline phosphatase associated antibodies with Fast BlueTM.

Fast Blue^{TM} and Napthol AS-MX phospate reagents (both Sigma) were stored at minus 20˚C and brought to room temperature before use. Four milligrams of Napthol AS-MX phosphate (Sigma) was placed in a glass bijou, to which 370 µl N-N-Dimethyl Formamide (Sigma) was added in a fume cupboard. The resulting solution was then added to 8mg Levamisole (Sigma) previously dissolved in Tris pH 9.2 (see section 3.1).

Into the resulting mixture was added 10-12 mg Fast Blue^{TM}, which was then mixed gently, and filtered before use. The final solution was protected from light if not used immediately. Approximately 100 µl was added to each slide, and the section observed by light microscopy to asses the progression of colour development. Once optimal development was achieved, the reaction was stopped by washing in Tris pH 7.4.

3.3.9.3 Final preparation of developed slides for permanent storage and use.

After development of the relevant substrates and washing in Tris pH 7.4, slides were briefly washed in distilled water before being allowed to dry. Sections were covered with glass cover-slips (Surgipath) using Immu-mount fluid (Thermo Electron Corporation).

3.3.10 Estimating splenic NP-specific AFC numbers by counting cells in histological sections.

Estimates of the relative number of NP-specific AFC present in mouse spleens were made using the Weible point counting method [196]. Six micrometre thick splenic sections, that had previously been immunohistochemically stained for anti-NP antibodies and for $CD138^+$ cells, were viewed at 100x magnification through an eyepiece with a 10x10 graticule. NP-stained cells that were overlain by intersections on the grid were counted (excluding those on the right and lower margins of the grid). An estimate for the relative number of cells per section, for each spleen of interest, by starting in one corner and sequentially moving the section back and forth, one 'row' at a time. An estimate of the relative number of cells per spleen was then obtained by multiplying the section's AFC count by the total splenic weight.

3.3.11 Photography of immunohistochemically stained tissue sections.

Photomicrographs of stained sections were obtained using a Hitachi HV-D30 digital camera attached to the P.A.L.M. microdissection platform (Microlaser Technologies

GmbH, Zeiss). Photomicrographs were saved as TIFF images. These were cropped or contrast-adjusted using Paint-Shop Pro Version 7 for windows.

3.3.12 Laser scanning confocal microscopy.

3.3.12.1 Incubation of tissues with antibodies.

Tissue sections were prepared in advance as described in section 3.3.8. Slides were brought to room temperature under a fan, for at least 15 minutes, before being rehydrated in PBS at room temperature for at least 10 minutes.

Primary antibodies were mixed and diluted as necessary. Five percent (by volume) NMS was then added to the antibody mixture, which was incubated at room temperature for 30 minutes before 75µl was added to each tissue section. Sections were incubated for 1 hour with primary antibody, at room temperature. During this, and subsequent, incubations slides were kept at room temperature in a moist cabinet. Slides were washed for at least 5 minutes in PBS with stirring, between each incubation step.

Second and subsequent layers of staining (up to 6 more per section), were performed in a similar manner. Antibodies were pre-mixed with 5% NMS, or another species' normal serum able to bind any residual antibody from the previous layer of staining. Seventy five microlitres of antibody mixture was added to the section each time. Second and subsequent incubations were all 30 minutes at room temperature. Once fluorochrome-conjugated antibodies had been applied, all incubations and wash steps were performed in the dark. Antibody combinations used are listed in Table 3-13 and Table 3-14.

After all staining was completed, sections were washed in fresh PBS. Excess liquid around the margin of the slide was removed, and sections were mounted in 2.5% [1,4-Diazabicyclo(2,2,2) octane] pH 8.6 in 90% glycerol in PBS.

Staining combinations displayed in thesis	**CD169** **F4/80** **anti-NP Ab** **IgM**	**F4/80** **Gr1** **anti-NP Ab** **IgM**	**CD11b** **Gr1** **anti-NP Ab** **IgM**	Corresponding Negative controls
Incubation phase	Staining combinations used			
Phase 1	**NP-Sheep Ig** **Rt @ F4/80** **NMS**	**NP-Sheep Ig** **NMS**	**NP-Sheep Ig** **NMS**	**NMS**
Phase 2	**Dk@Gt Cy-5** **NMS**	**Dk@Gt Cy-5** **NMS**	**Dk@Gt Cy-5** **NMS**	**Dk@Gt Cy-5** **NMS**
Phase 3	**NGS**	**NGS**	**NGS**	**NGS**
Phase 4	**Sh@ Rt bt** **NMS**	**Rt @ Gr1 bt** **NMS**	**Rt @ Gr1 bt** **NMS**	**NMS**
Phase 5	**Strepta Cy3** **NRS**	**Strepta Cy3** **NRS**	**Strepta Cy3** **NRS**	**Strepta Cy3** **NRS**
Phase 6	**Rt @ CD169** **FITC** **NMS**	**Rt @ F4/80** **FITC** **NMS**	**Rt @ CD11b** **FITC** **NMS**	**NMS**
Phase 7	**Rb @ FITC** **NMS**	**Rb @ FITC** **NMS**	**Rb @ FITC** **NMS**	**Rb @ FITC** **NMS**
Phase 8	**Gt @ Rb FITC** **Gt @ IgM AMCA**	**Gt @ Rb FITC** **Gt @ IgM AMCA**	**Gt @ Rb FITC** **Gt @ IgM AMCA**	**Gt @ Rb FITC** **Gt @ IgM AMCA**

Table 3-13 shows protocol for staining adjacent sections of mouse tissue for visualization of selected combinations of $CD169^+$ cells, $F4/80^+$ cells, $Gr1^+$ cells, $CD11b^+$ cells, cells specific for NP, and IgM^+ cells by confocal microscopy.
AMCA: 7-amino-4-methylcoumarin-3- acetic acid. NGS: Normal goat serum.
Reagents were obtained from the following sources: NP-Sheep Ig (Dr Khan), Dk@Gt Cy-5 (Jackson Immunoresearch), Sh@ Rt bt (Binding Site), Strepta Cy3 (Jackson Immunoresearch), Rt @ F4/80 FITC (Serotec), Rt @ CD11b FITC (e-Bioscience), Rb @ FITC (Dako), Gt @ Rb FITC (BD Pharmingen), Gt @ IgM AMCA (Jackson Immunoresearch), Rt@ CD169 FITC (Serotec). Normal animal sera were obtained from The Binding Site.

Staining combinations displayed in thesis	**F4/80** **CD11c** **CD4** **IgM**	Corresponding Negative controls
Incubation phase		
Phase 1	**Hs@ CD11c** **NMS**	**NMS**
Phase 2	**Gt @ Hs Cy3** **NMS**	**Gt @ Hs Cy3** **NMS**
Phase 3	**Rt @ F4/80 FITC** **NMS**	**NMS**
Phase 4	**Rb @ FITC** **NMS**	**Rb @ FITC** **NMS**
Phase 5	**Gt @ Rb-FITC** **Rt @ CD4-APC** **NMS**	**Gt @ Rb FITC** **NMS**
Phase 6	**Gt @ IgM AMCA**	**Gt@ IgM AMCA**

Table 3-14 shows protocol for staining sections of mouse tissue for visualization of F4/80$^+$ cells, CD11c$^+$ cells, CD4$^+$ cells and IgM$^+$ cells by confocal microscopy.
Hs: Hamster. Reagents were obtained from the following sources: Hs@ CD11c (Serotec), Gt @ Hs Cy3 (Jackson Immunoresearch), Rb @ FITC, Gt @ Rb-FITC (Dako), Rt @ CD4-APC (e-Bioscience), Gt @ IgM AMCA (Jackson Immunoresearch). Normal mouse serum was obtained from The Binding Site.

3.3.12.2 Confocal microscopy – image acquisition and analysis.

Sections were examined with a Zeiss LSM510 laser scanning confocal microscope using a x10 objective. A 488nm argon laser was used to excite FITC-conjugated antibodies; a 543nm HeNe laser was used for Cy3–conjugated antibodies; a 633nm helium laser for Cy5 conjugates, and 351 / 364nm lasers were used for AMCA conjugated antibodies. The four lasers scanned separately, to obtain discrete images of 2048x2048 resolution. These were analysed off line using Zeiss LSM image browser version 3,5,0,376 to generate combined images in false-colour.

3.3.13 Laser microdissection and capture of tissue sections for use in Real Time Reverse Transcriptase Polymerase Chain Reaction assays (RT_2-PCR).

3.3.13.1 Cresyl violet staining of sections for dissection.

Sections for subsequent microdissection were prepared and stored as for histology (section 3.3.8), except that PALM® MembraneSlides NF were used. For use, slides were removed from the freezer, and brought to room temperature under a fan, for at least 20 minutes. Sections were then rehydrated by passage through RNAse free 100% ethanol, 70% ethanol, and 50% ethanol (all from Sigma), and stained for 3 minutes with cresyl violet (sigma) 1% W/V in RNAse free 100% ethanol. Slides were then dipped sequentially in 50%, 70%, 100% to dehydrate, and air-dried.

3.3.13.2 Use of immunohistochemically stained slides to determine areas of splenic tissue for microdissection.

Two pairs of serial sections, cut before and after the sections intended for microdissection, were prepared for conventional histology (section 3.3.8). Within in each pair, one section was stained with NP and anti-IgD, the other with NP and anti-Ki67 (according to methods described in section 3.3.9).

Each section was photographed in entirety, and a composite image constructed in PowerPoint version 2002 (Microsoft). Tissue areas of interest were identified within this composite image – red pulp containing NP-specific antibody forming cells (AFC), red pulp not containing NP-specific AFC, IgD^+ areas, T zone, and extra-follicular foci (in

infected mice) – and cross-referenced with corresponding areas on the cresyl violet stained tissue for microdissection (Figure 3-1).

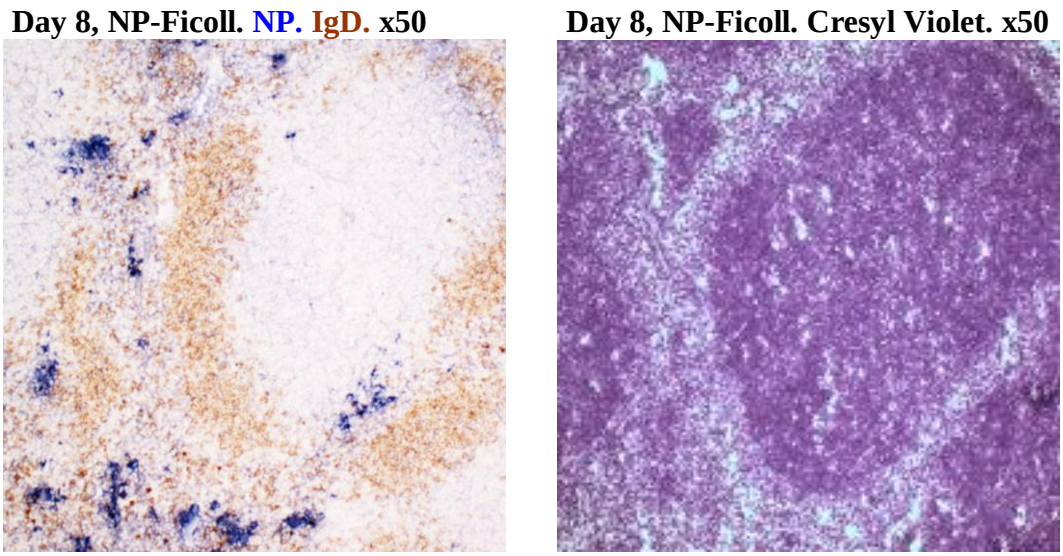

Figure 3-1 shows photomicrographs of two proximate splenic sections from a mouse sacrificed 8 days after NP-Ficoll immunization, demonstrating relationship between appearances after cresyl violet staining, and after immunohistochemical staining for IgD and anti-NP antibodies.
Left image shows section immunohistochemically stained for IgD (brown) and with NP (blue). Right image shows section stained with cresyl violet, revealing intense staining of the B cell follicle, slightly weaker staining of the T zone, and light staining of the red pulp.

In mice sacrificed at day 4 post NP-Ficoll immunization, no red pulp areas devoid of plasma cells could satisfactorily be identified for dissection (see section 6.4.2). Extra-follicular foci of antibody secreting cells, of adequate size for microdissection, were only satisfactorily identified in the *S.* Typhimurium infected mice.

3.3.13.3 Laser microdissection and tissue capture.

Laser microcapture was performed using a Microbeam HT microscope (PALM Microlaser Technologies). Twenty to forty similar areas were microdissected, and catapulted into twenty microlitres of RNeasy RLT buffer (Qiagen), and snap frozen on dry ice (-78˚C). Samples were stored at minus 20˚ C until use.

3.3.14 cDNA preparation for semi-quantitative RT_2-PCR.

3.3.14.1 RNA isolation from spleen cell suspensions.

This work was kindly performed by Dr Elodie Mohr.

Cell suspensions were previously prepared as described in section 3.3.7.2. The frozen pellets were resuspended in 1ml of RNABee (Tel-test Inc), and homogenised by pipetting up and down and then vortexing. The extraction was then performed by adding 200 µl of chloroform and vortexing for 30 sec. After centrifugation for 15 min at 16,060g at 4C, the aqueous phase was removed, and the RNA precipitated by incubation with 500 µl isopropanol for 10 min at room temperature. The RNA was pelletted by centrifugation for 5 min at 16,060g at 4C, and the pellet then washed twice in 1 ml of 75% ethanol, with similar centrifugations between washes.

After leaving the pellets to dry slightly, they were resuspended in 30 µl of diethyl pyrocarbonate (DEPC, Sigma-Aldrich)-treated water containing 20U of RNAseOUT^{TM} RNAse-inhibitor (Invitrogen).

The concentration of RNA obtained was estimated by optical density (at 260 nm), based on the assumption that 40 µg/µl of RNA gives an OD of 1. Two micrograms of RNA was used for cDNA preparation. This amount of RNA is incubated with 1ug random hexanucleotides (Promega) in 13 µl total.

3.3.14.2 RNA isolation from microdissected tissue.

RNA isolation and cDNA preparation were performed using RNAeasy Micro Kits (Qiagen), according to the manufacturer's instructions. Microdissected samples, contained with twenty microlitres of RLT buffer, were lysed by micropipetting in 350µl

of RLT buffer, to which β-mercaptoethanol (1%) and carrier RNA (to a final concentration of 57ng/ml) had been previously added. The lysed solution was then placed in a QIAShredder spin column, itself placed within a 2ml collection tube, and centrifuged for 2 minutes at 16,060g. The collected volume was mixed by pipetting with 350µl of RNAse free 70% Ethanol (sigma), placed in an RNeasy MinElute spin column, and centrifuged for 15 seconds at 8,000g. After discarding the flow through, the column contents were was washed by adding 350µl RW1 buffer and re-centrifuging at 8,000g for 15 seconds.

Eighty microlitres of diluted DNAse 1 solution (10µl of DNAse1 stock with 70 µl RDD buffer) was then added directly to the top of the column which was then incubated for 15 minutes at room temperature, before being washed by adding a further 350 µl RW1 buffer and then centrifuged at 15 seconds at 8,000g.

After placing the column into a new collection tube, 500µl RPE buffer was added to the column before centrifuging at 8,000g for 15 seconds, and discarding the flow through. Next 500µl 80% Ethanol (RNAse free) was added to the column which was centrifuged for 2 minutes at 8,000g, after which the flow through and collection tube were discarded.

After placing the column into a clean collection tube, it was centrifuged again, this time with the cap kept open, at 16,060g for 5 minutes to dry the column contents.

To elute the RNA, 22µl RNAse free water was added directly to the top of the column, which was centrifuged at 16,060g for 1 minute, with the flow through collected in a fresh 1.5ml eppendorf tube.

3.3.14.3 Preparation of cDNA from isolated RNA.

In preparing cDNA from bulk spleen cell suspensions, 2 µg extracted RNA was mixed with 1µl random primer hexa-nucleotides (3mg/ml, Promega) in 13µl RNAse free water. By contrast for microdissected samples, 2µl random primer hexa-nucleotides (3mg/ml, Promega), were mixed with 20µl of RNA containing eluate (see section 3.3.14.2). Thereafter similar methods were used for preparation of cDNA from both sources. Mixtures were denatured at 70˚C for 10 minutes, and shock cooled on ice to prevent re-annealing. Meanwhile the reverse transcriptase solution was prepared. This contained 6.4 µl RNAse free water, 8µl 5x first strand buffer (Promega), 1.5µl nucleotide mix (dATP, dCTP, dGTP, d, TTP at 10mM each), 0.625µl RNAseOUT^{TM} RNAse-inhibitor (40U/µl, Invitrogen), 1.5µl Moloney Murine Leukemia Virus reverse transcriptase (200U/ml, Promega). To this solution was added the 22µl water containing the RNA and primers, and the PCR tube contents were mixed well by pipetting.

The mixture was incubated at 42˚C for 1 hour, before being heated to 90˚C for 10 minutes to denature the reverse transcriptase, and then allowed to cool. The resulting cDNA was stored, without further dilution, at -20˚C.

3.3.15 Quantitative Reverse Transcriptase Polymerase Chain Reaction Assays (RT_2-PCR).

Assays for the relative quantification of target cDNA in samples were performed, where possible, in duplex with assays for β_2-Microglobulin or β-actin cDNA. Otherwise, relative amounts of target and reference gene cDNA were quantified in simultaneously performed, simplex, assays. Primers used had either been designed by others within the

research group using Primer Express computer software (Applied Biosystems) and then synthesized by Eurogenetec, or were purchased directly from Applied Biosystems. All primers were used at previously determined optimal concentrations and with standard reaction conditions for TaqMan PCR. Probes were detected by 5' conjugation to FAM (target species), or 5' conjugation to VIC or Yakima Yellow. Details of primer and probe sequences used, and their corresponding concentrations, are contained in Table 3-15.

mRNA species	Origin	Fluoro-phore	Assay configuration	Reference gene used	Final reagent concentration (nM) Forward primer	Reverse primer	Probe
IL6	MacLennan group	FAM	Simplex	β2-microglobulin	150	80	60
BAFF	MacLennan group	FAM	Simplex	β2-microglobulin	150	120	120
APRIL	MacLennan group	FAM	Simplex	β2-microglobulin	175	60	60
Blimp-1	MacLennan group	FAM	Duplex	β2-microglobulin	175	80	100
γ-IFN	MacLennan group	VIC	Simplex	β2-microglobulin	150	120	120
IL-21	MacLennan group	FAM	Simplex	β2-microglobulin	125	80	80
CXCL12	MacLennan group	FAM	Simplex	β2-microglobulin	175	80	80
BCMA	MacLennan group	FAM	Simplex	β2-microglobulin	80	80	175
CXCL9	Applied Biosystems	FAM	Duplex	β2-microglobulin	0.4µl per well		
CXCL10	Applied Biosystems	FAM	Duplex	β2-microglobulin	0.4µl per well		
CXCL11	Applied Biosystems	FAM	Duplex	β2-microglobulin	0.4µl per well		
TNF-α	Applied Biosystems	FAM	Duplex	β2-microglobulin	0.4µl per well		
CXCR3	Applied Biosystems	FAM	Duplex	β2-microglobulin	0.4µl per well		
CXCR4	Applied Biosystems	FAM	Duplex	β2-microglobulin	0.4µl per well		
β2-microglobulin	MacLennan group	Yakima Yellow	Both		175	60	80

Table 3-15 shows mRNA species analysed by RT_2-PCR, the fluorophore associated with each probe, their assay's configuration (duplex or simplex) and working concentrations of primers and probes used.
Primer and probe sequences are listed in Appendix 2, page 184. FAM: 6-carboxyfluoroscein. VICis a proprietary dye from Applied Biosystems.

RT_2-PCR assays were performed in 8µl final reaction volume. Quantities of target species' forward primers, reverse primers, and probes, sufficient to achieve the desired final concentrations, were mixed in advance with PCR master mix (Promega), and diluted to 7 µl with RNAse free water.

One microlitre of sample cDNA was added to the appropriate well of a 384 well MicroAmp plate (Applied Biosystems) which was then centrifuged for 2 minutes (200g). Seven microlitres of the previously prepared mix of primers, probes, enzymes and buffer

was then added to the sample cDNA, and the mixture re-centrifuged before being covered with an optically clear adhesive film (Absolute Q-PCR Seal, Thermo Scientific).

Assays were performed using an ABI 7900 machine (Applied Biosystems), in which samples were heated to 50˚C for 2 minutes, then to 95˚C for 10 minutes, followed by 40 cycles of high temperature (95˚C for 15 seconds) and lower temperature (60˚C for 60 seconds). Results were analyzed using SDS version 2.2.2 software (Applied Biosystems).

3.4 Statistical analysis and presentation of data.

Statistical analysis was performed using Prism software version 5.01 (GraphPad). Statistical comparisons were made with the two-tailed unpaired non-parametric Mann Whitney test. Figures presented either were created using Excel 2002 and PowerPoint 2002 (both Microsoft), or Prism software version 5.01 (GraphPad).

4 DEVELOPMENT OF MICROSPHERE BASED ASSAYS

4.1 Introduction.

There are considerable advantages to technologies that allow the accurate and reproducible performance of multiple assays, in parallel, using small amounts of a biological sample. In addition to their potential to save time, and minimise consumption of stored sera, such techniques (known as "multiplexing") eliminate intra-assay variability due to pipetting, and minor changes in experimental condition. These causes of variability are inherent in the execution of serial assays. This is of greatest relevance when performing within-subject comparisons amongst the relevant assays – an experimental design anticipated, and subsequently used, elsewhere in this thesis.

Prior studies have used "Luminex" microsphere based assays to measure, across a wide dynamic range, levels of antibodies specific to different pneumococcal capsular polysaccharides (PnCP) [193;197]. Although the appropriate machine was available, only preliminary steps towards establishing such assays had previously been made at the University of Birmingham. My project required accurate assays to determine within single samples specific class and subclass levels of antibody against all of the different recognized classes of antigen. Consequently I sought to establish, validate and standardise a local microsphere-based assay for this purpose. The aim was to use this approach to assess levels of antibodies against different serotype specific PnCP, as well as antibody specific for tetanus toxoid, phosphorylcholine (PC), or CWPS.

4.2 Principles of microsphere-based assays.

Microsphere assays are analogous to enzyme-lined immunospecific assays (ELISAs). The binding of a soluble factor (e.g. antibody) to an immobilised substrate (e.g. antigen) is not linearly related to the concentration of either, or the affinity of the interaction.

For microsphere-based assays the substrate is covalently bound to microscopic beads. These can be commercially obtained with substrate already attached (e.g. in cytokine assays) or purchased bearing carboxyl groups, for use in customised bead assays (see section 3.2.5.1 for conjugation method used in this work). Beads are available in a range of 'regions', which are distinguished by the relative amount of two fluorochromes they contain. Thus when run through an appropriate machine, analogous to a flow cytometer, distinct bead 'regions' can be identified by their fluorochrome signature (Figure 4-1).

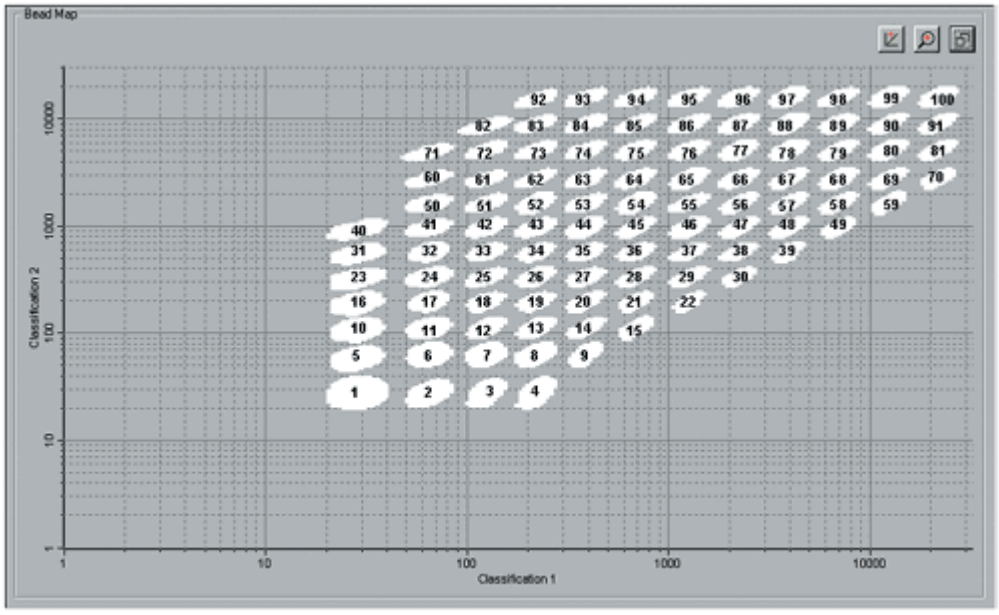

Figure 4-1 is a map of 100 distinct beads regions available for Luminex microsphere-based assays.
Figure downloaded from BioRad corporation website (http://www.bio-rad.com)

To quantify the amount of soluble factor binding to the bead-bound substrate, an excess of secondary antibody, which is usually directly conjugated to phycoerythrin (PE), is added to the sample well. Where additional amplification is needed (e.g. cytokine assays), biotinylated secondary antibodies can be used and binding of this is detected using an avidin-PE complex.

When running the assay, the machine reads a variable (pre-defined) number of beads (usually 100) of each region being studied. It measures the associated intensity of PE fluorescence for each bead and calculates a 'median fluorescence intensity' (MFI) for the region. This is assumed to be proportional to the amount of soluble factor associated with the bead.

Median fluorescence intensities assigned to a bead region are then compared to a standard curve (generated using dilutions of a standard preparation of the soluble factor in parallel wells) to obtain a measure of the relative or absolute quantity of the soluble factor in the sample fluid.

As various substrates can be bound to beads of different regions, which can then be distinguished when run on the machine, it is tempting to perform assays for multiple factors within the same well with consequent saving of time, and sample. This can be done so long as it is shown that there is minimal interference between the parallel assays. *A priori* where the soluble factor has a measurable affinity for another available substrate, the effective quantity of substrate is increased, and so binding to the 'true' substrate (bound to the relevant reporter bead) may be reduced. Conversely, where another soluble factor with measurable affinity for the 'true' substrate is present, the apparent binding of the factor being measured (via the reporter bead) may be increased. Confirming the non-

interference of assays performed in parallel was a crucial part of establishing confidence with this technique, especially as significant cross reactivity between antibodies against various PnCP has been reported [198]. It should be noted that experimental confirmation of non-interaction between different multiplexed assays does not exclude expected interference between antibodies of appropriate specificities, but differing isotypes (e.g. an IgM anti-PnCP-1 antibody, causing interference with an assay for IgG anti-PnCP-1).

4.3 Early assay development.

Preliminary experiments used beads that Dr Mark Cobbold had conjugated to pneumococcal antigens using periodate conjugation (after Biagini et al) [197]. Antibody binding to the coated beads was detected using PE conjugated anti-human IgG obtained from BD. Standard curves were produced, but with very poor signal/background ratios, and poor absolute signal strength compared to that achieved using published techniques. A poly-L-Lysine conjugation method derived from other published work [193] was then used, with limited improvements in signal/background ratio (Figure 4-2). Advice was then sought from Dr Lindsey Ashton (Institute of Child Health, London), in developing the protocol subsequently used and described in the methods chapter of this thesis (section 3.2.5.1). PE conjugated anti-human IgG supplied by BectonDickenson was replaced by antibody obtained from Southern BioTech, resulting in a marked improvement in the assay performance (Figure 4-2). Consequently, this reagent was used exclusively in subsequent studies.

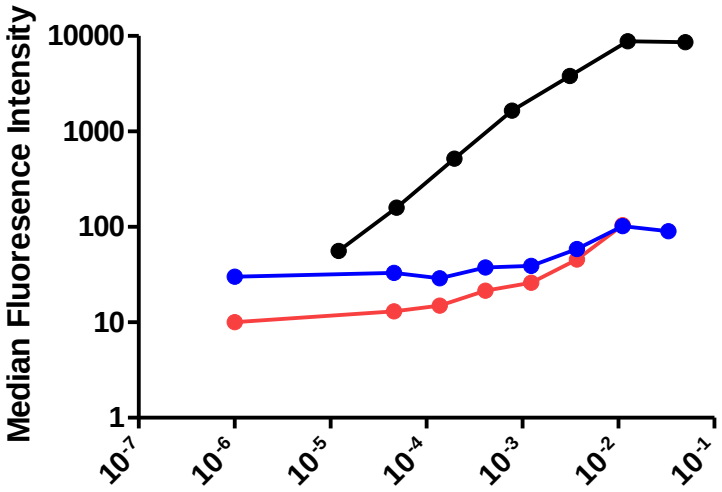

Figure 4-2 shows preliminary results in establishing microsphere assays.
Comparison of three different experimental techniques to assay IgG antibodies against pneumococcal capsular polysaccharide (Pn-CP) 19F, using antigen-conjugated microspheres. The blue line was obtained using beads conjugated using the periodate method, with anti-IgG antibody from BD (diluted 1 in 20). The red line was obtained using beads conjugated with the poly-L-lysine method, and IgG antibody from BD (diluted 1in 20). The black line was obtained in a separate experiment using beads conjugated with the poly-L-lysine method, and IgG antibody from Southern BioTech (diluted 1 in 200).

4.4 Suboptimal conjugation of substrate to bead affects assay performance.

As discussed above (section 4.1), first principles indicate that substrate density may affect assay performance. This was tested when developing the bead-based assay for antibodies to tetanus toxoid (Figure 4-3). When limiting amounts of tetanus toxoid were available during bead conjugation, subsequent assay performance was adversely affected in that the mean fluorescent intensity (MFI) was reduced, and prozone phenomena were noted.

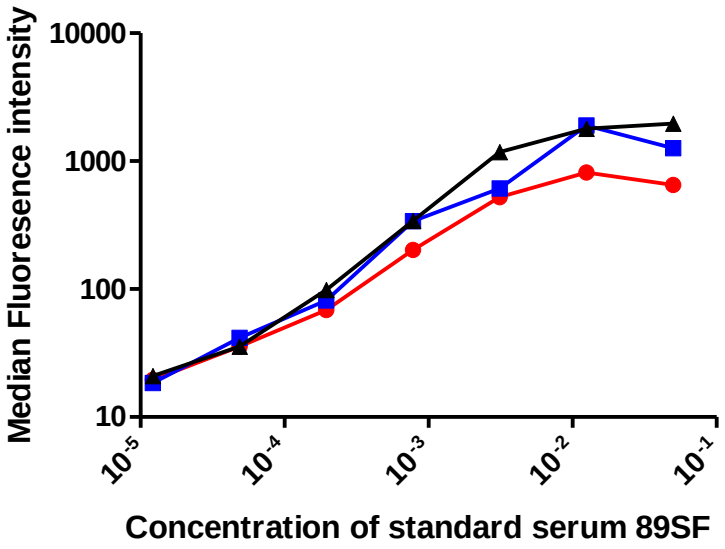

Figure 4-3 shows that limiting amounts of available antigen during conjugation to beads affects subsequent assay performance.
Comparison of three different experimental techniques to assay IgG antibodies against tetanus toxoid (in standard pneumococcal reference serum). Techniques varied only in the concentration of tetanus toxoid used during the bead-conjugation reaction - the red line represents a coating concentration of 5µg/ml, the blue line 7.5µg/ml and the back line 12µg/ml.

4.5 No evidence of inter-assay interactions within multiplexed system.

As discussed above, variations in bead's substrate density can affect assay performance, and certain anti-PnCP antibodies have been reported to be cross reactive with other PnCPs [198]. Thus it was important to confirm that anti-PnCP antibody assays were minimally affected by PnCPs bound to other beads present during multiplexed assays. Seven PnCP were selected for use to assay levels of specific anti-PnCP. Assays for antibodies against each PnCP were therefore performed separately (monoplex) and together (multiplex) (see Figure 4-4 for an example). Standard curves for each assay were comparable under the two conditions, and it was concluded that subsequently these assays could be performed as multiplex.

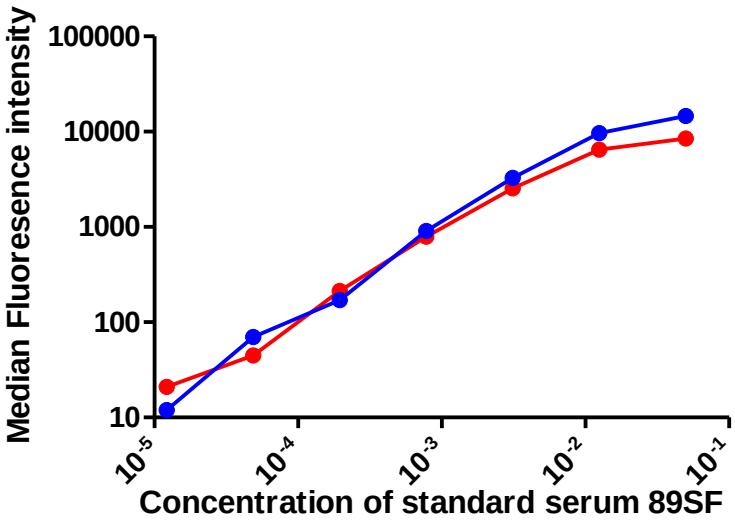

Figure 4-4 shows an assay of IgG antibodies against PnCP-9 – demonstrating consistency between monoplex and multiplex methods.
Detectable levels of anti-PnCP-9 antibody in serial dilutions of standard serum were comparable whether measured alone (monoplex) or in the presence of six other sets of beads; each set being coated with one of the six other PnCP serotypes.

4.6 Confirming optimal pre-absorbtion conditions for assay of serotype specific anti-pneumococcal antibodies.

Commercial preparations of PnCP contain contaminating CWPS [199]. Furthermore, as discussed in section 4.2, the WHO advises that sera are preabsorbed with CWPS and PnCP-22f, which has epitopes that cross react with other PnCP, prior to performing assays for serotype specific anti-PnCP antibodies, to reduce the levels of cross reactive antibodies present [194].

Optimal preabsorption conditions in the context of a microsphere-based assay were tested. A range of different concentrations for the two preabsorbing agents were used (Table 4-1), and their effect on subsequent assay performance was tested.

		Concentration of CWPS			
		0 μg/ml	0.5 μg/ml	1 μg/ml	2 μg/ml
Concentration of PnCP-22f	0 μg/ml	✓	✓		✓
	1.25 μg/ml		✓	✓	✓
	2.5 μg/ml		✓	✓	✓
	5 μg/ml		✓	✓	✓

Table 4-1 shows the range of concentrations of preabsorbing agents tested during development of pneumococcal antibody assay.

Representative examples of these experiments are shown in Figure 4-5. Measured levels of some, but not all, antibodies tested were reduced by pre-absorption with CWPS alone. Minimal incremental difference was noted with the higher concentration, but 2 μg/ml was chosen for subsequent experiments to ensure maximal efficacy. Similarly, pre-absorption with PnCP-22f, in addition to CWPS, attenuated the measured levels of some, but not all antibody specificities. Little difference was seen between the high concentrations used, and 5 μg/ml was chosen for subsequent experiments.

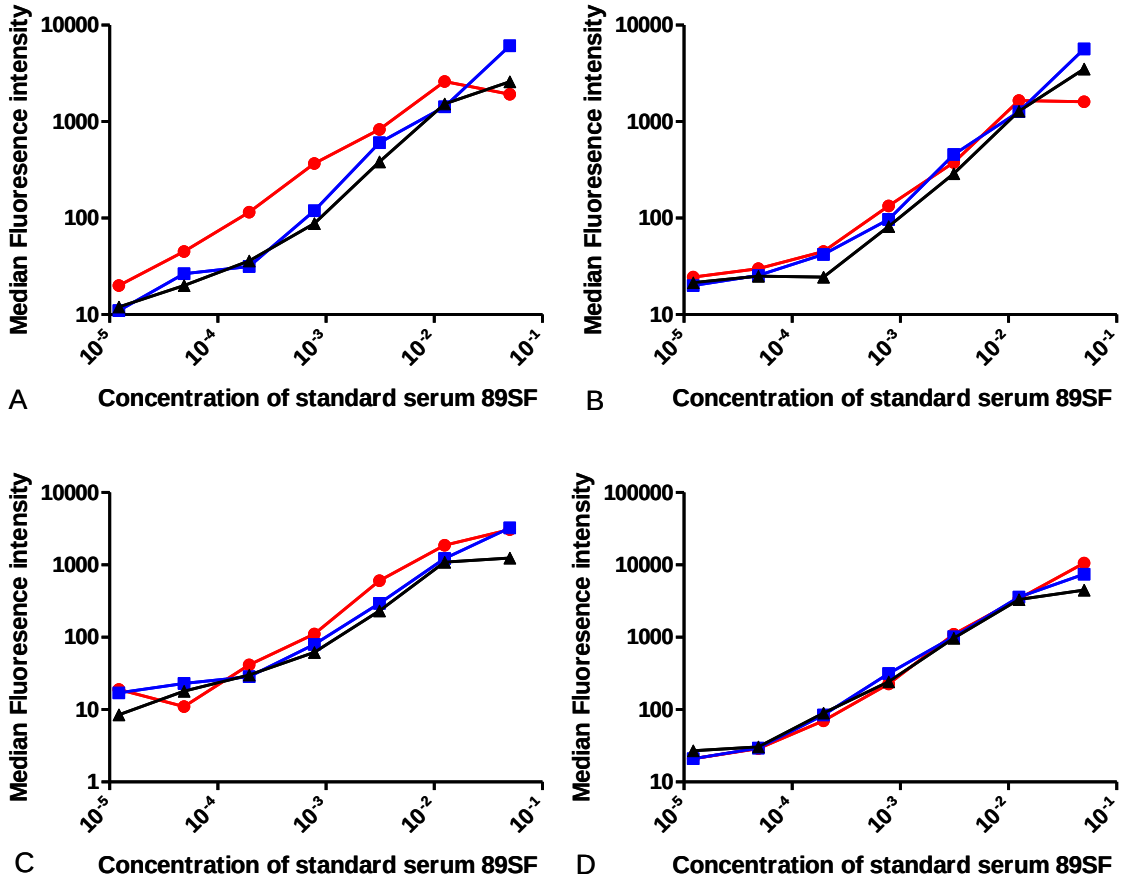

Figure 4-5 shows the effect of varying pre-absorption conditions on subsequent performance of IgG anti-PnCP antibody assays.

Panels A, and B: show the consequences of varying preabsorbing CWPS concentration. (No polysaccharide 22F was used). Red line – no CPS, Blue line – 0.5 µg/ml CWPS, black line – 2 µg/ml CWPS. Panel A – measuring antibody to PnCP-19f; panel B – measuring antibody to PnCP-23.

Panels C, and D: consequences of varying preabsorbing concentration of PnCP- 22f. (CWPS concentration kept constant at 2µg/ml). Red line – no PnCP22f, blue line – 2 µg/ml PnCP22f , black line – 5 µg/ml PnCP-22f. Panel C – measuring antibody to PnCP-1; panel D – measuring antibody to PnCP-14.

4.7 Specificity of anti-PnCP antibodies measured by multiplex assay.

The specificity of IgG and IgM antibodies measured in each multiplexed assay was then tested by separately pre-incubating eighty-fold dilutions of standard serum 89SF with excess amounts (2.5 μg/ml) of each test antigen in addition to standard pre-absorbents CPS (2 μg/ml) and PnCP-22f (5 μg/ml). Assay results for these antibody-depleted samples were compared with a standard curve from the same serum. This process was also subsequently used to confirm successful bead-antigen conjugations when preparing more assay reagents.

Pre-assay depletions resulted in mean reductions in the measured level of all corresponding IgG antibody specificities - ranging from 15 fold (PnCP-19f), to over 300 fold (for PnCP-14) (Figure 4-6, Figure 4-7, and Figure 4-8). Across all tested combinations of depleting-antigen and subsequently measured PnCP-specific IgG, the average inter-PnCP effect was an 18% reduction in measured specific IgG titre. The greatest inter-specificity effect was seen with pre-incubation with 2.5 μg/ml PnCP-1, which caused an average 41% reduction in IgG against PnCP-9v, but greater than 95% reduction in measured IgG anti-PnCP-1.

The effect of preabsorption on levels of IgM, specific for the same or other PnCPs, was tested once, in a similar manner, for each depleting PnCP (Figure 4-6, Figure 4-7, and Figure 4-8). Although depletion of the corresponding antibody was generally less, qualitatively analogous findings regarding test specificity were seen. It was concluded

that the assays were sufficiently independent during multiplexing that test sera could be measured in this manner.

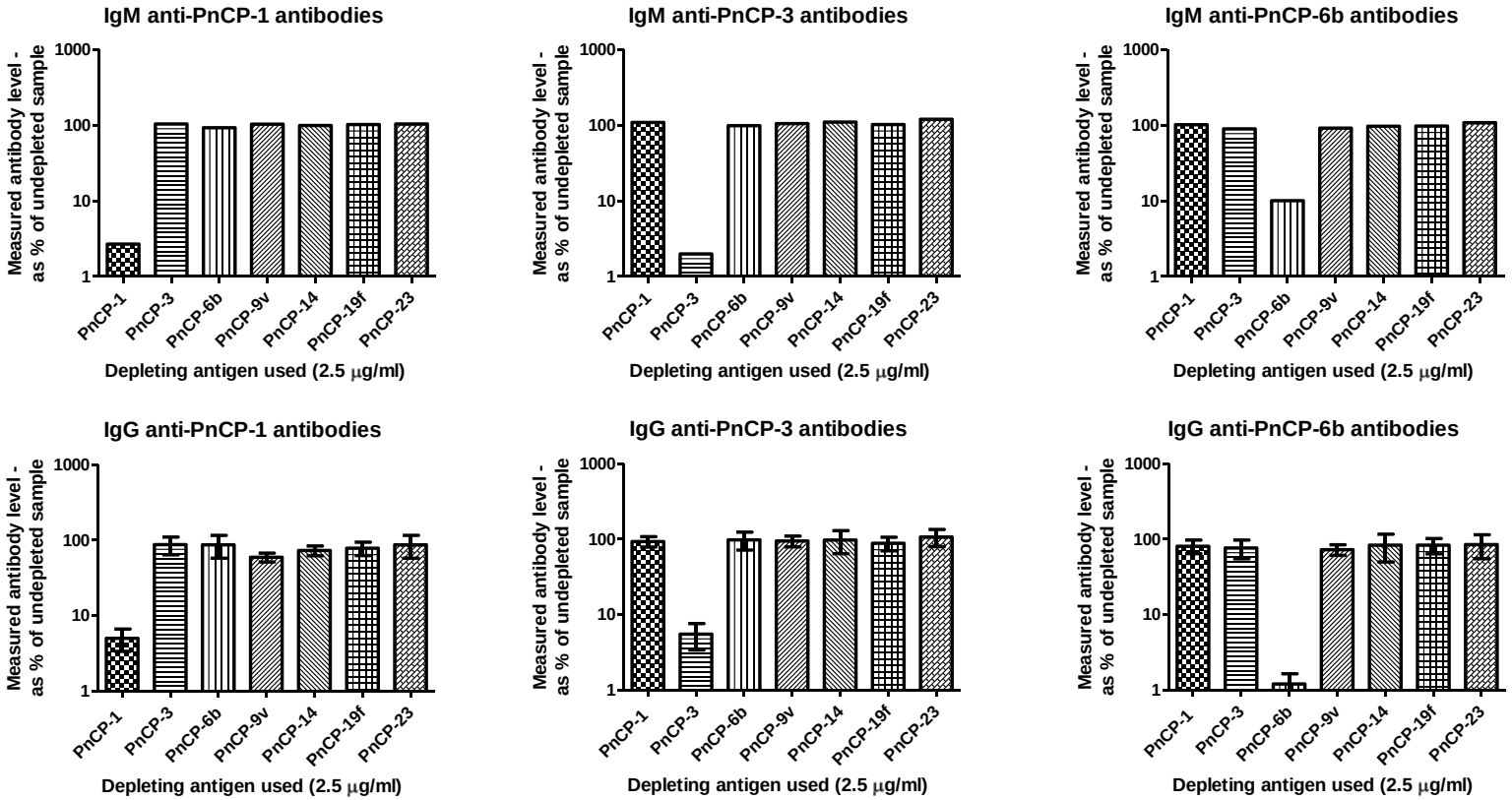

Figure 4-6 shows selective depletion of IgM and IgG serotype specific anti-pneumococcal capsular polysaccharide antibodies by excess antigen (serotypes 1, 3, and 6b).

Preabsorption of an 80 fold dilution of standard serum 89-SF with single PnCP specificities (at 2.5μg/ml) in addition to CWPS (2μg/ml) and PnCP-22f (5μg/ml) resulted in substantial depletion of serotype specific antibodies and modest or minimal depletion of other antibody specificities. Upper panels – one experiment measuring specific IgM titres after depletions. Lower panels – mean ± SD of 6 separate experiments to measure specific IgG titres; each experiment used separately prepared bead sets.

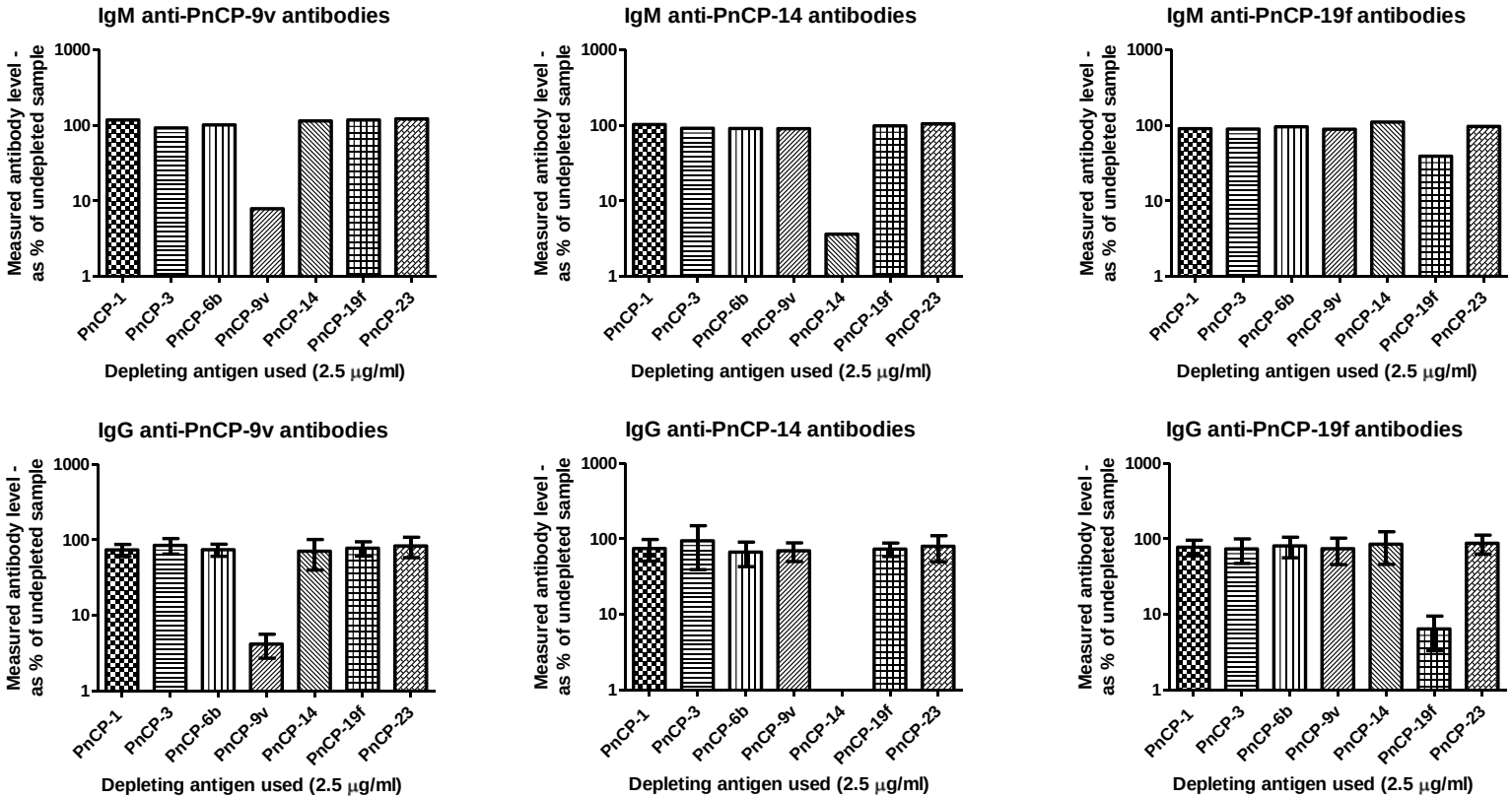

Figure 4-7 shows selective depletion of IgM and IgG serotype specific anti-PnCP antibodies by excess antigen (serotypes 9v, 14, and 19f).
Preabsorption of an 80 fold dilution of the standard serum 89-SF with single PnCP specificities (at 2.5 μg/ml) in addition to CWPS (2 μg/ml) and PnCP-22f (5 μg/ml) resulted in substantial depletion of serotype specific antibodies and modest or minimal depletion of other antibody specificities. Upper panels – one experiment measuring specific IgM titres after depletions. Lower panels – mean ± SD of 6 separate experiments to measure specific IgG titres; each experiment used separately prepared bead sets.

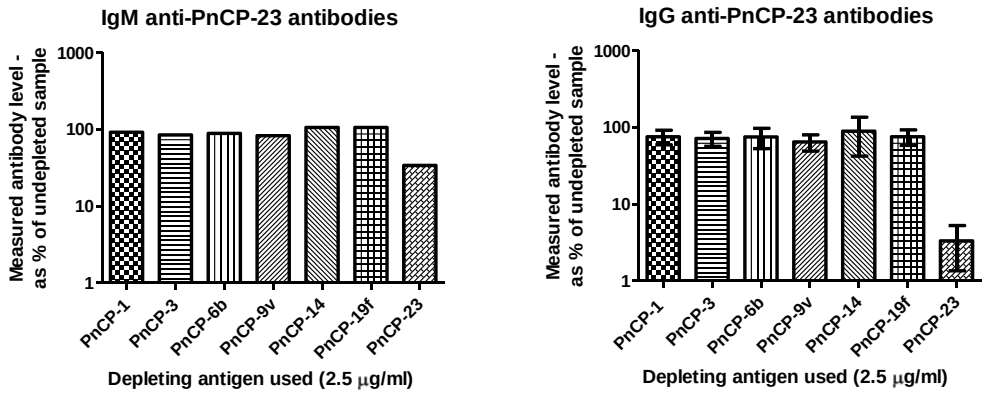

Figure 4-8 shows selective depletion of IgM and IgG serotype specific anti-PnCP antibodies by excess antigen (PnCP-23).
Preabsorption of an 80 fold dilution of the standard serum 89-SF with single PnCP specificities (at 2.5μg/ml) in addition to CWPS (2μg/ml) and PnCP-22f (5μg/ml) resulted in substantial depletion of serotype specific antibodies and modest or minimal depletion of other antibody specificities. Left panel – one experiment measuring specific IgM titres after depletions. Right panel – mean ± SD of 6 separate experiments to measure specific IgG titres; each experiment used separately prepared bead sets.

4.8 The human antibody response to phosphorylcholine does not fully reflect the response to Pneumococcal Cell Wall Polysaccharide.

It was also intended to establish assays for natural antibodies taken to be representative of the B1 cell repertoire (see section 2.5.2). So, based on published research in the mouse immune response [100], I sought to establish microsphere based assays for phosphorylcholine (PC), the proposed antigenic determinant of CWPS [200-202].

Antigens (either CWPS, or BSA-conjugated Phosphorylcholine) were conjugated to microspheres as described previously (see section 3.2.5.1). Assay specificities were tested by pre-absorption of 100-fold dilutions of standard serum with either reagent at concentrations of 2.5μg/ml, and 10μg/ml, without the addition of PnCP 22f (see Figure 4-9).

Depletion testing of the conjugated beads, with the identical antigen was consistent with successful conjugation of antigen to the relevant beads, though prozone phenomena were also seen on serial dilutions. Pre-absorption with 2.5 and 10 μg/ml PC-BSA reduced measured IgM anti-CWPS by 5-10 fold (median of 3 experiments), approximately comparable to its effect on IgM anti-PC Abs (10 fold reduction for each concentration, in the same experiment). In contrast pre-absorption with 2.5 and 10μg/ml CWPS resulted in greater depletion of measured IgM anti-CWPS titres, but less fall in measured IgM anti-PC levels.

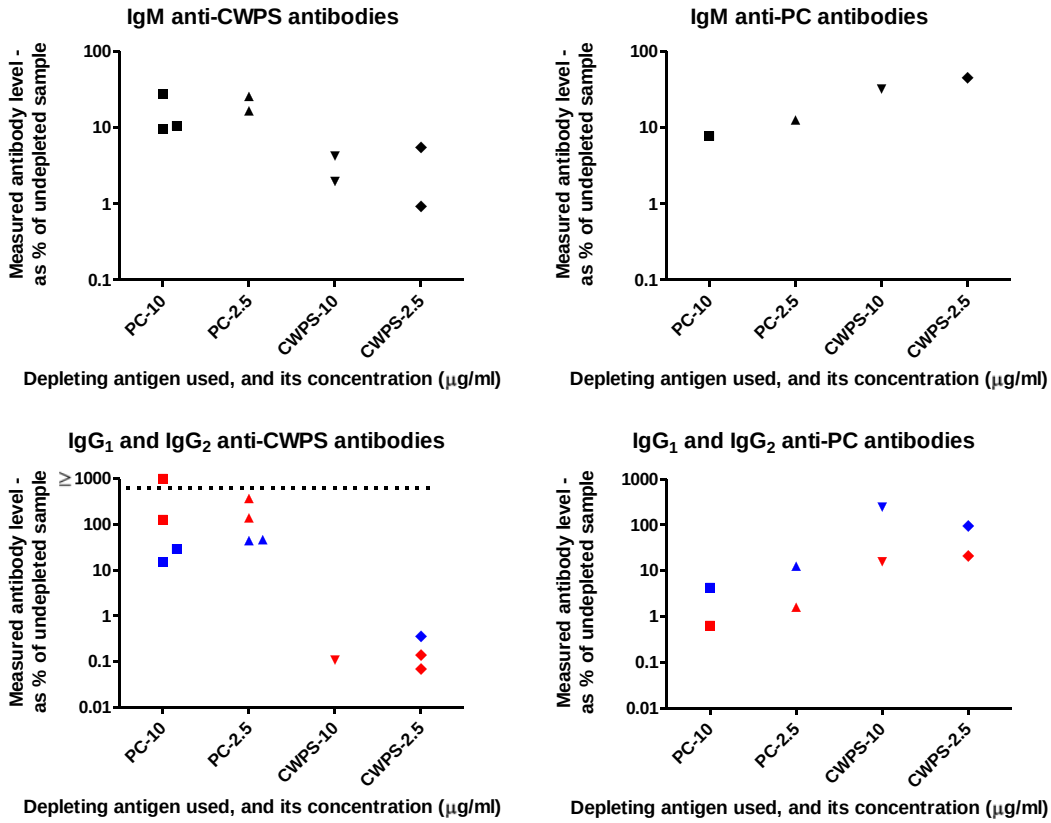

Figure 4-9 shows cross depletion testing of assays for IgM, IgG1, and IgG2 against phosphorylcholine (PC) and Cell wall polysaccharide (CWPS).
Pre-absorption of a one-hundred fold dilution of standard serum 89-SF with either PC, or CWPS resulted in depletion of the relevant IgM antibody specificity, but incomplete cross depletion (upper panel). Lower panel demonstrates comparable experiments for IgG_1 (blue) and IgG_2 (red); partial cross-specificity depletion was seen when measuring IgG_1 against CWPS and against PC, but measured levels of IgG_2 anti-CWPS increased after pre-absorption with PC. Duplicated symbols, where present, indicate results from separate experiments.

When testing the effect of depletions on specific IgG_1 levels, a comparable pattern was seen, except that pre-absorption with 2.5 μg/ml CWPS had minimal effect on IgG_1 anti-PC, whilst pre-absorption with 10 μg/ml appeared to increase measured levels of IgG_1. Replication of this experiment was not attempted, but it had been performed in parallel with the analogous experiment for IgM anti-PC, and one replicate of the tested anti-CWPS responses, using the same reagents for pre-absorption.

Further complexity was seen when studying IgG_2 responses to these antigens (Figure 4-9). Levels of IgG_2 anti-PC, and IgG_2 anti-CWPS were both depleted by pre-absorption with their corresponding antigen, but measured levels of IgG_2 against CWPS were raised by pre-absorption with both concentrations of PC.

In summary, the evaluation of the assays for antibodies against PC and CWPS identified the following:

1. The presence of prozones within serial dilution testing.
2. Non-identical depletion patterns by the two antigens - when 2.5μg/ml CWPS and 10μg/ml PC should contain approximately equimolar amounts of phosphorylcholine moieties.
3. Discrepant results between different antibody subclasses tested for the same putative antigen.
4. A substantial augmentation of some measured antibody titres after certain pre-absorption conditions.

It was thus concluded that PC is not likely to be the immuno-dominant epitope in all isotypes of the human response to CWPS, and so responses to both antigens should be

tested in subsequent experimental samples from patients. Nevertheless, sufficient evidence of cross-reactivity between the antibody specificities was obtained to preclude secure multiplexing of the two assays, and so subsequent testing of these two responses was performed separately.

4.9 Testing of anti-tetanus toxoid antibodies by microsphere assay.

The performance of microspheres coated with tetanus-toxoid was also tested by depletion assays. At the antigen concentration chosen for pre-absorption (2.5 μg/ml) measured IgG anti-tetanus toxoid in the pneumococcal standard serum 89-SF was reduced approximately 4 fold. In subsequent multiplex testing, pre-absorption with 2.5 μg/ml tetanus toxoid had minimal effects on measured levels of IgG against the 7 PnCP, and IgG anti-CWPS (data not shown), and *vice-versa*. It was concluded that anti-tetanus toxoid antibodies could be multiplexed with assays of anti-PnCP antibodies (in the presence of preabsorption with CWPS and PnCP-22f) or with an assay of anti-CWPS antibody.

4.10 Discussion.

This work, performed early in my MRC clinical training fellowship, sough to establish and validate the subsequent use of microsphere based assays for analysis of isotype specific antibodies to various PnCP, to CPS, PC, and to tetanus toxoid, and to perform them multiplex where possible.

The various experiments performed demonstrated satisfactory conditions for antigen-bead conjugation, and that antigenic epitopes within reagents appear to be maintained

after the chemical conjugation to Poly-L-lysine (where necessary), and subsequent conjugation to the microspheres themselves.

Ensuring the presence of excess antigen during conjugation reactions (Figure 4-3), and optimal preabsorption conditions (with CPS and PnCP-22f) before performing assays (Figure 4-5) minimised the presence of predicted prozone phenomena, but did not completely prevent them. It was thus decided that during the subsequent testing of multiple experimental sera (chapter 5), serial dilutions should be performed for all samples instead of using single dilutions of test sera to be compared with a standard curve.

In contrast, and despite theoretical concerns, extensive cross testing of reagents confirmed that there was remarkably little impact on anti-PnCP assay performance when performed in the presence of other bead specificities, thus such multiplexed assays were used for work described elsewhere in this thesis. Nevertheless, it was notable that during PnCP depletion testing, serotype specific IgM titres appeared to fall less than corresponding IgG titres (Figure 4-6, Figure 4-7, Figure 4-8). This is not due to the relative amounts of serotype specific IgM and IgG in the standard serum [203]. An explanation is offered by a recent publication by Baxendale et al [204] which studied several human IgM antibodies, produced by hybridomas derived from vaccinated volunteers. These antibodies had titratable anti-PnCP activity in a microsphere-based assay. In keeping with the findings reported in this thesis chapter, Baxendale et al demonstrated the limited sensitivity of their hybridoma-antibodies to depletion by excess PnCP, CWPS, or PC, but demonstrated additional poly-reactivity with other antigens including self antigens. Molecular analysis of the hybridomas demonstrated minimal

deviation from immunoglobulin V, D, and J germline sequences. Based on these findings they conclude these are likely to be natural antibody specificities produced by cells of the B-1 cell like lineage. They do not report the presence, or absence, of such polyreactive species within the IgM fraction of standard serum 89-SF, but if present, they could account for the findings shown here (in Figure 4-6, Figure 4-7, and Figure 4-8). Importantly, analogous work in isotype-switched, antibody responses to PnCPs do not seem derived from the same lineages [205;206].

As reported above, general opinion based on published literature from mouse studies [200-202] holds that PC is the immunodominant epitope in responses to CWPS. However experiments reported here using pooled human serum demonstrated complex and mutually-discrepant effects of pre-absorption with either reagent. The findings (Figure 4-9) are not consistent with the simple concept that PC is the immunodominant epitope to human CWPS responses. The published literature includes a report of similar findings, with additional variability between individual subjects, when using ELISA based assays of human sera [207]. Determining the true specificity, relative quantity, and affinity, of these antibodies was beyond the needs of this work as regards the development of the assays, but it serves to highlight the complexity of interactions underlying microsphere based assays (and ELISAs) and their vulnerability to effects arising from cross-reactive antibodies. It was not formally tested whether such interactions are greater in the context of multiplexing assays of antibody against CWPS and PC, but it was concluded that for subsequent assays of patient sera, these antibodies should be measured separately.

4.11 Future work.

The University of Birmingham Clinical Immunology service have expressed interest in further developing the PnCP antibody assays for clinical use, as at present the standard (semi-automated) pneumococcal antibody assay only measures bulk isotype-specific responses to a mixture of serotypes. The protocols developed during this work have been passed on to the clinical lab, but further work is likely to be needed before this assay can be offered for clinical use. Their parsimonious use of serum makes them suitable for studies where only small samples are available, for instance from infants.

In the setting of a clinical laboratory the ability to use point dilutions of test samples would be of great value, and the need to confirm the accuracy and precision of absolute measurements of antibody is essential. This is likely to involve further work to minimise, or control for, prozone phenomena, and validation with QC sera (available from NIBSC) would be required. All the serotypes chosen for this work are amongst those in Pneumovax II - the 23 valent polysaccharide vaccine, and include some but not all those in the 7 valent conjugate pneumococcal vaccine Prevnar, and it may be desirable to widen the assay repertoire accordingly. It is reasonable to speculate that other pneumococcal antigens could be conjugated to microspheres in a similar fashion, but the testing required to exclude significant cross reactivity would increase exponentially.

The recent paper by Baxendale et al [204] indicates that polyreactive IgM antibody produced after pneumococcal vaccination (and thus likely also to be produced after infection) can be detected by apparently serotype-specific microsphere based assays (and ELISAs) when configured to measure IgM antibody. Whilst it may yet be determined that the level of such ‘natural antibody’ proves to be the best measurable human correlate of

protection against pneumococal infection, its potential presence in serum samples has implications for the correct interpretation of apparently serotype specific anti-PnCP IgM assay results. This is especially so in clinically important settings where the proportion of 'natural antibody' may be increased, such as lymphoid malignancy [208], the response to microbial antigens [204;209], autoimmunity [210] or ageing [211]. Thus the ability to accurately determine amounts, in serum samples, of IgM that is truly specific for particular PnCP serotypes would appear to require further work to clarify this complex area.

5 AUTOANTIBODIES, UNLIKE ANTIBODIES TO ALL EXTRINSIC ANTIGEN GROUPS, FALL FOLLOWING B CELL DEPLETION WITH RITUXIMAB

5.1 Introduction.

Rituximab causes profound depletion of B cells, which express CD20, from blood and tissues [2]. It has been used successfully to treat a number of autoimmune diseases. Significant falls in disease-associated IgG and IgM autoantibody levels are often seen [3;6;12;212] although this does not always happen [22;23].

Autoantibodies against the neutrophil serine protease, proteinase-3 (PR3), are encoded by immunoglobulin V region genes that have acquired somatic mutations [24]. These findings are consistent with the autoantibodies being produced by plasma cells whose precursors have undergone affinity maturation through hypermutation of their immunoglobulin V-region genes and selection in GC [44], although immunoglobulin V-region mutations can be acquired without GC [77;78]. Plasma cells derived from GC in the spleen and peripheral LN against protein-based antigens, reside in the bone marrow, have the capacity to be very long lived, and typically do not express CD20 [58;59]. Nevertheless, as immunoglobulin levels are remarkably constant in adults [155] and responses giving persistent antibody levels to new antigens can be induced throughout life there must be some turnover of long-lived plasma cells. It is possible that if the production of new plasma cells is blocked, for example by B cell depletion with Rituximab, this turnover would cease and existing plasma cells would persist indefinitely.

Levels of affinity matured antibody against tetanus toxoid remain unchanged after B cell depletion by Rituximab [3] and falls in serum immunoglobulins are generally modest,

although falls in IgM have been seen after repeated cycles of treatment [192]. As levels of IgG autoantibodies fall following B cell depletion, we set out to test if this was attributable to them being produced by a population of intrinsically short-lived AFC.

Certain types of antigen seem to induce only extrafollicular antibody responses and many of the antibody forming cells produced in these responses are short-lived [74;75]. These antigens include those based on pure polysaccharides and lipopolysaccharides that are not able to complete the CD4 T cell-dependent selection process required for plasma cells to differentiate from GC B cells [44]. In addition, B1 cells produce extrafollicular antibody responses, but probably do not form GC [46].

B cell depletion by Rituximab allows the opportunity to investigate whether cells that maintain chronic antibody production after an extra-follicular response to antigen can be long-lived in the absence of B cell precursors. In this study these findings are directly compared to concurrent antibody production against T-dependent extrinsic antigens, and the autoantigen PR3. Such comparisons inform our understanding of why autoantibodies often fall after B cell depletion therapy.

5.2 B cell depletion, clinical responses and autoantibody level changes associated with Rituximab.

A criterion for treatment with Rituximab has been that patients should have active disease. This is shown by their pretreatment BVAS [17]. Following Rituximab 7 of the 11 patients were in clinical remission within 1 month and all patients were in remission by 5 months (Figure 5-1, top left). As observed by others [3;213;214], the number of $CD19^+$ lymphocytes in peripheral blood fell to undetectable levels within 2 weeks (all

patients) and remained depleted in 10 of 11 patients throughout the five-month observation period (Figure 5-1, top right). In one patient, a very low level of $CD19^+$ cells was detected 5 months after Rituximab but not on retesting one month later.

IgG anti-PR3 levels fell progressively in most patients, though in two patients little change in autoantibody titre was seen during the 4-5 month period studied. (Figure 5-1, bottom right). In two other patients titres became undetectable 2 weeks after treatment and remained so through 4-5 months. A further two patients' autoantibody titres became undetectable after 4-5 months. Clinical response characteristically antedated the fall in anti-PR3 levels.

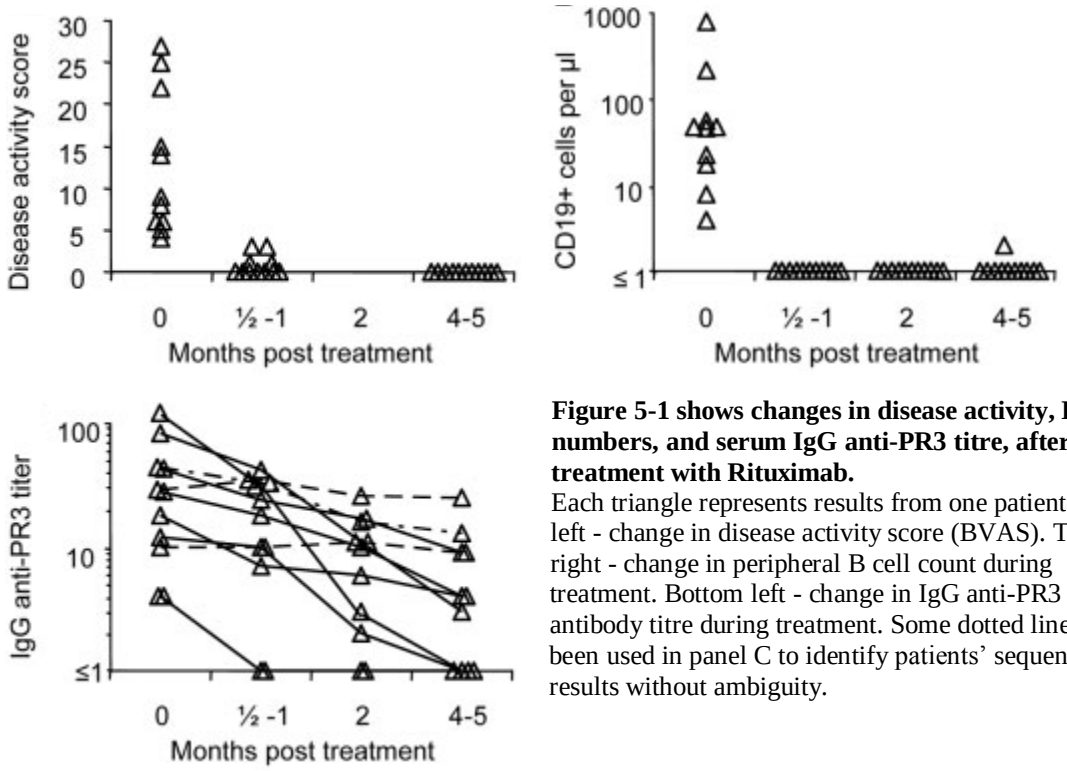

Figure 5-1 shows changes in disease activity, B cell numbers, and serum IgG anti-PR3 titre, after treatment with Rituximab.
Each triangle represents results from one patient. Top left - change in disease activity score (BVAS). Top right - change in peripheral B cell count during treatment. Bottom left - change in IgG anti-PR3 antibody titre during treatment. Some dotted lines have been used in panel C to identify patients' sequential results without ambiguity.

5.3 Resistance of serum antibody titres against extrinsic antigens to depletion by Rituximab.

The fall in anti-PR3 levels induced by Rituximab were not reflected by a parallel fall in antibody levels to different classes of antigen, including those that do not induce productive GC. Responses putatively induced from MZ B cells, B1 cells or both of these, were assessed by measuring antibody titres to PnCP 1, 3, 6b, 9v, 14, 19, and 23f, as well as PC and CWPS. PnCP 3 and CWPS evoke responses in the first year of life, perhaps from B1 cells. Other serotypes, including PnCP 1, 6, 14, and 23 produce responses later in infancy [102] and are candidate responses of MZ B cells; the antibody response to a purified PnCP serotype vaccine does not induce responses that are associated with affinity maturation [215]. Natural IgM antibody against A and B blood group antigens [103] were also measured. Finally, antibody against tetanus toxoid and EBV-CA – responses in which other studies have demonstrated affinity maturation [216-218] – were used as exemplars of TD responses with plasma cells arising GC.

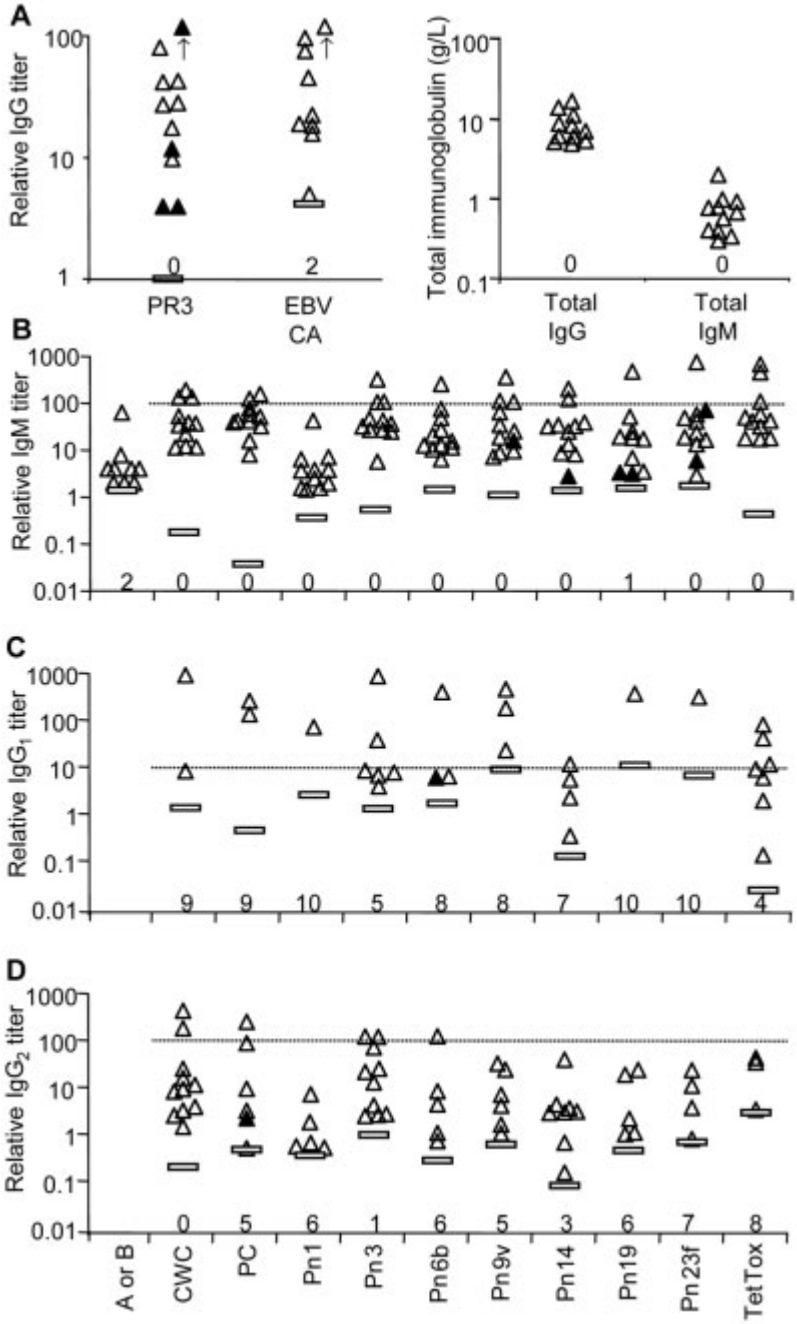

Figure 5-2 shows absolute levels of IgM and IgG, and relative titres of antibodies that are specific for either Proteinase 3 or one of a range of entrinsic antigens, in sera of patients about to receive treatment with Rituximab.
Panel **A** shows relative titres of IgG anti-Proteinase 3, and IgG anti-EBV CA, and the absolute serum levels of total IgM and IgG. Panels **B, C, and D** respectively show the serum titres of IgM, IgG_1 and IgG_2 specific for various extrinsic antigens, relative to the titre in pneumococcal standard serum 89SF (dotted line).Each △ represents a pre-treatment serum antibody titre in a patient for whom the same antibody was also detectable in the subsequent post-treatment sample. Each ▲ represents a pre-treatment serum antibody titre in a patient for whom the same antibody was not detectable in the subsequent post-treatment sample. ═ represent the lower limits of detection for each assay. In each panel, numbers just above the x axis report the number of patients in whom the relevant antibody could not be detected in serum prior to treatment.

Pre-treatment, relative antibody titres indicate that most patients had detectable IgM antibody for each antigenic specificity. Seven of eleven patients had IgG_1 against tetanus toxoid and each patient had IgG_2 against at least one PnCP other than PnCP 3. All had IgG_2 against CWPS (Figure 5-2). In striking contrast, $\log_{10}$ % change in titres for each antibody demonstrated that anti-PR3 antibodies are the exception, falling to a median of 22% of pre-treatment value in 4-5 months (Figure 5-3). IgM titres against all extrinsic antigens fell to medians around 70% of starting values (medians 83 to 40%). Comparable changes were seen in total serum IgM (median fall to 55% of original value). IgG titres against extrinsic antigens typically remained unchanged; only IgG_2 antibodies against PC fell to a median of 70% of the starting value. Analogous results were obtained for total serum IgG (median fall to 70% of original value). IgM antibody titres to A and B blood group antigens typically remained unchanged.

The percentage change in IgG anti-PR3 levels was significantly different to the changes in IgG_2 titres against all PnCP ($p<0.05$ for each comparison) and in IgG_2 against CWPS ($p<0.05$). Changes in levels of IgG anti-PR3 were also significantly different to those in IgG against EBV-CA and IgG_1 against tetanus toxoid (both $p<0.05$), and significantly different to changes in IgM against CWPS, and changes in IgM isohemagglutinins (both $p<0.05$). The differences between the changes in IgG anti-PR3 and that in IgM against PC ($p=0.08$) were not significant.

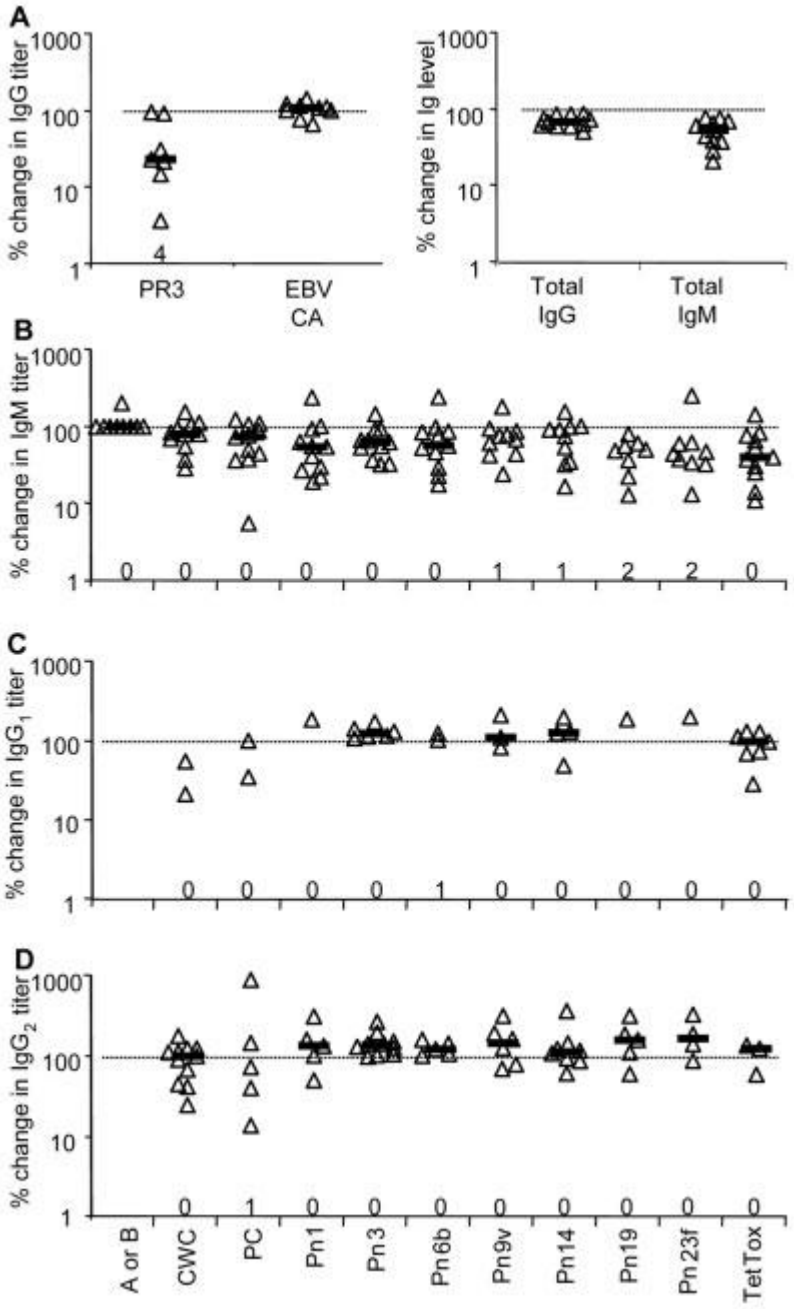

Figure 5-3 shows that patients' serum titres of IgG anti-PR3 typically fall substantially in 4-5 months after treatment with Rituximab, whereas serum levels of IgM and IgG_1 and IgG_2 specific for various extreinisc antigens are generally preserved. It also demonstrates that most patients' total serum IgG and IgM levels are little changed after Rituximab. Panel **A** shows post treatment serum titres of IgG anti-Proteinase 3 and IgG anti-EBV CA and total serum IgM and total serum IgG, expressed as a percentage of the level in the corresponding pre-treatment sample. Panels **B, C, and D** respectively show post treatment serum titres of IgM and IgG_1 and IgG_2 specific for various extrinisic antibodies, also expressed as a percentage of the level in the corresponding pre-treatment sample. The dotted lines (at 100%) represent no change in titre during the intervening time. Each △ represents a result from a patient in whom both samples contained detectable antibody. Numbers along each x axis report the small number of patients whose antibody titres became undetectable after treatment. (The initial antibody titre of these patients and the lower limit of detection of the antibody are shown in Figure 5-2.) ▬ represent median % change (where ≥3 paired values are available and all patients with antibody at presentation retained a detectable antibody titre).

5.4 Discussion and future work.

The falls in circulating anti-PR3 autoantibody levels seen in patients treated with Rituximab in this study are consistent with findings of other groups treating patients with ANCA-associated vasculitis [212;219;220] or rheumatoid arthritis [221] with this agent. The relative insensitivity to Rituximab of levels of antibody against some extrinsic antigens has also been reported previously [3;13;221]. The current work extends this by studying in greater detail antibodies to a wider range of antigens that have been found to have a different cellular basis for antibody production in experimental animals. The observed fall in autoantibody titres contrasts markedly with the relative preservation of antibody levels against extrinsic antigens of each of the classes studied.

Although many AFC resulting from extrafollicular responses in lymph nodes (LN) and spleen are short lived, close examination indicates that this short lifespan is not intrinsic. Rather it relates to limited local stroma that supports long-term plasma cell survival. Those plasma cells that gain access to this stroma can survive for extended periods [60]. If, against this evidence, antibody from extrafollicular responses is produced exclusively by short-lived plasma cells, Rituximab therapy would be expected to cause a fall in titres of antibody against antigens, like PnCP, that exclusively provoke extrafollicular responses. In autoimmune disease, where antigen is virtually limitless, plasmablasts could contribute substantially to antibody production. Available evidence indicates that unsupported AFC die well within a week of their precursor B cells being triggered by antigen [60]. Thus even if maximal tissue depletion of B cells by Rituximab took up to 4 weeks, it is likely that no AFC would exist outside supportive niches 5 weeks after Rituximab administration. If this resulted in the cessation of all anti-PR3 production,

levels of this autoantibody would be expected to halve in 20 days – the serum half life of IgG [222]. Complexation with circulating autoantigen would probably accelerate loss of anti-PR3 from the circulation, making the fall in titre even faster. All studies reporting the kinetics of change in IgG autoantibody levels following Rituximab [13;219;221] indicate a gradual fall in autoantibody titre that is not consistent with this scenario. Similarly, if production of antibody against extrinsic antigens also ceased, measured levels of antigen-specific IgG would fall to around 6% of their starting values by 4-5 months after Rituximab. With a half-life of 5 days [222], IgM antibodies would go through at least 17 half lives before the time when titres were remeasured. No such fall in IgM antibody titres was observed in patients during our study. These considerations indicate that, following Rituximab, there must be substantial ongoing production of all antibodies tested, and it is consistent with a hypothesis that chronic antibody production is predominantly by cells that can be long-lived in the absence of competition from newly-formed plasma cells.

We do not know if Rituximab treatment depleted all plasma cell precursors in patients. The loss of blood B cells is impressive, but tissue studies could not be performed, for ethical reasons. Rituximab therapy has been reported to deplete B cells from the appendix [223], and the spleen [224]. Vos et al have reported a reduction in $CD22^+$ cells in rheumatoid synovium one month after treatment [225]. More recently we have reported that $CD20^+$ cells were detectable in diseased lung tissue removed from a patient with WG who was relapsing at a time when peripheral B cells remained undetectable - 13 months after prior Rituximab therapy [226]. Recall responses to antigen are impaired (but not abolished) during the period of post-Rituximab B cell depletion, consistent with an effect

on non-circulating memory B cells [67]. Two other studies have reported residual B cells in lymphoid tissue after Rituximab, but both used suboptimal depletion regimes [214;227].

Studies of anti-CD20 antibody therapy in mice with B cells that express human CD20, show some non-circulating B cells are spared from depletion [40]. It is speculative whether this reflects B cell depletion by Rituximab in humans, for efficacy of antibody-mediated effector mechanisms – complement, and cell damage by phagocytes and antibody-dependent NK cell cell-mediated cytotoxicity – differs in humans and mice.

Serotype specific antibody responses to natural pneumococcal infection can include production of plasma cells that have acquired somatic mutations in immunoglobulin V-region genes [205;228]. This is likely to result from pneumococcal cell protein being associated with capsular polysaccharide forming a natural conjugate antigen. This could have occurred in the PnCP antibody responses measured in our patients.

After the bulk of the work contained in this chapter was published [229], Baxendale et al [204] have reported findings that indicate caution may be warranted in interpreting IgM anti-PnCP titres derived from luminex based assays. This issue is discussed in greater depth in section 4.10 above. Importantly, these concerns do not appear to relate to the measurement of IgG anti-PnCP titres.

Notwithstanding these caveats, the preservation of antibody levels against all extrinsic antigens assessed makes it unlikely that selective anti-PR3 loss reflects a type of antibody response that is uniquely sensitive to Rituximab.

If neither variations in the expected half-lives of different antibodies, nor differences between particular antibody production pathways, can account for the differential sensitivity of autoantibody production to Rituximab, why do autoantibody titres fall after Rituximab? Such observations are most comfortably explained by treatment destroying niches in inflammatory tissues that selectively support the survival of autoantibody secreting cells. 'Inflammatory' plasma cell niches may have biological value in the response to infection by linking the duration of antibody production to the duration of injury.

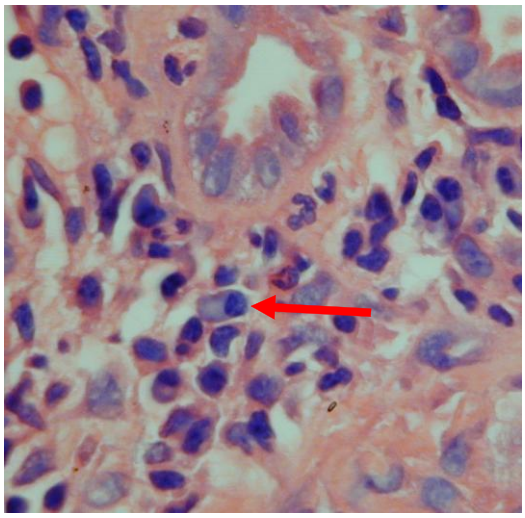

Figure 5-4 shows a plasma cell present in the renal interstitium of a patient with ANCA-associated renal vasculitis.
Photo courtesy of Dr Desley Neil, University of Birmingham. © European Journal of Immunology. 2008.

Plasma cells are present at inflamed sites in ANCA-associated vasculitis [49] (see also Figure 5-4), rheumatoid arthritis [53;230], lupus [231] and animal models of lupus [232;233]. Plasma cells are also reported in human kidney allografts [234] and liver allografts [235] that are undergoing rejection.

Furthermore, some reports indicate that a disproportionate number of plasma cells at these sites produce disease related autoantibodies [230;233]. Interestingly a recent publication reports that even where local lymphoid neogenesis occurs in inflamed tissue,

nearby plasma cells do not appear clonally related [53]. This implies that plasma cells migrate there from secondary lymphoid organs. Ectopic antibody production may not be confined to autoimmune inflammation, for AFC have been identified in inflammation associated with osteoarthritis, a disease that probably does not have an autoimmune aetiology [236].

Our hypothesis predicts that the plasma cells producing IgG anti-PR3 might have chemokine receptors and cell adhesion molecules that allow them to home to and adhere to stroma in inflammatory sites. Some appropriate chemokine ligands – CXCL9 and CXCL12 - have already been reported in other inflamed tissue [141;237].

The molecules present on autoantibody-producing plasma cells may differ from those that lead plasma cells in healthy subjects to find stroma in the bone marrow that sustains their survival. For example in mice there is evidence that AFC that express CXCR3 are attracted to chemokines produced in inflamed tissue [14]. Such differences, if confirmed, could have potential implications for the rational design of new therapeutic agents for use in autoimmune disease.

6 CUCKOO PLASMA CELLS IN INFLAMMATION

6.1 Introduction.

Chapter 5 reported the finding that serum levels of human autoantibodies fall after B cell depletion by Rituximab. This fall occurs despite preservation of levels of extrinsic antibodies representative of all known pathways of antibody production. The differential loss of autoantibody is consistent with the hypothesis that plasma cells can be sustained in additional niches intrinsically related to autoimmune inflammation. Upon resolution of inflammation, the related plasma cell population would be expected to wane, resulting in a selective fall of autoantibody levels.

There is no satisfactory animal model for the autoimmune nature of ANCA-associated vasculitis [21]. We therefore sought to test this hypothesis in a wider context – whether additional plasma cells could be sustained by 'newly-induced inflammatory niches', even if the immune response generating the plasma cells was unrelated to cause of the inflammation. Furthermore we sought to understand the mechanisms for retaining plasma cells in such a site, and the way these sites maintain plasma cell survival.

To this end, we combined two animal models that have been well characterised in our research laboratory:

1. The T-independent response to NP conjugated to the neutral polysaccharide Ficoll in QMxB6 mice. In these mice around 5% of the B cells carry a heavy chain transgene that renders them NP-specific. Massive numbers of red-pulp splenic plasmablasts are produced by 4 days after immunization with NP-Ficoll, but by 6 days over 95% of these cells have undergone apoptosis. Nevertheless, most of the

small proportion of plasmablasts that survive and differentiate into plasmablasts survive for more than 2 weeks. It was noted that after immunizing with a variety of antigens the number of red pulp antibody secreting cells sustained longer term is relatively stable, and consistent between models. The findings have been interpreted as evidence for an inherent limit on long-lived plasma cell numbers due to a finite number of supportive niches [60]. By using mice with transgenic NP-specific B cells massively more NP-specific plasma cells are produced in response to NP-Ficoll than can find niches that can secure their long term survival. QM mice are transgenic for a heavy chain that, when combined with any lambda light chain, confers NP-specificity on resultant immunoglobulins [123]. Of the 5% of the B cells in QM x B6 F1 hybrid (QMxB6) mice are NP-specific a high proportion are located in the marginal zone. As mentioned above, after immunizing these mice with NP-Ficoll there is a massive extrafollicular antibody response and 4 days after immunization the red pulp is crammed with NP-specific plasmablasts [128]. It is postulated that a lack of niches to sustain the survival results in the demise of >95% of the NP-specific antibody forming cells (AFC) on the 5^{th} day after immunization. It is also hypothesized that the scattered islands of AFC that remain in the red-pulp after this time are sustained by special plasma cell-sustaining microenvironments [60].

2. The response to attenuated *Salmonella enterica* serovar Typhimurium (*S.* Typhimurium). This infection induces a large number of AFC in the splenic red pulp and plasma cells can be seen in this site for weeks after immunization [57]. Intra-peritoneal infection of C57/B6 mice with 10^5 live organisms induces a

complex immune response, associated with splenomegally. Induction of the impressive early and sustained extrafollicular response is T independent, though the isotype switched response is a T dependent process. No germinal centres are induced in this response until the 4th week when the infection has largely cleared [57]. The important point, for our combined model, is that many of the AFC in the red pulp and extrafollicular foci persist through the first three weeks of infection [57]. The great majority of the AFC in the 3rd week from infection are mature (non-dividing) plasma cells. It is postulated that the infection induces a major increase in the number of niches that can secure plasma cell survival.

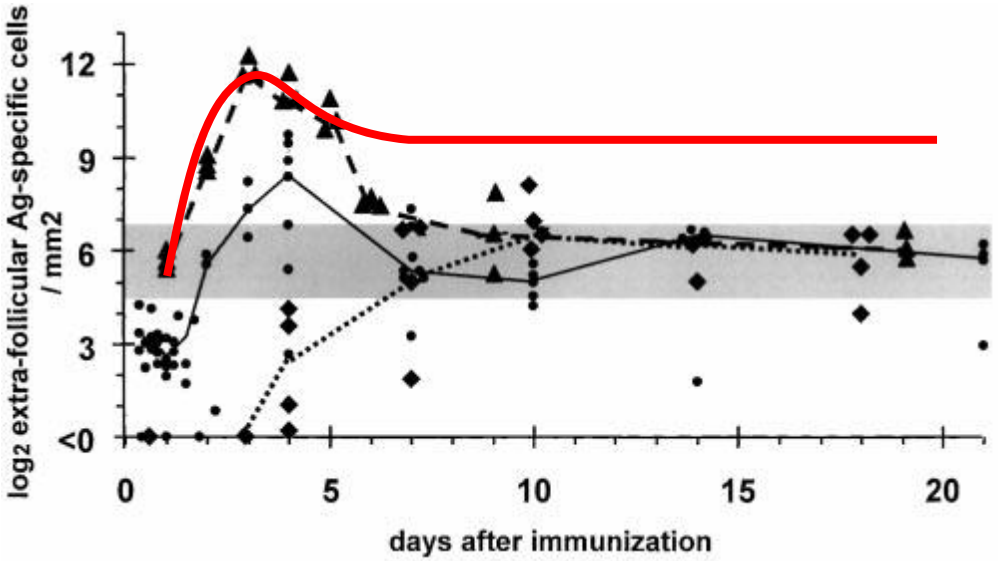

Figure 6-1 shows a schematic indication of the hypothesis that splenic inflammation results in increased numbers of sites that can sustain antibody forming cells beyond 6 days after immunization with NP-Ficoll.
This Figure modified from Sze et al (2000) [60] shows that peak AFC numbers in mouse spleen relate to the number of antigen-specific precursor B cells, but that the proportion of AFC sustained after 6 days is similar whatever the peak number of AFC produced. The black dashed line shows the AFC numbers in QM mice following immunization with NP-Ficoll. We postulated that NP-specific AFC survival might be more like the red curve if QMxB6 mice were infected with *S.* Typhimurium at the time they were immunized with NP-Ficoll, due to the increase in AFC-sustaining niches induced by the infection.

QMxB6 mice that have been infected with 10^5 live *S.* Typhimurium intra-peritoneally develop new AFC-sustaining niches in the red pulp. We hypothesised that if mice were immunized with 30 μg NP-Ficoll at the time of infection a proportion of the AFC

occupying the infection-induced niches would be NP-specific and NP-specific antibody titres would be higher than in control immunized but non-infected mice (Figure 6-1). In this scenario an increased proportion of the NP-specific AFC produced would survive past the first week after immunization. This has been a collaborative laboratory project involving several people, and a range of techniques. The division of work amongst members of the research group is summarised in Table 6-1.

	Dr Alastair Ferraro (PhD student)	Ms Jenny Marshall (PhD student)	Dr Elodie Mohr (Post-doctoral researcher)	Ms Saeeda Bobat (PhD student)
Immunizations, harvesting spleens and blood		✓		
Flow cytometric analyses of cell suspensions from spleens		✓	✓	
Quantification of serum antibody levels	✓			
Immunohistochemistry	✓	✓		
Cell counting from sections	✓			
Confocal microscopy	✓		✓	
RT-PCR analysis of bulk tissues			✓	
Microdissection and real-time RT-PCR of AFC-associated and control tissues	✓			
Culturing and quantification of attenuated *S.* Typhimurium				✓

Table 6-1 shows the division of laboratory work reported in this chapter.

6.2 Splenomegally induced in QMxB6 mice infected with *S.* Typhimurium.

As expected from published work, mice infected with *S.* Typhimurium developed splenomegally. This was generally seen by day 4 post immunization, was universal at day 8, and was somewhat reduced at day 35 (Figure 6-2). Additional co-immunization with NP-Ficoll had little effect on the development of splenomegally and immunization with NP-Ficoll alone did not induce splenomegally.

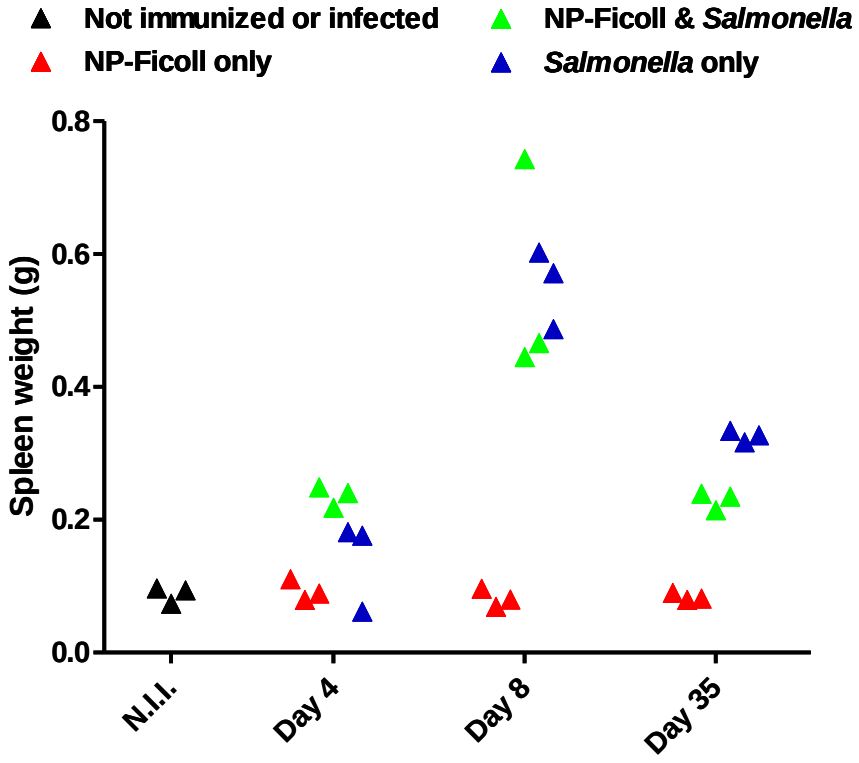

Figure 6-2 shows splenic weight increases following infection of QMxB6 mice with *S.* Typhimurium. Each symbol shows values from one mouse. The legend for the symbols is above the figure.

6.3 Infection with *S.* Typhimurium prolongs the serum IgM response to NP that follows immunization of QMxB6 mice with NP-Ficoll.

As previously reported for QMxB6 mice immunized with NP-Ficoll there is a 45 fold rise in the median IgM anti-NP antibody titre by 4 days after immunization. Strikingly this titre has already started to fall by day 8 (Figure 6-3). At four days after immunization and co-infection titres were if anything higher than in mice receiving only NP-Ficoll. In contrast to the non-infected mice the IgM titres in immunized and infected mice were sustained at day 8, and still higher than in non-infected animals at day 35. Thus on the basis of the serum IgM anti-NP titres co-infection with *S.* Typhimurium significantly augments the durability of the AFC response to NP-Ficoll. The next section probes the cellular basis for this difference. Interestingly the group of mice infected with *S.* Typhimurium without NP-Ficoll showed significant rises in IgM anti-NP titres.

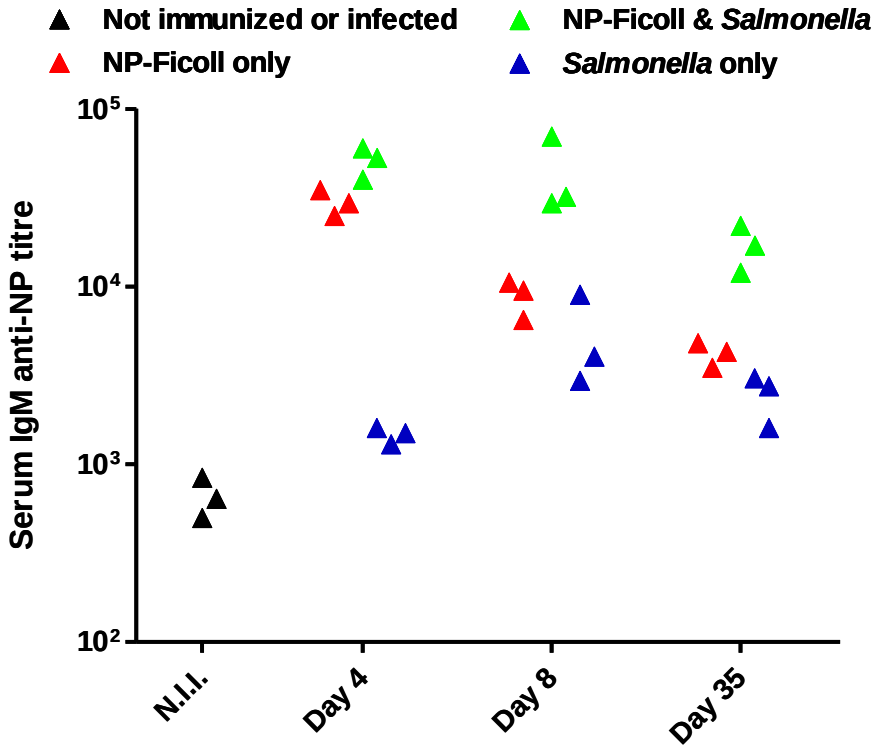

Figure 6-3 shows a graph of changes in IgM anti-NP titre in QMxB6 mice after immunization with NP-Ficoll, infection with *S.* Typhimurium, or both, which shows prolonged elevation of IgM anti-NP titre after immunization in the context of co-infection. Each symbol shows values from one mouse. The legend for the symbols is above the figure.

6.4 Splenic NP-specific antibody forming cell numbers are increased by concurrent *S.* Typhimurium infection.

The effect of co-infection with *S.* Typhimurium on the serum antibody response of QMxB6 mice to NP-Ficoll is reflected in the numbers of antibody producing cells induced. The number of such cells was estimated both by flow cytometric analysis of splenic cell suspensions, and by counting of cells in histological sections of spleen.

6.4.1 Splenic CD138$^+$ cell counts estimated by flow cytometry.

Flow-cytometry was used to identify the total number of CD138$^+$ cells present, and the number that also bound NP-phycoerythrin (NP-PE). Representative gating strategies are shown in Figure 6-4.

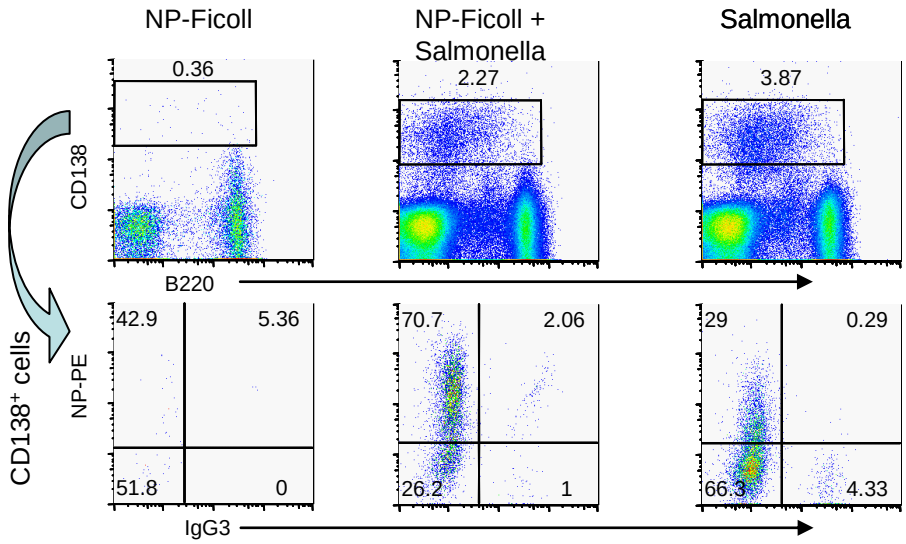

Figure 6-4 shows representative flow cytometry dot plots showing the proportion of CD138$^+$ cells staining for intracellular IgG_3 and anti-NP in individual mice at day 8 after infection or immunization.
Numbers on the dot plots show the percentage of cells in the corresponding gate.

By day 4, total CD138$^+$ cell numbers increased over 45-fold after immunization with NP Ficoll alone, and over 180-fold in those immunized and also infected with *S.* Typhimurium (Figure 6-5). An overwhelming proportion of these cells were specific for

NP, irrespective of co-infection with *S.* Typhimurium. Thus compared to naïve mice, NP-specific $CD138^+$ cell numbers were 100-fold higher in immunized mice, and more than 400-fold higher in those immunized and co-infected.

By day 8 median number of NP-specific $CD138^+$ cells in immunized mice then fell by 20 fold consistent with published reports [60]. In contrast, in mice immunized and co-infected with *S.* Typhimurium, the median number of NP-specific $CD138^+$ cells fell 8 fold. Thus, taking into account the higher day 4 AFC numbers in the mice coinfected with *S.* Typhimurium, at day 8, NP-specific $CD138^+$ cell numbers in immunized and infected mice were over 10 times higher than in mice immunized with NP-Ficoll only. This differential is substantially greater than the difference in median splenic weights (5 fold) indicating a greater frequency of $CD138^+$ cells in the infected mice.

At day 35, NP-specific cell numbers still remained approximately 2.5-fold higher in immunized and co-infected mice than in their non-infected peers, but this was no greater than the difference in median weights at the time.

Surprisingly the mice infected with *S.* Typhimurium but not immunized with NP-Ficoll mounted an NP-specific antibody response. Their total numbers of $CD138^+$ cells and numbers of NP-specific $CD138^+$ cells increased gradually until day 8. At this point the number of NP-specific AFC, as assessed by flow cytometry, was comparable to that in mice co-immunized with NP-Ficoll and this continued through to day 35. Not surprisingly the proportion of $CD138^+$ cells specific for NP was higher in those mice that were immunized with NP-Ficoll (Figure 6-5).

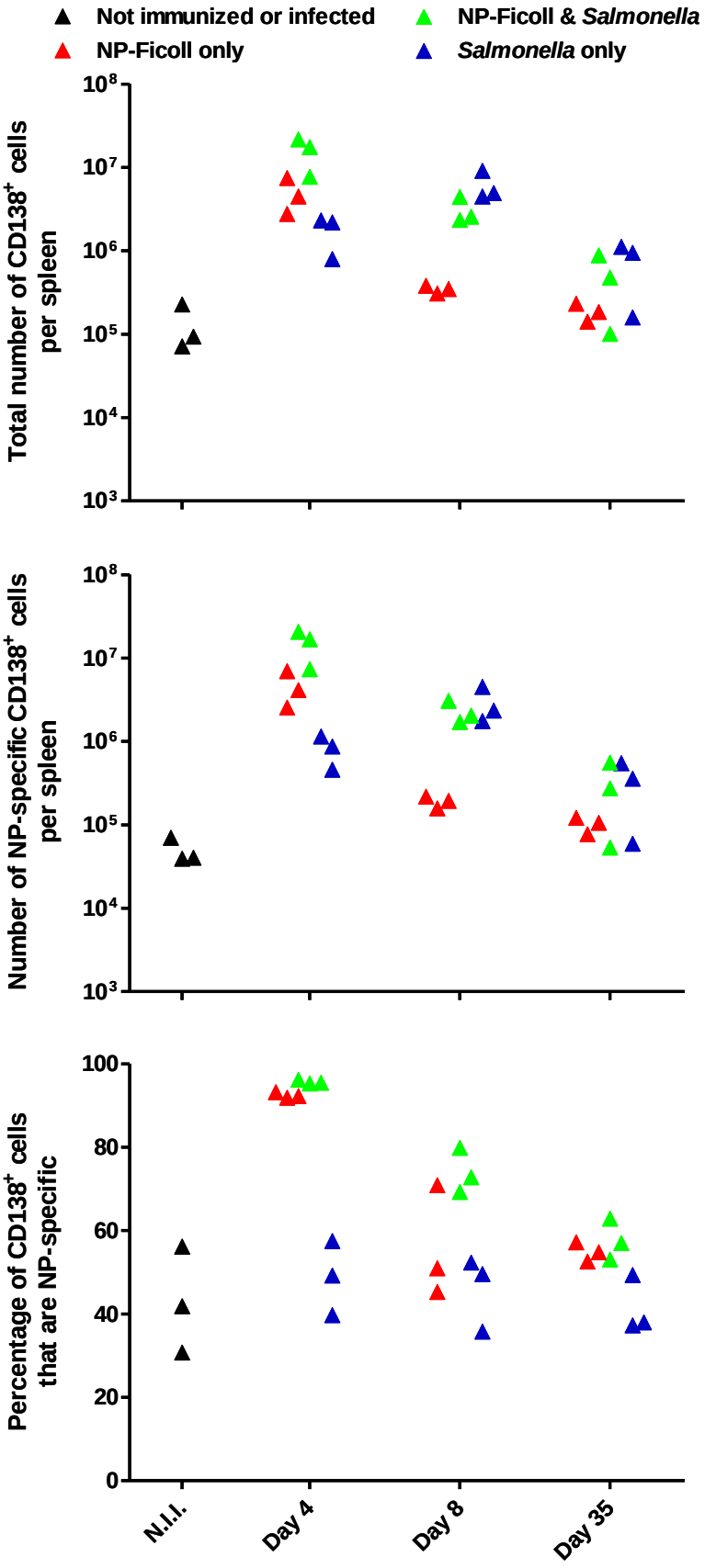

Figure 6-5 shows flow cytometric quantification of changes in the total numbers of CD138$^+$ cells, and changes in the proportion and absolute numbers of CD138$^+$ cells that were NP-specific, in spleens of mice immunized, infected, or both.
Within each panel, each triangle represents values from one mouse. The legend for the symbols is above the figures.

6.4.2 Co-infection with *S.* Typhimurium increases numbers of NP-specific AFC in the splenic red pulp after immunization with NP-Ficoll, but also generates extra-follicular foci of AFC.

Splenic sections from non-immunized mice, and those immunized with NP-Ficoll, infected with *S.* Typhimurium, or both, were examined using immunohistochemical techniques (Figure 6-6 and Figure 6-7). Anti-IgD antibody was used to identify the B cell follicles. These were usually seen adjacent to a T zone that stained strongly with anti-CD3 antibody (Figure 6-6B). Most NP-specific AFC were found in the red pulp, but in some sections, NP-specific AFC could be seen in extra-follicular foci. Extra-follicular foci are clusters of AFC located at the interface between the T zone and main red pulp area, and contiguous with both (see Figure 6-6F, and Figure 6-7).

Before immunization, sparse numbers of cells containing cytoplasmic anti-NP antibody were present in the splenic red pulp. Four days after immunization with NP-Ficoll, massively increased numbers of NP-specific AFC were present throughout the red pulp. In mice immunized with NP-Ficoll and infected with *S.* Typhimurium the enlarged red pulp is filled with even more impressive expanses of NP-specific AFC.

By day 8 after NP-Ficoll, far fewer NP-specific red pulp AFC are seen. This loss of cells was less marked in mice co-infected with *S.* Typhimurium. In the co-infected group but not the group receiving NP-Ficoll only, NP-specific AFC were also seen at day 8 in extra-follicular foci. By day 35 the differences in the number of NP-specific AFC between groups was not marked, except for the red pulp still being larger in the infected mice. Most NP-specific AFC at day 35 were in the red pulp.

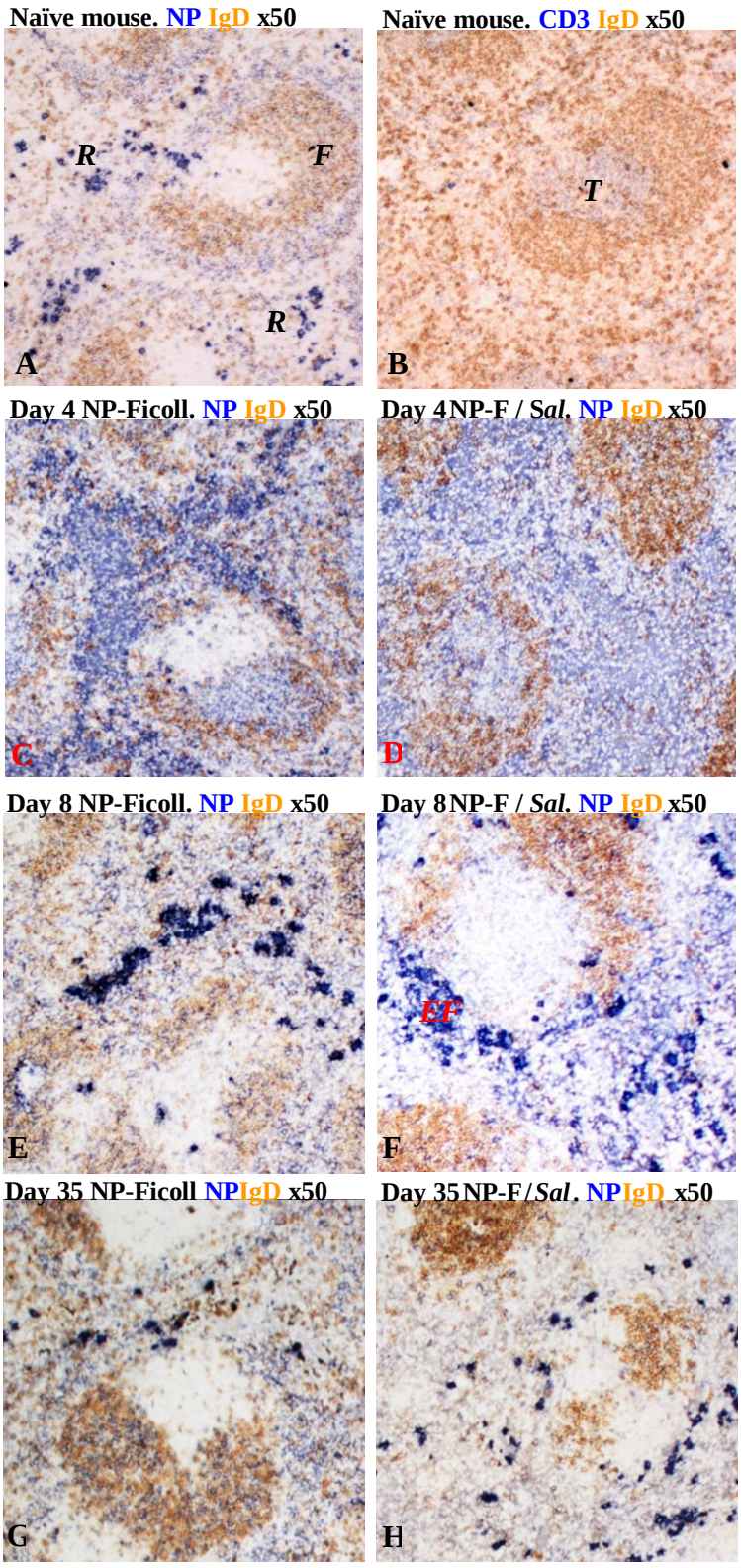

Figure 6-6 shows histological changes associated with immunizing QMxB6 mice with NP-Ficoll with or without coinfection with *S.* Typhimurium

The heading above each photomicrograph shows the mouse group in relation to immunization and/or infection and the staining used. NP-F / Sal = NP-Ficoll immunization with *S.* Typhimurium infection. Microscope magnification of the photomicrographs is x 50. **Panel A**, small background numbers of NP-specific AFC in the red pulp (*R*) and the concentration of NP-specific B cells in the marginal zone, which lies outside the IgD-staining follicles (*F*). In a serial section (**panel B**) CD3 staining cells identify the T zone (*T*). **Panels C and D** show the massive numbers of blue-staining AFC in the red pulp 4 days after immunization with NP-Ficoll Blue staining within the follicles identifies NP-specific germinal centres. The larger red pulp area seen in the co-infected mouse (panel D) compared to that in the non-infected group (panel C) is representative of all mice in the co-infected group. **Panels E and F** show that by 8 days after NP-Ficoll, AFC in the red pulp are now confined to discrete areas. In addition there are AFC in extrafollicular foci (*EF*). By day 35 after NP-Ficoll (**panels G and H)** NP-specific AFC in both infected and non-infected groups are confined to discrete areas in the red pulp.

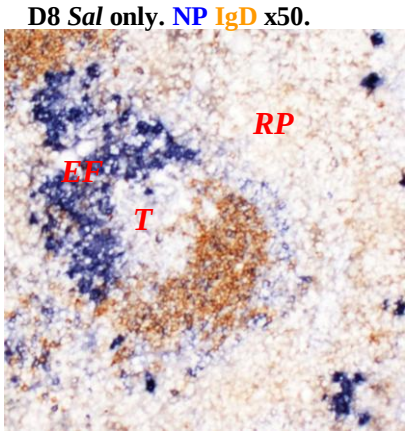

Figure 6-7 shows a representative photomicrograph of mouse spleen 8 days after infection with *S.* Typhimurium demonstrating prominent extra-follicular foci containing NP-specific AFC.
A large collection of NP-specific AFC is present in the extra-follicular focus (*EF)* adjacent to the T zone (*T*) (unstained). A few additional NP-specific AFC are seen in the red pulp (*R*). Original magnification x50.

Relatively few NP-specific AFC were seen in mice sacrificed 4 days after infection with *S.* Typhimurium alone. At day 8, these mice had impressive extra-follicular foci filled with clearly NP-specific AFC and some red pulp NP-specific AFC (Figure 6-7).

An estimate of NP-specific AFC numbers in the spleen of each mouse was also obtained by counting cells/unit area in histological sections using the Weibl point counting technique (Figure 6-8 top panel). Relative cell counts by this method broadly confirm the findings from flow cytometric studies.

Where possible, the location of NP-specific AFC cells was also recorded - as being either in the red pulp or in extra-follicular foci. This was not possible in spleens from mice sacrificed at day 4 after immunization with NP-Ficoll, whether co-infected or not, due to confluent areas of NP-specific AFC. As previously described [60], red pulp NP-specific AFC dominated the response arising after immunization with NP-Ficoll, as shown by the ratio between numbers of NP-specific AFC in red pulp to those in extra-follicular foci at day 8 and 35 (Figure 6-8 bottom panel). Thus in these mice, changes in red pulp NP-specific AFC numbers closely reflect changes in total numbers of NP-specific AFC (Figure 6-8 middle panel).

In mice infected with *S.* Typhimurium, and irrespective of prior co-immuinzation wih NP-Ficoll, the NP-specific AFC response was not so overwhelmingly confined to the red pulp at day 8; the median ratio between the number of NP-specific AFC in the red pulp and the number in extra-follicular foci was less than 4. These extra-follicular foci, prominent in infected mice, also contained many AFC that were not specific for NP (see Figure 6-16).

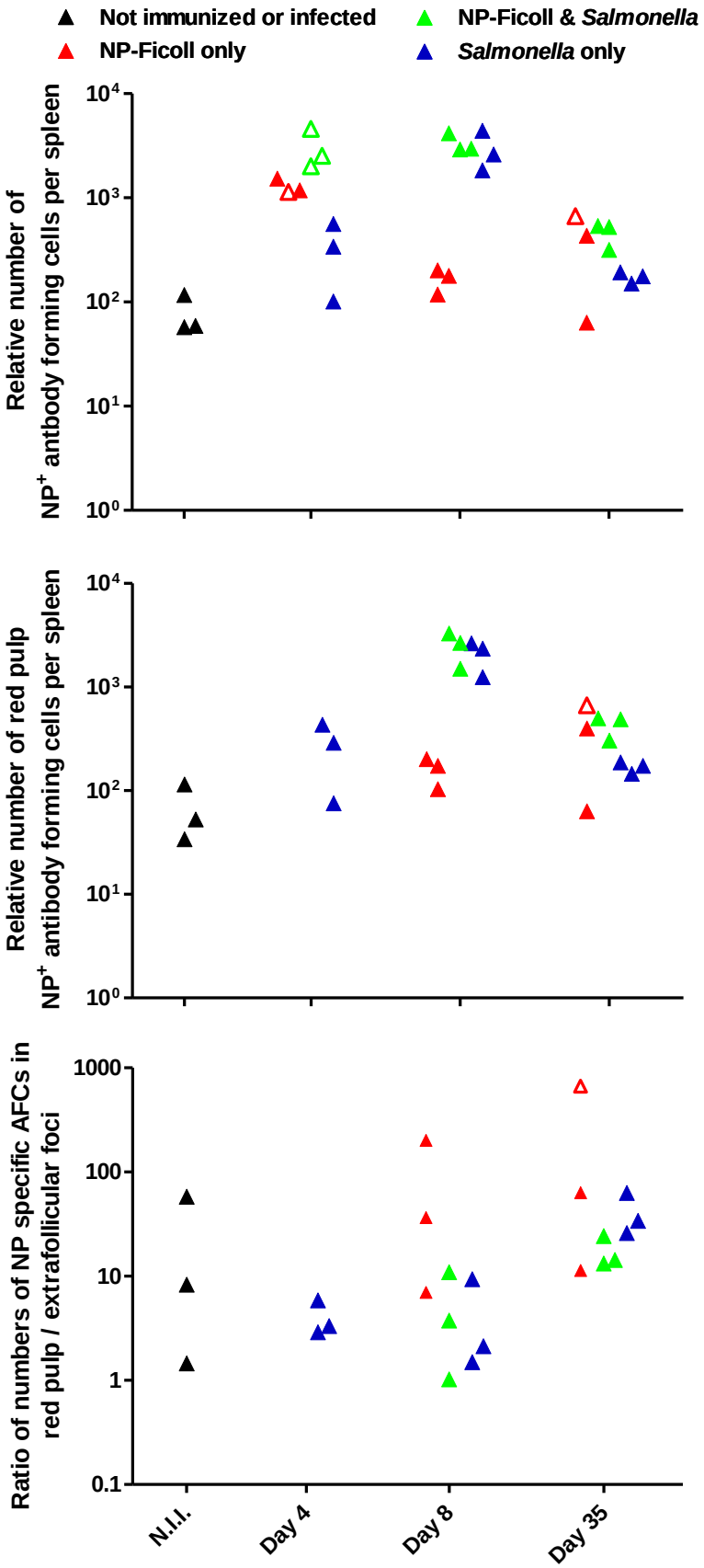

Figure 6-8 shows total numbers of splenic NP-specific AFC and their location following immunization with NP-Ficoll, with or without co-infection. Within each panel, each triangle represents the values from one mouse. Open triangles represent data from histological sections prospectively noted to have relatively indistinct staining.

6.5 AFC are still being produced at day 8 after infection as shown by the continued presence of plasmablasts.

Increased numbers of plasma cells in the red pulp at day 8 after NP-Ficoll and co-infection with *S.* Typhimurium could either be due to prolonged survival of AFC or their continued production, or a combination of both of these. To see if there were greater numbers of NP-specific plasmablasts in the co-infected mice compared to those receiving NP-Ficoll only histological sections were stained for anti-NP antibody and proliferation-associated nuclear antigen - Ki67. By day 8 after immunization with either NP-Ficoll, or infection with *S.* Typhimurium, or both, few red pulp NP-specific AFC contained nuclear staining for Ki67 (Figure 6-9, and Figure 6-10). Thus the AFC in the red pulp in all groups of mice at this stage are plasma cells. On the other hand, both groups of infected mice had extrafollicular foci with ~30% of $Ki67^+$ NP-specific AFC, while, as shown in the previous section, mice receiving NP-Ficoll had little or no evidence of extrafollicular foci. As expected at day 4 after NP-Ficoll, before the mass loss of NP-specific AFC from the red pulp, essentially all the NP-specific AFC that form sheets of cells in the red pulp were $Ki\text{-}67^+$.

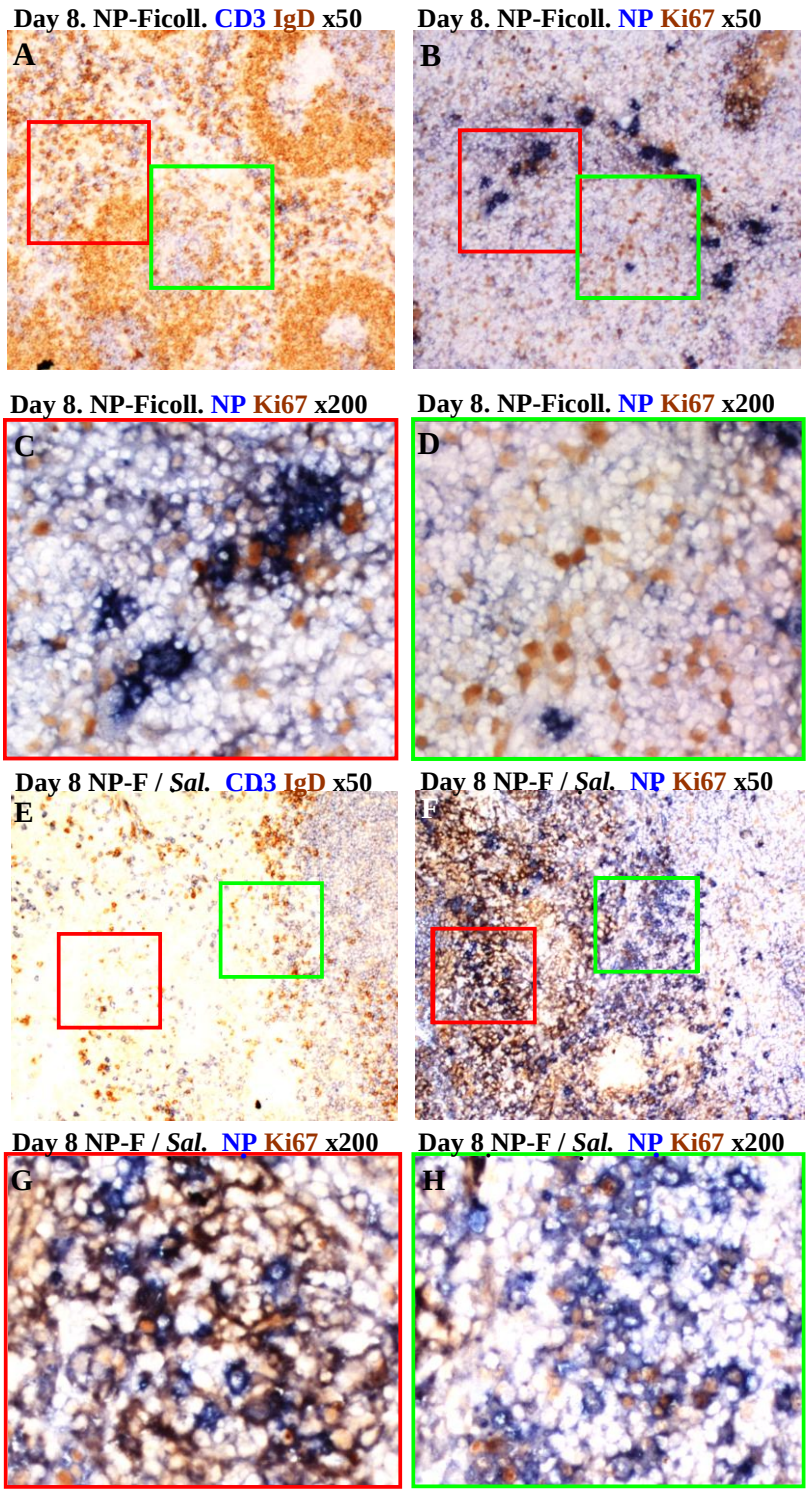

Figure 6-9 shows that eight days after immunization with NP-Ficoll almost all red pulp AFC have left cell cycle, while plasmablasts are still present in extrafollicular foci of mice infected with *S.* Typhimurium

The mouse group, staining patterns and objective magnification are shown above each photomicrograph. **Panels A-D** show QMxB6 spleen 8 days after NP-Ficoll. A) orients with CD3 and IgD staining while the same area of a serial section B) is co-stained for NP binding and the proliferation-associated nuclear marker - Ki67. The red box encompasses red pulp with a focus of NP-specific AFC and the green box red pulp largely devoid of AFC as well as an area of T zone red pulp junction, which typically is associated with extrafollicular focus formation; no AFC are in this area. C) and D) show the boxed areas of B) in higher power).

Panels E-H are analogous photomicrographs at day 8 after immunization and co-infection, but in this series the red box shows AFC-containing red pulp and the green box extra-follicular focus. Approximately one third of AFC in the latter are $Ki67^{+}$, indicating proliferation, while the red pulp AFC are $Ki67^{-}$. In infected mice, extensive red-pulp $Ki67^{+}$ staining that is not associated with NP-specific AFC is likely to reflect extra-medullary haemopoesis. Microscope magnification of the photomicrographs is either x50 or x200 as specified in the legend of each panel.

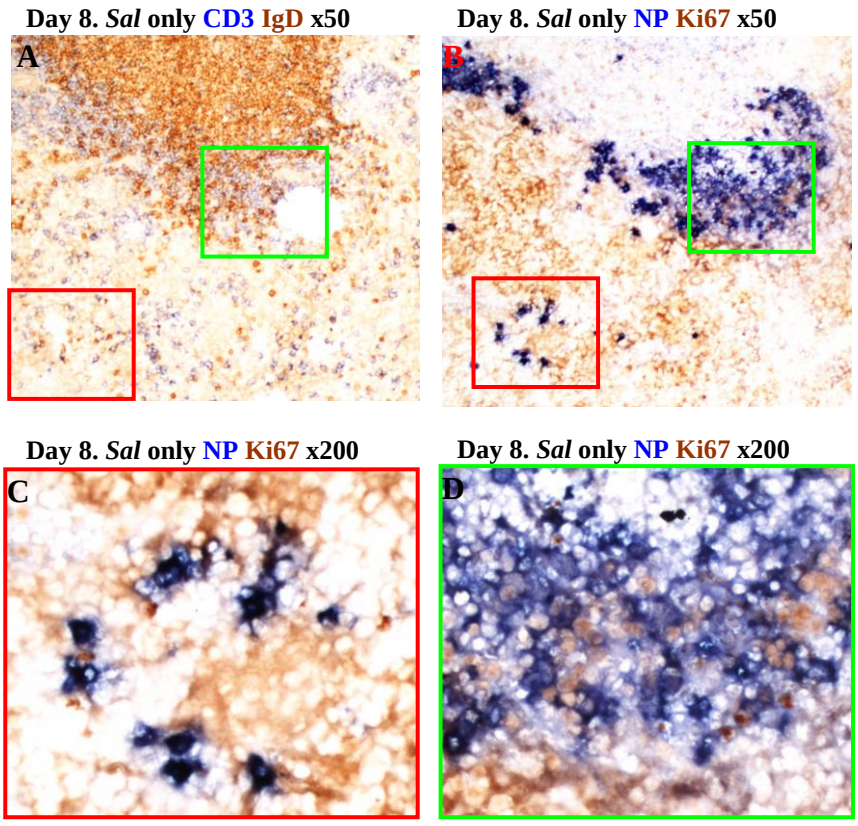

Figure 6-10 shows the distribution of NP-specific AFC in the spleen 8 days after infection alone, where proliferation amongst these AFC is again confined to extra-follicular foci.
The red box as in Fig 1-9 contains red pulp NP-specific AFC while the green box includes part of an extensive extrafollicular focus of NP-specific AFC. Red-pulp Ki67^{+} staining that is not associated with NP-specific AFC is likely to reflect extra-medullary haemopoesis. Microscope magnification of the photographs is either x50 or x200 as specified in the legend of each panel.

6.6 Increased numbers of non-proliferating splenic NP-specific plasma cells are sustained during *S.* Typhimurium infection.

The lack of Ki-67 staining by red pulp AFC at 8 d after immunization shows that these cells had differentiated into plasma cells. Nevertheless, the presence of proliferating NP-specific plasmablasts in extra-follicular foci is consistent with the possibility that these red pulp plasma cells are being rapidly renewed. To see if the new plasma cell niches were supporting longer term plasma cell survival we pulse labelled NP-specific AFC with

the thymidine analogue – 5-Bromo 2′-deoxyuridine (BrdU) and assessed if the labelled cells persisted in the red pulp niches. BrdU was provided in mice' drinking water from 24 hours to 120 hours after inoculations. During this time dividing cells, including plasmablasts, incorporate BrdU into cells' DNA but any division occurring after 120 hours will result in subsequent loss of any previously incorporated BrdU. Thus $BrdU^+$ AFC present at later timepoints will be those plasma cells terminally differentiated before day 5. As plasma cells may live up to three days without specific supportive factors [45], only survival beyond that time could be attributable to supportive niches. Enhanced survival of plasma cells was therefore examined in mice at days 9, and at 25 days after immunization i.e. 4 and 21days after the BrdU pulse.

Numbers of splenic $CD138^+$ cells and NP-specific $CD138^+$ cells as well as the proportion of NP-specific $CD138^+$ cells that was $BrdU^+$, were assessed by flow cytometry at 4 days (i.e. during the pulse), 9 day, and 25 days after the different inoculations. Representative flow cytometric dot plots are shown in Figure 6-11.

The results of the second experiment are shown in Figure 6-12. This confirms previous findings that at day 4 and at day 9, total numbers of $CD138^+$ cells (upper left panel), and also numbers of NP-specific $CD138^+$ cells (upper right panel), are higher in immunized and co-infected mice than in their immunized but not infected peers. A median of 97% of NP-specific $CD138^+$ cells had incorporated BrdU by 4 days after immunization with NP-Ficoll, irrespective of co-infection with *S.* Typhimurium, thus confirming technical success of the BrdU methodology at identifying proliferating AFC. Amongst day 9 mice, median numbers of NP-specific $CD138^+$ cells were 12-fold higher in immunized and co-infected mice, as compared to mice receiving NP-Ficoll only. This impressive difference

was greater than the 7.7-fold differential in median weights, between the same two groups of mice. No difference in median numbers of NP-specific $CD138^+$ cells was detectable between different groups of day 25 mice.

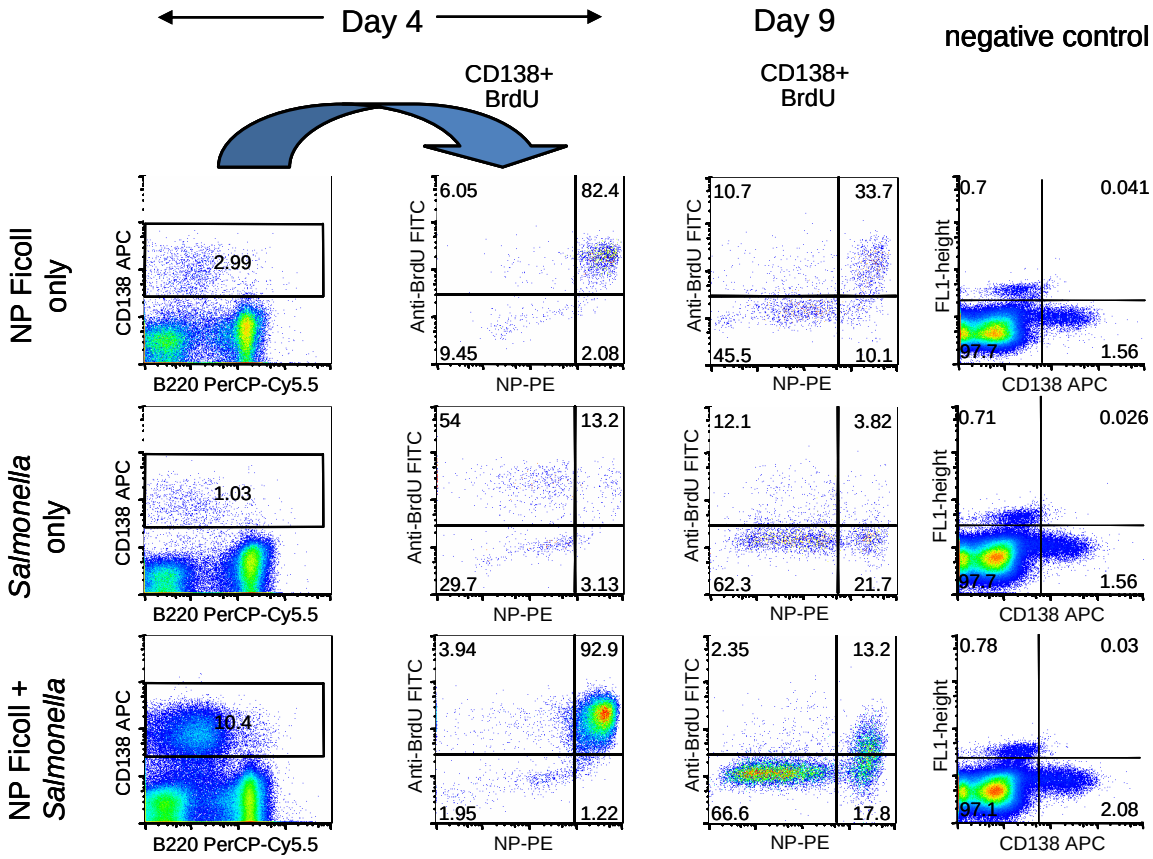

Figure 6-11 shows that many of the NP-specific $CD138^+$ cells present 9 days after immunization and/or infection retain BrdU taken up in the first 5 days of the response.
Representative flow cytometry dot plots are from mice given BrdU between 24 and 120 hours after inoculation(s). In the 2nd column, and 3rd columns gated $CD138^+$ cells in spleen suspensions are analysed for BrdU incorporated into DNA and NP binding.

In infected but not immunized mice, a median 82% of NP-specific cells had incorporated BrdU at day 4, consistent with the more gradual increase in NP-specific AFC numbers seen in this group. However, the absolute number of $BrdU^+$ NP-specific $CD138^+$ cells present at day 9 after infection alone, was still more than median 3 fold above numbers seen in immunized, but uninfected mice.

The number of $BrdU^-$ NP-specific $CD138^+$ cells present after 9 days of infection, and irrespective of co-immunization, was substantially higher than the number present at day 4. This is consistent with the ongoing plasmablast proliferation seen in extra-follicular foci of similar mice at day 8. It is likely to include both plasmablasts generated de-novo after day 5, or continued proliferation of plasmablasts that had previously incorporated BrdU between day 1 and the end of day 5.

Close examination of the flow cytometry dot plots (Figure 6-11 and data not shown) reveals that amongst day 9 mice the median BrdU fluorescence in NP-specific $CD138^+$ cells in spleens of immunized mice was some 8 fold higher than in corresponding cells from mice both immunized and infected. Thus it may be that some plasmablasts in infected and immunized mice continued to divide up to 3 times more after BrdU feeding ceased at 120 hours. Nevertheless, as plasmablast divisions occur at 8 hourly intervals or less [238], even these AFC will have ceased dividing by day 6, consequently the resultant terminally differentiated plasma cells will have survived for at least 3 days in an animal studied at day 9.

In conclusion, the results from the BrdU pulse chase extend the previously reported data, by providing evidence that extended survival of increased numbers of non-proliferating splenic NP-specific plasma cells can occur in the context of an unrelated source of inflammation. Histological examination of sections from these mice' spleens is yet to be performed, but will be likely to demonstrate that $BrdU^+$ NP-specific AFC are predominantly in the red pulp.

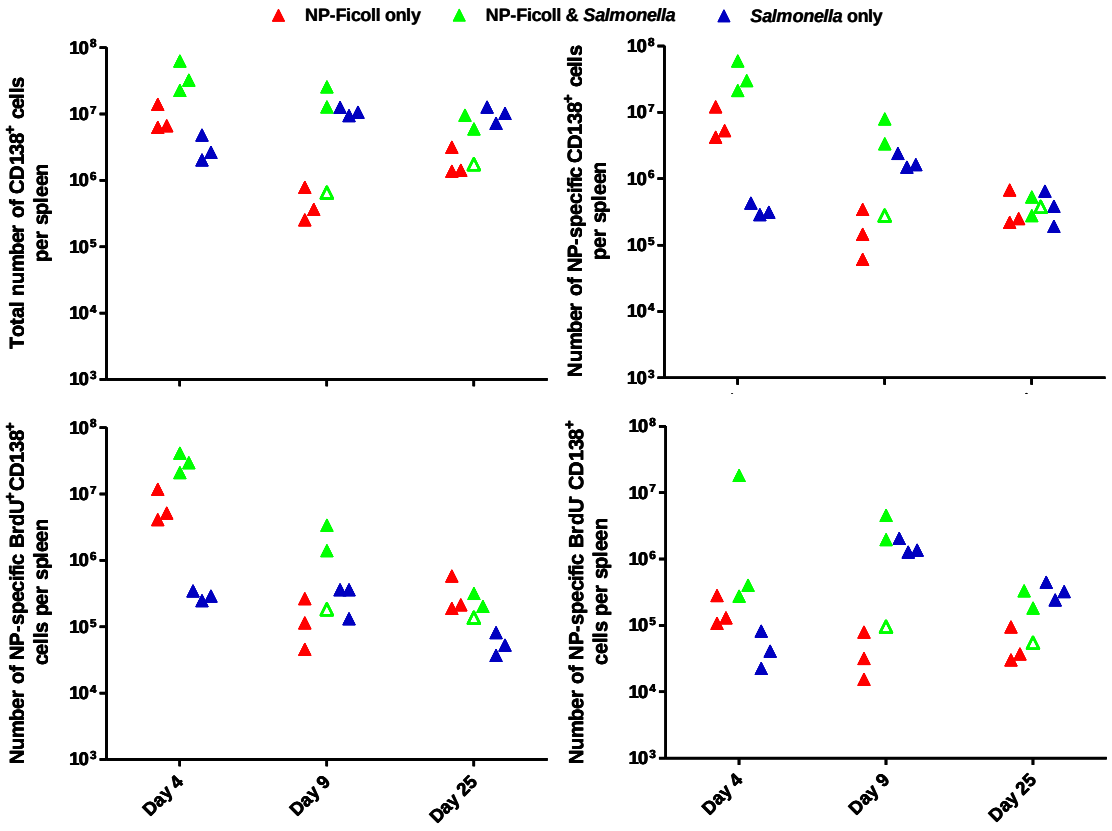

Figure 6-12 shows that the increased number of NP-specific red pulp plasma cells present 9 days after immunization with NP-Ficoll and co-infection with *S.* Typhimurium is attributable, at least in part, to an increased number of plasma cells surviving for more than 3 days.
The graphs show the number of NP-specific AFC that are labelled at 9 and 25 days after immunization with NP-Ficoll or infection or both by a BrdU pulse administered from days 2 to 5. The efficiency of the labelling was tested by assessing the proportion of plasmablasts labelled at 4 days; i.e. at the peak of the plasmablast response and before the onset of mass AFC apoptosis. Each symbol shows values for one mouse. Legend for the symbols is above the figure. The open triangles represent data from mice that were immunized and co-infected, but which did not demonstrate splenomegally, or other signs of infection with *S.* Typhimurium.

6.7 Strategies to identify infection-related niches for antibody forming cells.

Having obtained evidence to support the initial hypothesis, I sought to characterise the nature of the red-pulp niches that support survival of additional plasma cells during inflammation. Two broad approaches were used:

- To identify cell populations, whose numbers are increased during inflammation, for which there is evidence to indicate they contribute to increased plasma cell survival. Such cell populations would be expected to co-localise with plasma cells (or their precursor plasmablasts).
- To identify changes in the splenic microenvironment consistent with a mechanism to increase plasma cell retention and survival.

6.7.1 The potential role of phagocytes and dendritic cells in promoting prolonged survival of AFC in spleens of mice infected with *S.* Typhimurium.

Acute inflammation is characteristically associated with an infiltrate of neutrophils and macrophages. In addition a range of phagocytes and dendritic cells have been shown to associate with AFC even in immune responses where there is no infection. There is evidence that cells with both neutrophil and macrophage features as well as dendritic cells contribute to plasma cell survival through release of factors including BAFF and APRIL and IL-6 [174;239-241]. Recently published work from our laboratory, using a different model, provides evidence that macrophages are associated with non-proliferating AFC, and that they express substantial amounts of mRNA encoding for APRIL [130]. We thus considered the possible role of neutrophils, macrophages and dendritic cells in the maturation and survival of plasma cells in the models studied here.

6.7.1.1 Splenic numbers of $CD11b^{+}Gr1^{hi}F4/80^{neg}$ neutrophils and $CD11b^{+}Gr1^{intermediate}F4/80^{intermediate}$ macrophages increase after infection with *S.* Typhimurium.

Flow cytometric studies show S. typhimurium infection results in a significant increase in the numbers of both splenic $CD11b^{+}Gr1^{hi}F4/80^{neg}$ cells and $CD11b^{+}Gr1^{intermediate(int)}F4/80^{int}$ cells. Gating strategies are shown in Figure 6-13. Results show that median numbers in both cell populations were more than 3 fold higher by day 4, and at least 6 fold higher at day 8 after S. typhimurium infection (Figure 6-14). These increases occurred irrespective of co-immunization with NP-Ficoll, and were greater than the concurrent increases in splenic weight at the corresponding timepoints. By 35 days a more modest increase in number in each population compared with non-immunized non-infected mice was still present. Immunization with NP-Ficoll, in the absence of infection was associated with a gradual fall in numbers of $CD11b^{+}Gr1^{hi}F4/80^{-}$ cells, and $CD11b^{+}Gr1^{int}F4/80^{int}$ cells at day 4 through to day 35.

It will be seen that the Gr1+, F4/80+ cells separate into three subgroups on flow cytometry: $Gr1^{hi}F4/80^{int}$, $Gr1^{int}F4/80^{int}$ and $Gr1^{int}F4/80^{hi}$ cells (Figure 6-13). The numbers of all three of these subsets increased in a similar way in response to infection. The data for the $Gr1^{intermediate}F4/80^{intermediate}$ cells are shown in Figure 6-14B. The numbers of the cells in the other two subsets remained throughout approximately 10-fold lower, but changes in their number followed a similar pattern to that seen in $Gr1^{intermediate}F4/80^{intermediate}$ cells (data not shown).

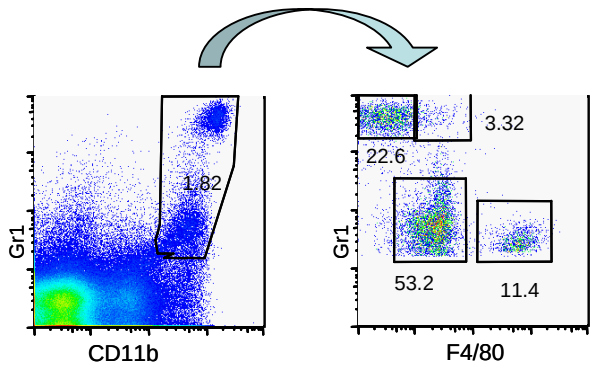

Figure 6-13 shows representative flow cytometry dot plot demonstrating gates used to define populations by surface expression of Gr1, F4/80, and CD11b.
Flow cytometric study of spleen removed 4 days after immunization with NP-Ficoll. **Left** – gating of $CD11b^+$ cells that are $Gr1^+$. **Right** – subgating according to intensity of staining with anti-Gr1 and anti-F4/80 antibodies. $Gr1^{hi}F4/80^-$ cells are likely to be neutrophils, whilst $Gr1^{int}F4/80^{int}$ cells are likely to be macrophages. The phenotype of the other two, smaller, gated populations of cells is not clear.

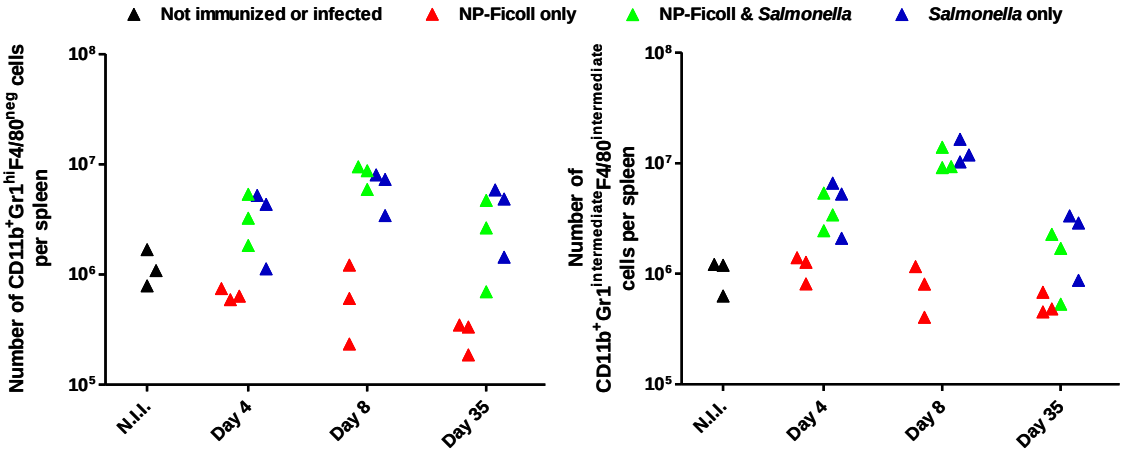

Figure 6-14 shows splenic numbers of $CD11b^+Gr1^{hi}F4/80^{neg}$ cells, and $CD11b^+Gr1^{int}F4/80^{int}$ cells rise after infection, but not immunization.
Changes in numbers of $CD11b^+Gr1^{hi}F4/80^{neg}$ cells (left), and in numbers of $CD11b^+Gr1^{int}F4/80^{int}$ cells (right), as measured by flow cytometry of splenic cell suspensions. Each symbol shows values for one mouse. Legend for the symbols is above the figure.

6.7.1.2 The relationship of red pulp AFC at day 8 with $CD11b^+Gr1^+$ cells and $F4/80^+$ cells.

Confocal microscopy was used to ascertain if NP-specific AFC were in proximity to $Gr1^+$ cells. The co-staining with Gr1 and F4/80 fails to show coincident staining (Figure 6-16 top row). This suggests that only the $Gr1^{high}$ cells and $F4/80^{high}$ cells are detectable by this methodology and that the major $Gr1^{int}F4/80^{int}$ subset may not be detected. In addition the small $Gr1^{high}F4/80^{int}$ subset is not distinguishable from the $Gr1^{high}F4/80^-$ cells.

Nevertheless, F4/80$^+$Gr1$^-$ cells are widely distributed in the red pulp. Consequently, red pulp AFC are never far from F4/80$^+$ cells. On the other hand there are large areas in the red pulp that contain F4/80$^+$ cells but lack AFC. It follows many F4/80 expressing cells are unlikely to be providing a microenvironment that can support red pulp AFC survival. It remains possible that those F4/80$^+$ cells that co-localize with AFC have a role in maintaining these AFC. Gr1$^+$ cells are more focused in the red pulp, but similar arguments to those used for F4/80 apply to Gr1$^+$ cell co-localization with red pulp AFC. Few Gr1$^+$ cells were associated with extrafollicular foci, but some F4/80$^+$ cells were in these foci. In keeping with data from flow cytometry, nearly all Gr1$^+$ cells were CD11b$^+$ by confocal microscopy (Figure 6-15).

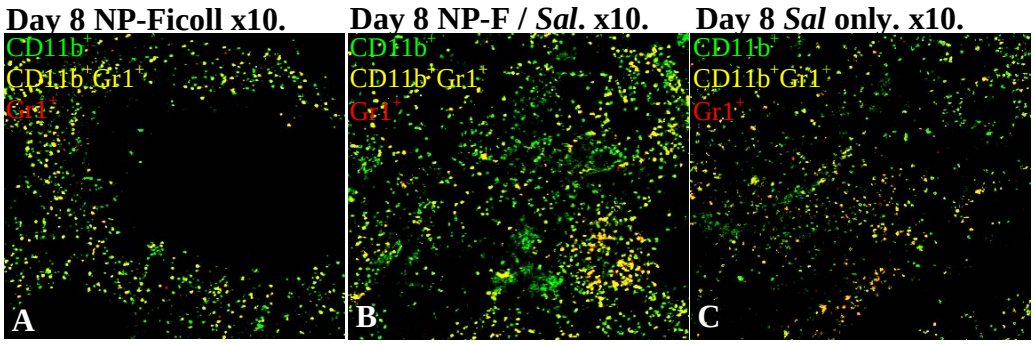

Figure 6-15 shows that in spleens of mice that were previously immunized or infected or both, nearly all Gr1$^+$ cells are CD11b$^+$ by confocal microscopy,
In spleens of mice sacrificed 8 days after **(A)** immunization, **(B)** immunization and co-infection, or **(C)** infection alone, almost all Gr1$^+$ cells (red) co-stain for CD11b (green) and so appear yellow. Original objective magnification x10 for all images.

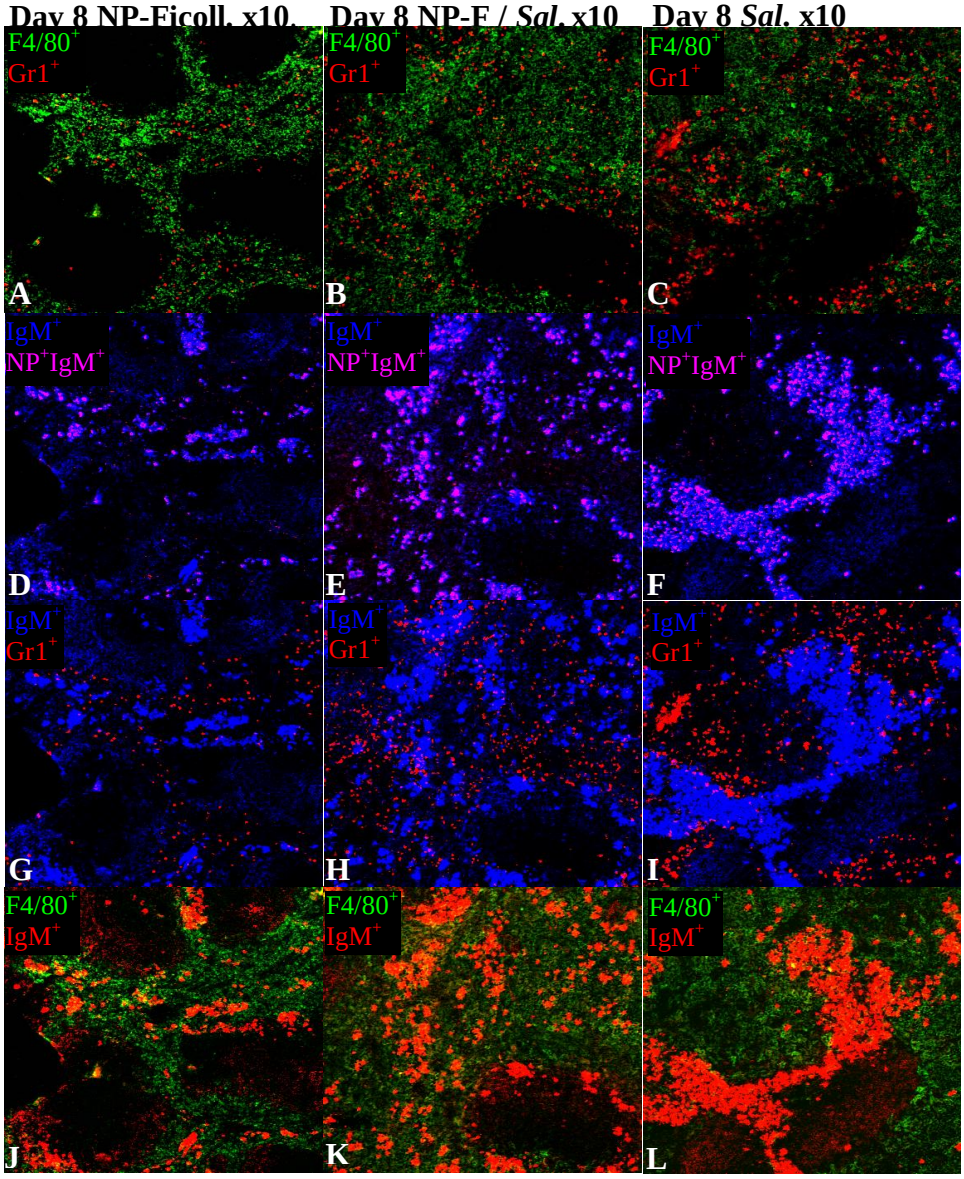

Figure 6-16 shows representative confocal microscopy images of spleens from mice sacrificed at day 8 after immunization, infection, or both. These show that in each tissue (i) no cells are seen to be $Gr1^+F4/80^+$, (ii) most red pulp NP-specific AFC are IgM^+, (iii) red pulp IgM^+ AFC are not restricted to the proximity of $Gr1^+$ cells and (iv) substantial areas of the red pulp contain $F4/80^+$ cells but no AFC.

Panels A, D, G and J show the same splenic section from one representative mouse 8 days after NP-Ficoll alone. **Panels B, E, H, and L** show the same splenic section from one representative mouse 8 days after immunization and co-infection. **Panels C, F, I and L** show the same splenic section from one representative mouse 8 days after *S.* Typhimurium infection alone. **Panels A-C** show $F4/80^+$ cells (green) and $Gr1^+$ cells (red). In confocal microscopy, no $Gr1^+$ cells co-stained for F4/80 (no yellow staining). $Gr1^+$ cells were more common in the red pulp of infected mice. **Panels D-F** show IgM^+ cells (blue) and NP-specific cells (red). NP-specific IgM^+ cells appear purple. In each experimental condition red pulp NP-specific AFC were overwhelmingly IgM^+. Extra-follicular foci in *S.* Typhimurium infected mice also included IgM^+ AFC not specific for NP. **Panels G-I** show $Gr1^+$ cells (red) and IgM^+ cells (blue). Neither red pulp IgM^+ AFC, nor extra-follicular IgM^+ AFC, were associated with $Gr1^+$ cells at 8 days after immunization, infection or both. **Panels J-L** show $F4/80^+$ cells (green) and IgM^+ cells (red). $F4/80^+$ cells are widely distributed within the red pulp and many areas containing F4/80 + cells do not contain IgM^+ AFC. All images were taken with x10 objective magnification.

6.7.1.3 Splenic numbers of CD11c^{+} dendritic cells, increase in mice infected with *S.* Typhimurium, but not those only immunized with NP-Ficoll.

Previously published reports have described a CD11c^{hi} cell population of dendritic phenotype that are associated AFC and may assist plasmablast maturation to plasma cells [128]. We therefore considered the possibility that infection related increases in CD11c^{hi} cells (or a subset thereof) might be causally associated with the increased numbers of AFC in infected mice on day 8 after NP-Ficoll.

Flow cytometric analyses were therefore performed on splenic cell suspensions from mice sacrificed after immunization or infection or both, in order to define a phenotype of one or more candidate cell populations. Previous work in our laboratory has divided CD11c^{+} cells into CD11c^{int} and CD11c^{hi} subsets of CD8α^{-} cells, and CD11c^{+}CD8α^{+} cells. These subsets are shown in Figure 6-17, which also shows that there is heterogeneity within each of these subsets based on the varying expression of F4/80 and CD4.

It will be seen from Figure 6-17 that infection results in major changes to the proportions of CD4^{+} and F4/80^{+} cells in the CD11c^{+} subsets. In particular the proportions of F4/80^{-}CD4^{+} cells falls, while F4/80^{+}CD4^{-} cell proportions increase. These changes expressed as numbers of cells per spleen are quantified in Figure 6-18. This shows that in the infected mice all 3 subsets defined by CD4 and F4/80 expression increase in number during infection, but this is most marked in the F4/80^{+} CD4^{-} subset. By contrast in mice immunized with NP-Ficoll, but not infected, only the F4/80^{-} subset increased and then only among the CD11c^{hi}CD8^{-} and the CD11c^{+}CD8^{+} subsets.

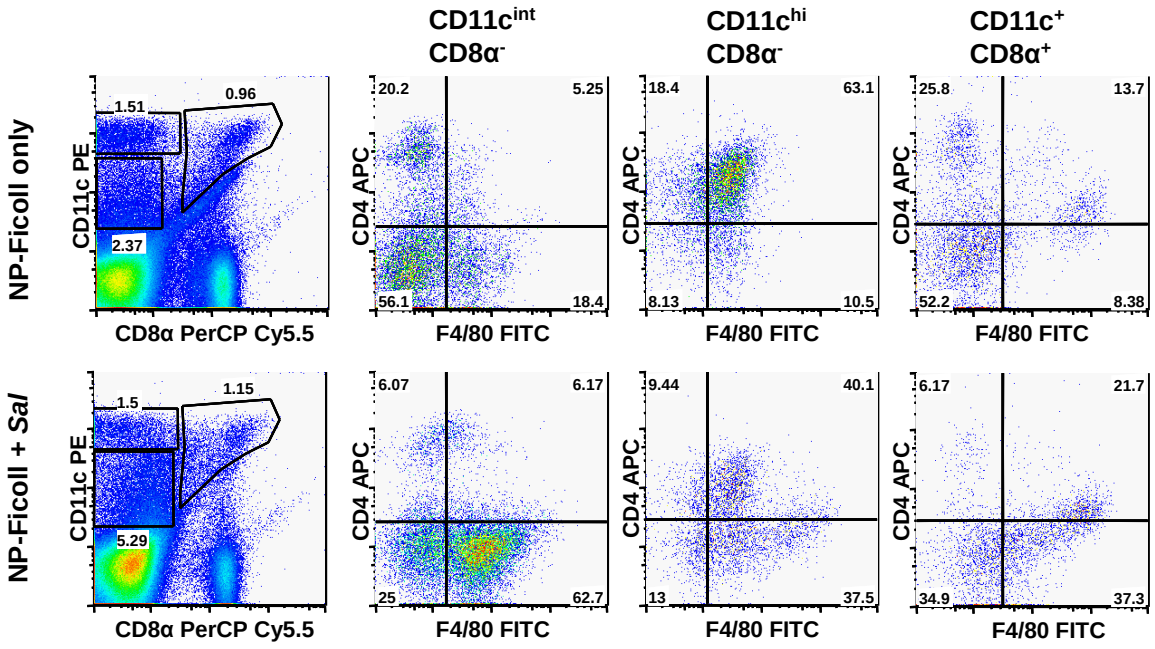

Figure 6-17 shows representative flow cytometry dot plots demonstrating gates used to define splenic cell populations according to staining with antibodies to CD11c, CD8α, CD4, and F4/80 in mice sacrificed after immunization, infection, or both.
Dot plots shown are from mice 8 days after immunization with NP-Ficoll (upper panels), and 8 days after immunization with NP-Ficoll and infection with *S.* Typhimurium (lower panels). For each row, the left dot plot shows the gating for 3 subsets of $CD11c^+$ cells, according to the intensity of staining with antibodies to CD11c and antibodies to CD8α. The remaining dot plots demonstrate subsets of these primary populations, according to intensity of staining for CD4 and F4/80.

The increase in the $CD11c^+CD8\alpha^+F4/80^+CD4^-$ subpopulation (maximal at day 8; a median 4.5 fold increase above baseline) was no greater than the concurrent changes in spleen weight in these mice. However the increase in median number of $CD11c^{hi}CD8\alpha^-F4/80^+CD4^-$ cells was greater, at 5-6 fold by day 8 after *S.* Typhimurium infection. The median number of cells within the $CD11c^{lo}F4/80^+CD4^-$ subset, increased more than 10 fold by day 8 after infection.

The $CD11c^{lo}F4/80^+CD4^+$ subset was also, more modestly, increased, in association with *S.* Typhimurium infection, but unaffected by immunization with NP-Ficoll. Some of this may have been attributable to cell populations spilling across the defined gating boundaries (Figure 6-17).

6.7.1.4 The relationship at day 8 between splenic AFC and $CD11c^+F4/80^+$ cells.

Flow cytometric studies indicate that some $CD11c^+F4/80^+$ cell populations were selectively increased in infected mice. Within the remaining time available for this thesis it was not possible to develop the technology to co-stain for CD11c and CD8 and CD4 and F4/80 and either NP or IgM in confocal microscopy. Confocal microscopy was therefore used to ascertain if AFC present at day 8 were associated with $CD11c^+F4/80^+$ cells.

As noted previously (Figure 6-16 panel J), and seen in the top left image of Figure 6-19, F4/80 cells (green) are seen scattered throughout the red pulp after immunization with NP-Ficoll. This is also the case for the expanded red pulp of infected mice (Figure 6-16 panel L, top right image of Figure 6-19). By contrast, F4/80 cells are not seen in the B cell follicle, which contains small IgM^+ B cells (white), in either group. Similarly, the T zone, which is devoid of either IgM^+ B cells or large IgM^+ AFC at day 8 after either inoculation, has few $F4/80^+$ cells either. However, at the edge of the T zone in infected mice there are clusters of AFC that are likely to be in extra-follicular foci, and these are amongst $F4/80^+$ cells.

Interestingly, when visualising binding to CD11c, as well as binding to F4/80 and IgM (Figure 6-19 lower panels), it is clear that $CD11c^+$ cells (red) encroach much further towards, and probably into, the T zone than $F4/80^+$ cells do. Furthermore at the sites of extra-follicular foci, but not elsewhere along the margin of the T zone, these $CD11c^+$ cells are $F4/80^+$ (and so appear yellow) (compare bottom right panel of Figure 6-19 and Figure 6-20).

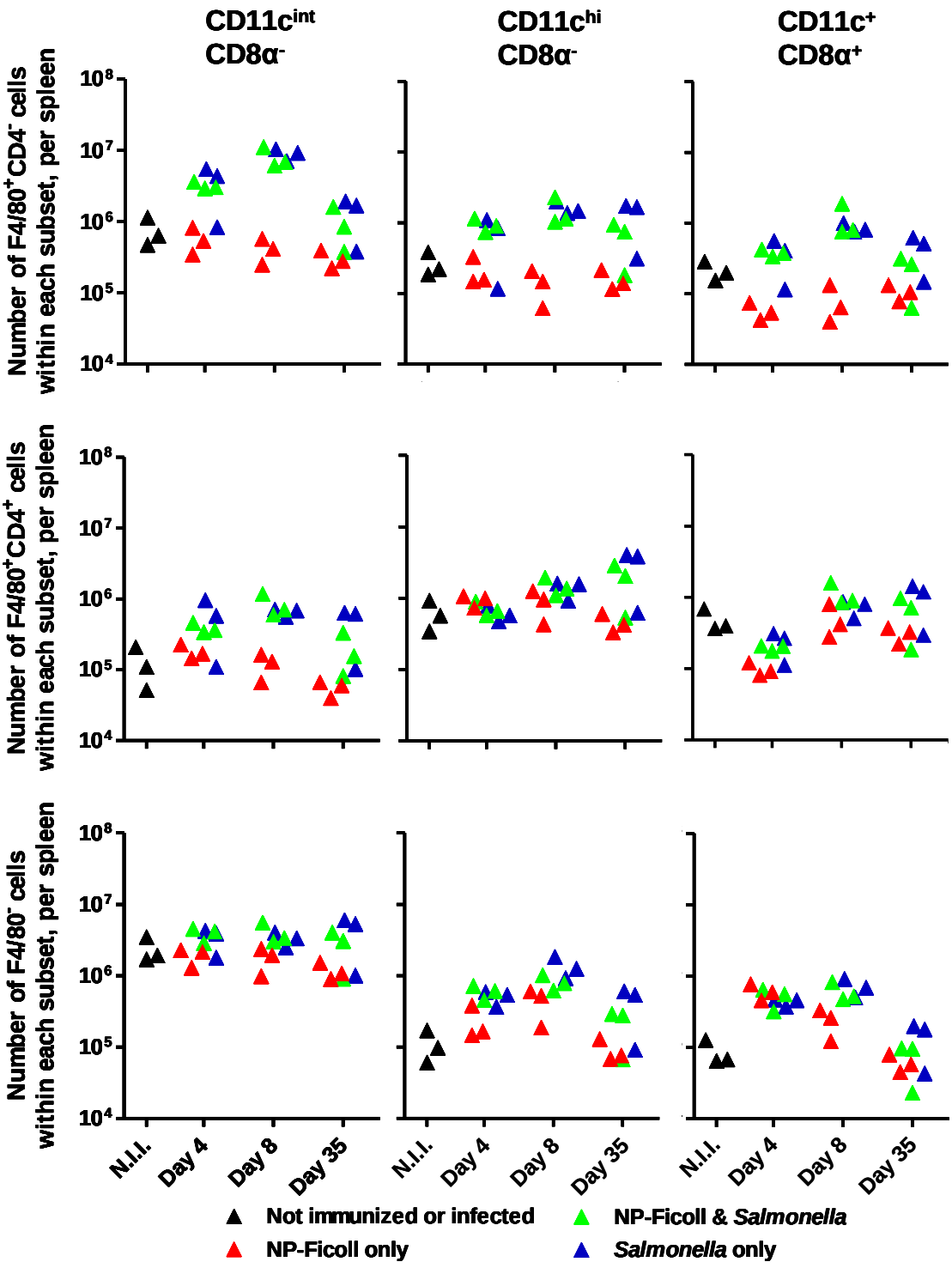

Figure 6-18 shows a summary of changes in splenic cell numbers within defined subsets of CD11c$^+$ cells, following infection or immunization or both, in which F4/80$^+$CD4$^-$ subsets of CD11c^{int}CD8α^- cells, CD11c^{hi}CD8α^- cells, and CD11c$^+$CD8α^+ cells are increased after infection but not immunization. Each symbol represents values from one mouse. The legend for the symbols is below the figure.

As seen in the lower panels of Figure 6-19, the $CD11c^{+}F4/80^{+}$ cells of greatest interest are distributed widely throughout the splenic red pulp in both conditions. Some, but not all, $CD11c^{+}F4/80^{+}$ cells are in contact with red pulp IgM^{+} AFC, though not all AFC are adjacent to $CD11c^{+}F4/80^{+}$ cells.

Flow cytometric studies (Figure 6-15) had also demonstrated further heterogeneity within $CD11c^{+}F4/80^{+}$ cells. It follows that the confocal microscopy images presented here cannot exclude the possibility that those $CD11c^{+}F4/80^{+}$ cells found near to red pulp plasma cells comprise a subpopulation that is able to contribute to the survival of some AFC. Nevertheless, as some day 8 red pulp AFC are not near any $CD11c^{+}F4/80^{+}$ cells, it is tempting to conclude that the survival of some red pulp plasma cells is independent of the any of $CD11c^{+}F4/80^{+}$ cells populations identified in flow cytometry as increased in infection. However there is an important caveat to this, which is analogous to the difficulties in identifying $F4/80^{int}$ staining on $CD11b^{+}$ cells (discussed in 6.7.1.2 above). Amongst the subsets of $CD11c^{+}$ cells defined by flow cytometry, $CD11c^{int}CD8\alpha^{-}$ contains the most cells, especially in infected mice (Figure 6-17). The majority of $CD11c^{int}CD8\alpha^{-}$ cells are $F4/80^{int}$. Thus $CD11c^{int}CD8\alpha^{-}F4/80^{+}$ cells comprise over half of all splenic $CD11c^{+}$ cells, as estimated by flow cytometry.

This is not apparent in confocal microscopy where there seem to be far fewer $CD11c^{+}F4/80^{+}$ cells than $CD11c^{+}F4/80^{-}$ cells (Figure 6-19). This could be due to insufficient expression of either F4/80, or CD11c, or both on cells that are $CD11c^{+}F4/80^{+}$ by flow cytometry. Irrespective of the technical cause, the likely failure to identify all $CD11c^{+}F4/80^{+}$ correctly in confocal microscopy leaves the possibility that infection-

related increases in numbers of $CD11c^{+}F4/80^{+}$ cells do contribute to enhanced survival of red pulp plasma cells in infected mice.

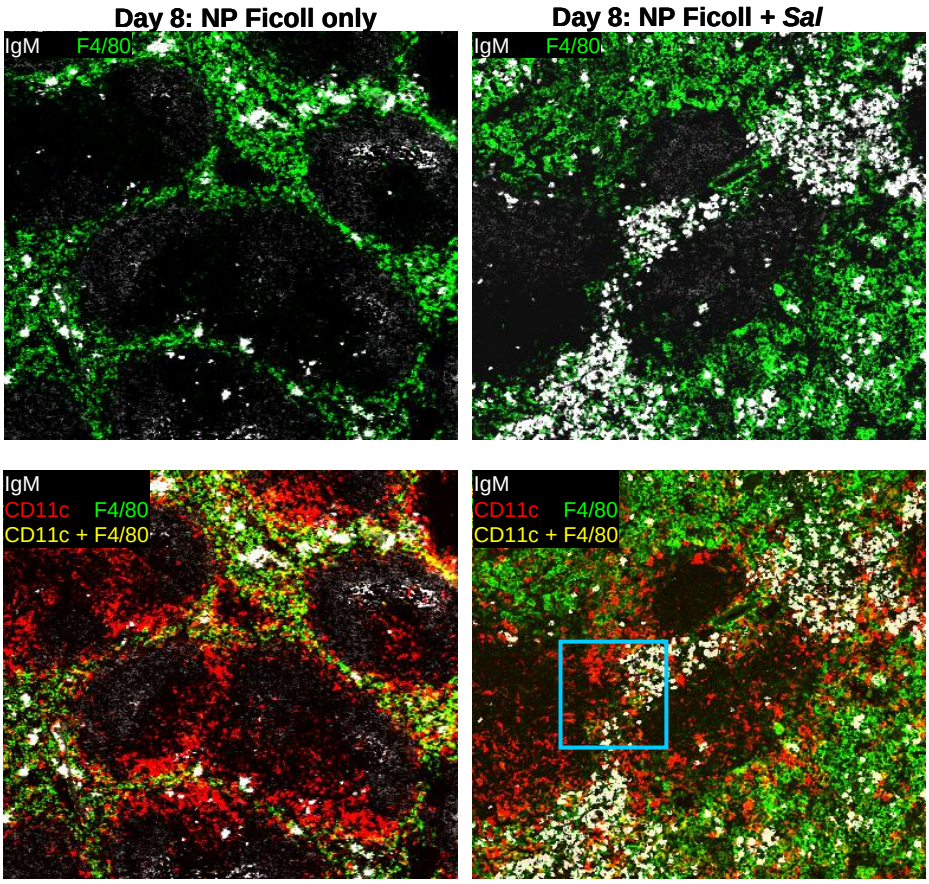

Figure 6-19 shows representative confocal microscopy images of spleens of mice 8 days after immunization with or without co-infection, and stained for IgM and F4/80 with or without staining for CD11c. These show that i) F4/80 cells are confined to the red pulp and extra-follicular foci and ii) some $CD11c^{+}F4/80^{+}$ cells are identifiable in the red pulp of both groups of mice, but that in each group, not all red pulp AFC (large IgM^{+} cells) are close to identified $CD11^{+}F4/80^{+}$ cells. The inoculations received by the mice are listed above each column. Images in one column are of the same splenic area. The colour coding for the antigens (and NP-binding cells) visualized in each image are shown in the top left corner of the image. All images taken at 10x original objective magnification. Blue box in lower right panel indicates area magnified in Figure 6-20.

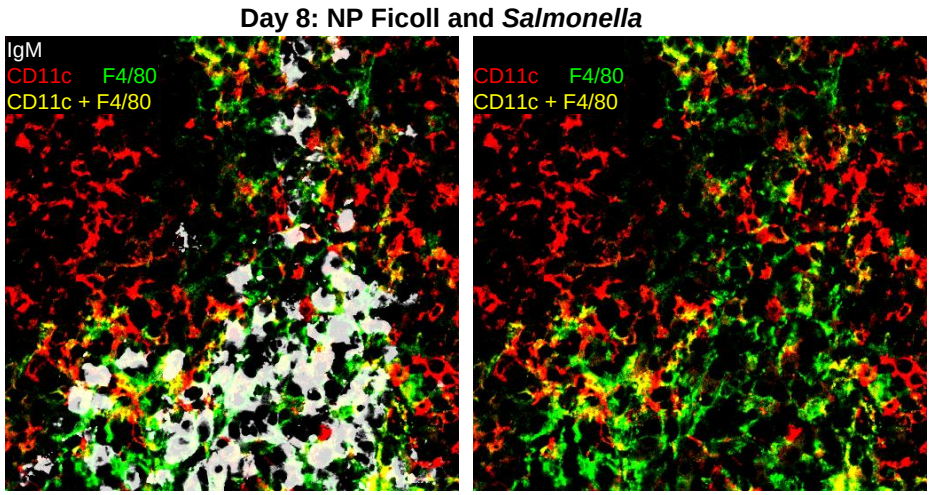

Figure 6-20 shows magnified images of an extra-follicular focus of AFC 8 days after NP-Ficoll with co-infection. Areas flanking the T zone and margin contain $CD11c^{+}F4/80^{-}$ cells, while the extra-follicular focus contains $CD11c^{+}F4/80^{+}$ cells and $CD11c^{-}F4/80^{+}$ cells.

Both images are of the same splenic area, which is also seen within the blue box in lower right panel of Figure 6-19. The colour coding for the antigens (and NP-binding cells) visualized in each image are shown in the top left corner of the image. All images taken at 63x original objective magnification.

6.7.2 An expansion in supportive niches near splenic trabeculae may accommodate some of the additional AFC sustained during infection.

Previous publications have reported that red pulp AFC aggregate around collagen fibres or trabeculae [45;133]. We thus considered the possibility that these structures support the additional plasma cells sustained in the red pulp of infected mice. Eight days after immunization with NP-Ficoll, some but not all red pulp NP-specific AFC are found near trabeculae that bind antibodies raised against human collagen III, and which appear to traverse the red pulp (Figure 6-21A). The specificity within mice of this cross reactive polyclonal antibody is not known, though splenic red pulp trabeculae also bind antibodies to laminins [121]. The same structures are identified by antibodies to ER-TR7 antigen [242] (see Appendix 5).

Interestingly, 8 days after immunization and co-infection with *S.* Typhimurium, increased numbers of NP-specific AFC were seen clustered around these trabeculae though additional NP-specific AFCs were also seen scattered elsewhere in the red pulp.

This association raises the possibility that the trabecular structures might themselves contribute to plasma cell survival either by direct interaction with plasma cells or by providing a niche where plasma cell-sustaining cells gather. Plasma cells express surface receptors that bind to extra-cellular proteins including fibronectin and some collagens [243;244]. Furthermore, signals transduced by one of these - VLA-4 - can enhance plasma cell survival, at least *in vitro* [160].

The association between the trabeculae and NP-specific AFCs was more closely examined in eight serial sections from the spleen of a mouse 8 days after infection and immunization. All sections were stained for NP binding, and with the antibody against human collagen III. Two separate trabeculae, that both had associated AFC aggregates, were followed through the multiple sections. Whilst this confirmed the close proximity of NP-specific AFCs to the trabeculae, at least some of the AFC in these clusters were not visibly in direct contact with the anti-collagen III stained fibres themselves (Figure 6-22).

Thus it appears that some red pulp NP-specific AFCs generated in the response to immunization reside in niches that are close to splenic trabeculae, but these niches are not defined by the trabeculae themselves. Further studies are required to characterize all the components of these peritrabecular zones. There may be other microenvironments in the red pulp that sustain plasma cell survival for a minority of red pulp plasma cells do not associate with fibrous trabeculae.

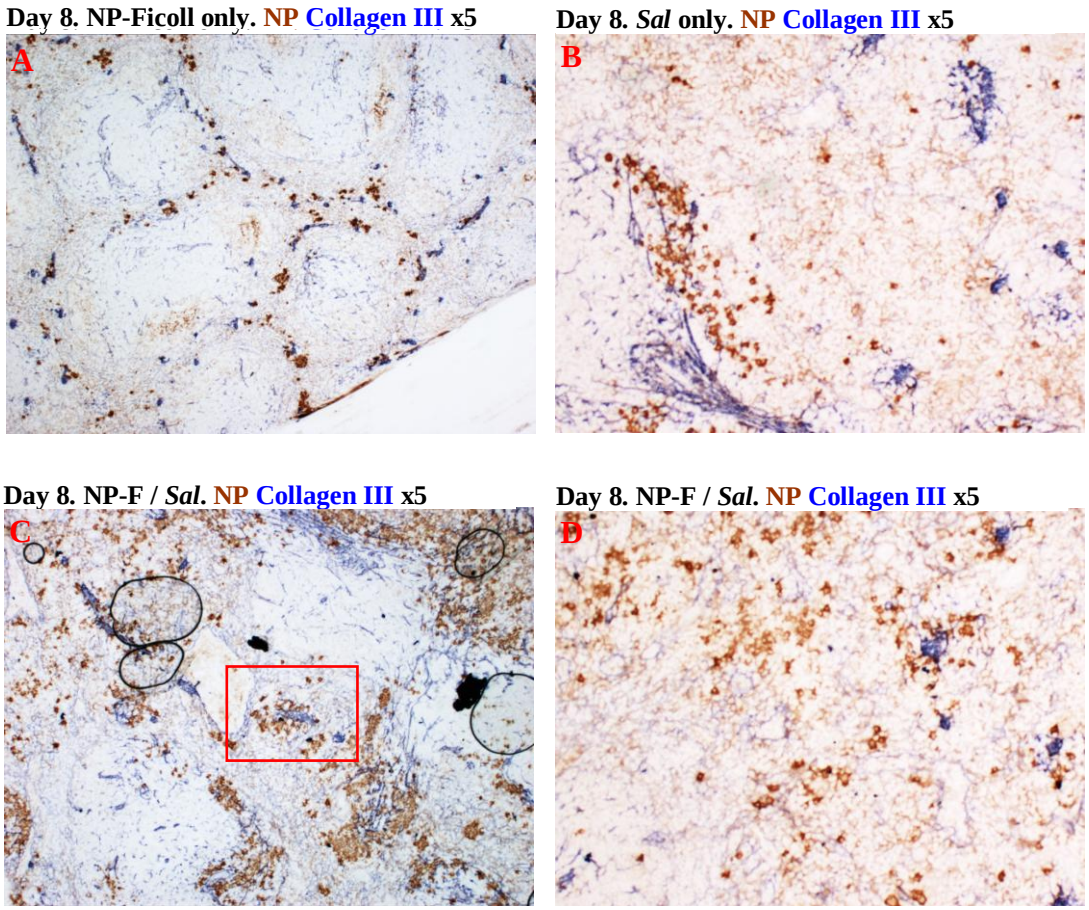

Figure 6-21 shows photomicrographs demonstrating that eight days after immunization with NP-Ficoll, some NP-specific AFCs are found clustered near splenic trabeculae that bind antibody raised against human collagen III, and that immunization and co-infection increases the number of such cells, but that infection *per se* does not.
Photomicrographs of splenic sections immunohistochemically stained with anti-human collagen III (blue) and with NP (brown), from representative mice sacrificed 8 days after **(A)** immunization with NP-Ficoll, **(B)** infection alone and **(C and D)** immunization with co-infection (two separate mice). After immunization some NP-specific AFCs are associated with trabeculae. The number of trabecula-associated cells is increased in co-infected mice. Infection alone is not associated with clusters of NP-specific AFCs around the trabeculae. Red box in panel C denotes approximate area shown in 8 serial sections in Figure 6-22. Images taken at x5 original objective magnification.

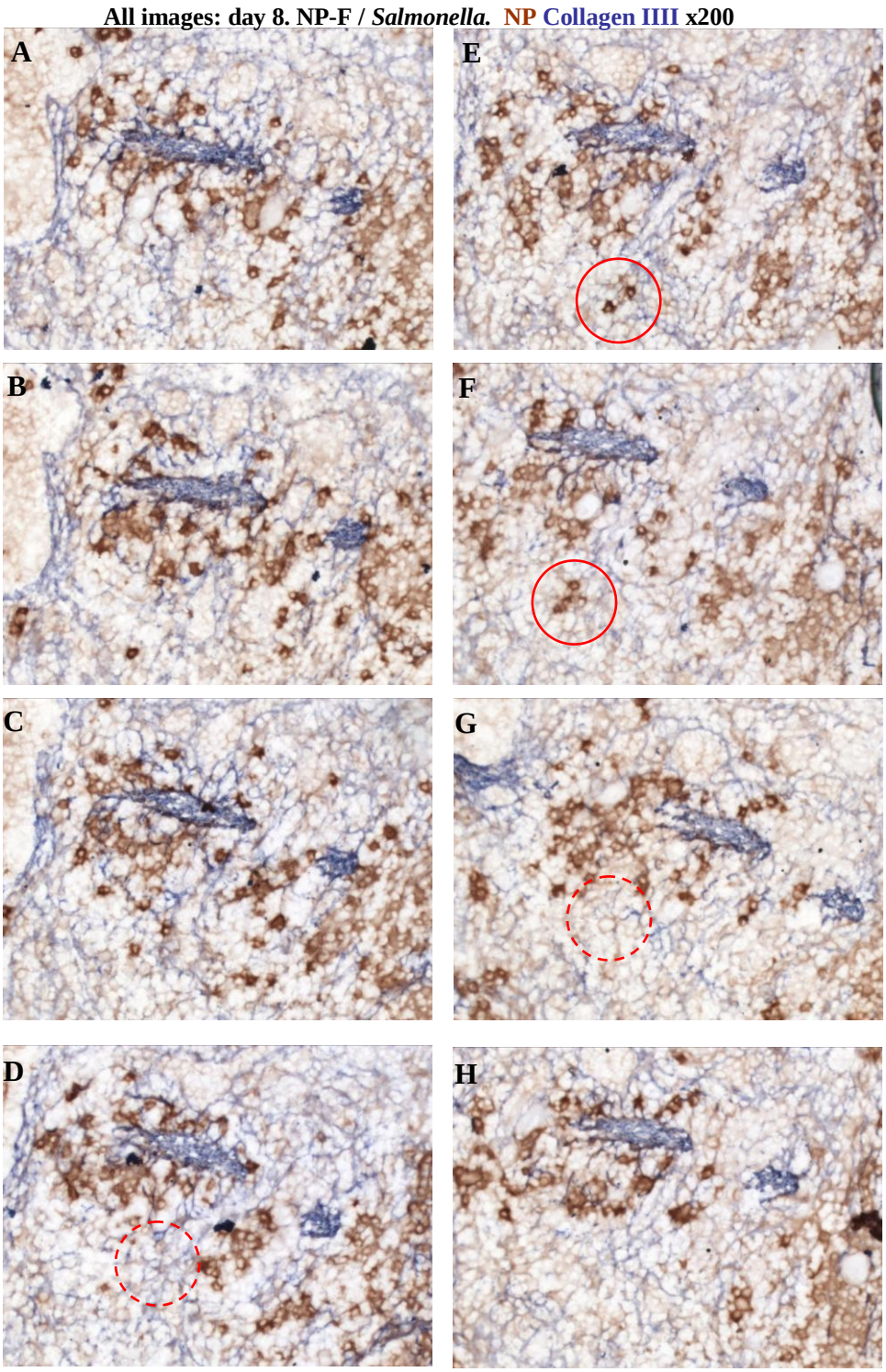

Figure 6-22 shows photomicrographs of eight serial sections through the spleen of a mouse 8 days post immunization with NP-Ficoll and co-infection, showing that some NP-specific AFC clustered around trabeculae are not in direct contact with the anti-collagen III stained fibres. Serial sections **(A-H)** were taken from the same mouse shown in Figure 6-21 (right image), and immunohistochemically stained with anti-human collagen III (blue) and with NP (brown). Red circles highlight the same cluster of AFC in two serial sections, close to, but not in contact with a bundle binding anti-collagen III antibody. Dotted red circles indicate the comparable areas in sections on either side, demonstrating the outer limits of the cluster.

6.7.3 Clusters of BP3$^+$ cells become prominent in the splenic red pulp of *S.* Typhimurium-infected mice, but are not consistently associated with plasma cells.

BP3$^+$ nurse like cells are present within the bone marrow, but also the inflamed rheumatoid joint [161]. Furthermore, rheumatoid BP3$^+$ cells are reported to produce IL-6 *in vitro* [161]. We thus considered the possibility that such BP3$^+$ cells could contribute to splenic plasma cell survival within the model studied here.

In non-immunized mice, a diffuse reticular staining pattern is seen with anti-BP3 antibody in the T zone, and inner B cell follicle. In addition isolated cells in the red pulp are also stained (Figure 6-23). These cells are not consistently associated with the small numbers of NP-specific AFC found in the red pulp of control mice.

Sections from mice 8 days after immunization with NP-Ficoll with or without co-infection with *S.* Typhimurium, were stained in parallel. In mice immunized with NP-Ficoll alone, the staining pattern was similar to that in naïve mice. In contrast, 8 days after immunization and co-infection with *S.* Typhimurium, the reticular staining for BP3 was less clear. Multiple clusters of cells staining for BP3 were seen in the red pulp. Some NP-specific AFC were seen on the outer rim of these BP3$^+$ clusters, but many plasma cells were distant from BP3$^+$ cells and some clusters of BP3$^+$ cells had no associated AFC (Figure 6-23). In mice infected with *S.* Typhimurium only, it was striking that the extrafollicular foci were located within the reticular network of BP3 positivity associated with the white pulp.

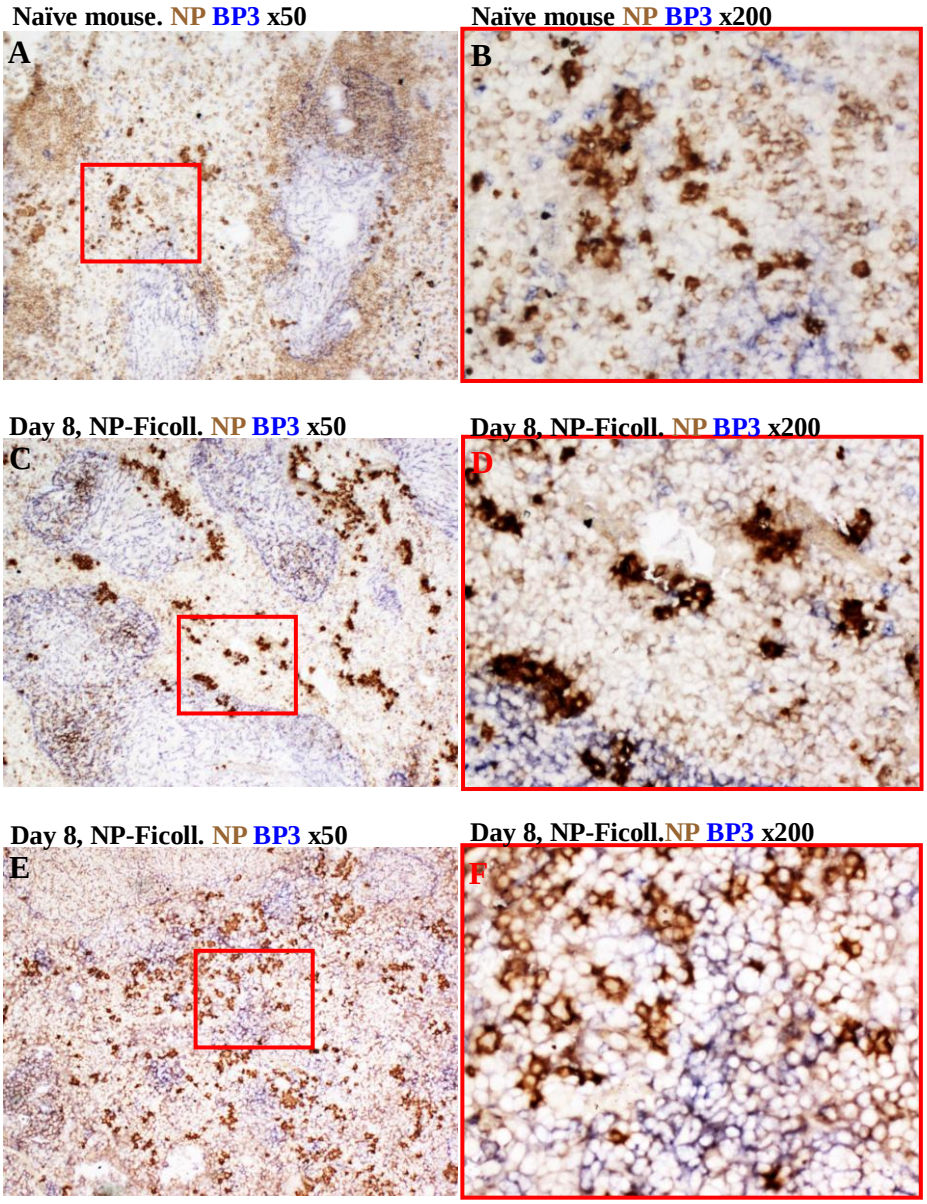

Figure 6-23 shows representative photomicrographs of splenic sections from non-immunized mice, and from mice 8 days after immunization with or without co-infection. Both are stained for BP3 antigen and NP binding. These show that infection increases the red pulp area stained with anti-BP3, but that these areas are not directly associated with NP-specific AFC.
In each row the right image (x200 microscope magnification) shows in detail the area enclosed in the red box in the left image (x50 microscope magnification). In naïve mice (**panels A and B),** and mice 8 days after immunization with NP-Ficoll (**panels C and D**) reticular expression of BP3 (blue) is seen in the T zone, and inner part of the B cell follicle. Isolated cells in the red pulp are also $BP3^+$, but NP-specific AFC (dark brown) are not consistently near the $BP3^+$ cells. In mice 8 days after immunization with co-infection (**panels E and F**) increased clusters of cells within the red pulp stain $BP3^+$, but few NP-specific AFC are amongst them.

6.7.4 CD169$^+$ cells are confined to the splenic marginal zone and not associated with AFC.

In a different experimental model used in our laboratory AFC appear associated with CD169$^+$ cells [130]. We thus considered the possibility that CD169$^+$ cells co-localise with splenic AFC in this model, and contribute to their survival.

Confocal microscopy was used to study the location of CD169$^+$ cells in non-immunized mice, and those 8 days after either immunization with NP-Ficoll, or after infection with *S.* Typhimurium and immunization with NP-Ficoll (Figure 6-24). In contrast to the other model, CD169$^+$ cells were confined to the marginal zone in the spleens of QMxB6 mice, irrespective of infection with *S.* Typhimurium. They were not associated with red pulp IgM$^+$ AFC.

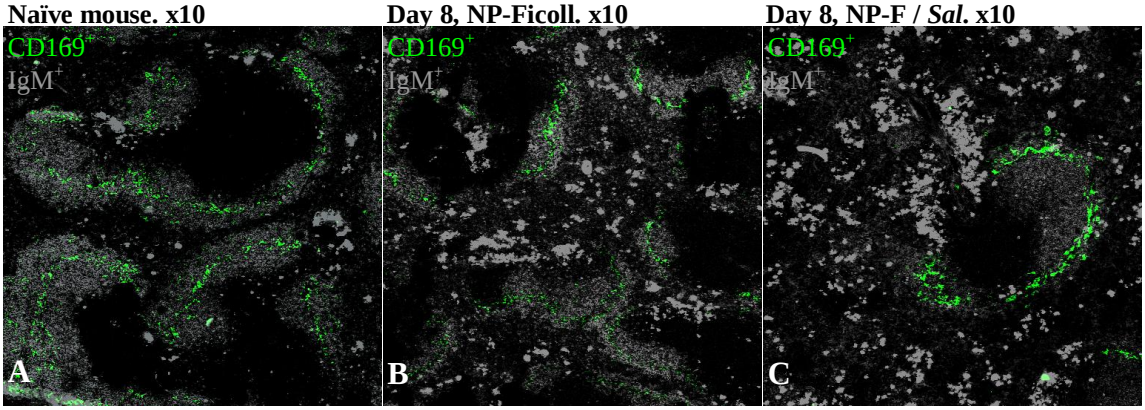

Figure 6-24 shows images from con-focal microscopy demonstrating that CD169$^+$ cells are confined to the splenic marginal zone, irrespective of immunization with NP-Ficoll, or co-infection with *S.* Typhimurium.
Representative splenic sections from **(A)** a non-immunized mouse, **(B)** a mouse 8 days after immunization with NP-Ficoll, and **(C)** a mouse 8 days after immunization and co-infection. CD169$^+$ cells appear green. These are confined to the splenic marginal zone, amongst small IgM$^+$ B cells (grey). Larger IgM$^+$ cells, AFC, are predominantly confined to the red pulp. All images were taken with x10 objective magnification.

6.8 Investigating the splenic expression of mRNA for known AFC chemotaxis, differentiation and survival factors.

There are likely to be two main components contributing to the long term survival of AFC:

(i) The presence of niches that provide factors that support long term survival.

(ii) Factors that induce AFC to home to these niches.

Splenic changes in either component could impact upon observed numbers of mature plasma cells in the splenic red pulp. Possible changes in both of these components associated with immunization and or infection are considered in this section.

The migration of AFC appears to occur in two phases: first the migration of activated B blasts from the T zone to extrafollicular foci, where the AFC grow as plasmablasts. The second phase is where mature plasma cells locate in niches in the splenic red pulp that secure their long term survival. In addition some of the AFC leave the spleen and find survival niches in the bone marrow. This movement from spleen to bone marrow and the bone marrow niches are not considered in this study.

The migration from the outer T zone to extrafollicular foci is coordinated by expression of chemokines and their receptors [133;134] and coincides with the differentiation of $CD138^{-}Blimp\text{-}1^{-}$ B blasts to $CD138^{+}Blimp\text{-}1^{+}$ plasmablasts [238;245]. The chemokine CXCL12 is chemotactic for plasmablasts which constitutively express the appropriate receptor CXCR4 [133;134]. This ligand-receptor pair contributes to homing of plasma cells to the bone marrow [133]. Expression of CXCR4 is maintained on most bone marrow plasma cells. These plasma cells do not respond to CXCL12 by migration [134],

although the interaction between this chemokine and its receptor may stabilize the localization of AFC in the marrow. There are conflicting reports of *in vitro* work as to whether CXCL12 supports plasma cell survival [149;162].

Available evidence indicates that a proportion of plasmablasts migrate towards CXCL9 or CXCL10 or CXCL11 [134]. All three chemokines are induced in cells of the monocyte-macrophage lineage (amongst other cell types) by stimulation with γ-IFN [138;139]. Furthermore, CXCL10 and CXCL11 are induced following direct lipopolysaccharide (LPS)-mediated activation of macrophages [147;148] and γ-IFN also acts synergistically on this response [147]. The receptor for all three of these chemokines is CXCR3, which itself can be upregulated by γ-interferon, at least *in vitro* [14]. There is no published evidence for, or against, the possibility that ligands for CXCR3 promote survival of any CXCR3-expressing plasma cells *in vitro* or *in vivo*.

Certain cytokines are known to favour AFC differentiation and survival. These have been most extensively studied *in vitro*, and in the context of bone marrow plasma cells *in vivo*.

IL-6 by itself can enhance plasma cell survival *in vitro,* though its efficacy is very much greater when acting synergistically with other plasma cell supporting factors [162]. Its *in vivo* role is less clear; long term antibody responses are reported to be unaffected in $IL6^{-/-}$ mice [162], though in the short term (up to 10 days after secondary immunization) the antibody response appears reduced. This may be due to an impact of IL-6 upon cell proliferation [246], and may be of relevance in the model studied here. Cassese et al also reports a modest *in vitro* effect of TNF-α on plasma cell survival [162].

IL-21 is one of a group of cytokines whose receptors share a common γ chain [247]. It is reported to act in concert with B cell receptor ligation to promote the production of Blimp-1 and thereby the terminal differentiation of B cells into plasma cells [184].

O'Connor et al have reported a non-redundant role for BCMA-mediated signalling in achieving bone marrow plasma cell survival [165]. Published data on adult mice indicates this is mediated via APRIL, one of the ligands for BCMA, but not by BCMA's other ligand BAFF [179].

The role of these various factors in splenic plasma cell survival is less clear. In contrast to their findings in bone marrow, Belnoue et al state (but do not provide data to show) that 48 hours after in-*vivo* transfer of antigen-specfic AFCs, the splenic recovery of these AFC was no different in $BAFF^{-/-}$ or $APRIL^{-/-}$ recipient mice compared to wild type recipient controls [179]. Furthermore bone marrow stromal cells sustain *in-vitro* plasma cell antibody production more effectively than splenic stromal cells, despite higher IL-6 production by the splenic cells [149].

The role of any of these factors in enhanced plasma cell survival in the context of splenic inflammation is not reported. Furthermore, such cytokines and chemokines may be produced by more than one cell type. When this is the case there would be sporadic rather than universal association of AFC with each of the different cell types that produced AFC-survival factors; a situation that makes interpretation of histological associations difficult.

Immunohistochemical staining of cytokine-producing cells in tissue sections generally has proved unreliable. Consequently two alternative approaches were used. In each, levels of cytokine mRNA were quantified using real time reverse transcriptase

polymerase chain reaction assays (RT_2-PCR). First levels of mRNA transcripts that encode for various cytokines, or chemokines, and their receptors, were measured in spleen cell suspensions from the different groups of mice. Although this will identify if leucocyte-produced cytokine message has increased it does not localize the cytokine production and would fail to detect cytokines produced by stromal cells that were not contained in the cell suspensions studied. Consequently mRNA levels were also assessed in microdissected areas taken from tissue sections.

In keeping with conventional methodology, changes in levels of mRNA species of interest were normalized by reporting changes relative to levels of reference gene mRNA in the same samples. Cellular levels of mRNA for reference genes (β_2-microglobulin and β-actin) are usually assumed to be unaffected by experimental conditions. However, total splenic cell numbers increase substantially following infection with *S.* Typhimurium, and all cells will express the reference gene mRNA. As only a subset of the cells is likely to be producing a plasma cell survival factor any observed increases in normalised levels of mRNA for the survival factor of interest will underestimate the upregulation of expression in the cell subset producing the mRNA for the factor.

Assays were also performed on the same tissues to estimate levels of mRNA encoding for BCMA, which in the spleen is solely expressed on differentiated AFC. This confirms that increases in BCMA mRNA levels following immunization, or infection, or both, broadly reproduce corresponding increases seen in total $CD138^+$ cell numbers as estimated by flow cytometry (Figure 6-25). For this reason BCMA mRNA levels have been used as a comparator with levels of different cytokines reported in Figure 6-26, Figure 6-30, and Figure 6-31.

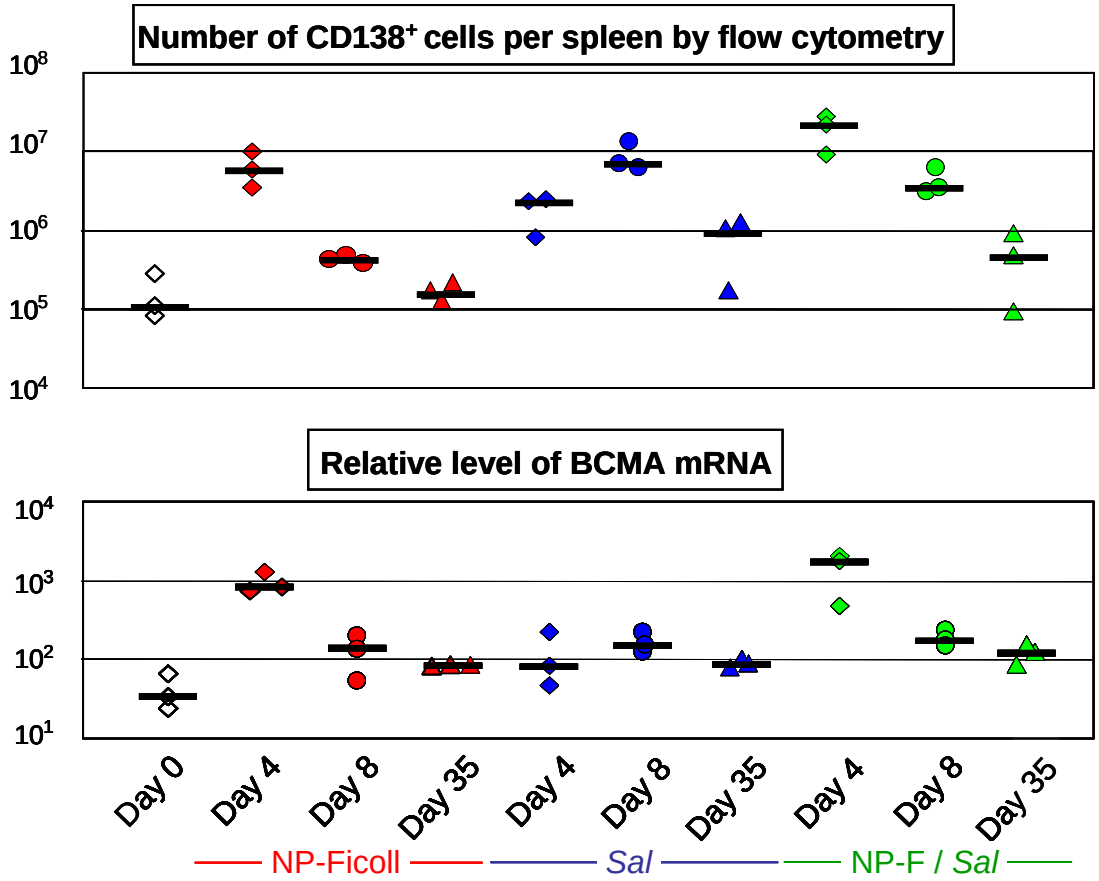

Figure 6-25 shows changes induced by immunization, infection or both in the absolute numbers of splenic CD138$^+$ cells reflect concurrent changes in relative levels of BCMA mRNA in splenic leucocyte suspensions.
Each symbol shows values for one mouse. Absolute numbers of CD138$^+$ cells were estimated by flow cytometry, and are replotted from Figure 6-5A. Levels of BCMA mRNA were measured by RT_2-PCR, and are reported relative to levels of β_2-microglobulin reference gene mRNA in the same sample.

6.8.1 In spleen cell suspensions infection induces mRNA for CXCR3-binding chemokines while the NP-Ficoll response in non-infected mice upregulates message for CXCR4-binding chemokine.

Changes in levels of mRNA for CXCL9, CXCL10, CXCL11 and CXCL12, were assessed by RT_2-PCR, in spleen cell suspensions from mice immunized with NP-Ficoll, infected with *S.* Typhimurium, or both. Consistent with published reports, levels of CXCL9, CXCL10 and CXCL11 increase substantially following infection, and

irrespective of co-immunization, but changes in these chemokines are modest after immunization alone. By contrast, increases in CXCL12 were greater in immunized but non-infected mice (Figure 6-26). Thus compared with naïve mice, peak median levels of CXCL9 mRNA were 11 fold above baseline, CXCL10 were 20 times baseline and 26 fold for CXCL11. By comparison immunization without infection resulted in changes that were never more than 4-fold above baseline for any of these chemokines. Unlike γ-IFN levels which were highest at day 35 after infection the levels of these chemokines, in parallel with the numbers of plasma cells declined between d8 and d35. Conversely the chemokine upregulation occurred earlier than that of γ-IFN, key cytokine produced in the T-helper type 1 (T_H-1) protective response against *S.* Typhimurium infection. These data raise the possibility that increased splenic expression of CXCL9, CXCL10 or CXCL11 during *S.* Typhimurium could alter the migration patterns of emergent NP-specific plasmablasts, if such AFC express CXCR3.

6.8.2 CXCR4 protein is expressed on the surface of AFC from all groups of mice although some late switched plasma cells, again from all groups of mice, express CXCR3.

We sought evidence of increased CXCR3 expression within the spleen of infected mice as: i) spleens of infected mice have increased splenic expression of CXCL9, and CXCL10 and CXCL11 (section 6.8.1 above); ii) some AFC migrate towards these chemokines [134] and iii) γ-IFN can increase expression of CXCR3 on AFC [14] In the first instance RT_2-PCR of splenic cell suspensions was used to assess levels of mRNA for CXCR3 as well as CXCR4, which is expressed on most AFC [133].

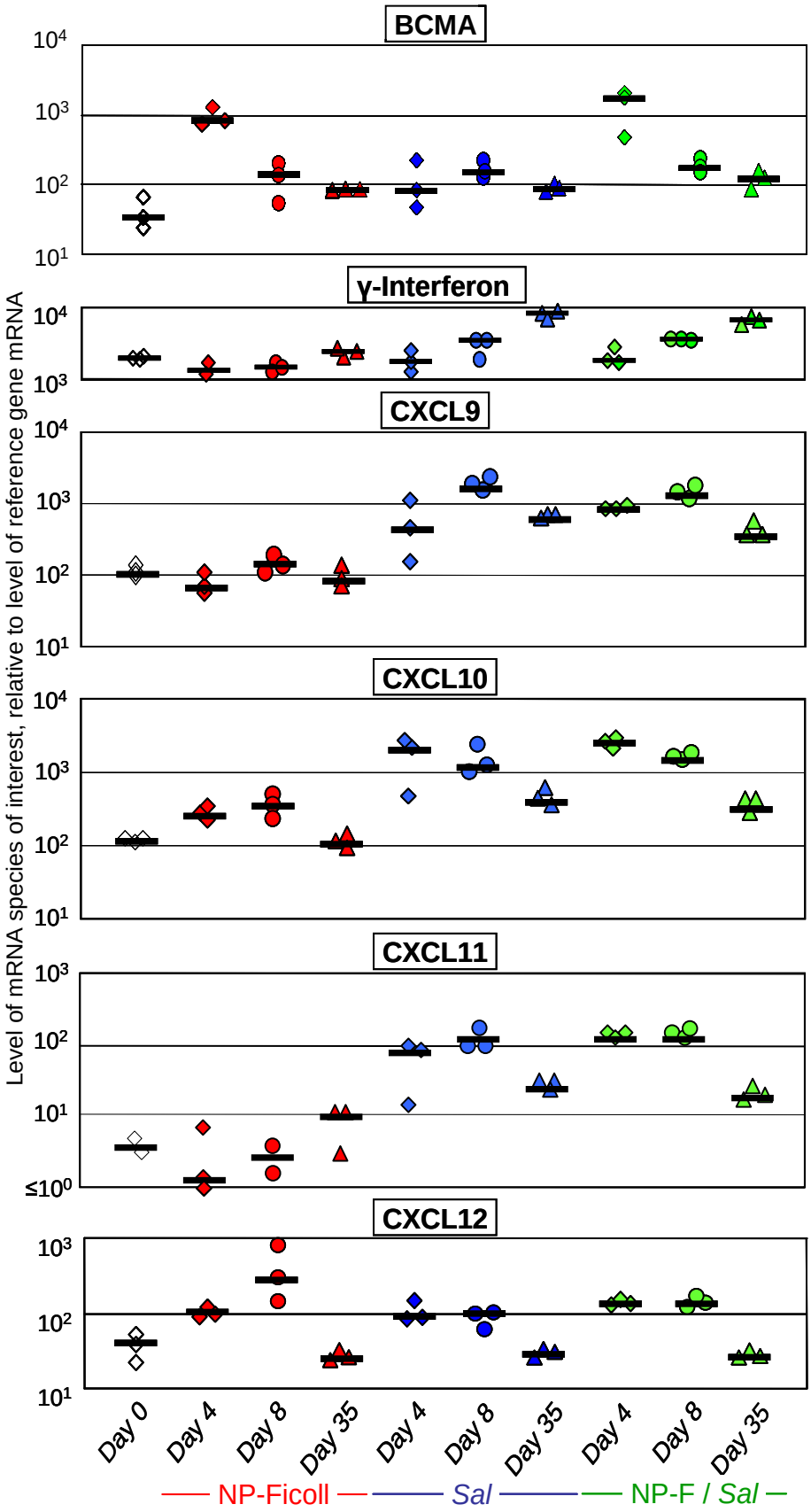

Figure 6-26 shows that in splenic cell suspensions, levels of mRNA for γ-IFN, and CXCL9, CXCL10, and CXCL11, but not CXCL12, increase more after infection than after immunization. Each symbol represents values from one mouse. Levels of mRNA were measured by RT_2-PCR and are all reported relative to reference gene (β2-microglobulin) mRNA levels in the same sample. Where less than three symbols are shown per group, no mRNA was detected in samples from unreported mice. Changes in BCMA mRNA levels, which broadly reproduce changes in $CD138^+$ cell numbers estimated by flow cytometry, are shown for comparison.

The results of these experiments are shown in Figure 6-27. Levels of CXCR3 mRNA in spleen cell suspensions were little changed after either infection, or immunization, or both. Surprisingly, levels of CXCR4 mRNA were found to be lower than baseline for at least 8 days after all types of inoculation. This decrease was most marked in infected mice.

These findings contrast with the changes in BCMA mRNA following inoculation, which are represented on the same figure – and which are a reasonable surrogate for total $CD138^{+}$ cell numbers in these mice. It can be concluded from this that much of the CXCR3 and CXCR4 expressed within the leucocyte suspension is not present in AFC. At least in CD4 T cells, surface turnover of CXC4 can be substantial and intracellular stores exist, thus dissociation of mRNA levels from surface expression of the corresponding protein is likely [153;248].

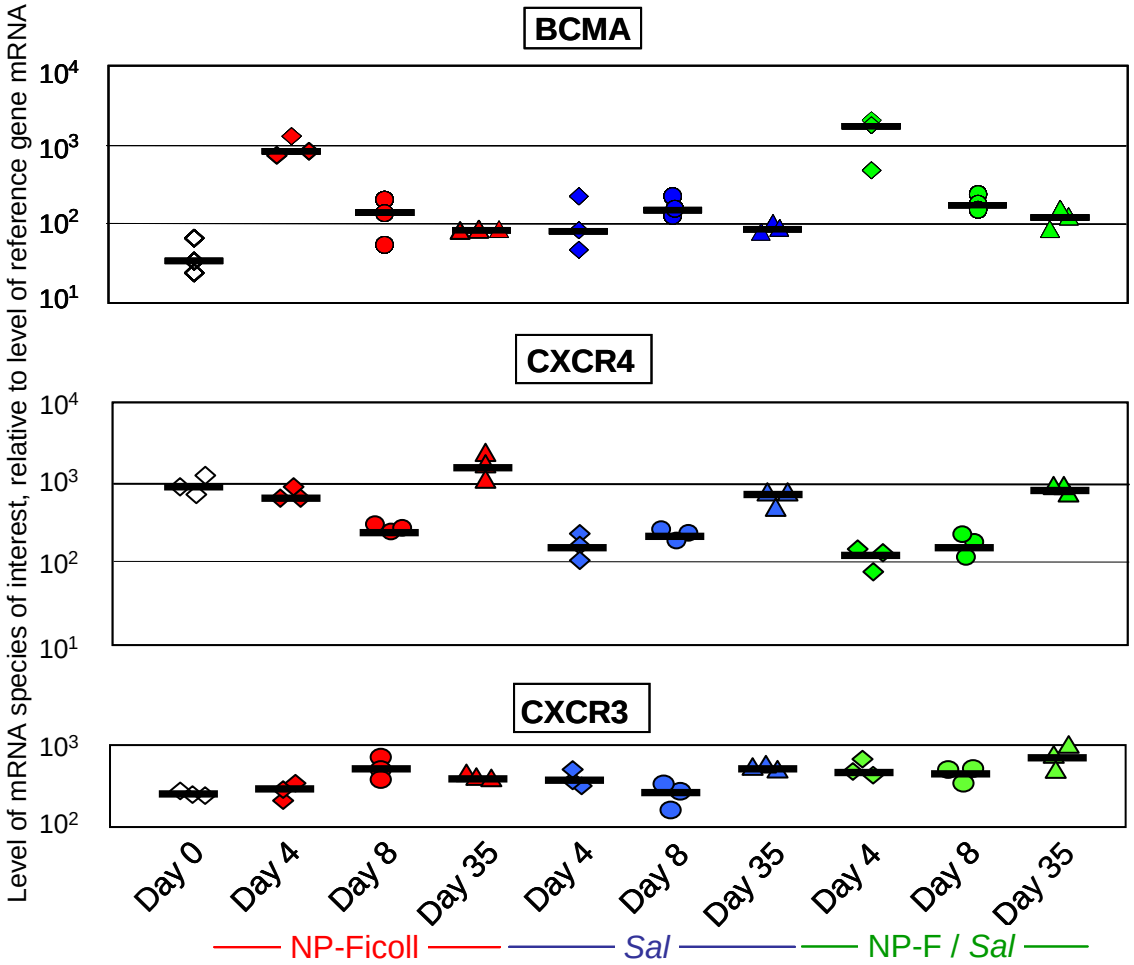

Figure 6-27 shows that in spleen cell suspensions, relative levels of CXCR4 mRNA are below baseline levels for at least 8 days after immunization, or infection or both, whilst CXCR3 mRNA levels change little in the same mice, over the same time.
Figure also shows contemporary changes in BCMA mRNA that reflect changes in splenic $CD138^+$ cell numbers. Each symbol represents values from one mouse. Levels of mRNA were measured by RT_2-PCR and are reported relative to levels of β_2-microglobulin reference gene mRNA in the same sample.

Given these difficulties with the assessment of CXCR3 and CXCR4 expression on AFC by mRNA, in the repeat experiment the surface expression of these molecules on NP-specific AFC was assessed by flow cytometry. Technical issues precluded co-staining for CD138 expression with either chemokine receptor, so intracellular NP^{high} staining was used to identify NP-specific AFC. As most NP-specific AFC generated after infection alone are NP^{int} (Figure 6-4), AFC chemokine expression could not be studied in these

mice. Representative flow cytometry dot plots for mice that were immunized, and those that were immunized and co-infected, are shown in figure Figure 6-28.

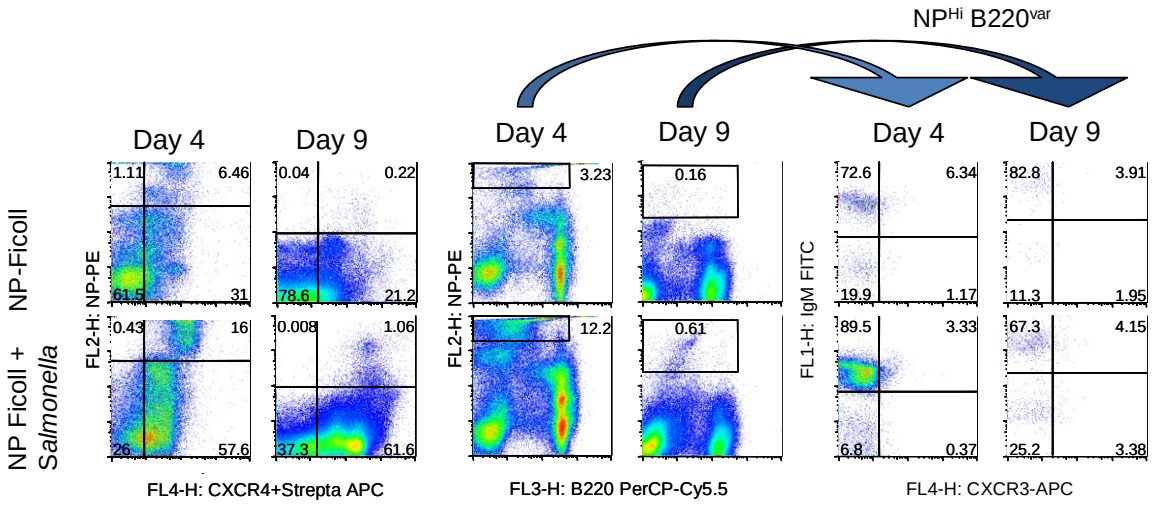

Figure 6-28 shows that although NP-specific AFC express CXCR4 they are only a small proportion of the CXCR4-expressing cells in the spleens of responding mice and few AFC express CXCR3 and these are mainly a subset of non-switched AFC in co-infected and immunized mice.
The 2 left columns show representative dot plots CXCR4 expression related to cytoplasmic+surface NP binding. The centre columns show gated cells showing cytoplasmic + surface NP-binding and the right two columns IgM and CXCR3 expression in the gated NP-specific AFC.showing the proportion of NP-specific AFC that are $CXCR4^+$, and the proportions of IgM NP-specific AFC and isotype switched NP-specific AFC that are $CXCR3^+$, at 4 and 9 days after immunization, with or without co-infection. Numbers on the dot plots show the percentage of cells in the corresponding gate.

In all mice studied at day 4 - irrespective of inoculation received - more than 95% of NP-specific AFC had detectable CXCR4 expression (Figure 6-29, top left panel). CXCR4 expresion was also detectable on more than 85% of NP-specific AFC in each of the day 9 mice. Amongst the few mice studied it appeared that the the proportion of NP-specific AFC expressing CXCR4 was slighly lower in uninfected mice than their infected peers. Importantly only a small proportion of the cells expressing CXCR4 are NP-specific AFC.

Surface expression of CXCR3 was examined separately on IgM^+ NP-specific AFC and isotype-switched NP-specific AFC. At both timepoints studied, most NP-specific AFC were IgM^+ (Figure 6-29, top right panel). Irrespective of timepoint studied or inoculation receieved, fewer than 10% of IgM^+ NP-specific AFC were $CXCR3^+$ (Figure 6-29, bottom

left panel). At 4 days after either inoculation, a median of 5% of isotype switched NP-specific AFC are $CXCR3^+$. (Figure 6-29, bottom right panel). Strikingly, however, the proportion of splenic isotype-switched NP-specific AFC that are $CXCR3^+$ in all day 9 mice is signifcantly higher than that in all day 4 mice ($p<0.01$, Mann Whitney test). It was not possible to discern any additional effect of infection on the proprotion of isotype switched NP-specific AFC were $CXCR3^+$ at day 9.

It is tempting to conclude that the rise in the proportion of isotype switched NP-specific AFC that express CXCR3 reflects either i) preferential retention of $CXCR3^+$ AFC in the spleen or ii) a survival advantage for such AFC relative to other AFC retained within the spleen. Two other observations from these data do not concur with this:

i) at day 4, the proportion of IgM^+ NP-specific AFC that are $CXCR3^+$ is not less than the proportion amongst the switched NP-specific AFC – and no equivalent enrichment for CXCR3 expressing IgM NP-specific AFC is seen between day 4 and day 9.

ii) the proportion of isotype switched NP-specific AFC that are $CXCR3^+$ increases between 4 and 9 days after immunization alone – but the proportion of all splenic NP-specific AFC that is isotype switched does not (Figure 6-29, top right panel).

These results still need to be repeated, but an alternative explanation is possible. The median proportion of day 9 NP-specific $CD138^+$ cells that were $BrdU^-$ was 25% in immunized mice, and 57% in immunized and co-infected mice (see Figure 6-12). Thus many AFC present at day 9 developed after day 5. Any alteration, between day 4 and day 9, in the proportion of newly emergent AFC that are $CXCR3^+$ could influence the

proportion of prevalent AFC that are CXCR3$^+$ at day 9. This scenario seems most plausible in the context of evolving *S.* Typhimuruim infection though it remains unproven, and could be the subject of future work.

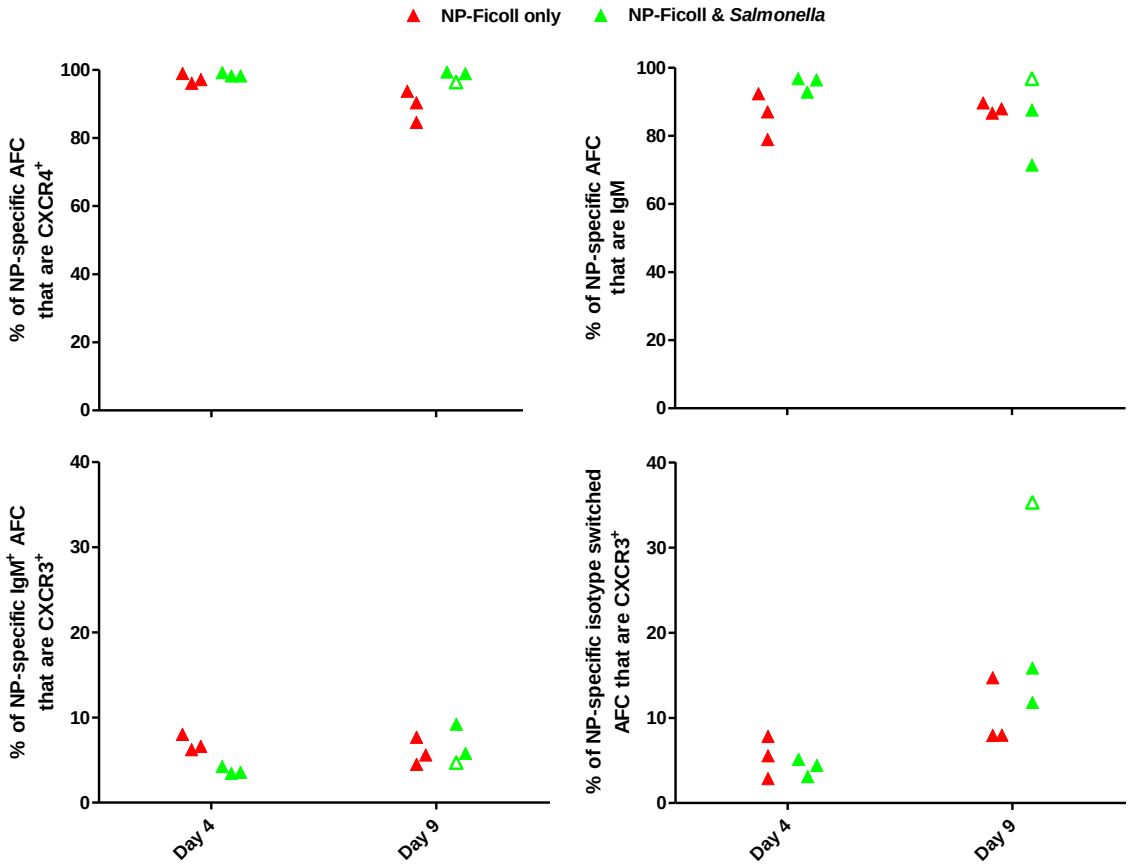

Figure 6-29 shows the proportion ofNP-specific AFC that express CXCR4$^+$ or CXCR3$^+$.
Each symbol shows values for one mouse. The legend for the symbols is above the figure. The open triangle represents one mouse that was inoculated with NP-Ficoll and *S.* Typhimurium, but did not develop splenomegally or any other signs of infection.

B blasts usually migrate from the white pulp as they differentiate into plasmblasts; i.e. the migration occurs in proliferating cells. Thus the plasma cells that at day 9 retain BrdU taken up before day 6 are likely to have migrated from the white pulp several days before. The continued expression of CXCR4 in day 9 plasma cells may refect retention in red pulp niches rater than migration to these niches. The high splenic levels of CXCL9 or

CXCL10 or CXCL11 seem unlikely to be having influence more than a small proportion of AFC from infected day 9 mice.

6.8.3 Levels of mRNA for IL-6 and IL-21, but not mRNA for TNF-α or BAFF or APRIL, are selectively increased in spleens of mice infected with *S.* Typhimurium.

RT_2-PCR assays were performed to assess changes induced by infection and/or immunization in mRNA encoding the putative AFC survival and maturation factors in spleen cell suspensions. The factors assessed were IL-6, IL-21, TNF-α, BAFF and APRIL.

Levels of IL-6 and IL-21 mRNA are increased more after infection than after immunization (Figure 6-30). In contrast levels of mRNA for TNF-α, BAFF and APRIL changed remarkably little following any inoculation (Figure 6-31).

Amongst both groups of infected mice changes in IL-6 mRNA levels tracked changes in levels of BCMA mRNA and hence, by inference, the numbers of AFC. The highest measured levels of IL-6 mRNA (median 16-fold above baseline) were found at day 4 after infection and co-immunization, whilst levels in infected but not-immunized mice peaked at median 7-fold above baseline, at day 8. In both groups of infected mice, levels of IL-6 mRNA were still elevated at day 35. By contrast, in immunized but not infected mice, no correlation between levels of IL-6 mRNA and BCMA mRNA was seen, and median levels remained within 2-fold of baseline throughout.

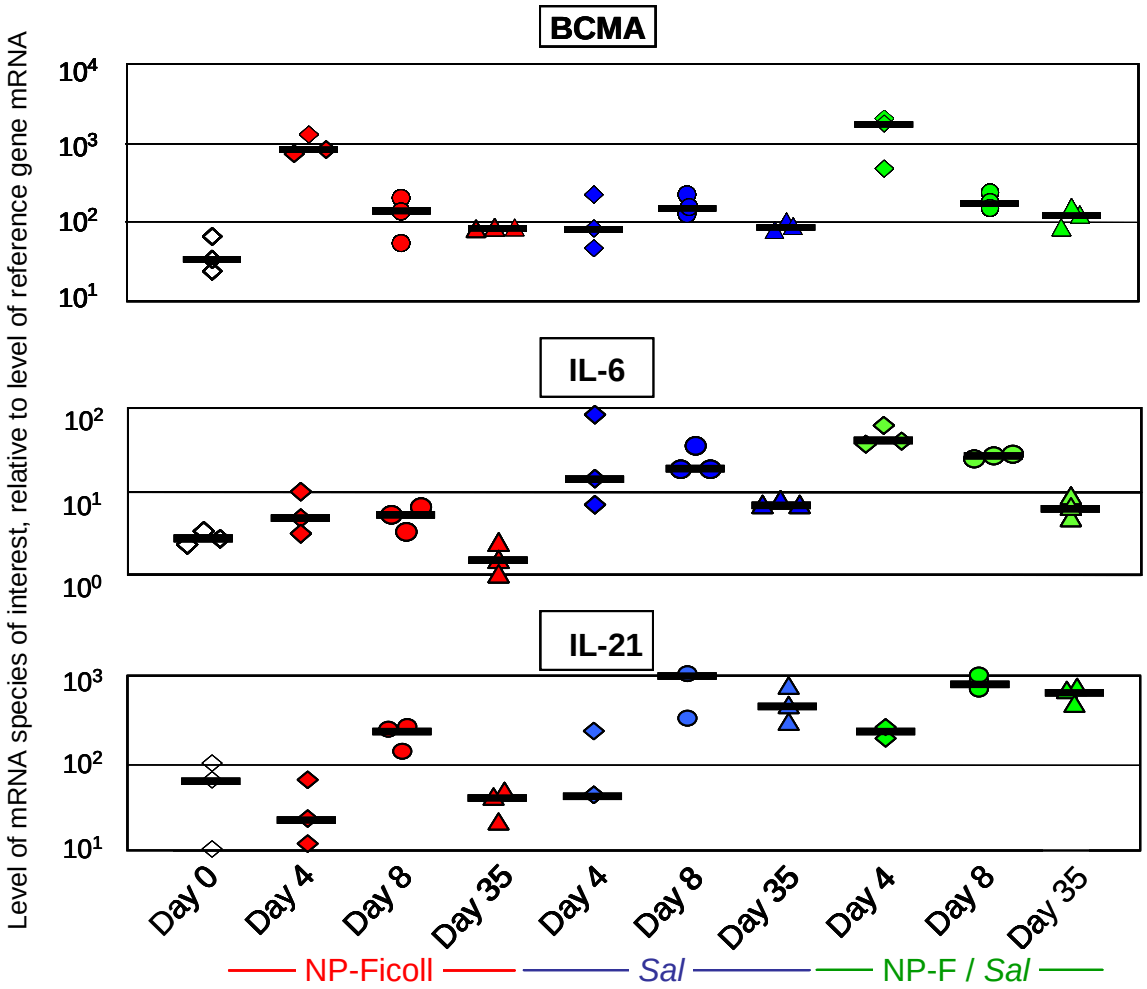

Figure 6-30 shows that in splenic cell suspensions, levels of IL-6 and IL-21 mRNA are more substantially increased after infection, than after immunization.
Each symbol represents values from one mouse. Levels of mRNA were measured by RT_2-PCR and are reported relative to reference gene (β2-microglobulin) mRNA levels in the same sample. Where less than three symbols are shown per group, no mRNA was detected in the samples from unreported mice. Changes in BCMA mRNA levels, which broadly reproduce changes in $CD138^+$ cell numbers estimated by flow cytometry, are shown for comparison.

Irrespective of co-immunization, in infected mice peak levels of IL-21 mRNA were seen at day 8, and the medians were more than 10-fold above baseline. Levels in both these groups declined only marginally by day 35. The only impact of co-immunization of IL-21 mRNA levels was seen at day 4; levels had already begun to climb in this group, whereas they were virtually unchanged in mice that were infected but not immunized. Whereas infection, and to a lesser extent additional co-immunization, has a substantial effect on

IL-21 mRNA levels, immunization alone only resulted in median 3-fold rise in levels seen at day 8.

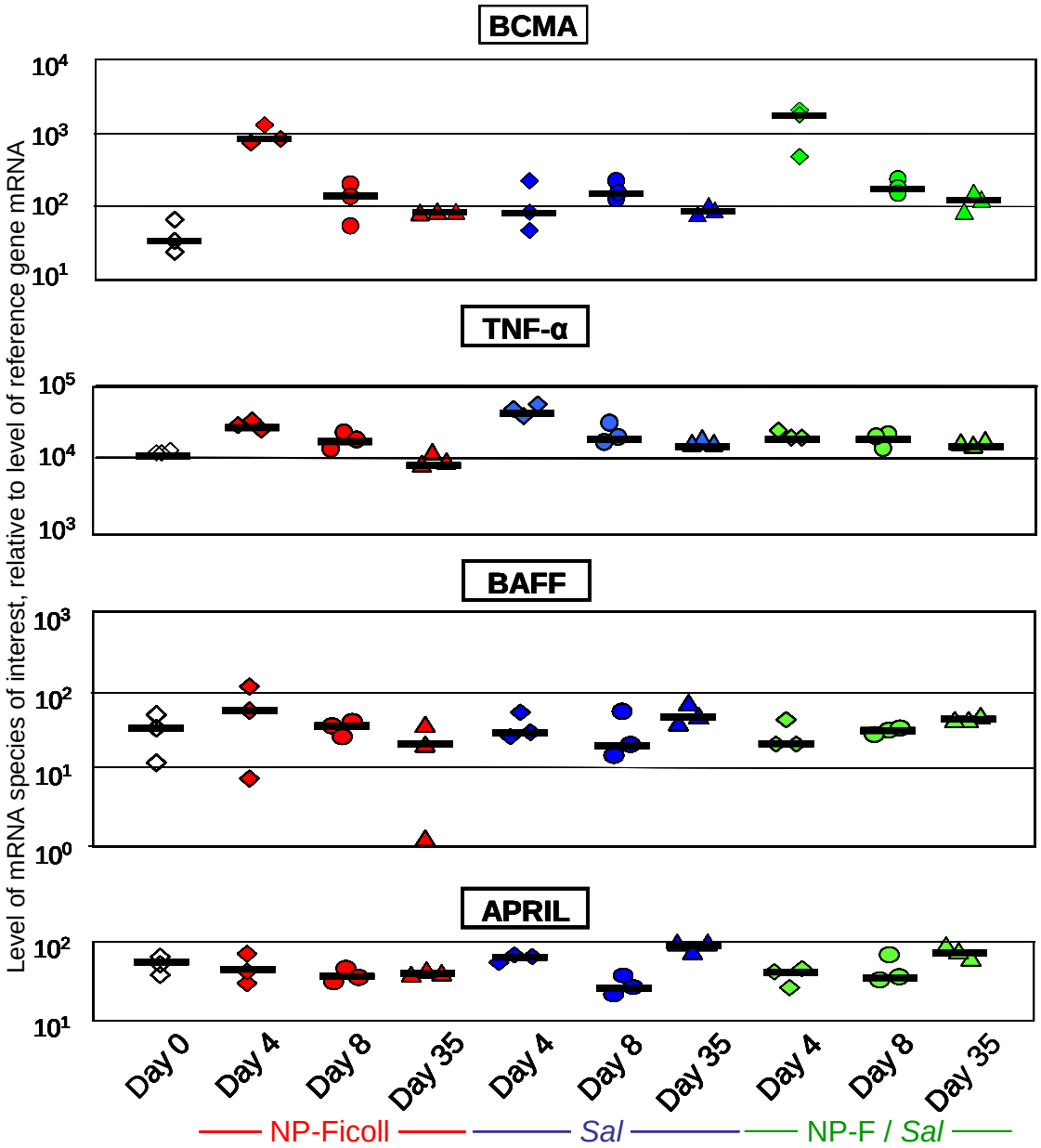

Figure 6-31 shows that in splenic cell suspensions, levels of mRNA encoding for TNF-α, BAFF and APRIL are little changed after infection, immunization or both, and that none of these mRNA species increase more after infection than after immunization.
Each symbol represents values from one mouse. Levels of mRNA were measured by RT_2-PCR and are reported relative to reference gene (β_2-microglobulin) mRNA levels in the same sample. Changes in BCMA mRNA levels, which broadly reproduce changes in $CD138^+$ cell numbers estimated by flow cytometry, are shown for comparison.

Surprisingly, and in contrast to levels of IL-6 and IL-21 mRNA in spleen cell suspensions, levels of mRNA encoding TNF-α, or BAFF, or APRIL changed relatively little after immunization, or infection, or both. Changes in the levels of all 3 mRNA species varied no more than 4-fold different from baseline at any timepoint.

Thus amongst the mRNA species studied here in spleen cell suspensions, only IL-6 and IL-21 mRNA shows increases in levels in bulk splenic cell suspensions that are plausibly associated with the increased numbers of splenic AFC present in *S.* Typhimurium infected mice.

6.9 Estimation of regional variations in mRNA levels within the spleen by RT_2-PCR of laser microdissected sections.

To look for regional variations in the levels of AFC-supporting chemokines and cytokines that can influence AFC-survival *in vivo,* levels of mRNA encoding these were assessed in different compartments of the spleen. In order to obtain reliable data multiple dissected areas, each representative of the compartment of interest, are needed. Multiple sections of a tissue are cut and placed on a single, membrane coated slide, which is subsequently stained with cresyl violet to assist the identification of compartments within the tissue. However additional localisation techniques are needed to identify splenic compartments with confidence, and AFCs themselves cannot be identified by cresyl violet staining alone. Two additional sections were thus cut before the sections to be used for microdissection, and two additional sections cut after. These four were stained by immunohistochemical techniques. Within each flanking pair, one was stained for NP-specific AFC and for IgD^+ cells, whilst the other was stained for $Ki67^+$, a nuclear marker

of proliferation, and for IgD^+ cells. By cross reference between composite photomicrographs of the immunohistochemically stained slides and the cresyl-violet stained sections we identified AFC-rich and AFC-sparse areas of red pulp, and plasmablast-rich extrafollicular foci for microdissection. In addition areas of B cell follicles with continuous IgD^+ small recirculating B cells ($Ki67^-$ areas) and central T zones were dissected. Further details of this technique are provided in the methods chapter (section 3.3.13.3). Previous work had shown that the majority of red pulp AFC at day 4 and day 8 after immunization or infection or both, were NP-specific IgM^+ AFC, (Figure 6-5, Figure 6-16, and Figure 6-29).

Localisation of splenic compartments by this process, and the laser microdissection itself are highly time-consuming and so only selected tissues that were expected to be informative were to be used. These were spleens from mice sacrificed at day 4 and day 8 after immunization, day 8 spleens from infected mice, and day 8 spleens from infected and co-immunized mice. In the event, tissue from the 3 mice sacrificed at day 8 after infection and co-immunization had become unavailable. Three mouse spleens were available for each of the other conditions of interest. Extra-follicular foci of AFC, of sufficient size to microdissect accurately, could only be identified in infected mice. Additionally, the presence of confluent red pulp plasma cells in day 4 mice precluded the identification of AFC-sparse red pulp areas in these mice. The tissues examined, and the splenic compartments that were successfully identified and microdissected are summarised in Table 6-2.

Levels of Blimp-1 mRNA, and BCMA mRNA were measured in the dissected tissues, to test the technical success in discriminating AFC-rich red pulp areas, and AFC-sparse red

pulp areas, and in identifying AFC-rich extra-follicular foci. The results, which are shown in Figure 6-32, confirm the association between the levels of each of these mRNA species, and also the association of each with the relative frequency of NP-specific AFCs in corresponding immunohistochemically stained sections. Blimp-1 mRNA levels are thus used as a comparator with levels of different cytokines reported in Figure 6-33 and Figure 6-34 and Figure 6-35 in the next section).

Splenic Compartment	Corresponding legend on Figure 6-32 through to Figure 6-35	Day 4 after NP-Ficoll	Day 8 after NP-Ficoll	Day 8 after *S.* Typhimurium infection.
AFC rich red pulp	Red pulp NP^+	✓	✓	✓
AFC sparse red pulp	Red pulp NP^-		✓	✓
Extra-follicular foci	EF Foci			✓
Primary B cell follicles	IgD^+	✓	✓	✓
Central T zone	T zone	✓	✓	✓

Table 6-2 shows the range of mouse spleen compartments identified and microdissected, according to the experimental conditions and timepoints chosen.
Three mice were available for each condition and splenic tissue was obtained from each.

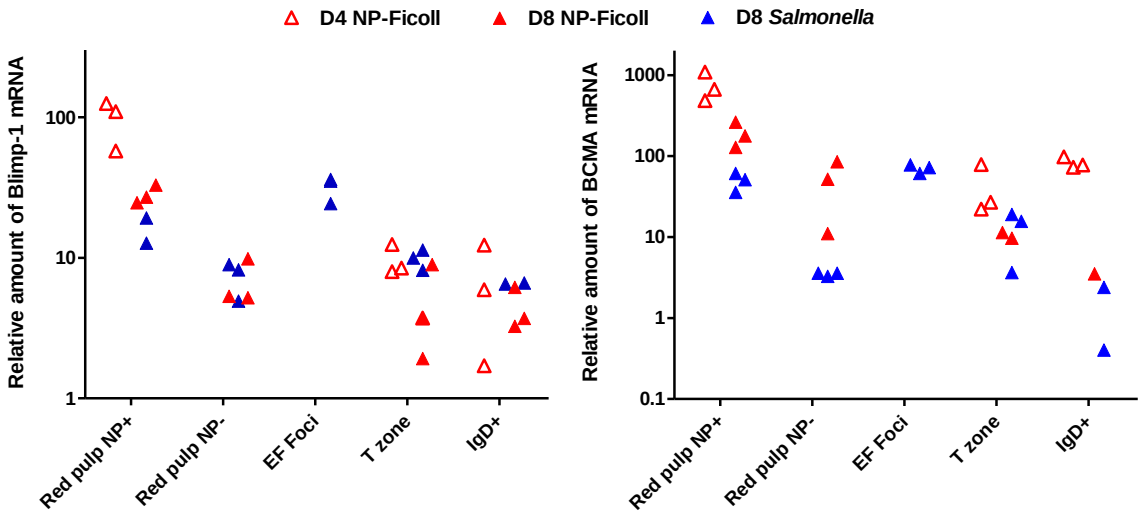

Figure 6-32 shows relative amounts of Blimp-1 mRNA, and BCMA mRNA in different splenic regions, at day 4 and day 8 after NP-Ficoll immunization, and at day 8 of *S.* Typhimurium infection. These both closely reflect the distribution of AFCs in the corresponding tissue sections as identified by immunohistochemistry.

Each symbol represents values from one mouse. Levels of Blimp-1 mRNA and BCMA mRNA were measured by RT_2-PCR, and are each reported relative to levels of β_2-microglobulin reference gene mRNA in the same sample. The legend for the symbols is shown above the figure. Where less than three symbols are shown per group, no mRNA was detected in the samples from unreported mice. Red pulp NP^+ = NP-specific AFC-rich areas of red pulp. Red pulp NP^- = NP-specific AFC-sparse areas of red pulp. EF foci = Extra-follicular foci. T zone = central T zone. IgD^+ = primary B cell follicles.

6.9.1 Evidence for different chemokines present in the splenic red pulp of infected mice compared to those responding to NP-Ficoll only

Levels of mRNA encoding for the chemokines CXCL9, CXCL10, CXCL11, and CXCL12, and for γ-IFN were studied in the different microdissected splenic compartments. The results were consistent with those from spleen cell suspension RT_2-PCR assays. As seen in Figure 6-33, levels of the inflammation related chemokines CXCL9, CXCL10 and CXCL11, and also levels of γ-IFN mRNA, are higher in day 8 infected mice, than in day 8 immunized peers. Red pulp levels of these same mRNA species are also generally higher 8 days than 4 days after immunization. By contrast

CXCL12 mRNA levels are similar at day 4 and day 8 after NP-Ficoll, and these levels are higher than those at day 8 after infection alone.

The microdissection methodology provides location specific information at different timepoints, so additional, and much more detailed, analysis is possible. At day 4 after NP-Ficoll, CXCL12 mRNA levels were highest in the red pulp (Figure 6-33 bottom right panel). This gradient, if reflected in CXCL12 protein expression, would favour migration of $CXCR4^+$ AFC towards the red pulp. Histological evidence (Figure 6-6) and compartmental levels of Blimp-1 mRNA (Figure 6-33, top left panel) indicate that much migration of AFC has already occurred by this time. There is no co-existing gradient in levels of mRNA for CXCL9 or CXCL10 or CXCL11. It is therefore unlikely that the few $CXCR3^+$ NP-specific AFC use these chemokines to migrate to the red pulp (Figure 6-33, middle panels and bottom left panel). As the proportion of cells expressing CXCR3 and the proportion expressing CXCR4 totals more than 100% (Figure 6-29), it is likely that some of these $CXCR3^+$ AFC also express CXCR4.

Eight days after NP-Ficoll, the CXCL12 gradient persists. However, there is no difference in CXCL12 levels between red pulp areas still rich in Blimp-1 mRNA, and red pulp areas with lower levels of Blimp-1 mRNA. Differential CXCL12 expression cannot therefore account for the selective survival to day 8 of AFC in some red pulp areas but not others.

In the same day 8 immunized mice a gradient in CXCL10 mRNA levels is present that, if present at the protein level, would favour migration to the red pulp of late emerging $CXCR3^+$ AFC. There is no detectable difference in CXCL10 mRNA between AFC-rich and AFC-spare red pulp areas, but there are differences between these areas in levels of

mRNA for γ-IFN (Figure 6-33, top right panel) and CXCL11 (Figure 6-33, bottom left panel). The significance of these findings, if any, is not clear.

Eight days after infection, there is no CXCL12 gradient to favour migration of new AFC to the red pulp, but CXCL12 mRNA levels in these mice are marginally higher in the extra-follicular foci than the T zone. Since at day 9 after infection, the majority of NP-specific AFC are $BrdU^-$ (Figure 6-12), it is likely that most of the AFC present at day 8 after infection are formed after day 5. The continued formation of AFC, in the absence of a CXCL12 gradient to guide migration to the red pulp, may account for the substantial accumulation of NP-specific AFC seen in the extra-follicular foci of these mice. Similar factors likely account for the same observation at day 8 after infection with co-immunization.

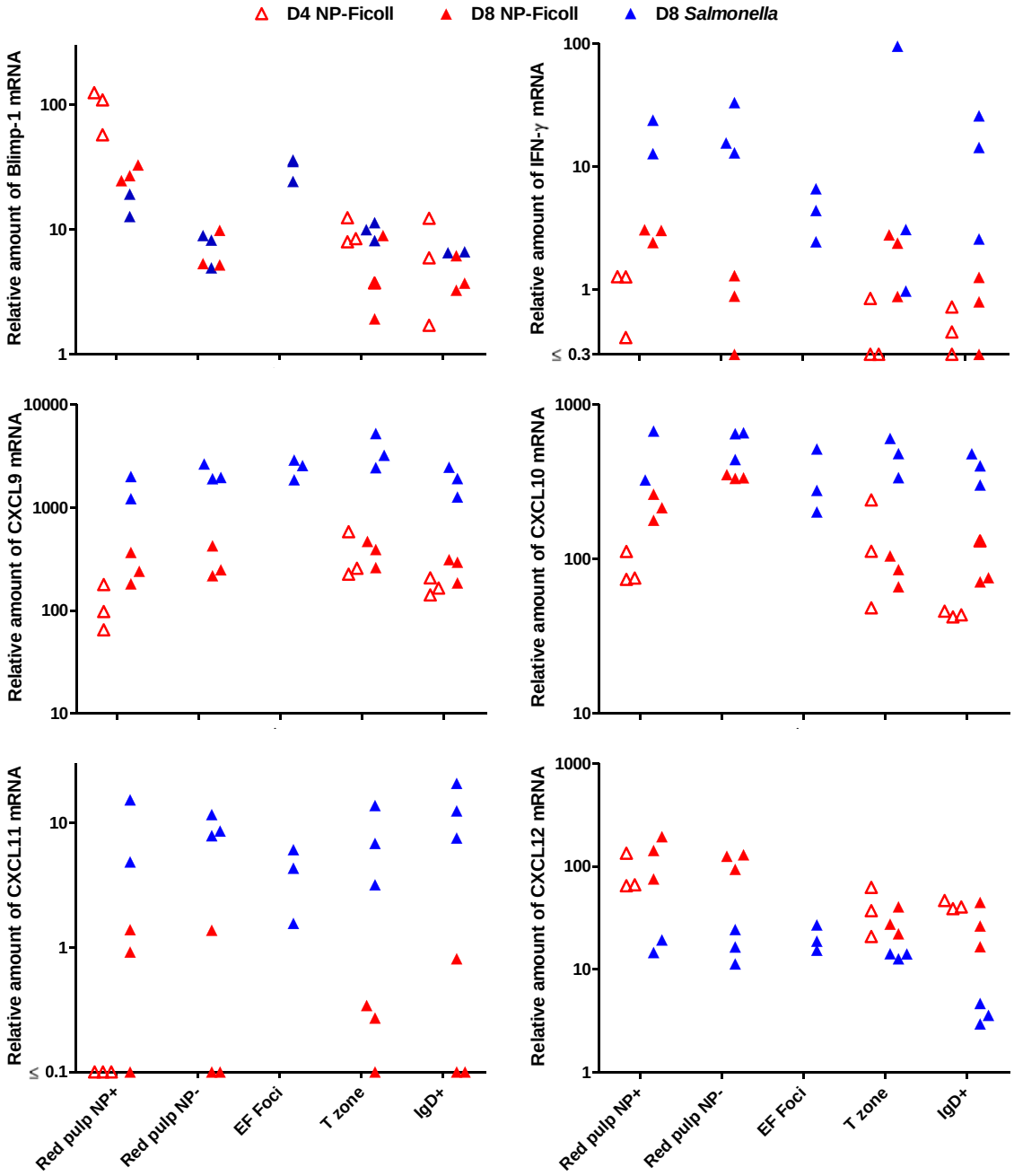

Figure 6-33 shows that mNA for CXCL9, CXCL10 and CXCL11 and IFN-γ are selectively induced by infection rather than immunization, but do not relate specifically to sites where AFC are located. CXCL12 by contrast is increased in immunized rather than infected mice, but again this is not clearly associated to AFC-containing areas.

Corresponding levels of mRNA for Blimp-1, which is only expressed in AFCs are shown for comparison. Each symbol represents values from one mouse. The legend for the symbols is shown above the figure. Levels of mRNA were measured by RT_2-PCR; mRNA species of interest are reported relative to levels of β_2-microglobulin reference gene mRNA in the same sample. Where less than three symbols are shown per group, no mRNA was detected in the samples from unreported mice. Red pulp NP^+ = NP-specific AFC-rich areas of red pulp. Red pulp NP^- = NP-specific AFC-sparse areas of red pulp. EF foci = Extra-follicular foci. T zone = central T zone. IgD^+ = primary B cell follicles.

In these day 8 infected mice there is no evidence of a gradient in CXCL9 or CXCL10 or CXCL11 that could favour migration of newly formed $CXCR3^+$ AFC from the T zone to extra-follicular foci. CXCL11 is higher in the red pulp of these mice than in their extra-follicular foci so one might consider that any extra-follicular $CXCR3^+$ AFC could use this to migrate to the red pulp, but levels are also higher in the T zone and no accumulation of AFC is seen there.

Nevertheless, the red pulp of day 8 infected mice does contain NP-specific AFC, and it is likely – but as yet unproven – that these include relatively long lived AFC. Circumstantial evidence in support of this is that i) NP-specific AFC are already present in the red pulp 4 days post infection (Figure 6-8) but that ii) most NP-specific $CD138^+$ cells present at 4 days after infection are newly formed ($BrdU^+$) (Figure 6-12) and – as discussed above – iii) it is not clear how migration to the red pulp can occur at later timepoints.

Spleens of day 4 infected mice were not examined by RT_2-PCR analysis of microdissected areas. It seems possible that early in infection a CXCL12 gradient still exists in these mice to favour migration to the red pulp. A similar argument holds for AFC migration to the red pulp by day 4 after immunization with co-infection – especially as for these mice it has been shown that almost all their NP-specific AFC are $CXCR4^+$, and relatively few are $CXCR3^+$ (Figure 6-29).

None of the inflammatory chemokines, nor γ-IFN, nor CXCL12, exhibit differential mRNA expression between AFC-rich and AFC-sparse areas of red pulp in infected mice so it is unlikely that these factors contribute to extended survival of AFC in selected areas of these mice' spleens.

6.9.2 Levels of BAFF mRNA, but not APRIL or TNF-α mRNA, correlate with AFC frequency in splenic red-pulp areas, eight days after immunization or infection.

Levels of mRNA encoding for TNF-α, BAFF and APRIL (all AFC-supporting factors in the TNF-α superfamily) were also measured in the microdissected compartments of the selected mouse spleens (Figure 6-34). For each of these three cytokines, comparison of overall levels of mRNA in microdissected tissues revealed only modest differences between groups of mice subjected to different inoculations. As with the data on chemokine mRNA, levels of BAFF, APRIL and TNF-α mRNA were comparable in microdissected tissues to those in spleen cell suspensions (Figure 6-31).

Within spleens of mice BAFF mRNA levels were appreciably higher 8 days after NP-Ficoll or *S.* Typhimurium in AFC-rich red pulp areas than in AFC-sparse red pulp areas (Figure 6-34, top right panel). Median levels of BAFF mRNA were also selectively raised in AFC-rich extra-follicular foci of infected mice. Thus, 8 days after either infection or immunization, levels of mRNA encoding for BAFF are raised in areas where AFC were located and the presence of AFC is confirmed by the high levels of Blimp-1 mRNA in these areas (Figure 6-34, top left panel). There was no clear association between levels of TNF-α mRNA, or APRIL mRNA and AFC containing areas. The high levels of BAFF in the white pulp may well reflect the known roles of this cytokine in homeostasis of resting and activated B cells [86].

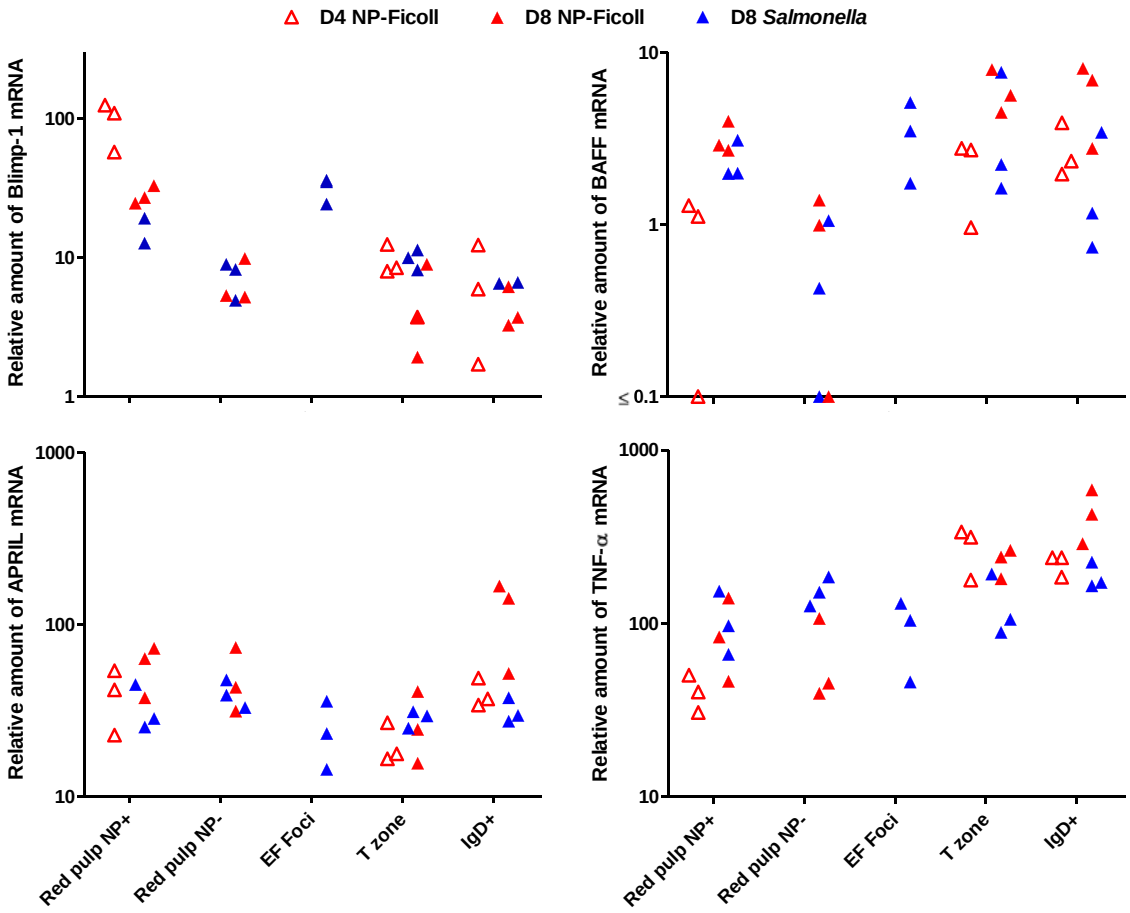

Figure 6-34 shows higher levels of BAFF mRNA, but not mRNA for TNF-α, or APRIL, are present in NP-specific AFC containing splenic regions of mice sacrificed 8 days after immunization or infection. Corresponding levels of mRNA for Blimp-1, which is only expressed in AFCs, are shown for comparison. Each symbol represents values from one mouse. The legend for the symbols is shown above the figure. Levels of mRNA were measured by RT2-PCR, and mRNA species of interest are reported relative to levels of β_2-microglobulin reference gene mRNA in the same sample. Where less than three symbols are shown per group, no mRNA was detected in the samples from unreported mice. Red pulp NP+ = NP-specific AFC-rich areas of red pulp. Red pulp NP- = NP-specific AFC-sparse areas of red pulp. EF foci = Extra-follicular foci. T zone = central T zone. IgD+ = primary B cell follicles.

6.9.3 IL6 and IL21 mRNA are selectively up regulated in infected mice.

The studies of spleen cell suspensions showed selective upregulation of IL-6 and IL-21 in infected mice. Microdissection confirms this association with *S.* Typhimurium infection but fails to identify any differences between AFC-containing and other compartments for

IL-6. It does show higher IL-21 levels in both the T and B cell areas of the white pulp compared to the red pulp (Figure 6-35).

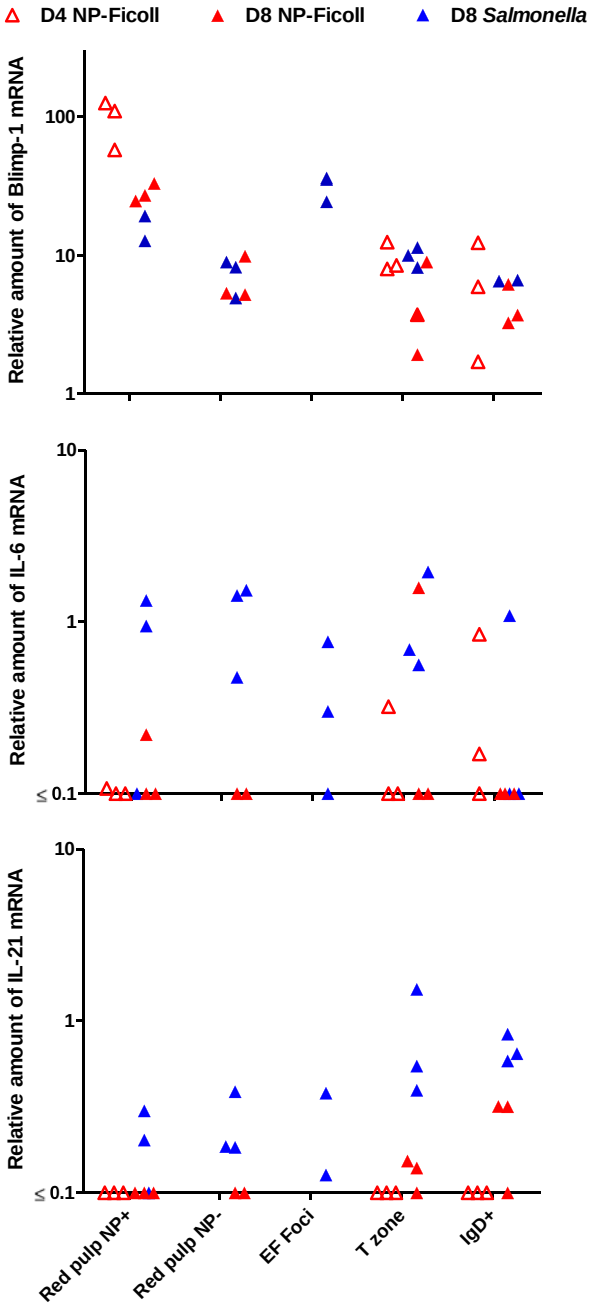

Figure 6-35 shows that mRNA for IL-6 and IL-21are rarely detectable in different splenic regions of uninfected mice and that in different splenic regions of mice infected 8 days previously levels of these mRNA species do not correlate with corresponding numbers of prevalent NP-specific AFC present. Corresponding levels of mRNA for Blimp-1, which is only expressed in AFC, are shown for comparison. Each symbol represents values from one mouse. The legend for the symbols is shown above the figure. Levels of mRNA were measured by RT_2-PCR, and mRNA species of interest are reported relative to levels of β_2-microglobulin reference gene mRNA in the same sample. Where less than three symbols are shown per group, no mRNA was detected in the samples from unreported mice. Red pulp NP^+ = NP-specific AFC-rich areas of red pulp. Red pulp NP^- = NP-specific AFC-sparse areas of red pulp. EF foci = Extra-follicular foci. T zone = central T zone. IgD^+ = primary B cell follicles.

6.10 Discussion and future work.

Detailed results are reported here of an experiment designed to test the hypothesis that 'inflammatory niches' can secure extended survival of additional plasma cells, even those unrelated to the cause of the inflammation. Available results from a repeat experiment have also been included. A preliminary experiment – not reported here – had measured serum levels of IgM anti-NP and numbers of splenic AFC at days 4, 10 and 35 after immunization with or without co-infection. All three experiments have consistent results and support the original hypothesis that more NP-specific AFC survive in QM x B6 mice immunized with NP-Ficoll if AFC sustaining niches are induced by co-infection with *S.* Typhimurium.

Splenic red pulp niches supporting NP-specific AFC 8 days after immunization with co-infection appear close to, but not necessarily in contact with, red pulp fibrous trabeculae (Figure 6-21 and Figure 6-22). Similar co-localization of AFC and splenic trabeculae was seen in immunized but not infected mice (Figure 6-21), as has been reported previously [45;133]. Further studies are needed to test whether most trabecula-associated plasma cells are actually long lived. The repeat experiment that included BrdU administration to immunised mice was designed to do this. Histological examination of spleens of mice sacrificed at day 9 or later should confirm that most trabecula-associated plasma cells are $BrdU^{+}$.

Our RT_2-PCR assays of microdissected splenic compartments also identify high levels of BAFF mRNA level as a feature of red pulp areas that contain plasma cells at day 8 after infection and immunization. It was unfortunate that doubly inoculated mice were not

available for microdissection and subsequent RT_2-PCR in the first experiment. This will need to be performed on spleens of mice in the repeat experiment, but there is no reason to expect a different result in this group.

The implied requirement for BAFF in achieving plasma cell survival is consistent with the reports that BCMA is essential for plasma cell survival (albeit in a study of bone marrow plasma cells) [165]. This contrasts with published work on plasma cell survival in the bone marrow [179], in the medullary cords of the lymph node [130], and the tonsil [249]. All of these associate the local production of APRIL with plasma cell survival. We have not been able to find a report of the roles of BAFF and APRIL in sustaining AFC survival at inflamed sites.

Locally elevated BAFF levels, and proximity to trabeculae, are features common to AFC-niches in both immunized, and infected, mice. It therefore appears that the infection-related increase in red pulp niches reflects increased capacity at 'conventional' trabecula-associated niches. If so, why does infection render them capable of supporting more AFC? The data do not indictate that increased levels of BAFF contribute to the increased numbers of NP-specific AFC at 8 d after immunization in the infected mice. In contrast, though levels of neither IL-6 nor IL-21 vary substantially between AFC-rich and AFC-sparse areas (Figure 6-35), levels of IL-6 mRNA and levels of IL-21 mRNA are higher in infected mice, than in their immunized but uninfected peers (Figure 6-30). Of these two cytokines, IL-6 levels seems the more likely to have a role in AFC survival *in vivo*, as i) IL-6 supports AFC survival *in vitro* [162], ii) levels of IL-6, but not levels of IL-21, have already risen by day 5 post infection (Figure 6-30), when apoptosis of most unsupported

splenic AFC occurs, and iii) in infected mice levels of IL-6 mRNA, but not IL-21 mRNA, are typically highest in the red pulp (Figure 6-35).

O'Connor et al report that IL-6 and BAFF have additive effects on plasma cell survival, at least *in vitro* [165]. In the context of our study, it is therefore tempting to speculate that additional red pulp IL-6 enables plasma cell to survive at lower levels of BAFF and/or APRIL. If this effect is superimposed upon levels of BAFF that decline with distance from a trabeculae-related source, the net result would be an enlarged peri-trabecular area capable of supporting plasma cell survival. This, in turn, would increase the number of NP-specific AFC supported in the red pulp of infected mice (Figure 6-36).

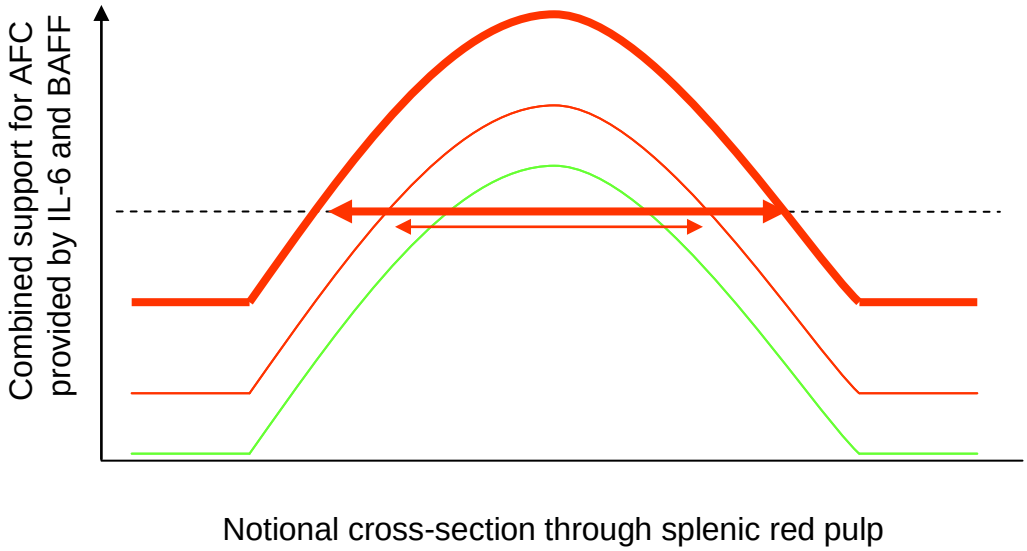

Figure 6-36 is a schematic diagram illustrating how the effective size of a BAFF-dependent AFC niche might be increased by a diffuse increase in levels of red pulp IL-6, without a change in localiazed levels of BAFF.
The minimum support sufficient to sustain AFC survival remains constant throughout the red pulp, and is indicated by the dashed black line. BAFF levels vary within the splenic red pulp, and provide dose-dependent support to AFC (green line). The effective support to AFC provided in uninfected mice by a combination of uniformly low levels of IL-6, and locally variable levels of BAFF is represented by the thin red line. This results in a narrow region where total support is sufficient for AFC survival (thin red double ended arrow). In infected mice BAFF levels do not change, but the uniformly higher levels of red pulp IL-6 increase the total support provided at any location (thick red line) results in an increased size of red pulp niche (thick double ended red arrow).

It is remarkable that even infected, and not immunized, QMxB6 mice have more long-lived NP-specific plasma cells at day 9 than their conventionally immunized QMxB6 peers (Figure 6-12). This may reflect LPS mediated 'bystander' activation of available B cells [250;251], alternatively, it may be due to cross reactivity between antigens from *S.* Typhimurium and surface immunoglobulin on NP-specific B cells.

Hargreaves et al have previously demonstrated that most migration of AFC to the red pulp is CXCR4 dependent [133]. The present study supports this in identifying, in mice that received NP-Ficoll, a CXCL12 gradient favouring migration of $CXCR4^+$ AFC to the red pulp. It is striking that in infected mice there is no such gradient, and many AFC accumulate in extra-follicular foci. Only a minority of these are still proliferating ($Ki67^+$), and BAFF levels at this site are comparable to AFC-supporting areas of the red pulp. It therefore seems possible that, in *S.* Typhimurium-infected mice, extra-follicular foci comprise an additional niche to sustain long term plasma cell survival. Again, histological examination of BrdU fed mice can examine this possibility.

In addition to the marked accumulation of AFC in extra-follicular foci, infected but non-immunized mice have some NP-specific red-pulp AFC. No evidence was found for significant $CXCR3^+$ mediated migration of AFC within the spleen. A recent report has described a new chemokine receptor, CXCR7, which binds CXCL11 and CXCL12 [252]. This report indicates widespread expression of CXCR7 mRNA in a range of tissues (including the spleen). However it appears that expression of the corresponding protein, at least in adult mice and humans, is confined to transformed cells. A detailed examination of the presence or absence of CXCR7 in various immune cells is yet to be reported, but could be of great interest – e.g. in CXCR4-independent AFC migration

within the spleen. Others have previously demonstrated expression of CXCR6 on human plasma cells [253], and expression of CXCL16, the ligand for CXCR6 in the spleen, the bone marrow and the inflamed rheumatoid joint [253;254]. The possibility that CXCR6 mediates splenic plasma-cell migration has not explored here.

Splenic $CD11b^{+}F4/80^{+}$ macrophages, and some splenic $CD11c^{+}F4/80^{+}$ dendritic cells, could not be satisfactorily identified by presently available confocal microscopy techniques. This is particularly frustrating as these cell types are increased in the spleen after *S.* Typhimurium infection, and could produce either BAFF or IL-6 or both [170;241;255]. It may yet be possible to identify other antigenic markers for these cells that enable their identification using confocal microscopy. It is possible that more than one cell type is capable of providing all sufficient support for AFC - perhaps by producing the necessary BAFF, with or without IL-6. If so then the histological approaches just discussed – and those reported elsewhere in this chapter – will fail to identify the association between AFC and any of the relevant cell types.

Flow-assisted cytometric cell sorting (FACS) of splenic cell types, and subsequent RT_2-PCR analysis of homogeneous post-sort populations could at least address the relative contribution of these various cell types to overall splenic production of various putative AFC-survival factors, including BAFF and IL-6. This approach has already been applied in our laboratory in other models.

Previous publications have reported that, in addition to the AFC-supportive molecules studied here, other factors can enhance plasma cell survival, at least *in vitro*. IL-5 can promote plasma cell survival *in vitro* although there appears to be functional redundancy in its action [162], and so we did not explore any role for IL-5 in the present model. The

plasma cell surface receptors VLA-4, and CD44 may contribute to the cells' survival, though the published findings are not consistent [160;162].

At least one ligand for VLA-4 – fibronectin – is widely expressed in the spleen [256], and so it alone cannot be a determinant of a plasma cell niche. In contrast histologically detectable expression of hyaluronic acid (a ligand for CD44) in the splenic red pulp is restricted to vascular structures [257]. As production of hyaluronic acid is widely upregulated in inflammation [258;259] infection-related increases in splenic expression of hyaluronic acid might provide additional support to plasma cells. This merits investigation but was not undertaken here.

A large part of information in this report regarding niches, and infection-related changes in the spleen, was derived from RT_2-PCR based assays of mRNA levels. This is necessary given the difficulties in interpreting histological staining for cytokines, and chemokines. Nevertheless, inferences about protein levels from levels of corresponding mRNA as measured by RT_2-PCR requires caution - and even more so in the context of a substantial, and changing, cellular infiltrate. Levels of mRNA are expressed relative to levels of reference gene mRNA. As discussed in section 6.8 above, increased production of reference gene mRNA due to infection related increases in cell numbers will tend to result in underestimation of absolute levels of mRNA species of interest. This, in turn, many results in more modest infection-related changes in mRNA levels being overlooked. The use of microdissection did enable us to test if mRNA detected in spleen cell suspensions was localized within certain compartments in the spleen.

Furthermore, the sequential relationship between cellular mRNA expression, cellular protein synthesis, cellular secretion of protein, and extra-cellular (or cell surface)

persistence of protein is not invariable. The example of variable cell surface expression of CXCR4 has already been cited [153;248], but there are other examples pertinent to this work. CXCL12 can bind to CXCR4$^-$ cells via cell-surface heparin sulphate, and can bind to other negatively-charged glycosaminoglycans in the extra-cellular matrix [260]. In both circumstances the CXCL12 retains functional activity. Neutrophils can store BAFF, and possibly APRIL, in cytoplasmic granules, with secretion of granule contents after stimulation [255;261]. Secreted APRIL can also bind to extra-cellular proteoglycans and may thus accumulate there [177]. All these phenomena would result in levels of functional protein that are not reflected in contemporary local mRNA production. This could, for example, result in a failure to detect a true association between APRIL and supportive niches.

Although interesting, and contrasting, observations were made in the various groups of mice, the experiments reported here cannot confirm a causal, and non-redundant, relationship between BAFF and niche-related support for AFC. It is common to test such observations by the use of mice genetically deficient for the critical factor, or its ligand, or the addition of blocking substances (e.g. anti-BAFF antibodies, or BAFF-receptor Ig). However, BAFF has multiple roles within the B cell lineage and elsewhere so interpretation of the results obtained would be virtually impossible in the present model that involves active infection.

The present study indicates that AFC survival in spleens of uninfected mice is also through a similar BAFF-dependent pathway. This has previously been investigated experimentally. Consistent with our findings, Ingold et al have reported that post-immunisation BAFF-selective blockade reduces the number of splenic NP-specific AFCs

present [177]. Others have reported strain-dependent effects when using such approaches [262].

The more complex infection/immunization model reported here has many potentially interesting, and informative, permutations. One could administer antibiotics to previously infected and co-immunized mice – a crude analogy to the therapeutic role of Rituximab in autoimmune disease. The resultant, accelerated, resolution of inflammation would be expected to cause a loss of established splenic NP-specific plasma cells.

Alternatively one might consider immunization with a T-dependent antigen (preferably with prior priming) instead of NP-Ficoll. This scenario may test more fully any role for CXCR3 in splenic AFC migration or survival as in published reports that used recall responses to antigen, the proportion of AFC that are $CXCR3^{+}$ is higher than seen in our present work [14;134].

It would also be interesting, and useful, to confirm the original hypothesis – namely that plasma cells unrelated to a cause of inflammation can be sustained in inflammatory sites – in mice suffering an alternative form of inflammation that does not involve an infection (or autoimmunity). The study of a non-lymphoid organ may also simply the interpretation of the findings. One such model is that of ischaemia reperfusion injury in the kidney [263].

7 GENERAL DISCUSION AND IMPLICATIONS FOR FUTURE RESEARCH

The studies presented here arose from the surprising clinical observations that in patients with various autoimmune diseases, including Wegener's granulomatosis, serum titres of disease-associated IgG autoantibodies fall after therapeutic B cell depletion with Rituximab, while total serum IgG levels show little change.

First we considered whether such sensitivity to Rituximab was a) a feature of a certain pathway of antibody production, or b) a feature of antibody producing cells arising from a particular B cell subset, or c) a feature of autoantibies that are produced exclusively by short lived plasma cells. Initially we developed the technology to measure antibodies of several different specificities in parallel (Chapter 4), This technology, and other established techniques, were then deployed to measure levels of antibodies against different classes of antigen from in sera from patients with active disease, and paired samples from the same patients after treatment with Rituximab (Chapter 5). The findings were most consistent with the following hypothesis:

1. Plasma cells, including those producing autoantibody, accumulate in sites of inflammation.
2. Inflamed sites provide supportive niches that enhance the survival of such plasma cells.
3. Treatment of autoimmune disease by Rituximab, results in resolution of the disease related inflammation.
4. As the inflammation resolves, the unsupported plasma cells die.

5. Subsequently the serum autoantibody titres, previously maintained by those plasma cells, then fall.

Further work sought to test, in an experimental model, the underlying hypothesis that long lived plasma cells can be supported in inflamed tissues. Results obtained following intra-peritoneal inoculation of QM x B6 mice, in which some 5% of their B cells are NP-specific, with either NP-Ficoll, or live attenuated *S.* Typhimurium or both. *S.* Typhimurium infection creates new niches that support plasma cells in the spleen. The finding that increase numbers of NP-specific plasma cells survived in those mice that were infected with *S.* Typhimurium as well as immunized with NP-Ficoll is consistent with the hypothesis set out above.

Based on the published literature one may conclude that emergent AFC are likely to migrate to inflamed sites through interactions between CXCR3 and its ligands CXCL9, CXCL10 and CXCL11 [264]. These publications include reports that:

- Indicate CXCL9 and CXCL11 are present in at least some inflamed tissues, including the rheumatoid joint [141;265], and CXCL9 is upregulated in inflamed lymph nodes [266]. These nodes become enriched for $CXCR3^+$ monocytes [266]. Additionally, CXCL10 is induced in experimental models of renal injury [267].
- Show $CXCR3^+$ plasmablasts can migrate to these ligands [134].
- Plasma cells are found at non-lymphoid sites of inflammation in mouse models [232], and in many inflamed human tissues [49;53;230;231;234-236] (see also Figure 5-4 in this thesis).

- Provide evidence that indicates that some plasma cells in rheumatoid joints are indeed $CXCR3^{+}$ [141].

The proportion of new AFC that express CXCR3 may be increased in certain circumstances. Thus:

- *In vitro* studies have found that γ-IFN increases surface expression of CXCR3 during in the process of memory B cell differentiation into AFC [14], at least in the subpopulation switched to IgG_1.
- Others have found, in patients with SLE, an unusual circulating population of $CD19^{hi}$ cells that is enriched for autoreactive specificities [268]. These $CD19^{hi}$ cells, which appear to be memory B cells [268], typically express higher levels of CXCR3 than $CD19^{lo/normal}$ cells from the same subject and exhibit chemotaxis to CXCL9 [269].

Why then do findings presented in Chapter 6 not support this model of CXCR3 mediated AFC migration? There are several possibilities. These include:

1. The time constraints and resources of the mice studies mean that findings should be considered as provisional until they have been repeated.
2. The timepoints chosen for study may not reveal the impact of infection and related inflammation on AFC expression of CXCR3.
3. *S.* Typhimurium may prevent increases in AFC expression of CXCR3 as a virulence strategy.
4. CXCR3 expression on AFC might only be modulated by T-dependent responses, or perhaps only in responses derived from memory B cells. The

mouse studies reported in Chapter 6 involved T-independent responses to NP-Ficoll.

By contrast we did find evidence that most intra-splenic AFC migration in our model is mediated by CXCR4. This is consistent with some published literature [133]. Upregulated expression of CXCL12 has also been reported at several inflamed sites including the rheumatoid synovium [270], and in more than one model of renal inflammation [271;272]. Interestingly, in NZB/W mice – animals whose kidneys are recognised to be a major site of AFC accumulation [232] – treatment with anti-CXCL12 mAb results in a fall in serum anti-DNA IgG, but not total levels of serum IgG [272].

Other work presented in Chapter 6, which still needs to be replicated, raises the possibility that during *S.* Typhimurium infection the increased splenic capacity for supporting plasma cells – above and beyond that attributable to splenomegally alone – is attributable to a combination of a) inflammation related increases in local IL-6 production and b) local production of BAFF.

Could a similar mechanism apply in human autoimmune disease? Published work indicates that levels of IL-6 are higher in the inflamed rheumatoid synovium than in the serum [273] consistent with local production. Others have found direct [274] and indirect [275] evidence of local IL-6 production in renal lupus nephritis. To our knowledge, only indirect evidence has so far been published regarding locally increased IL-6 production in kidneys affected by ANCA-vasculitis [275], but this seems a plausible possibility given the available evidence, and the biology of IL-6 production (2.8.1.1). Appendices 3 and 4 report our findings that serum levels of IL-6 are greatly elevated in patients with active

vasculitis, and that these systemic levels fall after remission induction with Rituximab based treatment.

The published literature also includes several reports of local BAFF production at sites of clinical inflammation [276-278]. Given that BAFF can be produced by neutrophils and macrophages [170;255], and that both cell types can be activated by ANCA antibodies present in WG [21], it is possible that BAFF is present at sites of vasculitic damage in patients with WG.

As with IL-6, serum levels of BAFF are elevated in most patients with WG, compared to healthy controls [279]. Serum BAFF levels are also elevated in most patients with SLE or RA [277;280]. Serum levels of BAFF correlate with disease activity score (and serum auto-antibody titres) in patients with conventionally treated SLE [281]. However, available evidence indicates that therapeutic B cell depletion in patients with SLE [282] and in patients with Rheumatoid Arthritis [221] is associated with a rise in serum BAFF levels, whilst autoantibody levels fall in such patients [11;23]. The rise in serum BAFF may be due to the operation of homeostatic mechanisms, but superficially does contradict the hypothesis offered here. However, there is no published information on levels of BAFF at inflamed sites (or their anatomical correlates during clinical remission), and only local levels are likely to be of relevance regarding local AFC survival.

The emergent hypothesis from this work – that antibody producing plasma cells, including autoantibody producing plasma cells, are supported and sustained at sites of disease related inflammation – remains an attractive candidate explanation for the selective falls in most serum autoantibody titres after Rituximab. However it appears that not all autoantibody titres fall in this way – even within a common patient cohort. For

example amongst 16 patients with SLE treated with Rituximab, reported in detail by Cambridge et al [23], serum titres of anti-nucleosome antibodies (n=11) and anti-dsDNA antibodies (n=14) fell significantly whilst serum levels of antibodies against histone (n=10), SSA (n=9), and ribonucleoproteins (n=7) did not.

In SLE some autoantibodies are circulating in significant quantities several years before symptoms develop [283]. The corresponding autoantibody-producing AFC are therefore presumably present before significant disease related inflammation develops. One might expect that the autoantibody-producing AFCs that emerge during this prodromal phase would mostly accumulate in 'conventional' niches within the bone marrow. Our model would predict that such autoantibody production from these AFC would not be sensitive to Rituximab.

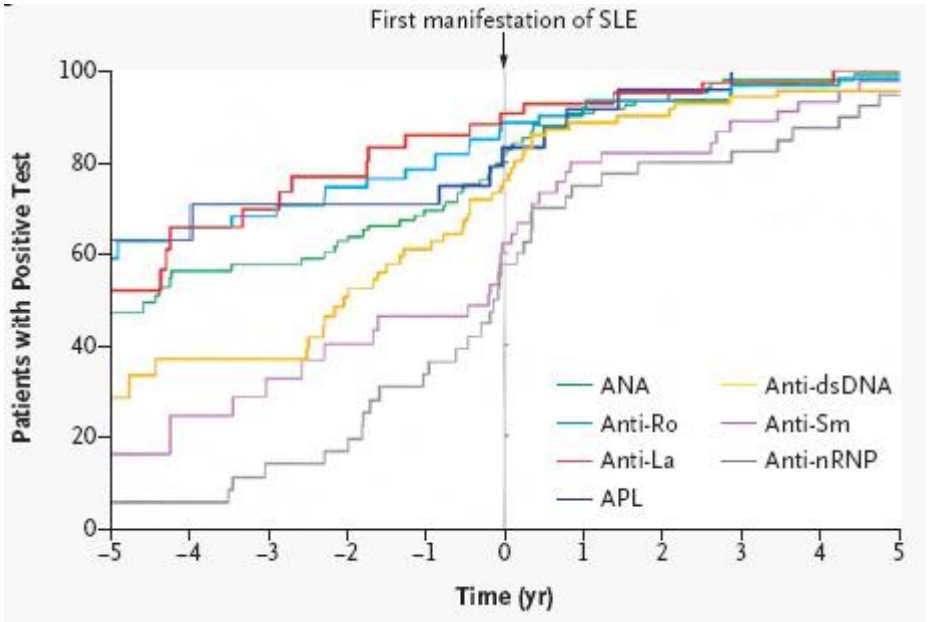

Figure 7-1 shows the gradual development of autoantibodies prior to the emergence of symptoms of SLE. Taken from Arbukle et al 2003 [283].
In patients that subsequently develop SLE, auto-antibodies become detectable at variable intervals before clinical symptoms. Some, such as anti-Ro antibodies, are present long before disease, and their titres appear relatively preserved after Rituximab [23]. Others, such as anti-DNA antibodies, often emerge soon before symptoms, and more often fall after Rituximab therapy. ANA – Anti nuclear antibody. APL – Anti phospholipid antibody. dsDNA – double stranded DNA. nRNP – nuclear ribonucleoprotein.

The available evidence supports this to a certain extent. As shown in Figure 7-1, anti-dsDNA antibodies emerge relatively late in pre-clinical SLE [283], and as previously noted, seem relatively sensitive to Rituximab treatment [23]. Conversely anti-Ro (SSA) antibodies emerge earlier [283], and are reported to be less Rituximab sensitive [23]. As such comparisons would be better made within one patient cohort, the value of this evidence is limited at present. No published reports describe the timescale of ANCA emergence prior to clinical ANCA-associated vasculitis.

It may be that important differences between the animal model used in this work and the human diseases of interest limit the capacity to translate mechanisms from one to the other. Nevertheless, the technologies successfully applied to the 'cuckoo project' (Chapter 6) ought to be adaptable to the studies of human pathological tissue. Such work, an obvious extension of the research reported here, would test whether local production of one or more factors that support AFC survival contributes to the survival of $CXCR3^+$ AFC, or $CXCR4^+$ AFC, at sites of pathological inflammation. Alternatively, as discussed at the end of Chapter 6, different animal models could be used that bear closer analogy to the clinical scenarios of interest.

Finally, whilst Rituximab is clearly finding a role as a valuable new therapeutic option in the treatment of autoimmune disease, it is likely that further biological therapies will continue to emerge. For example, a therapeutic agent that antagonises BAFF is already being developed [284]. As several life threatening autoimmune diseases, such as Wegener's granulomatosis, have less than ideal conventional therapies, it is likely that difficult clinical scenarios will continue to arise in patients are treated with new agents

that are at early stages of clinical development [21]. Some of these new treatments in time may find their own ‘niches’ in the therapeutic arsenal.

The experience with Rituximab over the last 5-8 years sets a precedent for further treatment development. It provides the hope that ‘experiments of medicine’ that deploy specific therapeutic agents in a clinical setting will provide unexpected insights into human immunology.

8 APPENDIX 1: PROFORMA FOR BIRMINGHAM VASCULITIS ACTIVITY SCORE (BVAS)

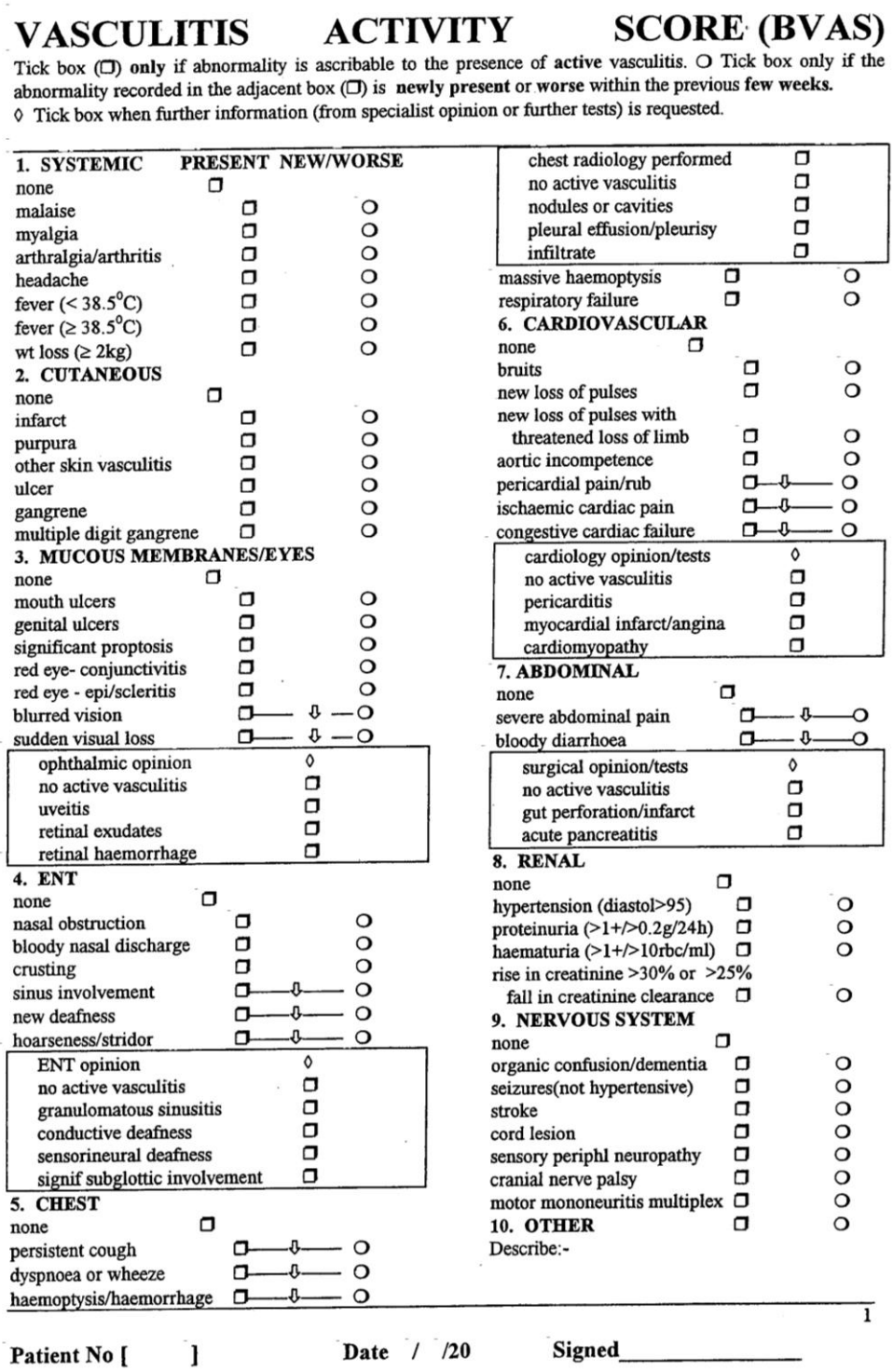

VASCULITIS ACTIVITY SCORE (BVAS)

Tick box (☐) **only** if abnormality is ascribable to the presence of **active** vasculitis. ○ Tick box only if the abnormality recorded in the adjacent box (☐) is **newly present** or **worse** within the previous **few weeks.**
◊ Tick box when further information (from specialist opinion or further tests) is requested.

1. SYSTEMIC	PRESENT	NEW/WORSE
none	☐	
malaise	☐	○
myalgia	☐	○
arthralgia/arthritis	☐	○
headache	☐	○
fever (< 38.5°C)	☐	○
fever (≥ 38.5°C)	☐	○
wt loss (≥ 2kg)	☐	○
2. CUTANEOUS		
none	☐	
infarct	☐	○
purpura	☐	○
other skin vasculitis	☐	○
ulcer	☐	○
gangrene	☐	○
multiple digit gangrene	☐	○
3. MUCOUS MEMBRANES/EYES		
none	☐	
mouth ulcers	☐	○
genital ulcers	☐	○
significant proptosis	☐	○
red eye- conjunctivitis	☐	○
red eye - epi/scleritis	☐	○
blurred vision	☐ ⇩ ○	
sudden visual loss	☐ ⇩ ○	
ophthalmic opinion	◊	
no active vasculitis	☐	
uveitis	☐	
retinal exudates	☐	
retinal haemorrhage	☐	
4. ENT		
none	☐	
nasal obstruction	☐	○
bloody nasal discharge	☐	○
crusting	☐	○
sinus involvement	☐ ⇩ ○	
new deafness	☐ ⇩ ○	
hoarseness/stridor	☐ ⇩ ○	
ENT opinion	◊	
no active vasculitis	☐	
granulomatous sinusitis	☐	
conductive deafness	☐	
sensorineural deafness	☐	
signif subglottic involvement	☐	
5. CHEST		
none	☐	
persistent cough	☐ ⇩ ○	
dyspnoea or wheeze	☐ ⇩ ○	
haemoptysis/haemorrhage	☐ ⇩ ○	
chest radiology performed	☐	
no active vasculitis	☐	
nodules or cavities	☐	
pleural effusion/pleurisy	☐	
infiltrate	☐	
massive haemoptysis	☐	○
respiratory failure	☐	○
6. CARDIOVASCULAR		
none	☐	
bruits	☐	○
new loss of pulses	☐	○
new loss of pulses with threatened loss of limb	☐	○
aortic incompetence	☐	○
pericardial pain/rub	☐ ⇩ ○	
ischaemic cardiac pain	☐ ⇩ ○	
congestive cardiac failure	☐ ⇩ ○	
cardiology opinion/tests	◊	
no active vasculitis	☐	
pericarditis	☐	
myocardial infarct/angina	☐	
cardiomyopathy	☐	
7. ABDOMINAL		
none	☐	
severe abdominal pain	☐ ⇩ ○	
bloody diarrhoea	☐ ⇩ ○	
surgical opinion/tests	◊	
no active vasculitis	☐	
gut perforation/infarct	☐	
acute pancreatitis	☐	
8. RENAL		
none	☐	
hypertension (diastol>95)	☐	○
proteinuria (>1+/>0.2g/24h)	☐	○
haematuria (>1+/>10rbc/ml)	☐	○
rise in creatinine >30% or >25% fall in creatinine clearance	☐	○
9. NERVOUS SYSTEM		
none	☐	
organic confusion/dementia	☐	○
seizures(not hypertensive)	☐	○
stroke	☐	○
cord lesion	☐	○
sensory periphl neuropathy	☐	○
cranial nerve palsy	☐	○
motor mononeuritis multiplex	☐	○
10. OTHER	☐	○
Describe:-		

1

Patient No [ ] **Date / /20** **Signed**_____

Figure 8-1 is reproduced from Luqmani et al, 1994, [17] and shows the standard proforma used to assess disease activity in ANCA associated vasculitis.

9 APPENDIX 2: RT_2-PCR PRIMER AND PROBE SEQUENCES

mRNA species	Origin	Forward primer sequence	Reverse primer sequence	Probe sequence
IL6	MacLennan group	TCGGAGGCTTAATTACACATGTTC	AAGTGCATCATCGTTGTTCATACA	CAGAATTGCCATTGCACAACTCTTTTCTCAT
BAFF	MacLennan group	GAAGTGTGCCATGTGAGTTATGAGA	TCACCCAAGGCAAAAAGCA	TCCTTTGCCAACACGCACCGC
APRIL	MacLennan group	CGAGTCTGGGACACTGGAATTT	AGATACCACCTGACCCATTGTGA	CTGCTCTATAGTCAGGTCCTGTTTCATGATGTGAC
Blimp-1SC	MacLennan group	CAAGAATGCCAACAGGAAGTATTTT	CCATCAATGAAGTGGTGGAACTC	TCTCTGGAATAGATCCGCCA-MGB
γ-IFN	MacLennan group	TCTTCTTGGATATCTGGAGGAACTG	GAGATAATCTGGCTCTGCAGGATT	TTCATGTCACCATCCTT-MGB
IL-21	MacLennan group	ACACCCAAAGAATTCCTAGAAAGACTAA	TGCATTCGTGAGCGTCTATAGTG	AGCATCTCTCCTAGAACACATAGGACCCGAAGAT
CXCL12	MacLennan group	CAAGCATCTGAAAATCCTCAACAC	CACTTTAATTTCGGGTCAATGCA	TGCACGGCTGAAGAACAACAACAGACAA
BCMA	MacLennan group	TCCAACCCTCCTGCAACCT	CGTGTACGTCCCTTTCACTGAA	TCAGCCTTACTGTGATCCAAGCGTGACC
CXCL9	Applied Biosystems	Unknown	Unknown	Unknown
CXCL10	Applied Biosystems	Unknown	Unknown	Unknown
CXCL11	Applied Biosystems	Unknown	Unknown	Unknown
TNF-α	Applied Biosystems	Unknown	Unknown	Unknown
CXCR3	Applied Biosystems	Unknown	Unknown	Unknown
CXCR4	Applied Biosystems	Unknown	Unknown	Unknown
β2-microglobulin	MacLennan group	CATACGCCTGCAGAGTTAAGCA	ATCACATGTCTCGATCCCAGTAGA	CAGTATGGCCGAGCCCAAGACCG

Table 9-1 lists the source of RNA primers and probes used in RT_2-PCR assays, and the probes' RNA sequences where known.

10 APPENDIX 3: SERUM LEVELS OF CYTOKINES IN PATIENTS WITH ACTIVE ANCA-ASSOCIATED VASCULITIS, COMPARED TO LEVELS IN HEALTHY CONTROLS

	Naïve patients		Relapsed patients		
Cytokine	Median serum level as multiple of controls' median serum level	Significant difference with controls	Median serum level as multiple of controls' median serum level	Significant difference with controls	Significant difference between naïve and relapsed patients
IL-1β	2.2 x	✓✓✓	1.6 x	✓✓	
IL-1Rα	2.8 x	✓✓✓	2.6 x	✓✓	
IL-2	5.9 x	✓	2.7 x		
IL-4	2.1 x	✓✓	1.1 x		
IL-5	10.2 x	✓✓	3.9 x		
IL-6	5.7 x	✓✓✓	3.0 x	✓✓	
IL-7	3.2 x	✓✓	2.0 x	✓	
IL-8	3.2 x	✓✓✓	1.5 x		✓
IL-9	4.9 x	✓✓	4.4 x	✓	
IL-10	8.5 x	✓✓✓	4.7 x	✓	
IL-12	4.8 x	✓✓	3.1 x	✓	
IL-13	3.8 x	✓	3.2 x		
IL-17	8.5 x	✓	6.7 x	✓	
Eotaxin	1.6 x		2.3 x	✓✓	
G-CSF	1.2 x		1.2 x		
GM-CSF	2.7 x	✓✓	1.5 x		
γ-IFN	1.5 x		1.1 x		
IP-10	1.9 x		1.2 x		
MCP-1	4.1 x	✓✓✓	3.4 x	✓✓✓	
MIP-1α	1.9 x	✓✓	1.3 x		
MIP-1β	2.7 x	✓✓	2.1 x		
PDGF	1.1 x		1.6 x		
TNF-α	1.4 x		1.1 x		
VEGF	7.9 x	✓✓✓	5.7 x	✓	

Table 10-1 summarizes the serum levels of various cytokines in treatment-naïve patients with ANCA-vasculitis, and in patients with relapsed ANCA-vasculitis relative to levels in healthy controls' serum. Subsequent pages show dot plots with results for individual patients and controls.

Levels of each cytokine (listed in far left column) in patients with untreated ANCA associated vasculitis (n=19; left columns), and those with relapsed ANCA-associated vasculitis (n=13; right columns) are reported relative to the median level amongst healthy controls (n=8). Statistical significance (Mann Whitney test) for each comparison is reported is as follows: $p<0.05$ (✓), $p<0.01$ (✓✓), or $p<0.001$ (✓✓✓).

Scatter plots representing results for each patient or control subjects (where appropriate) regarding parameters of disease activity, serum autoantibody titres, and levels of each cytokine, are presented below. Dotted lines, where present, indicate the limits of the assay's range. Statistical significance (Mann Whitney test) for each comparison is reported as follows: $p<0.05$ (☆), $p<0.01$ (☆☆), or $p<0.001$ (☆☆☆).

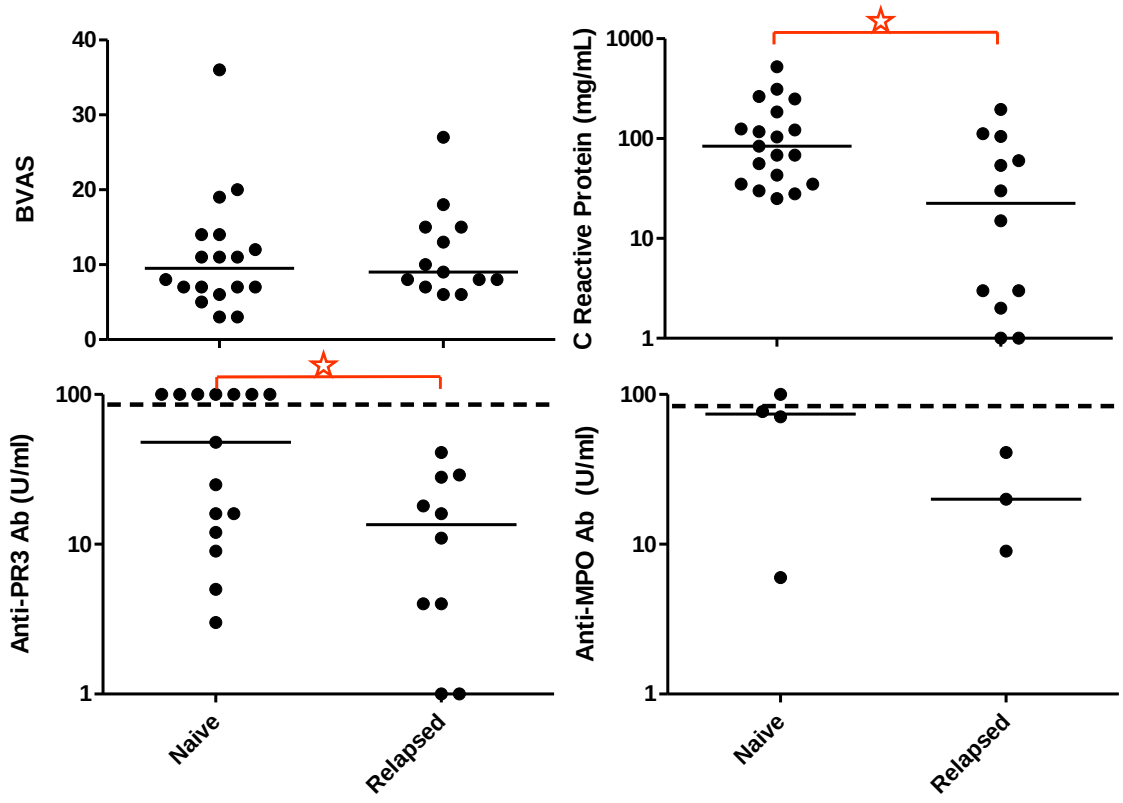

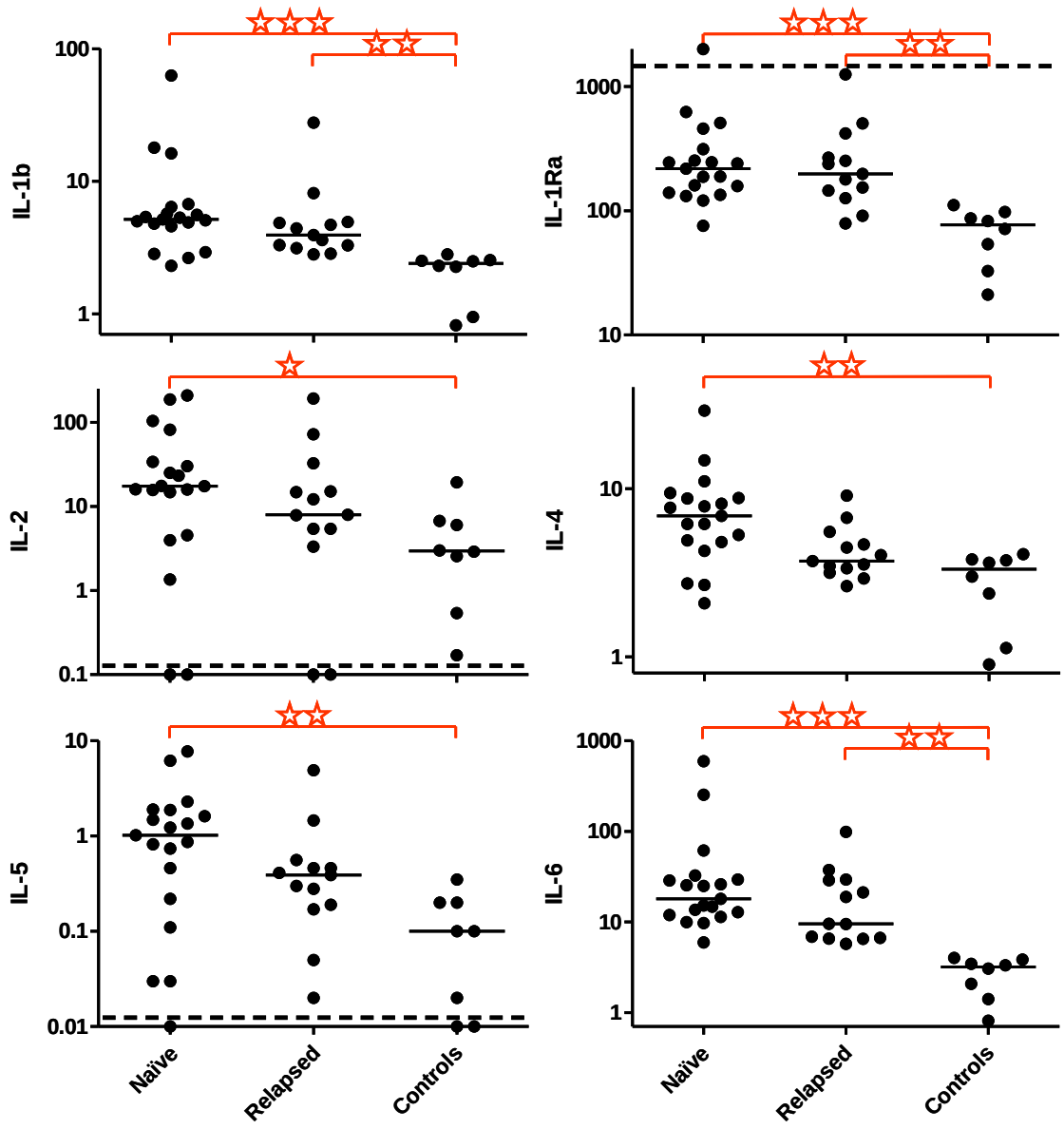
IL-1b
100
10
1
IL-1Ra
1000
100
10
IL-2
100
10
1
0.1
IL-4
10
1
IL-5
10
1
0.1
0.01
IL-6
1000
100
10
1
Naïve
Relapsed
Controls
Naïve
Relapsed
Controls

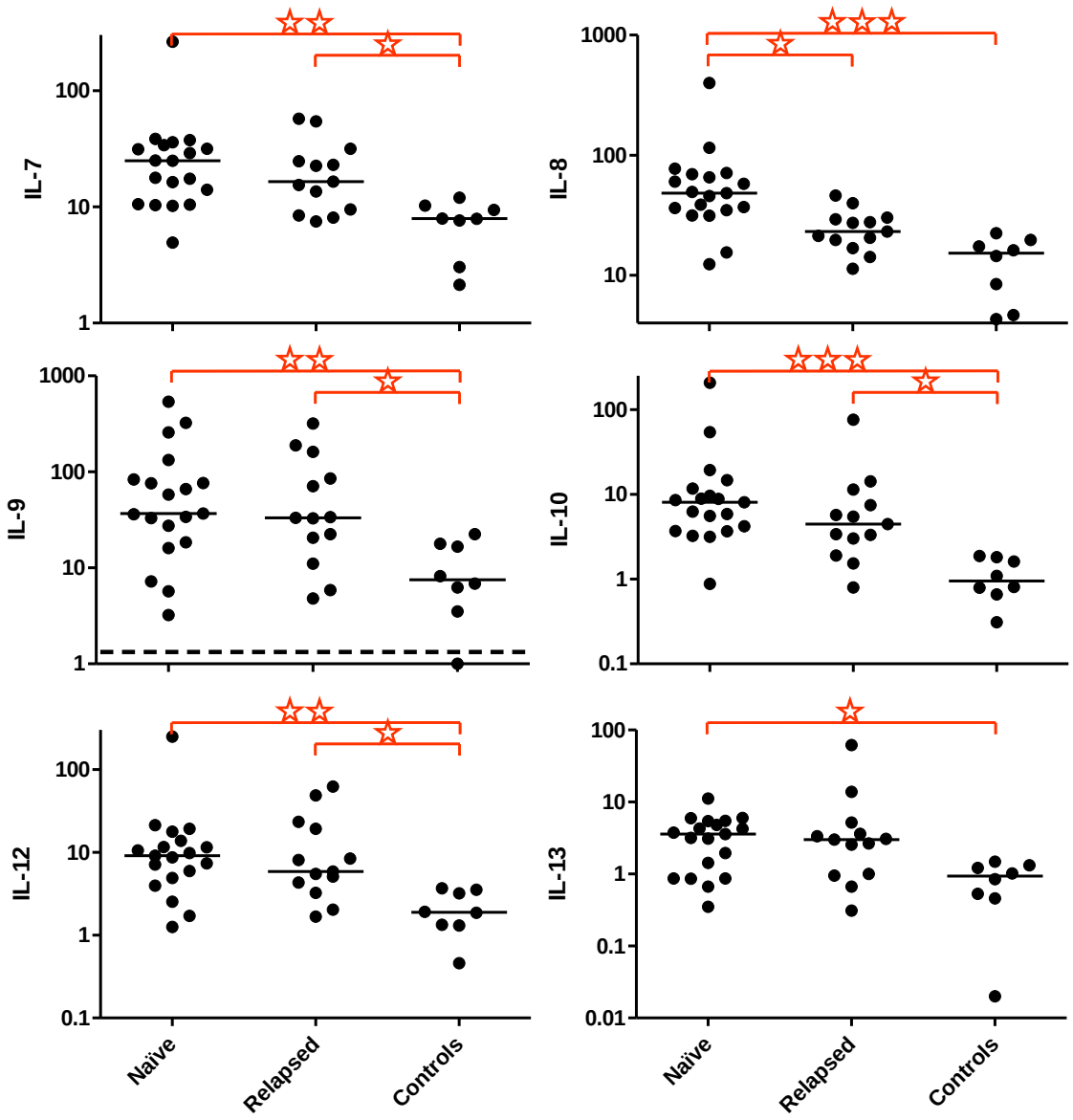
IL-7
IL-8
IL-9
IL-10
IL-12
IL-13
Naïve
Relapsed
Controls

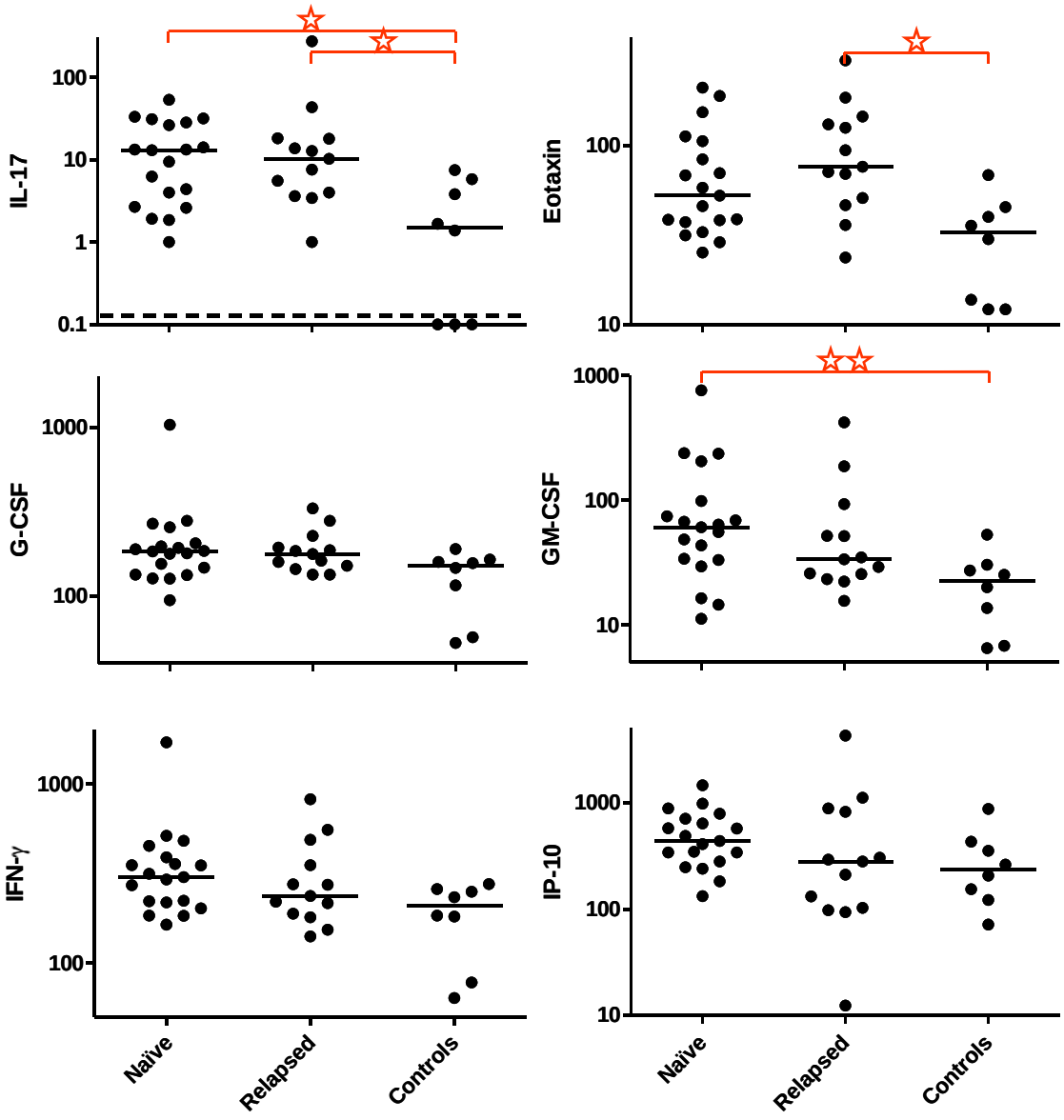
IL-17
100
10
1
0.1
Eotaxin
100
10
G-CSF
1000
100
GM-CSF
1000
100
10
IFN-γ
1000
100
IP-10
1000
100
10
Naïve
Relapsed
Controls
Naïve
Relapsed
Controls

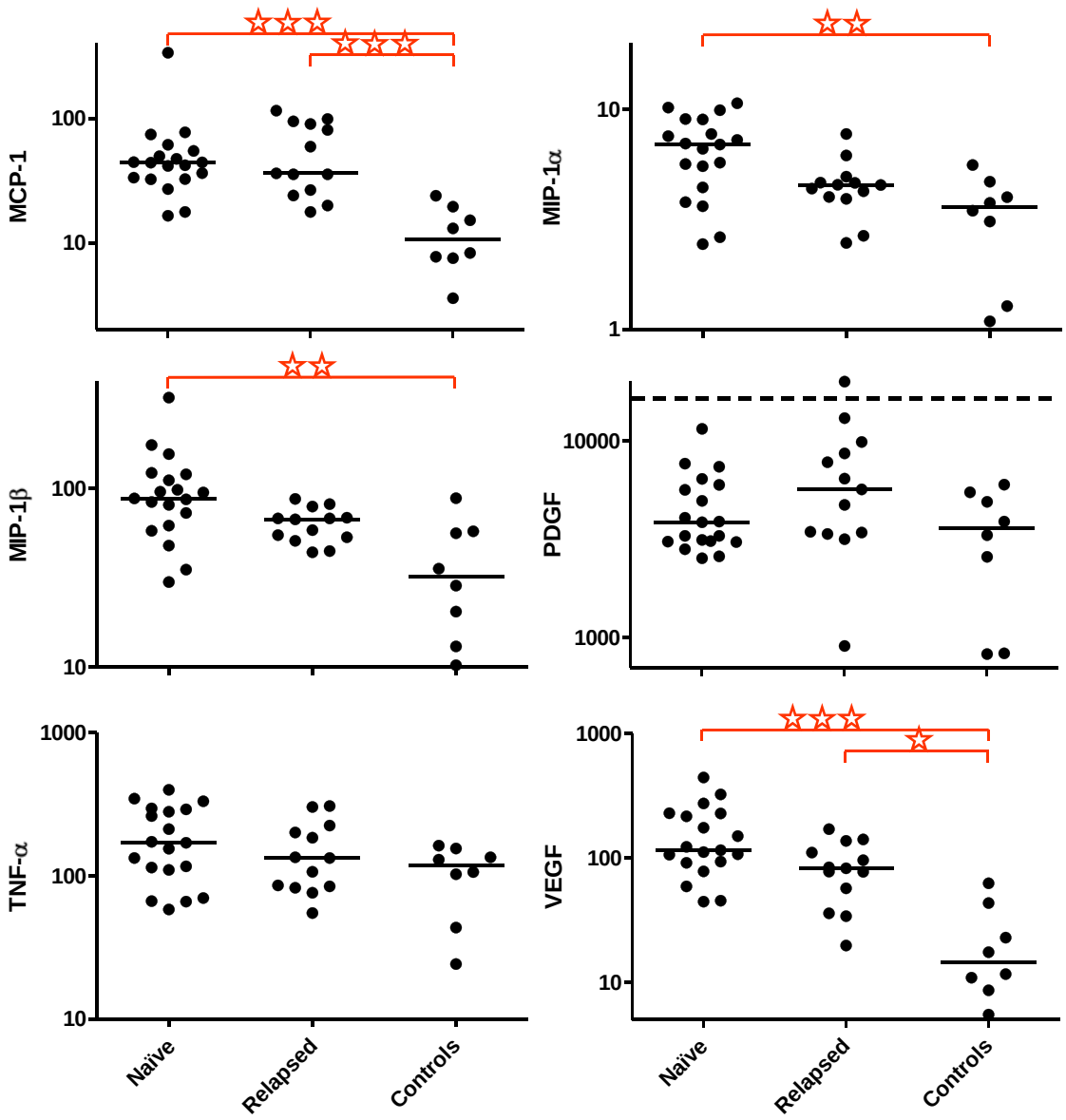
MCP-1
100
10
MIP-1α
10
1
MIP-1β
100
10
PDGF
10000
1000
TNF-α
1000
100
10
VEGF
1000
100
10
Naïve
Relapsed
Controls
Naïve
Relapsed
Controls

11 APPENDIX 4: CHANGES IN SERUM LEVELS OF CYTOKINES IN PATIENTS WITH ANCA- ASSOCIATED VASCULITIS AFTER TREATMENT WITH CYCLOPHOSPHAMIDE OR RITUXIMAB

Cytokine	Changes in 5 months after Cyclophosphamide based therapy		Changes in 5 months after Rituximab based therapy	
	Median % fall (*or rise*)	Significance of change ($p<0.05$)	Median % fall (*or rise*)	Significance ($p<0.05$)
IL-1β	8%		28%	✓
IL-1Rα	35%	✓	4%	
IL-2	87-93%		86%	✓
IL-4	18%	✓	33%	✓
IL-5	70-72%	✓	83%	✓
IL-6	70%	✓	67%	✓
IL-7	64%	✓	48%	✓
IL-8	33%		48%	
IL-9	69%	✓	40%	✓
IL-10	57%		35%	✓
IL-12	52%		46%	✓
IL-13	71%		69%	✓
IL-17	35%	✓	*45% rise*	
Eotaxin	*77% rise*		*42% rise*	
G-CSF	11%		31%	✓
GM-CSF	44%	✓	43%	✓
γ-IFN	28%		25%	✓
IP-10	50%		*113% rise*	
MCP-1	10%		*9% rise*	
MIP-1α	34%		28%	
MIP-1β	9%		*32% rise*	✓
PDGF	36%	✓	4%	
TNF-α	12%		57%	✓
VEGF	66%	✓	29%	

Table 11-1 summarizes the changes in serum levels of various cytokines in the 5 months following treatment of ANCA-associated vasculitis with either cyclophosphamide or Rituximab based regimes. Subsequent pages show dot plots with results for individual patients and controls.

The table reports the median percentage change in various cytokines (far-left column) in the 5 months following treatment with either a cyclophosphamide based regime (left columns; n=7) or a Rituximab based regime (right columns; n=6). Percentage changes were calculated for each cytokine in each patient and the median percentage in each treatment group is reported here. Statistical significance (Wilcoxon signed rank test) for each comparison is reported is $p<0.05$ (✓). No tests reached significance of $p<0.01$.

Scatter plots representing the changes within each patient, in levels of parameters indicating disease activity, in serum levels of autoantibody, and in serum levels of each cytokine, are presented on the subsequent pages. In each plot two dots, linked by a solid line, represent the results from one patient. Horizontal dotted lines, where present indicate the limits of the assay's range. Where appropriate, levels in control patients (n=8) are included for comparison. Statistical significance (Wilcoxon signed rank test) for each comparison is reported as follows: $p<0.05$ (☆).

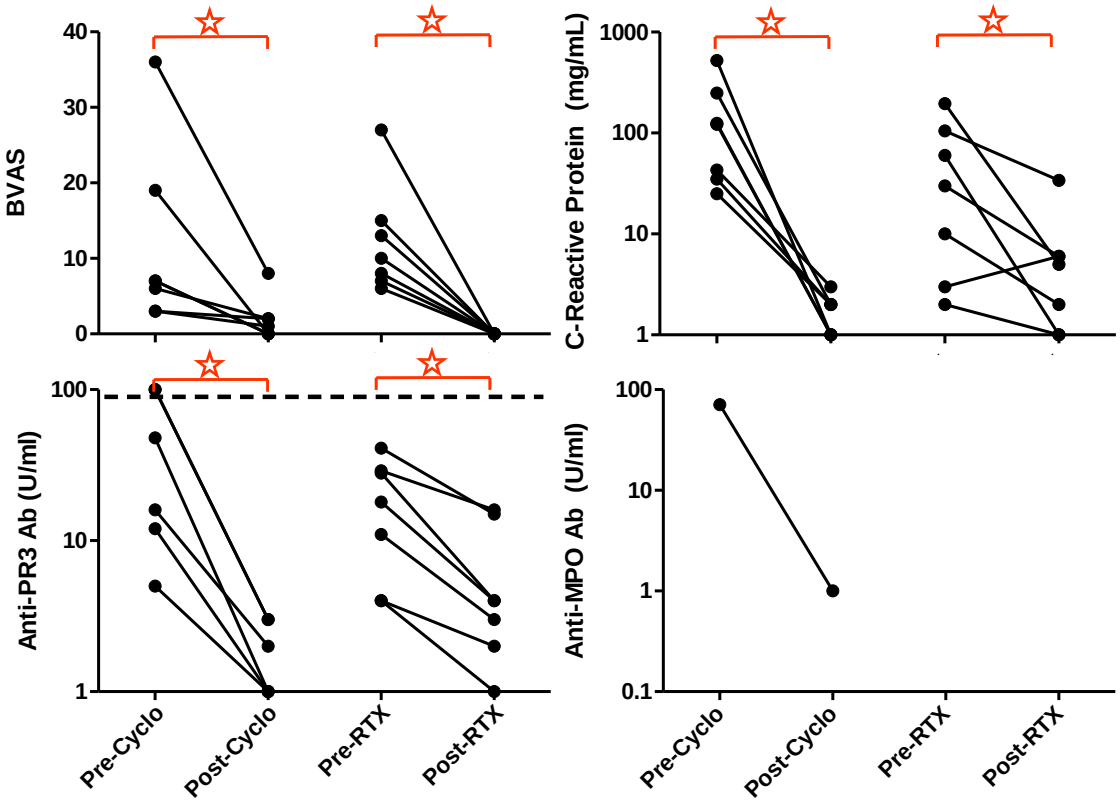

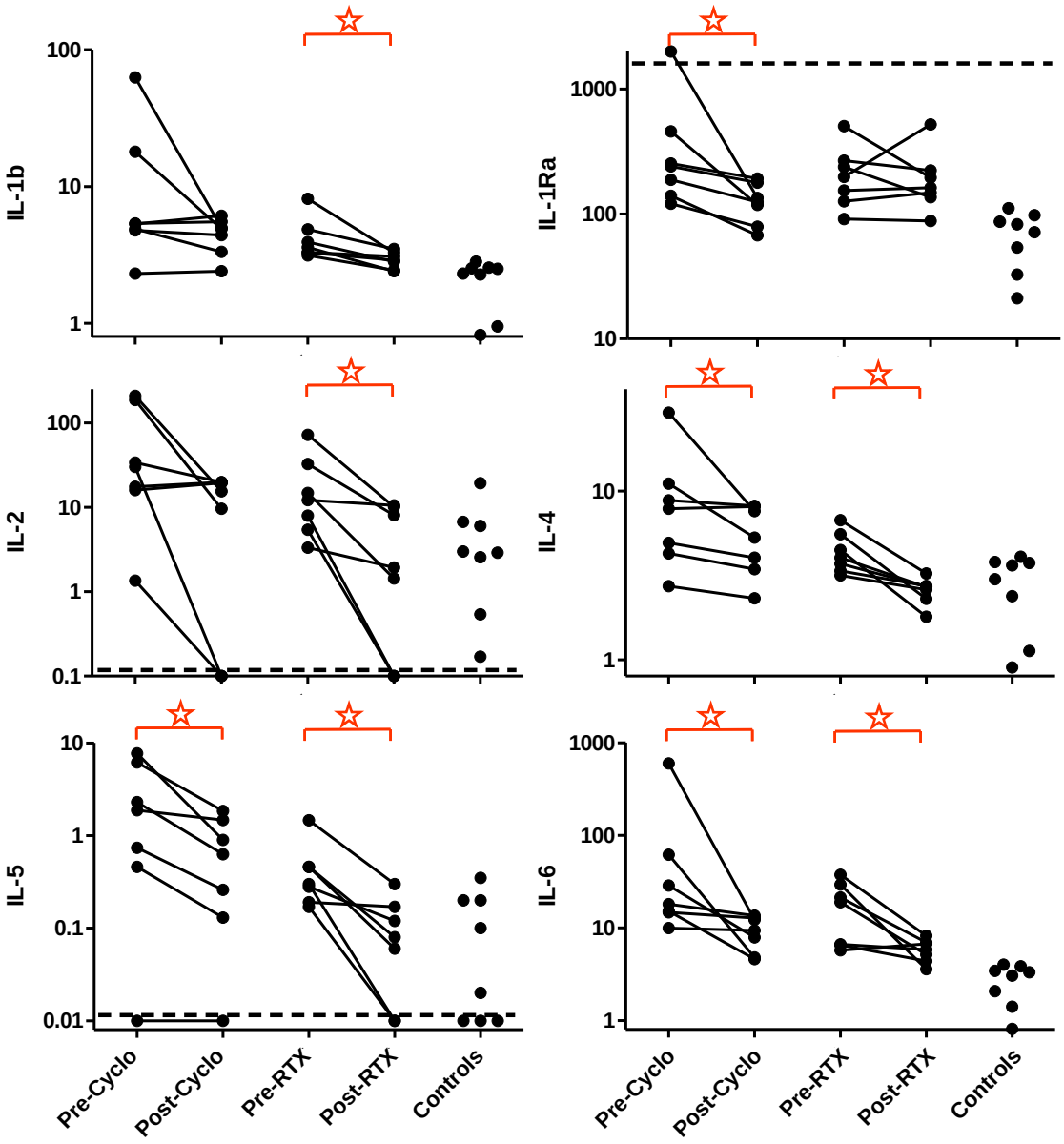
IL-1b
100
10
1
IL-1Ra
1000
100
10
IL-2
100
10
1
0.1
IL-4
10
1
IL-5
10
1
0.1
0.01
IL-6
1000
100
10
1
Pre-Cyclo
Post-Cyclo
Pre-RTX
Post-RTX
Controls

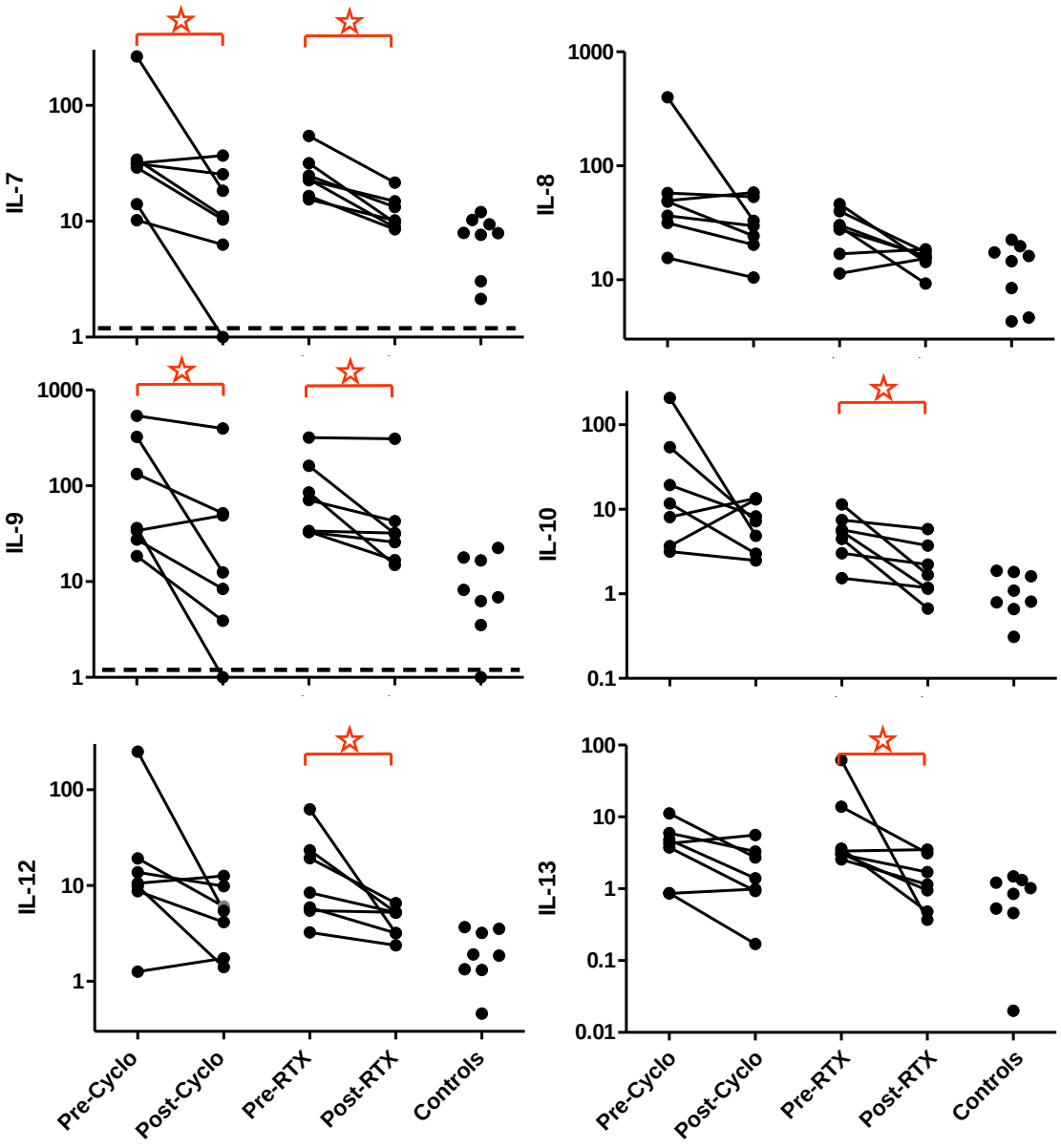
IL-7
IL-8
IL-9
IL-10
IL-12
IL-13
Pre-Cyclo
Post-Cyclo
Pre-RTX
Post-RTX
Controls

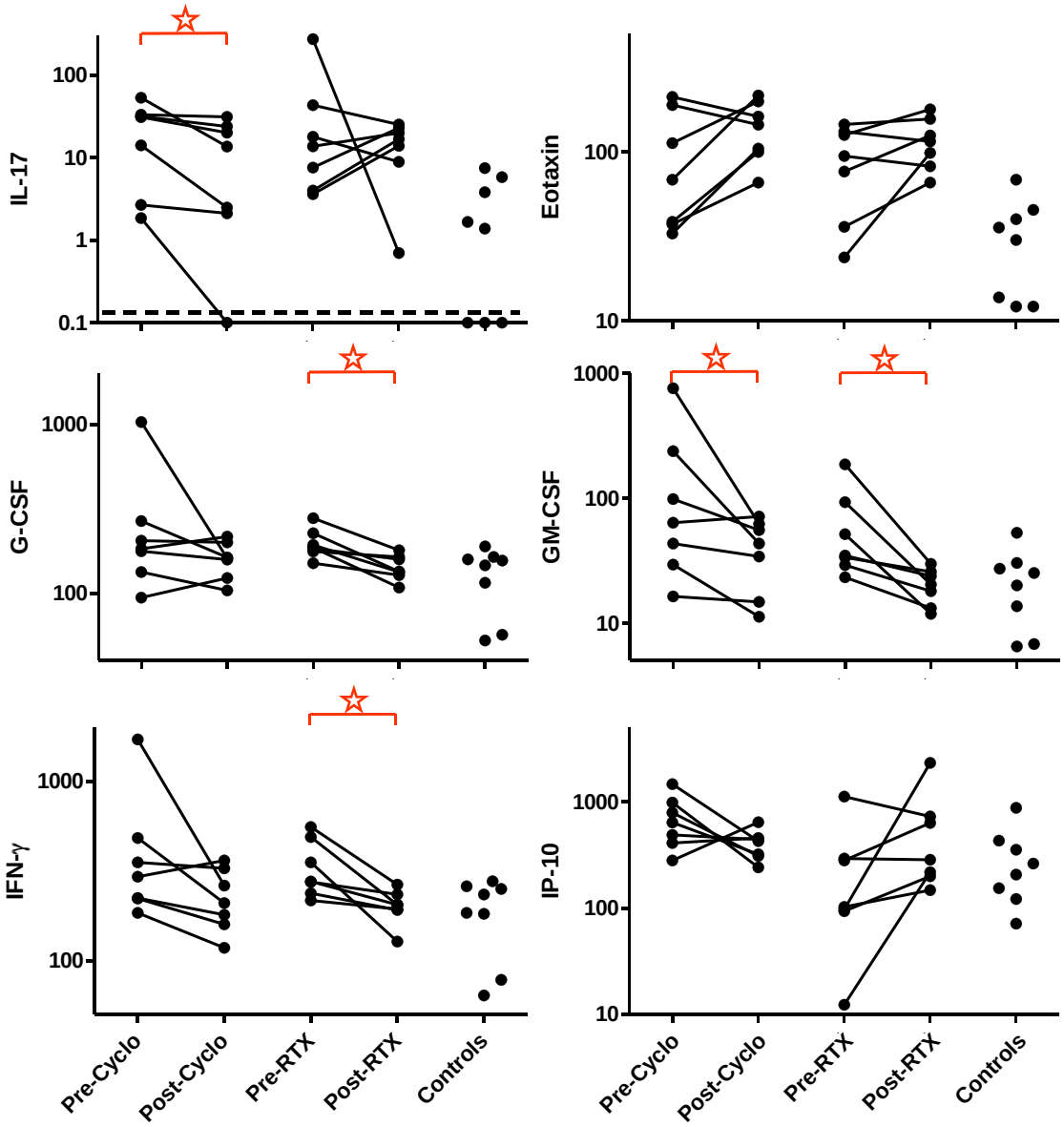
IL-17
100
10
1
0.1
Eotaxin
100
10
G-CSF
1000
100
GM-CSF
1000
100
10
IFN-γ
1000
100
IP-10
1000
100
10
Pre-Cyclo
Post-Cyclo
Pre-RTX
Post-RTX
Controls

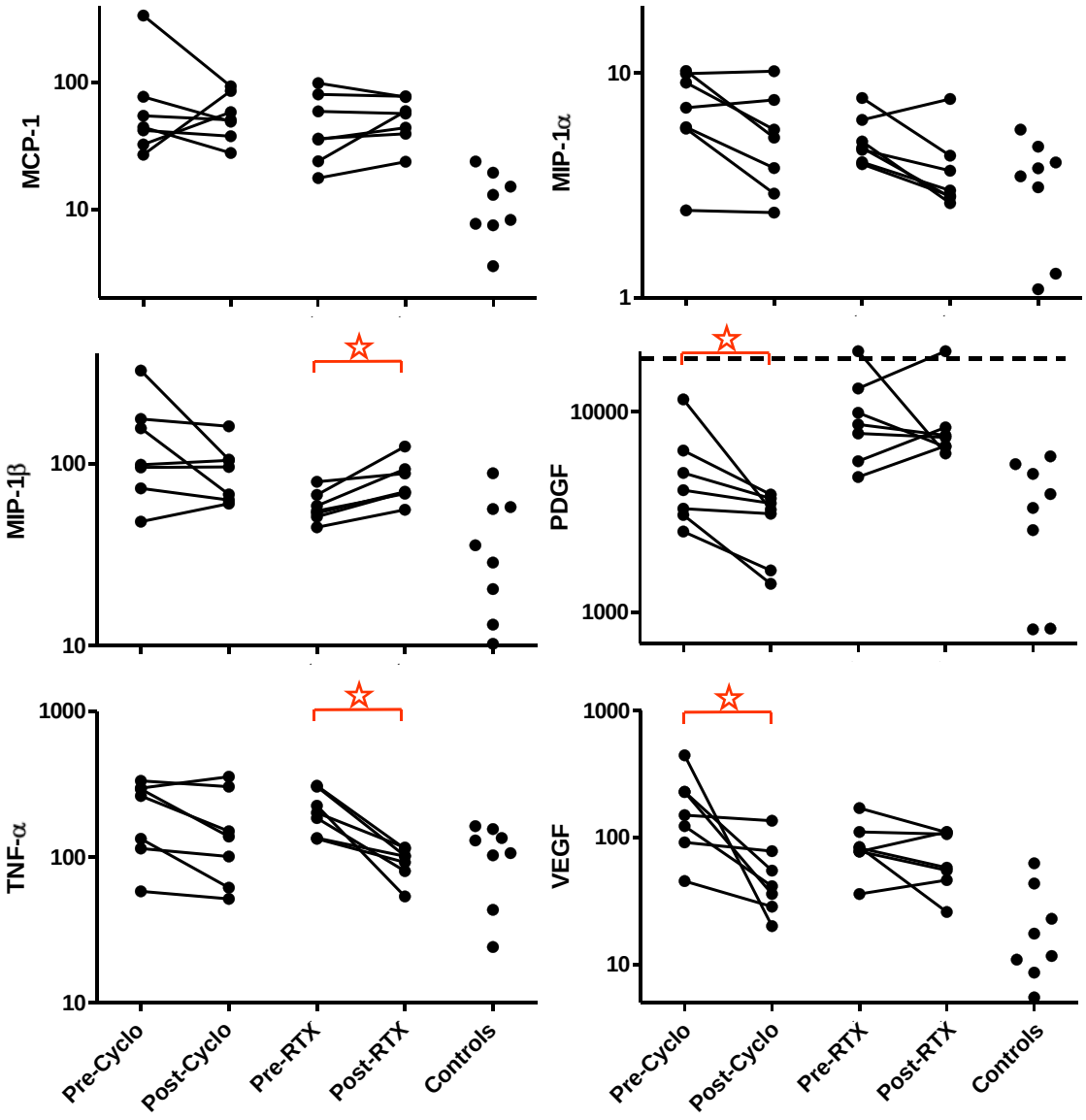
MCP-1
100
10
MIP-1α
10
1
MIP-1β
100
10
PDGF
10000
1000
TNF-α
1000
100
10
VEGF
1000
100
10
Pre-Cyclo
Post-Cyclo
Pre-RTX
Post-RTX
Controls
Pre-Cyclo
Post-Cyclo
Pre-RTX
Post-RTX
Controls

12 APPENDIX 5: IMMUNOHISTOCHEMICAL STAINING WITH ANTIBODIES AGAINST ER-TR7 AND AGAINST HUMAN COLLAGEN III

Additional immunohistochemical studies indicated that antibodies against human Collagen III and antibodies against ER-TR7 [242] identify similar structures in the spleens of naïve QMxB6 mice, and those inoculated with NP-Ficoll, or *S.* Typhimurium or both. Examples are shown in Figure 12-1.

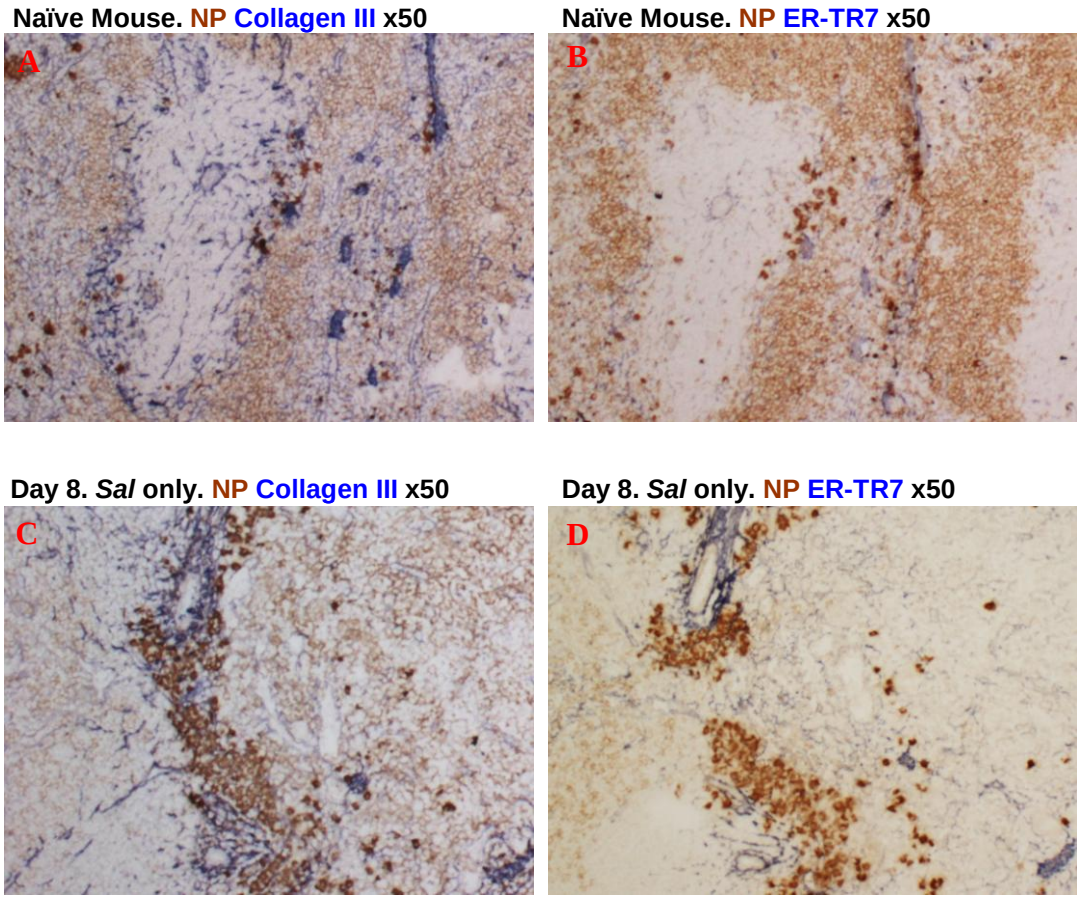

Figure 12-1 shows that in the spleens of QMxB6 mice, analogous trabecular structures are identified by antibodies against human Collagen III, and antibodies against ER-TR7 [242].
The mouse group, staining patterns and original magnification are shown above each photomicrograph. **Panels A and B** are photomicrographs of proximate spleen sections from one representative naïve mouse, whilst **Panels C & D** are photomicrographs of proximate spleen sections from a representative mouse 8 days after *S.* Typhimurium infection. All sections were stained for antibodies to NP (brown). **Panels A & C** are also stained with antibodies against human Collagen III (blue), whilst **panels B & D** are stained with antibodies against ER-TR7 (brown). Analogous structures, including red pulp trabeculae, are identified by the antibody against human Collagen III and the antibody against ER-TR7.

13 REFERENCES

1. **Mason,D.Y. and Jones,M.,** B-Cell Antigens. In **Kishimoto,T., Kikutani,H., and et al** (Eds.) *Leucocyte Typing VI*. Garland Publishing, 1997, pp 127-262.

2. **Reff,M.E., Carner,K., Chambers,K.S., Chinn,P.C., Leonard,J.E., Raab,R., Newman,R.A., Hanna,N., and Anderson,D.R.,** Depletion of B cells in vivo by a chimeric mouse human monoclonal antibody to CD20. *Blood* 1994. **83**: 435-445.

3. **Edwards,J.C., Szczepanski,L., Szechinski,J., Filipowicz-Sosnowska,A., Emery,P., Close,D.R., Stevens,R.M., and Shaw,T.,** Efficacy of B-cell-targeted therapy with rituximab in patients with rheumatoid arthritis. *New England Journal of Medicine* 2004. **350**: 2572-2581.

4. **Specks,U., Fervenza,F., McDonald,T.J., and Hogan,M.C.E.,** Response of Wegener's granulomatosis to anti-CD20 chimeric monoclonal antibody therapy. *Arthritis and Rheumatism* 2001. **44**: 2836-2840.

5. **Keogh,K.A., Wylam,M.E., Stone,J.H., and Specks,U.,** Induction of remission by B lymphocyte depletion in eleven patients with refractory antineutrophil cytoplasmic antibody-associated vasculitis. *Arthritis & Rheumatism* 2005. **52**: 262-268.

6. **Leandro,M.J., Edwards,J.C., Cambridge,G., Ehrenstein,M.R., and Isenberg,D.A.,** An open study of B lymphocyte depletion in systemic lupus erythematosus. *Arthritis & Rheumatism* 2002. **46**: 2673-2677.

7. **Jy,W., Gagliano-DeCesare,T., Kett,D.H., Horstman,L.L., Jimenez,J.J., Ruiz-Dayao,Z., Santos,E.S., and Ahn,Y.S.,** Life-threatening bleeding from refractory acquired FVIII inhibitor successfully treated with rituximab. *Acta Haematologica* 2003. **109**: 206-208.

8. **Braendstrup,P., Bjerrum,O.W., Nielsen,O.J., Jensen,B.A., Clausen,N.T., Hansen,P.B., Andersen,I., Schmidt,K., Andersen,T.M., Peterslund,N.A., Birgens,H.S., Plesner,T., Pedersen,B.B., and Hasselbalch,H.C.,** Rituximab chimeric anti-CD20 monoclonal antibody treatment for adult refractory idiopathic thrombocytopenic purpura. *American Journal of Hematology* 2005. **78**: 275-280.

9. "RAVE - Rituximab for ANCA associated Vasculitis", at http://www.immunetolerance.org/RAVE/ and last accessed on 5-8-2009

10. "Clinical Trials by EUVAS", at http://www.vasculitis.org/acttrials.htm and last accessed on 5-8-0209

11. **Cambridge,G., Leandro,M.J., Edwards,J.C., Ehrenstein,M.R., Salden,M., Bodman-Smith,M., and Webster,A.D.,** Serologic changes following B

lymphocyte depletion therapy for rheumatoid arthritis. *Arthritis & Rheumatism* 2003. **48**: 2146-2154.

12. **Ferraro,A.J., Day,C.J., Drayson,M.T., and Savage,C.O.,** Effective therapeutic use of rituximab in refractory Wegener's granulomatosis. *Nephrol.Dial.Transplant.* 2005. **20**: 622-625.

13. **Vallerskog,T., Gunnarsson,I., Widhe,M., Risselada,A., Klareskog,L., van Vollenhoven,R., Malmstrom,V., and Trollmo,C.,** Treatment with rituximab affects both the cellular and the humoral arm of the immune system in patients with SLE. *Clinical Immunology* 2007. **122**: 62-74.

14. **Muehlinghaus,G., Cigliano,L., Huehn,S., Peddinghaus,A., Leyendeckers,H., Hauser,A.E., Hiepe,F., Radbruch,A., Arce,S., and Manz,R.A.,** Regulation of CXCR3 and CXCR4 expression during terminal differentiation of memory B cells into plasma cells. *Blood* 2005. **105**: 3965-3971.

15. **Leavitt,R.Y., Fauci,A.S., Bloch,D.A., Michel,B.A., Hunder,G.G., Arend,W.P., Calabrese,L.H., Fries,J.F., Lie,J.T., Lightfoot,R.W., Masi,A.T., Mcshane,D.J., Mills,J.A., Stevens,M.B., Wallace,S.L., and Zvaifler,N.J.,** The American College of Rheumatology 1990 criteria for the classification of Wegener granulomatosis. *Arthritis and Rheumatism* 1990. **33**: 1101-1107.

16. **Watts,R.A., Gonzalez-Gay,M.A., Lane,S.E., Garcia-Porrua,C., Bentham,G., and Scott,D.G.I.,** Geoepidemiology of systemic vasculitis: comparison of the incidence in two regions of Europe. *Ann Rheum Dis* 2001. **60**: 170-172.

17. **Luqmani,R.A., Bacon,P.A., Moots,R.J., Janssen,B.A., Pall,A., Emery,P., Savage,C., and Adu,D.,** Birmingham Vasculitis Activity Score (BVAS) in systemic necrotizing vasculitis. *Qjm* 1994. **87**: 671-678.

18. **Hagen,E.C., Daha,M.R., Hermans,J., Andrassy,K., Csernok,E., Gaskin,G., Lesavre,P., Ludemann,J., Rasmussen,N., Sinico,R.A., Wiik,A., and Van Der Woude,F.J.,** Diagnostic value of standardized assays for anti-neutrophil cytoplasmic antibodies in idiopathic systemic vasculitis. *Kidney International* 1998. **53**: 743-753.

19. **Bosch,X., Guilabert,A., and Font,J.,** Antineutrophil cytoplasmic antibodies. *The Lancet* 2006. **368**: 404-418.

20. **Harper,L. and Savage,C.O.S.,** Pathogenesis of ANCA-associated systemic vasculitis. *Journal of Pathology* 2000. **190**: 349-359.

21. **Ferraro,A.J., Hassan,B., and Savage,C.O.,** Pathogenic mechanisms of anti-neutrophil cytoplasm antibody-associated vasculitis. *Expert Review of Clinical Immunology* 2007. **3**: 543-555.

22. **Looney,R.J., Anolik,J.H., Campbell,D., Felgar,R.E., Young,F., Arend,L.J., Sloand,J.A., Rosenblatt,J., and Sanz,I.,** B cell depletion as a novel treatment for systemic lupus erythematosus: a phase I/II dose-escalation trial of rituximab. *Arthritis & Rheumatism* 2004. **50**: 2580-2589.

23. **Cambridge,G., Leandro,M.J., Teodorescu,M., Manson,J., Rahman,A., Isenberg,D.A., and Edwards,J.C.,** B cell depletion therapy in systemic lupus erythematosus - Effect on autoantibody and antimicrobial antibody profiles. *Arthritis and Rheumatism* 2006. **54**: 3612-3622.

24. **Sibilia,J., Benlagha,K., Vanhille,P., Ronco,P., Brouet,J.C., and Mariette,X.,** Structural analysis of human antibodies to proteinase 3 from patients with Wegener granulomatosis. *Journal of Immunology* 1997. **159**: 712-719.

25. **van Esch,W.J., Reparon-Schuijt,C.C., Hamstra,H.J., van Kooten,C., Logtenberg,T., Breedveld,F.C., and Verweij,C.L.,** Human IgG Fc-binding phage antibodies constructed from synovial fluid CD38+ B cells of patients with rheumatoid arthritis show the imprints of an antigen-dependent process of somatic hypermutation and clonal selection. *Clinical & Experimental Immunology* 2003. **131**: 364-376.

26. **Victor,K.D., Randen,I., Thompson,K., Forre,O., Natvig,J.B., Fu,S.M., and Capra,J.D.,** Rheumatoid Factors Isolated from Patients with Autoimmune Disorders Are Derived from Germline Genes Distinct from Those Encoding the

Wa, Po, and Bla Cross-Reactive Idiotypes. *Journal of Clinical Investigation* 1991. **87**: 1603-1613.

27. **Davis,J.A., Peen,E., Williams,R.C., Perkins,S., Malone,C.C., McCormack,W.T., Csernok,E., Gross,W.L., Kolaskar,A.S., and Kulkarni-Kale,U.,** Determination of primary amino acid sequence and unique three-dimensional structure of WGH1, a monoclonal human IgM antibody with anti-PR3 specificity. *Clinical Immunology and Immunopathology* 1998. **89**: 35-43.

28. **Esposito,G., Scarselli,E., and Traboni,C.,** Phage display of a human antibody against Clostridium tetani toxin. *Gene* 1994. **148**: 167-168.

29. **Ernst,J.A., Li,H., Kim,H.S., Nakamura,G.R., Yansura,D.G., and Vandlen,R.L.,** Isolation and characterization of the B-cell marker CD20. *Biochemistry* 2005. **44**: 15150-15158.

30. **Algino,K.M., Thomason,R.W., King,D.E., Montiel,M.M., and Craig,F.E.,** CD20 (pan-B cell antigen) expression on bone marrow-derived T cells. *American Journal of Clinical Pathology* 1996. **106**: 78-81.

31. **Leandro,M.J., Cambridge,G., Ehrenstein,M.R., and Edwards,J.C.W.,** Reconstitution of peripheral blood B cells after depletion with rituximab in patients with rheumatoid arthritis. *Arthritis & Rheumatism* 2006. 613-620.

32. **Hultin,L.E., Hausner,M.A., Hultin,P.M., and Giorgi,J.V.,** CD20 (pan-B cell) antigen is expressed at a low level on a subpopulation of human T lymphocytes. *Cytometry* 1993. **14**: 196-204.

33. **Storie,I., Wilson,G.A., Granger,V., Barnett,D., and Reilly,J.T.,** Circulating CD20dim T-lymphocytes increase with age: evidence for a memory cytotoxic phenotype. *Clinical & Laboratory Haematology* 1995. **17**: 323-328.

34. **Bubien,J.K., Zhou,L.J., Bell,P.D., Frizzell,R.A., and Tedder,T.F.,** Transfection of the CD20 cell surface molecule into ectopic cell types generates a Ca2+ conductance found constitutively in B lymphocytes. *Journal of Cell Biology* 1993. **121**: 1121-1132.

35. **Li,H., Ayer,L.M., Lytton,J., and Deans,J.P.,** Store-operated cation entry mediated by CD20 in membrane rafts. *J.Biol.Chem.* 2003. **278**: 42427-42434.

36. **Uchida,J., Lee,Y., Hasegawa,M., Liang,Y., Bradney,A., Oliver,J.A., Bowen,K., Steeber,D.A., Haas,K.M., Poe,J.C., and Tedder,T.F.,** Mouse CD20 expression and function. *International Immunology* 2004. **16**: 119-29.

37. **Uchida,J., Hamaguchi,Y., Oliver,J.A., Ravetch,J.V., Poe,J.C., Haas,K.M., and Tedder,T.F.,** The innate mononuclear phagocyte network depletes B lymphocytes through Fc receptor-dependent mechanisms during anti-CD20

antibody immunotherapy. *Journal of Experimental Medicine* 2004. **199**: 1659-1669.

38. **Cartron,G., Dacheux,L., Salles,G., Solal-Celigny,P., Bardos,P., Colombat,P., and Watier,H.,** Therapeutic activity of humanized anti-CD20 monoclonal antibody and polymorphism in IgG Fc receptor Fcgamma RIIIa gene. *Blood* 2002. **99**: 754-758.

39. **Anolik,J.H., Campbell,D., Felgar,R.E., Young,F., Sanz,I., Rosenblatt,J., and Looney,R.J.,** The relationship of FcgammaRIIIa genotype to degree of B cell depletion by rituximab in the treatment of systemic lupus erythematosus. *Arthritis & Rheumatism* 2003. **48**: 455-459.

40. **Gong,Q., Ou,Q., Ye,S., Lee,W.P., Cornelius,J., Diehl,L., Lin,W.Y., Hu,Z., Lu,Y., Chen,Y., Wu,Y., Meng,Y.G., Gribling,P., Lin,Z., Nguyen,K., Tran,T., Zhang,Y., Rosen,H., Martin,F., and Chan,A.C.,** Importance of cellular microenvironment and circulatory dynamics in B cell immunotherapy. *Journal of Immunology* 2005. **174**: 817-826.

41. **MacLennan,I.C., Campbell,A.C., and Gale,D.G.,** Quantitation of K cells. In **Bloom,B.R. and David,J.R.** (Eds.) *In vitro methods in cell-mediated immunity.* Academic Press, New York 1976, pp 511-522.

42. **Treon,S.P., Mitsiades,C., Mitsiades,N., Young,G., Doss,D., Schlossman,R., and Anderson,K.C.,** Tumor cell expression of CD59 is associated with resistance to CD20 serotherapy in patients with B-cell malignancies. *Journal of Immunotherapy* 2001. **24**: 263-271.

43. **Pedersen,I.M., Buhl,A.M., Klausen,P., Geisler,C.H., and Jurlander,J.,** The chimeric anti-CD20 antibody rituximab induces apoptosis in B-cell chronic lymphocytic leukemia cells through a p38 mitogen activated protein-kinase-dependent mechanism. *Blood* 2002. **99**: 1314-1319.

44. **MacLennan,I.C.M.,** Germinal-Centers. *Annual Review of Immunology* 1994. **12**: 117-139.

45. **MacLennan,I.C., Toellner,K.M., Cunningham,A.F., Serre,K., Sze,D.M., Zuniga,E., Cook,M.C., and Vinuesa,C.G.,** Extrafollicular antibody responses. *Immunological Reviews* 2003. **194**: 8-18.

46. **Hsu,M.-C., Toellner,K.-M., Vinuesa,C.G., and MacLennan,I.C.M.,** B cell clones that sustain long-term plasmablast growth in T-independent extrafollicular antibody responses. *Proceedings of the National Academy of Sciences of the United States of America* 2006. **103**: 5905-5910.

47. **Obukhanych,T.V. and Nussenzweig,M.C.,** T-independent type II immune responses generate memory B cells. *Journal of Experimental Medicine* 2006. **203**: 305-310.

48. **Klimiuk,P.A., Goronzy,J.J., Bjornsson,J., Beckenbaugh,R.D., and Weyand,C.M.,** Tissue cytokine patterns distinguish variants of rheumatoid synovitis. *American Journal of Pathology* 1997. **151**: 1311-1319.

49. **Voswinkel,J., Mueller,A., Kraemer,J.A., Lamprecht,P., Herlyn,K., Holl-Ulrich,K., Feller,A.C., Pitann,S., Gause,A., and Gross,W.L.,** B lymphocyte maturation in Wegener's granulomatosis: a comparative analysis of VH genes from endonasal lesions. *Ann Rheum Dis* 2006. **65**: 859-864.

50. **Stott,D.I., Hiepe,F., Hummel,M., Steinhauser,G., and Berek,C.,** Antigen-driven clonal proliferation of B cells within the target tissue of an autoimmune disease. The salivary glands of patients with Sjogren's syndrome. *Journal of Clinical Investigation* 1998. **102**: 938-946.

51. **Wagner,U.G., Kurtin,P.J., Wahner,A., Brackertz,M., Berry,D.J., Goronzy,J.J., and Weyand,C.M.,** The role of CD8(+) CD40L(+) T cells in the formation of germinal centers in rheumatoid synovitis. *Journal of Immunology* 1998. **161**: 6390-6397.

52. **Kim,H.J., Krenn,V., Steinhauser,G., and Berek,C.,** Plasma cell development in synovial germinal centers in patients with rheumatoid and reactive arthritis. *Journal of Immunology* 1999. **162**: 3053-3062.

53. **Cantaert,T., Kolln,J., Timmer,T., van der Pouw Kraan,T., Vandooren,B., Thurlings,R.M., Canete,J.D., Catrina,A.I., Out,T., Verweij,C.L., Zhang,Y., Tak,P.P., and Baeten,D.,** B Lymphocyte Autoimmunity in Rheumatoid Synovitis Is Independent of Ectopic Lymphoid Neogenesis. *J Immunol* 2008. **181**: 785-794.

54. **Bos,N.A., Meeuwsen,C.G., Wostmann,B.S., Pleasants,J.R., and Benner,R.,** The influence of exogenous antigenic stimulation on the specificity repertoire of background immunoglobulin-secreting cells of different isotypes. *Cellular Immunology* 1988. **112**: 371-380.

55. **Haury,M., Sundblad,A., Grandien,A., Barreau,C., Coutinho,A., and Nobrega,A.,** The repertoire of serum IgM in normal mice is largely independent of external antigenic contact. *European Journal of Immunology* 1997. **27**: 1557-1563.

56. **Martin,F., Oliver,A.M., and Kearney,J.F.,** Marginal zone and B1 B cells unite in the early response against T-independent blood-borne particulate antigens. *Immunity* 2001. **14**: 617-629.

57. **Cunningham,A.F., Gaspal,F., Serre,K., Mohr,E., Henderson,I.R., Scott-Tucker,A., Kenny,S.M., Khan,M., Toellner,K.M., Lane,P.J.L., and MacLennan,I.C.M.,** Salmonella induces a switched antibody response without germinal centers that impedes the extracellular spread of infection. *Journal of Immunology* 2007. **178**: 6200-6207.

58. **Slifka,M.K., Antia,R., Whitmire,J.K., and Ahmed,R.,** Humoral immunity due to long-lived plasma cells. *Immunity* 1998. **8**: 363-372.

59. **Manz,R.A., Lohning,M., Cassese,G., Thiel,A., and Radbruch,A.,** Survival of long-lived plasma cells is independent of antigen. *International Immunology* 1998. **10**: 1703-1711.

60. **Sze,D.M., Toellner,K.M., Garcia,d., V, Taylor,D.R., and MacLennan,I.C.,** Intrinsic constraint on plasmablast growth and extrinsic limits of plasma cell survival. *Journal of Experimental Medicine.* 2000. **192**: 813-821.

61. **Ahuja,A., Anderson,S.M., Khalil,A., and Shlomchik,M.J.,** Maintenance of the plasma cell pool is independent of memory B cells. *Proceedings of the National Academy of Sciences of the United States of America* 2008. **105**: 4802-4807.

62. **DiLillo,D.J., Hamaguchi,Y., Ueda,Y., Yang,K., Uchida,J., Haas,K.M., Kelsoe,G., and Tedder,T.F.,** Maintenance of long-lived plasma cells and

serological memory despite mature and memory B cell depletion during CD20 immunotherapy in mice. *Journal of Immunology* 2008. **180**: 361-371.

63. **Coico,R.F., Bhogal,B.S., and Thorbecke,G.J.,** Relationship of Germinal-Centers in Lymphoid-Tissue to Immunological Memory .6. Transfer of B-Cell Memory with Lymph-Node Cells Fractionated According to Their Receptors for Peanut Agglutinin. *Journal of Immunology* 1983. **131**: 2254-2257.

64. **Weller,S., Braun,M.C., Tan,B.K., Rosenwald,A., Cordier,C., Conley,M.E., Plebani,A., Kumararatne,D.S., Bonnet,D., Tournilhac,O., Tchernia,G., Steiniger,B., Staudt,L.M., Casanova,J.L., Reynaud,C.A., and Weill,J.C.,** Human blood IgM "memory" B cells are circulating splenic marginal zone B cells harboring a prediversified immunoglobulin repertoire. *Blood* 2004. **104**: 3647-3654.

65. **Liu,Y.J., Oldfield,S., and MacLennan,I.C.M.,** Memory B-Cells in T-Cell-Dependent Antibody-Responses Colonize the Splenic Marginal Zones. *European Journal of Immunology* 1988. **18**: 355-362.

66. **Ling,N.R., MacLennan,I., and Mason,D.Y.,** B cell and plasma cell antigens: new and previously defined clusters. In **McMichael,A.J.** (Ed.) *Leucocyte Typing III*. Oxford University Press, Oxford 1987, pp 302-335.

67. **van der Kolk,L.E., Baars,J.W., Prins,M.H., and van Oers,M.H.J.,** Rituximab treatment results in impaired secondary humoral immune responsiveness. *Blood* 2002. **100**: 2257-2259.

68. **Bearden,C.M., Agarwal,A., Book,B.K., Vieira,C.A., Sidner,R.A., Ochs,H.D., Young,M., and Pescovitz,M.D.,** Rituximab inhibits the in vivo primary and secondary antibody response to a neoantigen, bacteriophage phiX174. *American Journal of Transplantation* 2005. **5**: 50-57.

69. **Bernasconi,N.L., Traggiai,E., and Lanzavecchia,A.,** Maintenance of serological memory by polyclonal activation of human memory B cells. *Science* 2002. **298**: 2199-2202.

70. **Amanna,I.J., Carlson,N.E., and Slifka,M.K.,** Duration of humoral immunity to common viral and vaccine antigens. *New England Journal of Medicine* 2007. **357**: 1903-1915.

71. **Ahuja,A., Shupe,J., Dunn,R., Kashgarian,M., Kehry,M.R., and Shlomchik,M.J.,** Depletion of B cells in murine lupus: efficacy and resistance. *Journal of Immunology* 2007. **179**: 3351-3361.

72. **Liu,Y.J., Zhang,J., Lane,P.J., Chan,E.Y., and MacLennan,I.C.,** Sites of specific B cell activation in primary and secondary responses to T cell-dependent

and T cell-independent antigens.[erratum appears in Eur J Immunol 1992 Feb;22(2):615]. *European Journal of Immunology* 1991. **21**: 2951-2962.

73. **Vinuesa,C.G., Sunners,Y., Pongracz,J., Ball,J., Toellner,K.M., Taylor,D., MacLennan,I.C., and Cook,M.C.,** Tracking the response of Xid B cells in vivo: TI-2 antigen induces migration and proliferation but Btk is essential for terminal differentiation. *European Journal of Immunology* 2001. **3**: 1340-1350.

74. **Ho,F., Lortan,J.E., MacLennan,I.C., and Khan,M.,** Distinct short-lived and long-lived antibody-producing cell populations. *European Journal of Immunology* 1986. **16**: 1297-1301.

75. **Smith,K.G., Hewitson,T.D., Nossal,G.J., and Tarlinton,D.M.,** The phenotype and fate of the antibody-forming cells of the splenic foci. *European Journal of Immunology* 1996. **26**: 444-448.

76. **Toellner,K.M., Jenkinson,W.E., Taylor,D.R., Khan,M., Sze,D.M., Sansom,D.M., Vinuesa,C.G., and MacLennan,I.C.,** Low-level hypermutation in T cell-independent germinal centers compared with high mutation rates associated with T cell-dependent germinal centers. *Journal of Experimental Medicine* 1996. **195**: 383-389.

77. **William,J., Euler,C., Christensen,S., and Shlomchik,M.J.,** Evolution of autoantibody responses via somatic hypermutation outside of germinal centers. *Science* 2002. **297**: 2066-2070.

78. **Weller,S., Faili,A., Garcia,C., Braun,M.C., Le Deist,F.F., Saint Basile,G.G., Hermine,O., Fischer,A., Reynaud,C.A., and Weill,J.C.,** CD40-CD40L independent Ig gene hypermutation suggests a second B cell diversification pathway in humans. *Proceedings of the National Academy of Sciences of the United States of America* 2001. **98**: 1166-1170.

79. **William,J., Euler,C., Leadbetter,E., Marshak-Rothstein,A., and Shlomchik,M.J.,** Visualizing the onset and evolution of an autoantibody response in systemic autoimmunity. *Journal of Immunology* 2005. **174**: 6872-6878.

80. **Herlands,R.A., William,J., Hershberg,U., and Shlomchik,M.J.,** Anti-chromatin antibodies drive in vivo antigen-specific activation and somatic hypermutation of rheumatoid factor B cells at extrafollicular sites. *European Journal of Immunology* 2007. **37**: 3339-3351.

81. **Kiyoi,H., Naito,K., Ohno,R., and Naoe,T.,** Comparable profiles of the immunoglobulin heavy chain complementarity determining region (CDR)-3 in CD5+ and CD5- human cord blood B lymphocytes. *Immunology* 1995. **85**: 236-240.

82. **Ebeling,S.B., Schutte,M.E., and Logtenberg,T.,** Peripheral human CD5+ and CD5- B cells may express somatically mutated VH5- and VH6-encoded IgM receptors. *Journal of Immunology* 1993. **151**: 6891-6899.

83. **MacLennan,I. and Chan,E.,** The dynamic relationship between B-cell populations in adults. *Immunology Today* 1993. **14**: 29-34.

84. **Hao,Z. and Rajewsky,K.,** Homeostasis of peripheral B cells in the absence of B cell influx from the bone marrow. *Journal of Experimental Medicine* 2001. **194**: 1151-1164.

85. **Kumararatne,D.S., Gagnon,R.F., and Smart,Y.,** Selective loss of large lymphocytes from the marginal zone of the white pulp in rat spleens following a single dose of cyclophosphamide. A study using quantitative histological methods. *Immunology* 1980. **40**: 123-131.

86. **Smith,S.H. and Cancro,M.P.,** Cutting edge: B cell receptor signals regulate BLyS receptor levels in mature B cells and their immediate progenitors. *Journal of Immunology* 2003. **170**: 5820-5823.

87. **Bossen,C., Cachero,T.G., Tardivel,A., Ingold,K., Willen,L., Dobles,M., Scott,M.L., Maquelin,A., Belnoue,E., Siegrist,C.A., Chevrier,S., cha-Orbea,H., Leung,H., Mackay,F., Tschopp,J., and Schneider,P.,** TACI, unlike

BAFF-R, is solely activated by oligomeric BAFF and APRIL to support survival of activated B cells and plasmablasts. *Blood* 2008. **111**: 1004-1012.

88. **Sprent,J., Schaefer,M., Hurd,M., Surh,C.D., and Ron,Y.,** Mature murine B and T cells transferred to SCID mice can survive indefinitely and many maintain a virgin phenotype. *Journal of Experimental Medicine* 1991. **174**: 717-728.

89. **Fulcher,D.A., Lyons,A.B., Korn,S.L., Cook,M.C., Koleda,C., Parish,C., Fazekas de St,G.B., and Basten,A.,** The fate of self-reactive B cells depends primarily on the degree of antigen receptor engagement and availability of T cell help. *Journal of Experimental Medicine* 1996. **183**: 2313-2328.

90. **Luther,S.A., Gulbranson-Judge,A., Acha-Orbea,H., and MacLennan,I.C.,** Viral superantigen drives extrafollicular and follicular B cell differentiation leading to virus-specific antibody production. *Journal of Experimental Medicine* 1997. **185**: 551-562.

91. **Toellner,K.M., Luther,S.A., Sze,D.M., Choy,R.K., Taylor,D.R., MacLennan,I.C., and Acha-Orbea,H.,** T helper 1 (Th1) and Th2 characteristics start to develop during T cell priming and are associated with an immediate ability to induce immunoglobulin class switching. *Journal of Experimental Medicine* 1998. **187**: 1193-1204.

92. **Vinuesa,C.G., Sze,D.M., Cook,M.C., Toellner,K.M., Klaus,G.G., Ball,J., and MacLennan,I.C.,** Recirculating and germinal center B cells differentiate into cells responsive to polysaccharide antigens. *European Journal of Immunology* 2003. **33**: 297-305.

93. **Lane,P.J., Gray,D., Oldfield,S., and MacLennan,I.C.,** Differences in the recruitment of virgin B cells into antibody responses to thymus-dependent and thymus-independent type-2 antigens. *European Journal of Immunology* 1986. **16**: 1569-1575.

94. **Goodnow,C.C., Cyster,J.G., Hartley,S.B., Bell,S.E., Cooke,M.P., Healy,J.I., Akkaraju,S., Rathmell,J.C., Pogue,S.L., and Shokat,K.P.,** Self-tolerance checkpoints in B lymphocyte development. *Advances in Immunology* 1995. **59**: 279-368.

95. **Berland,R. and Wortis,H.H.,** Origins and functions of B-1 cells with notes on the role of CD5. *Annual Review of Immunology* 2002. **20**: 253-300.

96. **Dzierzak,E., Medvinsky,A., and de Bruijn,M.,** Qualitative and quantitative aspects of haematopoietic cell development in the mammalian embryo. *Immunology Today*. 1998. **19**: 228-236.

97. **Montecino-Rodriguez,E., Leathers,H., and Dorshkind,K.,** Identification of a B-1 B cell-specified progenitor. *Nat Immunol* 2006. **7**: 293-301.

98. **Kantor,A.B., Merrill,C.E., Herzenberg,L.A., and Hillson,J.L.,** An unbiased analysis of V(H)-D-J(H) sequences from B-1a, B-1b, and conventional B cells. *Journal of Immunology* 1997. **158**: 1175-1186.

99. **Forster,I., Gu,H., and Rajewsky,K.,** Germline antibody V regions as determinants of clonal persistence and malignant growth in the B cell compartment. *EMBO Journal* 1988. **7**: 3693-3703.

100. **Briles,D.E., Nahm,M., Schroer,K., Davie,J., Baker,P., Kearney,J., and Barletta,R.,** Antiphosphocholine antibodies found in normal mouse serum are protective against intravenous infection with type 3 streptococcus pneumoniae. *Journal of Experimental Medicine* 1981. **153**: 694-705.

101. **Haas,K.M., Poe,J.C., Steeber,D.A., and Tedder,T.F.,** B-1a and B-1b cells exhibit distinct developmental requirements and have unique functional roles in innate and adaptive immunity to S. pneumoniae. *Immunity* 2005. **23**: 7-18.

102. **Cowan,M.J., Ammann,A.J., Wara,D.W., Howie,V.M., Schultz,L., Doyle,N., and Kaplan,M.,** Pneumococcal polysaccharide immunization in infants and children. *Pediatrics* 1978. **62**: 721-727.

103. Naturally arising antibodies. In **Mollison,P.L., Engelfriet,C.P., and Contreras,M.** (Eds.) *Blood Transfusion in Clinical Medicine*. Blackwell Scientific, London 1993, pp 100-102.

104. **Zhou,W., Ohdan,H., Tanaka,Y., Hara,H., Tokita,D., Onoe,T., and Asahara,T.,** NOD/SCID mice engrafted with human peripheral blood lymphocytes can be a model for investigating B cells responding to blood group A carbohydrate determinant. *Transplant Immunology* 2003. **12**: 9-18.

105. **Ohdan,H., Swenson,K.G., Kruger Gray,H.S., Yang,Y.G., Xu,Y., Thall,A.D., and Sykes,M.,** Mac-1-negative B-1b phenotype of natural antibody-producing cells, including those responding to Gal alpha 1,3Gal epitopes in alpha 1,3-galactosyltransferase-deficient mice. *Journal of Immunology* 2000. **165**: 5518-5529.

106. **Tiegs,S.L., Russell,D.M., and Nemazee,D.,** Receptor editing in self-reactive bone marrow B cells. *Journal of Experimental Medicine* 1993. **177**: 1009-1020.

107. **Hartley,S.B., Crosbie,J., Brink,R., Kantor,A.B., Basten,A., and Goodnow,C.C.,** Elimination from peripheral lymphoid tissues of self-reactive B lymphocytes recognizing membrane-bound antigens. *Nature* 1991. **353**: 765-769.

108. **Goodnow,C.C., Crosbie,J., Jorgensen,H., Brink,R.A., and Basten,A.,** Induction of self-tolerance in mature peripheral B lymphocytes. *Nature* 1989. **342**: 385-391.

109. **Lam,K.P. and Rajewsky,K.,** B cell antigen receptor specificity and surface density together determine B-1 versus B-2 cell development. *Journal of Experimental Medicine* 1999. **190**: 471-477.

110. **Watanabe,N., Nisitani,S., Ikuta,K., Suzuki,M., Chiba,T., and Honjo,T.,** Expression levels of B cell surface immunoglobulin regulate efficiency of allelic exclusion and size of autoreactive B-1 cell compartment. *Journal of Experimental Medicine* 1999. **190**: 461-469.

111. **Ferry,H., Crockford,T.L., Leung,J.C.H., and Cornall,R.J.,** Signals from a Self-Antigen Induce Positive Selection in Early B Cell Ontogeny but Are Tolerogenic in Adults. *J Immunol* 2006. **176**: 7402-7411.

112. **Murakami,M., Yoshioka,H., Shirai,T., Tsubata,T., and Honjo,T.,** Prevention of autoimmune symptoms in autoimmune-prone mice by elimination of B-1 cells. *International Immunology* 1995. **7**: 877-882.

113. **Hardy,R.R., Hayakawa,K., Shimizu,M., Yamasaki,K., and Kishimoto,T.,** Rheumatoid factor secretion from human Leu-1+ B cells. *Science* 1987. **236**: 81-83.

114. **Casali,P., Burastero,S.E., Balow,J.E., and Notkins,A.L.,** High-Affinity Antibodies to Ssdna Are Produced by CD5- B-Cells in Systemic Lupus-Erythematosus Patients. *Journal of Immunology* 1989. **143**: 3476-3483.

115. **Tyden,G., Kumlien,G., and Fehrman,I.,** Successful ABO-incompatible kidney transplantations without splenectomy using antigen-specific immunoadsorption and rituximab. *Transplantation* 2003. **76**: 730-731.

116. **Kawahara,T., Ohdan,H., Zhao,G., Yang,Y.G., and Sykes,M.,** Peritoneal cavity B cells are precursors of splenic IgM natural antibody-producing cells. *Journal of Immunology* 2003. **171**: 5406-5414.

117. **Spalter,S.H., Kaveri,S.V., Bonnin,E., Mani,J.C., Cartron,J.P., and Kazatchkine,M.D.,** Normal human serum contains natural antibodies reactive with autologous ABO blood group antigens. *Blood* 1999. **93**: 4418-4424.

118. **Rieben,R., Buchs,J.P., Fluckiger,E., and Nydegger,U.E.,** Antibodies to Histo-Blood Group Substances-A and Substances-B - Agglutination Titers, Ig Class, and Igg Subclasses in Healthy-Persons of Different Age Categories. *Transfusion* 1991. **31**: 607-615.

119. **Martin,F. and Kearney,J.F.,** B1 cells: similarities and differences with other B cell subsets. *Current Opinion in Immunology* 2001. **13**: 195-201.

120. **Ferry,H., Jones,M., Vaux,D.J., Roberts,I.S., and Cornall,R.J.,** The cellular location of self-antigen determines the positive and negative selection of autoreactive B cells. *Journal of Experimental Medicine* 2003. **198**: 1415-1425.

121. **Lokmic,Z., Lammermann,T., Sixt,M., Cardell,S., Hallmann,R., and Sorokin,L.,** The extracellular matrix of the spleen as a potential organizer of immune cell compartments. *Seminars in Immunology* 2008. **20**: 4-13.

122. **Kraal,G. and Janse,M.,** Marginal Metallophilic Cells of the Mouse Spleen Identified by A Monoclonal-Antibody. *Immunology* 1986. **58**: 665-669.

123. **Cascalho,M., Ma,A., Lee,S., Masat,L., and Wabl,M.,** A quasi-monoclonal mouse. *Science* 1996. **272**: 1649-1652.

124. **Gray,D., MacLennan,I.C.M., Bazin,H., and Khan,M.,** Migrant Mu+ Delta+ and Static Mu+ Delta- Lymphocyte-B Subsets. *European Journal of Immunology* 1982. **12**: 564-569.

125. **Cinamon,G., Zachariah,M.A., Lam,O.M., Frank,W.J., and Cyster,J.G.,** Follicular shuttling of marginal zone B cells facilitates antigen transport. *Nature Immunology* 2008. **9**: 54-62.

126. **de Vinuesa,C.G., Cook,M.C., Ball,J., Drew,M., Sunners,Y., Cascalho,M., Wabl,M., Klaus,G.G.B., and MacLennan,I.C.M.,** Germinal centers without T cells. *Journal of Experimental Medicine* 2000. **191**: 485-493.

127. **Shapiro-Shelef,M., Lin,K.I., Heyzer-Williams,L.J., Liao,J., Heyzer-Williams,M.G., and Calame,K.,** Blimp-1 is required for the formation of

immunoglobulin secreting plasma cells and pre-plasma memory B cells. *Immunity* 2003. **19**: 607-620.

128. **de Vinuesa,C.G., Gulbranson-Judge,A., Khan,M., O'Leary,P., Cascalho,M., Wabl,M., Klaus,G.G.B., Owen,M.J., and MacLennan,I.C.M.,** Dendritic cells associated with plasmablast survival. *European Journal of Immunology* 1999. **29**: 3712-3721.

129. **Hebel,K., Griewank,K., Inamine,A., Chang,H.D., Muller-Hilke,B., Fillatreau,S., Manz,R.A., Radbruch,A., and Jung,S.,** Plasma cell differentiation in T-independent type 2 immune responses is independent of CD11c(high) dendritic cells. *European Journal of Immunology* 2006. **36**: 2912-2919.

130. **Mohr,E., Serre,K., Manz,R.A., Cunningham,A.F., Khan,M., Hardie,D.L., Bird,R., and MacLennan,I.C.M.,** Dendritic Cells and Monocyte/Macrophages That Create the IL-6/APRIL-Rich Lymph Node Microenvironments Where Plasmablasts Mature. *Journal of Immunology* 2009. **182**: 2113-2123.

131. **Leduc,E.H., Coons,A.H., and Connolly,J.M.,** Studies on Antibody Production .2. the Primary and Secondary Responses in the Popliteal Lymph Node of the Rabbit. *Journal of Experimental Medicine* 1955. **102**: 61-&.

132. **Nossal,G.J.V.,** Antibody Production by Single Cells .3. the Histology of Antibody Production. *British Journal of Experimental Pathology* 1959. **40**: 301-311.

133. **Hargreaves,D.C., Hyman,P.L., Lu,T.T., Ngo,V.N., Bidgol,A., Suzuki,G., Zou,Y.R., Littman,D.R., and Cyster,J.G.,** A Coordinated Change in Chemokine Responsiveness Guides Plasma Cell Movements. *J.Exp.Med.* 2001. **194**: 45-56.

134. **Hauser,A.E., Debes,G.F., Arce,S., Cassese,G., Hamann,A., Radbruch,A., and Manz,R.A.,** Chemotactic responsiveness toward ligands for CXCR3 and CXCR4 is regulated on plasma blasts during the time course of a memory immune response. *J Immunol* 2002. **169**: 1277-1282.

135. **Rossi,D. and Zlotnik,A.,** The biology of chemokines and their receptors. *Annual Review of Immunology* 2000. **18**: 217-242.

136. **Qin,S.X., Rottman,J.B., Myers,P., Kassam,N., Weinblatt,M., Loetscher,M., Koch,A.E., Moser,B., and Mackay,C.R.,** The chemokine receptors CXCR3 and CCR5 mark subsets of T cells associated with certain inflammatory reactions. *Journal of Clinical Investigation* 1998. **101**: 746-754.

137. **Cole,K.E., Strick,C.A., Paradis,T.J., Ogborne,K.T., Loetscher,M., Gladue,R.P., Lin,W., Boyd,J.G., Moser,B., Wood,D.E., Sahagan,B.G., and Neote,K.,** Interferon-inducible T cell alpha chemoattractant (I-TAC): a novel non-

ELR CXC chemokine with potent activity on activated T cells through selective high affinity binding to CXCR3. *Journal of Experimental Medicine* 1998. **187**: 2009-2021.

138. **Mantovani,A., Sica,A., Sozzani,S., Allavena,P., Vecchi,A., and Locati,M.,** The chemokine system in diverse forms of macrophage activation and polarization. *Trends in Immunology* 2004. **25**: 677-686.

139. **Rani,M.R., Foster,G.R., Leung,S., Leaman,D., Stark,G.R., and Ransohoff,R.M.,** Characterization of beta-R1, a gene that is selectively induced by interferon beta (IFN-beta) compared with IFN-alpha. *J.Biol.Chem.* 1996. **271**: 22878-22884.

140. **Indraccolo,S., Pfeffer,U., Minuzzo,S., Esposito,G., Roni,V., Mandruzzato,S., Ferrari,N., Anfosso,L., Dell'Eva,R., Noonan,D.M., Chieco-Bianchi,L., Albini,A., and Amadori,A.,** Identification of genes selectively regulated by IFNs in endothelial cells. *Journal of Immunology* 2007. **178**: 1122-1135.

141. **Tsubaki,T., Takegawa,S., Hanamoto,H., Arita,N., Kamogawa,J., Yamamoto,H., Takubo,N., Nakata,S., Yamada,K., Yamamoto,S., Yoshie,O., and Nose,M.,** Accumulation of plasma cells expressing CXCR3 in the synovial sublining regions of early rheumatoid arthritis in association with production of Mig/CXCL9 by synovial fibroblasts. *Clinical & Experimental Immunology* 2005. **141**: 363-371.

142. **Proost,P., Verpoest,S., Van de,B.K., Schutyser,E., Struyf,S., Put,W., Ronsse,I., Grillet,B., Opdenakker,G., and Van,D.J.,** Synergistic induction of CXCL9 and CXCL11 by Toll-like receptor ligands and interferon-gamma in fibroblasts correlates with elevated levels of CXCR3 ligands in septic arthritis synovial fluids. *J Leukoc Biol* 2004. **75**: 777-784.

143. **Ueno,A., Yamamura,M., Iwahashi,M., Okamoto,A., Aita,T., Ogawa,N., and Makino,H.,** The production of CXCR3-agonistic chemokines by synovial fibroblasts from patients with rheumatoid arthritis. *Rheumatology International* 2005. **25**: 361-367.

144. **Dajotoy,T., Andersson,P., Bjartell,A., Lofdahl,C.G., Tapper,H., and Egesten,A.,** Human eosinophils produce the T cell-attracting chemokines MIG and IP-10 upon stimulation with IFN-gamma. *J Leukoc Biol* 2004. **76**: 685-691.

145. **Park,M.K., Amichay,D., Love,P., Wick,E., Liao,F., Grinberg,A., Rabin,R.L., Zhang,H.W.H., Gebeyehu,S., Wright,T.M., Iwasaki,A., Weng,Y.M., DeMartino,J.A., Elkins,K.L., and Farber,J.M.,** The CXC chemokine murine monokine induced by IFN-gamma (CXC chemokine ligand 9) is made by APCs, targets lymphocytes including activated B cells, and supports antibody responses to a bacterial pathogen in vivo. *Journal of Immunology* 2002. **169**: 1433-1443.

146. **Gattass,C.R., King,L.B., Luster,A.D., and Ashwell,J.D.,** Constitutive expression of interferon gamma-inducible protein 10 in lymphoid organs and

inducible expression in T cells and thymocytes. *Journal of Experimental Medicine* 1994. **179**: 1373-1378.

147. **Widney,D.P., Xia,Y.R., Lusis,A.J., and Smith,J.B.,** The murine chemokine CXCL11 (IFN-inducible T cell alpha chemoattractant) is an IFN-gamma- and lipopolysaccharide-inducible glucocorticoid-attenuated response gene expressed in lung and other tissues during endotoxemia. *Journal of Immunology* 2000. **164**: 6322-6331.

148. **Ohmori,Y. and Hamilton,T.A.,** Requirement for STAT1 in LPS-induced gene expression in macrophages. *J Leukoc Biol* 2001. **69**: 598-604.

149. **Minges Wols,H.A., Ippolito,J.A., Yu,Z., Palmer,J.L., White,F.A., Le,P.T., and Witte,P.L.,** The effects of microenvironment and internal programming on plasma cell survival. *International Immunology*. 2007. **19**: 837-846.

150. **Pablos,J.L., Santiago,B., Galindo,M., Torres,C., Brehmer,M.T., Blanco,F.J., and Garcia-Lazaro,F.J.,** Synoviocyte-derived CXCL12 is displayed on endothelium and induces angiogenesis in rheumatoid arthritis. *Journal of Immunology* 2003. **170**: 2147-2152.

151. **Bleul,C.C., Fuhlbrigge,R.C., Casasnovas,J.M., Aiuti,A., and Springer,T.A.,** A highly efficacious lymphocyte chemoattractant, stromal cell-derived factor 1 (SDF-1). *Journal of Experimental Medicine* 1996. **184**: 1101-1109.

152. **Zaitseva,M., Blauvelt,A., Lee,S., Lapham,C.K., Klaus-Kovtun,V., Mostowski,H., Manischewitz,J., and Golding,H.,** Expression and function of CCR5 and CXCR4 on human Langerhans cells and macrophages: implications for HIV primary infection. *Nature Medicine* 1997. **3**: 1369-1375.

153. **Forster,R., Kremmer,E., Schubel,A., Breitfeld,D., Kleinschmidt,A., Nerl,C., Bernhardt,G., and Lipp,M.,** Intracellular and surface expression of the HIV-1 coreceptor CXCR4/fusin on various leukocyte subsets: Rapid internalization and recycling upon activation. *Journal of Immunology* 1998. **160**: 1522-1531.

154. **Nanki,T., Hayashida,K., El-Gabalawy,H.S., Suson,S., Shi,K.R., Girschick,H.J., Yavuz,S., and Lipsky,P.E.,** Stromal cell-derived factor-1-CXC chemokine receptor 4 interactions play a central role in CD4(+) T cell accumulation in rheumatoid arthritis synovium. *Journal of Immunology* 2000. **165**: 6590-6598.

155. **Bienvenu,J., Whicher,J., Chir,B., and Aguzzi,F.,** Immunoglobulins. In **Ritchie,R.F. and Navolotskaia,O.** (Eds.) *Serum Proteins in Clinical Medicine*. Found. Blood. Res., Scarborough, ME 1996, pp 1-16.

156. **Odendahl,M., Mei,H., Hoyer,B.F., Jacobi,A.M., Hansen,A., Muehlinghaus,G., Berek,C., Hiepe,F., Manz,R., Radbruch,A., and Dorner,T.,** Generation of migratory antigen-specific plasma blasts and mobilization of

resident plasma cells in a secondary immune response. *Blood* 2005. **105**: 1614-1621.

157. **Manz,R.A., Thiel,A., and Radbruch,A.,** Lifetime of plasma cells in the bone marrow. *Nature* 1997. **388**: 133-134.

158. **Tarlinton,D., Radbruch,A., Hiepe,F., and Dorner,T.,** Plasma cell differentiation and survival. *Current Opinion in Immunology* 2008. **20**: 162-169.

159. **Kopf,M., Herren,S., Wiles,M.V., Pepys,M.B., and Kosco-Vilbois,M.H.,** Interleukin 6 influences germinal center development and antibody production via a contribution of C3 complement component. *Journal of Experimental Medicine* 1998. **188**: 1895-1906.

160. **Wols,H.A.M., Underhill,G.H., Kansas,G.S., and Witte,P.L.,** The role of bone marrow-derived stromal cells in the maintenance of plasma cell longevity. *Journal of Immunology* 2002. **169**: 4213-4221.

161. **Shimaoka,Y., Attrep,J.F., Hirano,T., Ishihara,K., Suzuki,R., Toyosaki,T., Ochi,T., and Lipsky,P.E.,** Nurse-like cells from bone marrow and synovium of patients with rheumatoid arthritis promote survival and enhance function of human B cells. *Journal of Clinical Investigation* 1998. **102**: 606-618.

162. **Cassese,G., Arce,S., Hauser,A.E., Lehnert,K., Moewes,B., Mostarac,M., Muehlinghaus,G., Szyska,M., Radbruch,A., and Manz,R.A.,** Plasma cell survival is mediated by synergistic effects of cytokines and adhesion-dependent signals. *J Immunol* 2003. **171**: 1684-1690.

163. **Suematsu,S., Matsuda,T., Aozasa,K., Akira,S., Nakano,N., Ohno,S., Miyazaki,J., Yamamura,K., Hirano,T., and Kishimoto,T.,** IgG1 plasmacytosis in interleukin 6 transgenic mice. *Proceedings of the National Academy of Sciences of the United States of America* 1989. **86**: 7547-7551.

164. **Dienz,O., Eaton,S.M., Bond,J.P., Neveu,W., Moquin,D., Noubade,R., Briso,E.M., Charland,C., Leonard,W.J., Ciliberto,G., Teuscher,C., Haynes,L., and Rincon,M.,** The induction of antibody production by IL-6 is indirectly mediated by IL-21 produced by CD4+ T cells. *Journal of Experimental Medicine* 2009. **206**: 69-78.

165. **O'Connor,B.P., Raman,V.S., Erickson,L.D., Cook,W.J., Weaver,L.K., Ahonen,C., Lin,L.L., Mantchev,G.T., Bram,R.J., and Noelle,R.J.,** BCMA is essential for the survival of long-lived bone marrow plasma cells. *Journal of Experimental Medicine* 2004. **199**: 91-97.

166. **Bradley,J.R.,** TNF-mediated inflammatory disease. *Journal of Pathology* 2008. **214**: 149-160.

167. **Li,Y.Y.Y., Yang,Y., Bao,M., Edwards,C.K., and Parnes,J.R.,** Mouse splenic B lymphocyte activation using different activation stimuli induces in vitro splicing of tumor necrosis factor-alpha nuclear pre-mRNA. *Molecular Immunology* 2006. **43**: 613-622.

168. **Sung,S.S.J., Jung,L.K.L., Walters,J.A., Chen,W., Wang,C.Y., and Fu,S.M.,** Production of Tumor Necrosis Factor Cachectin by Human B-Cell Lines and Tonsillar B-Cells. *Journal of Experimental Medicine* 1988. **168**: 1539-1551.

169. **Yazdani-Biuki,B., Stadlmaier,E., Mulabecirovic,A., Brezinschek,R., Tilz,G., Demel,U., Mueller,T., Brickmann,K., Graninger,W.B., and Brezinschek,H.P.,** Blockade of tumour necrosis factor {alpha} significantly alters the serum level of IgG- and IgA-rheumatoid factor in patients with rheumatoid arthritis. *Ann Rheum Dis* 2005. **64**: 1224-1226.

170. **Mackay,F., Silveira,P.A., and Brink,R.,** B cells and the BAFF/APRIL axis: fast-forward on autoimmunity and signaling. *Current Opinion in Immunology* 2007. **19**: 327-336.

171. **Litinskiy,M.B., Nardelli,B., Hilbert,D.M., He,B., Schaffer,A., Casali,P., and Cerutti,A.,** DCs induce CD40-independent immunoglobulin class switching through BLyS and APRIL. *Nature Immunology* 2002. **3**: 822-829.

172. **Ohata,J., Zvaifler,N.J., Nishio,M., Boyle,D.L., Kalled,S.L., Carson,D.A., and Kipps,T.J.,** Fibroblast-like synoviocytes of mesenchymal origin express functional B cell-activating factor of the TNF family in response to proinflammatory cytokines. *Journal of Immunology.* 2005. **174**: 864-870.

173. **Schaumann,D.H.S., Tuischer,J., Ebell,W., Manz,R.A., and Lauster,R.,** VCAM-1-positive stromal cells from human bone marrow producing cytokines for B lineage progenitors and for plasma cells: SDF-1, flt3L, and BAFF 6. *Molecular Immunology* 2007. **44**: 1606-1612.

174. **Scapini,P., Nardelli,B., Nadali,G., Calzetti,F., Pizzolo,G., Montecucco,C., and Cassatella,M.A.,** G-CSF-stimulated neutrophils are a prominent source of functional BLyS. *Journal of Experimental Medicine* 2003. **197**: 297-302.

175. **Assi,L.K., Wong,S.H., Ludwig,A., Raza,K., Gordon,C., Salmon,M., Lord,J.M., and Scheel-Toellner,D.,** Tumor necrosis factor alpha activates release of B lymphocyte stimulator by neutrophils infiltrating the rheumatoid joint. *Arthritis & Rheumatism* 2007. **56**: 1776-1786.

176. **Chu,V.T., Enghard,P., Riemekasten,G., and Berek,C.,** In vitro and in vivo activation induces BAFF and APRIL expression in B cells. *Journal of Immunology* 2007. **179**: 5947-5957.

177. **Ingold,K., Zumsteg,A., Tardivel,A., Huard,B., Steiner,Q.G., Cachero,T.G., Qiang,F., Gorelik,L., Kalled,S.L., cha-Orbea,H., Rennert,P.D., Tschopp,J., and Schneider,P.,** Identification of proteoglycans as the APRIL-specific binding partners. *Journal of Experimental Medicine* 2005. **201**: 1375-1383.

178. **Mackay,F. and Leung,H.,** The role of the BAFF/APRIL system on T cell function. *Seminars in Immunology* 2006. **18**: 284-289.

179. **Belnoue,E., Pihlgren,M., Mcgaha,T.L., Tougne,C., Rochat,A.F., Bossen,C., Schneider,P., Huard,B., Lambert,P.H., and Siegrist,C.A.,** APRIL is critical for plasmablast survival in the bone marrow and poorly expressed by early-life bone marrow stromal cells. *Blood* 2008. **111**: 2755-2764.

180. **Tokoyoda,K., Egawa,T., Sugiyama,T., Choi,B.I., and Nagasawa,T.,** Cellular niches controlling B lymphocyte behavior within bone marrow during development. *Immunity* 2004. **20**: 707-718.

181. **Nie,Y.C., Waite,J., Brewer,F., Sunshine,M.J., Littman,D.R., and Zou,Y.R.,** The role of CXCR4 in maintaining peripheral B cell compartments and humoral immunity. *Journal of Experimental Medicine* 2004. **200**: 1145-1156.

182. **Parrish-Novak,J., Dillon,S.R., Nelson,A., Hammond,A., Sprecher,C., Gross,J.A., Johnston,J., Madden,K., Xu,W.F., West,J., Schrader,S., Burkhead,S., Heipel,M., Brandt,C., Kuijper,J.L., Kramer,J., Conklin,D.,**

Presnell,S.R., Berry,J., Shiota,F., Bort,S., Hambly,K., Mudri,S., Clegg,C., Moore,M., Grant,F.J., Lofton-Day,C., Gilbert,T., Raymond,F., Ching,A., Yao,L., Smith,D., Webster,P., Whitmore,T., Maurer,M., Kaushansky,K., Holly,R.D., and Foster,D., Interleukin 21 and its receptor are involved in NK cell expansion and regulation of lymphocyte function. *Nature* 2000. **408**: 57-63.

183. **Spolski,R. and Leonard,W.J.,** Interleukin-21: Basic biology and implications for cancer and autoimmunity. *Annual Review of Immunology* 2008. **26**: 57-79.

184. **Ozaki,K., Spolski,R., Ettinger,R., Kim,H.P., Wang,G., Qi,C.F., Hwu,P., Shaffer,D.J., Akilesh,S., Roopenian,D.C., Morse,H.C., III, Lipsky,P.E., and Leonard,W.J.,** Regulation of B cell differentiation and plasma cell generation by IL-21, a novel inducer of Blimp-1 and Bcl-6. *Journal of Immunology* 2004. **173**: 5361-5371.

185. **Ozaki,K., Spolski,R., Feng,C.G., Qi,C.F., Cheng,J., Sher,A., Morse,H.C., III, Liu,C., Schwartzberg,P.L., and Leonard,W.J.,** A critical role for IL-21 in regulating immunoglobulin production. *Science* 2002. **298**: 1630-1634.

186. **Jin,H.L., Carrio,R., Yu,A.X., and Malek,T.R.,** Distinct activation signals determine whether IL-21 induces B cell costimulation, growth arrest, or bim-dependent apoptosis. *Journal of Immunology* 2004. **173**: 657-665.

187. **Lax,S., Hou,T.Z., Jenkinson,E., Salmon,M., MacFadyen,J.R., Isacke,C.M., Anderson,G., Cunningham,A.F., and Buckley,C.D.,** CD248/endosialin is dynamically expressed on a subset of stromal cells during lymphold tissue development, splenic remodeling and repair. *Febs Letters* 2007. **581**: 3550-3556.

188. **Kaisho,T., Ishikawa,J., Oritani,K., Inazawa,J., Tomizawa,H., Muraoka,O., Ochi,T., and Hirano,T.,** Bst-1, A Surface-Molecule of Bone-Marrow Stromal Cell-Lines That Facilitates Pre-B-Cell Growth. *Proceedings of the National Academy of Sciences of the United States of America* 1994. **91**: 5325-5329.

189. **McNagny,K.M., Bucy,R.P., and Cooper,M.D.,** Reticular cells in peripheral lymphoid tissues express the phosphatidylinositol-linked BP-3 antigen. *European Journal of Immunology* 1991. **21**: 509-515.

190. **Itoh,M., Ishihara,K., Hiroi,T., Lee,B.O., Maeda,H., Iijima,H., Yanagita,M., Kiyono,H., and Hirano,T.,** Deletion of bone marrow stromal cell antigen-1 (CD157) gene impaired systemic thymus independent-2 antigen-induced IgG3 and mucosal TD antigen-elicited IgA responses. *Journal of Immunology* 1998. **161**: 3974-3983.

191. **Oetke,C., Vinson,M.C., Jones,C., and Crocker,P.R.,** Sialoadhesin-deficient mice exhibit subtle changes in B- and T-cell populations and reduced immunoglobulin M levels. *Molecular & Cellular Biology* 2006. **26**: 1549-1557.

192. **Edwards,J.C.W., Cambridge,G., and Leandro,M.J.,** B cell depletion therapy in rheumatic disease. *Best Practice & Research in Clinical Rheumatology* 2006. **20**: 915-928.

193. **Lal,G., Balmer,P., Stanford,E., Martin,S., Warrington,R., and Borrow,R.,** Development and validation of a nonaplex assay for the simultaneous quantitation of antibodies to nine Streptococcus pneumoniae serotypes. *Journal of Immunological Methods* 2005. **296**: 135-147.

194. "Training manual for Enzyme linked immunosorbent assay for the quantitation of *Streptococcus pneumoniae* serotype specific IgG (Pn PS ELISA).", at http://www.vaccine.uab.edu/ELISA%20Protocol.pdf and last accessed on 30-11-2006

195. **Hoiseth,S.K. and Stocker,B.A.D.,** Aromatic-Dependent Salmonella-Typhimurium Are Non-Virulent and Effective As Live Vaccines. *Nature* 1981. **291**: 238-239.

196. **Weible,E.R.,** Principle and methods for the morphometric study of the lung and other organs. *Laboratory Investigation* 1963. **12**: 131-135.

197. **Biagini,R.E., Schlottmann,S.A., Sammons,D.L., Smith,J.P., Snawder,J.C., Striley,C.A., MacKenzie,B.A., and Weissman,D.N.,** Method for simultaneous

measurement of antibodies to 23 pneumococcal capsular polysaccharides. *Clinical & Diagnostic Laboratory Immunology* 2003. **10**: 744-750.

198. **Concepcion,N.F. and Frasch,C.E.,** Pneumococcal Type 22F Polysaccharide Absorption Improves the Specificity of a Pneumococcal-Polysaccharide Enzyme-Linked Immunosorbent Assay. *Clinical and Vaccine Immunology* 2001. **8**: 266-272.

199. **Sorensen,U.B. and Henrichsen,J.,** C-polysaccharide in a pneumococcal vaccine. *Acta Pathol.Microbiol.Immunol.Scand.Sect.C* 1984. **92**: 351-356.

200. **Young,N.M., Jocius,I.B., and Leon,M.A.,** Binding Properties of A Mouse Immunoglobulin-M Myeloma Protein with Carbohydrate Specificity. *Biochemistry* 1971. **10**: 3457-&.

201. **Claflin,J.L., LIEBERMA.R, and Davie,J.M.,** Clonal Nature of Immune-Response to Phosphorylcholine .2. Idiotypic Specificity and Binding Characteristics of Antiphosphorylcholine Antibodies. *Journal of Immunology* 1974. **112**: 1747-1756.

202. **Briles,E.B. and Tomasz,A.,** Pneumococcal Forssman Antigen - Choline-Containing Lipoteichoic Acid. *J.Biol.Chem.* 1973. **248**: 6394-6397.

203. **Quataert,S.A., Kirch,C.S., Wiedl,L.J.Q., Phipps,D.C., Strohmeyer,S., Cimino,C.O., Skuse,J., and Madore,D.V.,** Assignment of Weight-Based Antibody Units to A Human Antipneumococcal Standard Reference Serum, Lot 89-S. *Clinical and Diagnostic Laboratory Immunology* 1995. **2**: 590-597.

204. **Baxendale,H.E., Johnson,M., Stephens,R.C.M., Yuste,J., Klein,N., Brown,J.S., and Goldblatt,D.,** Natural human antibodies to pneumococcus have distinctive molecular characteristics and protect against pneumococcal disease. *Clinical and Experimental Immunology* 2008. **151**: 51-60.

205. **Baxendale,H.E., Davis,Z., White,H.N., Spellerberg,M.B., Stevenson,F.K., and Goldblatt,D.,** Immunogenetic analysis of the immune response to pneumococcal polysaccharide. *European Journal of Immunology* 2000. **30**: 1214-1223.

206. **Lucas,A.H., Moulton,K.D., Tang,V.R., and Reason,D.C.,** Combinatorial library cloning of human antibodies to Streptococcus pneumoniae capsular polysaccharides: Variable region primary structures and evidence for somatic mutation of Fab fragments specific for capsular serotypes 6B, 14, and 23F. *Infect.Immun.* 2001. **69**: 853-864.

207. **Frasch,C.E. and Concepcion,N.F.,** Specificity of human antibodies reactive with pneumococcal C polysaccharide. *Infect.Immun.* 2000. **68**: 2333-2337.

208. **Broker,B.M., Klajman,A., Youinou,P., Jouquan,J., Worman,C.P., Murphy,J., Mackenzie,L., Quartey-Papafio,R., Blaschek,M., and Collins,P.,** Chronic lymphocytic leukemic (CLL) cells secrete multispecific autoantibodies. *Journal of Autoimmunity* 1988. **1**: 469-481.

209. **Ray,S.K., Putterman,C., and Diamond,B.,** Pathogenic autoantibodies are routinely generated during the response to foreign antigen: a paradigm for autoimmune disease. *Proceedings of the National Academy of Sciences of the United States of America* 1996. **93**: 2019-2024.

210. **Yurasov,S., Wardemann,H., Hammersen,J., Tsuiji,M., Meffre,E., Pascual,V., and Nussenzweig,M.C.,** Defective B cell tolerance checkpoints in systemic lupus erythematosus. *Journal of Experimental Medicine* 2005. **201**: 703-711.

211. **Weksler,M.E., Schwab,R., Huetz,F., Kim,Y.T., and Coutinho,A.,** Cellular Basis for the Age-Associated Increase in Autoimmune Reactions. *International Immunology* 1990. **2**: 329-335.

212. **Keogh,K.A., Ytterberg,S.R., Fervenza,F.C., Carlson,K.A., Schroeder,D.R., and Specks,U.,** Rituximab for refractory Wegener's granulomatosis. Report of a prospective, open label, pilot trial. *Am.J.Respir.Crit.Care Med.* 2006. **173**: 180-187.

213. **Vieira,C.A., Agarwal,A., Book,B.K., Sidner,R.A., Bearden,C.M., Gebel,H.M., Roggero,A.L., Fineberg,N.S., Taber,T., Kraus,M.A., and Pescovitz,M.D.,** Rituximab for reduction of anti-HLA antibodies in patients awaiting renal transplantation: 1. Safety, pharmacodynamics, and pharmacokinetics. *Transplantation* 2004. **77**: 542-548.

214. **Genberg,H., Hansson,A., Wernerson,A., Wennberg,L., and Tyden,G.,** Pharmacodynamics of rituximab in kidney allotransplantation. *American Journal of Transplantation* 2006. **6**: 2418-2428.

215. **Konradsen,H.B.,** Quantity and avidity of pneumococcal antibodies before and up to 5 years after pneumococcal vaccination of elderly persons. *Clinical Infectious Diseases* 1995. **21**: 616-620.

216. **Gray,J.J.,** Avidity of EBV VCA-specific IgG antibodies: distinction between recent primary infection, past infection and reactivation. *Journal of Virological Methods* 1995. **52**: 95-104.

217. **Marchant,A., Pihlgren,M., Goetghebuer,T., Weiss,H.A., Ota,M.O.C., Schlegel-Hauter,S.E., The Medical Research Council Gambia Twin Study Group, Whittle,H., Lambert,P.H., Newport,M.J., and Siegrist,C.A.,** Predominant influence of environmental determinants on the persistence and avidity maturation of antibody responses to vaccines in infants. *J Infect Dis* 2006. **193**: 1598-1605.

218. **Schallert,N., Pihlgren,M., Kovarik,J., Roduit,C., Tougne,C., Bozzotti,P., Del Giudice,G., Siegrist,C.A., and Lambert,P.H.,** Generation of adult-like antibody avidity profiles after early-life immunization with protein vaccines. *European Journal of Immunology* 2002. **32**: 752-760.

219. **Smith,K.G., Jones,R.B., Burns,S.M., and Jayne,D.R.,** Long-term comparison of rituximab treatment for refractory systemic lupus erythematosus and vasculitis: Remission, relapse, and re-treatment. *Arthritis & Rheumatism* 2006. **54**: 2970-2982.

220. **Stasi,R., Stipa,E., Del Poeta,G., Amadori,S., Newland,A.C., and Provan,D.,** Long-term observation of patients with anti-neutrophil cytoplasmic antibody-associated vasculitis treated with rituximab. *Rheumatology* 2006. **45**: 1432-1436.

221. **Cambridge,G., Stohl,W., Leandro,M.J., Migone,T.-S., Hilbert,D.M., and Edwards,J.C.W.,** Circulating levels of B lymphocyte stimulator in patients with rheumatoid arthritis following rituximab treatment: Relationships with B cell depletion, circulating antibodies, and clinical relapse. *Arthritis & Rheumatism* 2006. **54**: 723-732.

222. **Barth,W.F., Fahey,J.L., Waldmann,T.A., and Wochner,R.D.,** Metabolism of human gamma macroglobulins. *Journal of Clinical Investigation* 1964. **43**: 1036-1048.

223. **Paran,D., Trej'o,L., and Caspi,D.,** Clinical images: B cell depletion in the appendix following rituximab treatment. *Arthritis & Rheumatism* 2006. **54**: 2151.

224. **Kneitz,C., Wilhelm,M., and Tony,H.,** Effective B cell depletion with rituximab in the treatment of autoimmune diseases. *Immunobiology* 2002. **206**: 519-527.

225. **Vos,K., Thurlings,R.M., Wijbrandts,C.A., van Schaardenburg,D., Gerlag,D.M., and Tak,P.P.,** Early effects of rituximab on the synovial cell infiltrate in patients with rheumatoid arthritis. *Arthritis and Rheumatism* 2007. **56**: 772-778.

226. **Ferraro,A.J., Smith,S.W., Neil,D., and Savage,C.O.S.,** Relapsed Wegener's granulomatosis after rituximab therapy--B cells are present in new pathological lesions despite persistent 'depletion' of peripheral blood. *Nephrol.Dial.Transplant.* 2008. **23**: 3030-3032.

227. **Ramos,E.J., Pollinger,H.S., Stegall,M.D., Gloor,J.M., Dogan,A., and Grande,J.P.,** The effect of desensitization protocols on human splenic B-cell populations in vivo. *American Journal of Transplantation* 2007. **7**: 402-407.

228. **Zhou,J., Lottenbach,K.R., Barenkamp,S.J., and Reason,D.C.,** Somatic hypermutation and diverse immunoglobulin gene usage in the human antibody response to the capsular polysaccharide of streptococcus pneumoniae type 6B. *Infect.Immun.* 2004. **72**: 3505-3514.

229. **Ferraro,A.J., Drayson,M.T., Savage,C.O., and MacLennan,I.C.,** Levels of autoantibodies, unlike antibodies to all extrinsic antigen groups, fall following B cell depletion with Rituximab. *European Journal of Immunology* 2008. **38**: 292-298.

230. **Reparon-Schuijt,C.C., van Esch,W.J., van Kooten,C., Levarht,E.W., Breedveld,F.C., and Verweij,C.L.,** Functional analysis of rheumatoid factor-producing B cells from the synovial fluid of rheumatoid arthritis patients. *Arthritis & Rheumatism* 1998. **41**: 2211-2220.

231. **Hutloff,A., Buchner,K., Reiter,K., Baelde,H.J., Odendahl,M., Jacobi,A., Dorner,T., and Kroczek,R.A.,** Involvement of inducible costimulator in the exaggerated memory B cell and plasma cell generation in systemic lupus erythematosus. *Arthritis & Rheumatism* 2004. **50**: 3211-3220.

232. **Cassese,G., Lindenau,S., de Boer,B., Arce,S., Hauser,A., Riemekasten,G., Berek,C., Hiepe,F., Krenn,V., Radbruch,A., and Manz,R.A.,** Inflamed kidneys of NZB / W mice are a major site for the homeostasis of plasma cells. *European Journal of Immunology* 2001. **31**: 2726-2732.

233. **Sekine,H., Watanabe,H., and Gilkeson,G.S.,** Enrichment of anti-glomerular antigen antibody-producing cells in the kidneys of MRL/MpJ-Fas(lpr) mice. *Journal of Immunology* 2004. **172**: 3913-3921.

234. Personal communication from Roberts, I. S.

235. **Krukemeyer,M.G., Moeller,J., Morawietz,L., Rudolph,B., Neumann,U., Theruvath,T., Neuhaus,P., and Krenn,V.,** Description of B lymphocytes and plasma cells, complement, and chemokines/receptors in acute liver allograft rejection. *Transplantation* 2004. **78**: 65-70.

236. **Krenn,V., Hensel,F., Kim,H.J., Carneiro,M.M.S., Starostik,P., Ristow,G., Konig,A., Vollmers,H.P., and Muller-Hermelink,H.K.,** Molecular IgV(H) analysis demonstrates highly somatic mutated B cells in synovialitis of osteoarthritis: A degenerative disease is associated with a specific, not locally generated immune response. *Laboratory Investigation* 1999. **79**: 1377-1384.

237. **van Oosterhout,M., Levarht,E.W., Sont,J.K., Huizinga,T.W., Toes,R.E., and van Laar,J.M.,** Clinical efficacy of infliximab plus methotrexate in DMARD naive and DMARD refractory rheumatoid arthritis is associated with decreased synovial expression of TNF alpha and IL18 but not CXCL12. *Ann Rheum Dis* 2005. **64**: 537-543.

238. **Hsu, M.-C.** PhD thesis. *University of Birmingham* 1995.

239. **Nardelli,B., Belvedere,O., Roschke,V., Moore,P.A., Olsen,H.S., Migone,T.S., Sosnovtseva,S., Carrell,J.A., Feng,P., Giri,J.G., and Hilbert,D.M.,** Synthesis

and release of B-lymphocyte stimulator from myeloid cells. *Blood* 2001. **97**: 198-204.

240. **Moreaux,J., Cremer,F.W., Reme,T., Raab,M., Mahtouk,K., Kaukel,P., Pantesco,V., De,V.J., Jourdan,E., Jauch,A., Legouffe,E., Moos,M., Fiol,G., Goldschmidt,H., Rossi,J.F., Hose,D., and Klein,B.,** The level of TACI gene expression in myeloma cells is associated with a signature of microenvironment dependence versus a plasmablastic signature. *Blood* 2005. **106**: 1021-1030.

241. **Terebuh,P.D., Otterness,I.G., Strieter,R.M., Lincoln,P.M., Danforth,J.M., Kunkel,S.L., and Chensue,S.W.,** Biologic and immunohistochemical analysis of interleukin-6 expression in vivo. Constitutive and induced expression in murine polymorphonuclear and mononuclear phagocytes. *American Journal of Pathology* 1992. **140**: 649-657.

242. **Vanvliet,E., Melis,M., Foidart,J.M., and Vanewijk,W.,** Reticular Fibroblasts in Peripheral Lymphoid Organs Identified by A Monoclonal-Antibody. *Journal of Histochemistry & Cytochemistry* 1986. **34**: 883-890.

243. **Wayner,E.A., Garcia-Pardo,A., Humphries,M.J., McDonald,J.A., and Carter,W.G.,** Identification and characterization of the T lymphocyte adhesion receptor for an alternative cell attachment domain (CS-1) in plasma fibronectin. *J.Cell Biol.* 1989. **109**: 1321-1330.

244. **San Antonio,J.D., Karnovsky,M.J., Gay,S., Sanderson,R.D., and Lander,A.D.,** Interactions of syndecan-1 and heparin with human collagens. *Glycobiology* 1994. **4**: 327-332.

245. **Marshall, J.** PhD thesis (in preparation). *University of Birmingham* 2009.

246. **Vink,A., Coulie,P.G., Wauters,P., Nordan,R.P., and Van,S.J.,** B cell growth and differentiation activity of interleukin-HP1 and related murine plasmacytoma growth factors. Synergy with interleukin 1. *European Journal of Immunology* 1988. **18**: 607-612.

247. **Asao,H., Okuyama,C., Kumaki,S., Ishii,N., Tsuchiya,S., Foster,D., and Sugamura,K.,** Cutting edge: the common gamma-chain is an indispensable subunit of the IL-21 receptor complex. *Journal of Immunology* 2001. **167**: 1-5.

248. **Bermejo,M., Martin-Serrano,J., Oberlin,E., Pedraza,M.A., Serrano,A., Santiago,B., Caruz,A., Loetscher,P., Baggiolini,M., renzana-Seisdedos,F., and Alcami,J.,** Activation of blood T lymphocytes down-regulates CXCR4 expression and interferes with propagation of X4 HIV strains. *European Journal of Immunology* 1998. **28**: 3192-3204.

249. **Huard,B., McKee,T., Bosshard,C., Durual,S., Matthes,T., Myit,S., Donze,O., Frossard,C., Chizzolini,C., Favre,C., Zubler,R., Guyot,J.P., Schneider,P., and Roosnek,E.,** APRIL secreted by neutrophils binds to heparan sulfate

proteoglycans to create plasma cell niches in human mucosa. *Journal of Clinical Investigation* 2008. **118**: 2887-2895.

250. **Turner,M.L., Hawkins,E.D., and Hodgkin,P.D.,** Quantitative Regulation of B Cell Division Destiny by Signal Strength. *J Immunol* 2008. **181**: 374-382.

251. **Genestier,L., Taillardet,M., Mondiere,P., Gheit,H., Bella,C., and Defrance,T.,** TLR agonists selectively promote terminal plasma cell differentiation of B cell subsets specialized in thymus-independent responses. *Journal of Immunology* 2007. **178**: 7779-7786.

252. **Burns,J.M., Summers,B.C., Wang,Y., Melikian,A., Berahovich,R., Miao,Z., Penfold,M.E., Sunshine,M.J., Littman,D.R., Kuo,C.J., Wei,K., McMaster,B.E., Wright,K., Howard,M.C., and Schall,T.J.,** A novel chemokine receptor for SDF-1 and I-TAC involved in cell survival, cell adhesion, and tumor development. *Journal of Experimental Medicine* 2006. **203**: 2201-2213.

253. **Nakayama,T., Hieshima,K., Izawa,D., Tatsumi,Y., Kanamaru,A., and Yoshie,O.,** Cutting edge: profile of chemokine receptor expression on human plasma cells accounts for their efficient recruitment to target tissues. *Journal of Immunology* 2003. **170**: 1136-1140.

254. **Ruth,J.H., Haas,C.S., Park,C.C., Amin,M.A., Martinez,R.J., Haines,G.K., Shahrara,S., Campbell,P.L., and Koch,A.E.,** CXCL16-mediated cell recruitment to rheumatoid arthritis synovial tissue and murine lymph nodes is dependent upon the MAPK pathway. *Arthritis and Rheumatism* 2006. **54**: 765-778.

255. **Scapini,P., Carletto,A., Nardelli,B., Calzetti,F., Roschke,V., Merigo,F., Tamassia,N., Pieropan,S., Biasi,D., Sbarbati,A., Sozzani,S., Bambara,L., and Cassatella,M.A.,** Proinflammatory mediators elicit secretion of the intracellular B-lymphocyte stimulator pool (BLyS) that is stored in activated neutrophils: implications for inflammatory diseases. *Blood* 2005. **105**: 830-837.

256. **Lo,C.G., Lu,T.T., and Cyster,J.G.,** Integrin-dependence of lymphocyte entry into the splenic white pulp. *Journal of Experimental Medicine* 2003. **197**: 353-361.

257. **Till,K.J., Zuzel,M., and Cawley,J.C.,** The role of hyaluronan and interleukin 8 in the migration of chronic lymphocytic leukemia cells within lymphoreticular tissues. *Cancer Research* 1999. **59**: 4419-4426.

258. **Dechert,T.A., Ducale,A.E., Ward,S.I., and Yager,D.R.,** Hyaluronan in human acute and chronic dermal wounds. *Wound Repair & Regeneration* 2006. **14**: 252-258.

259. **Day,A.J. and de la Motte,C.A.,** Hyaluronan cross-linking: a protective mechanism in inflammation? *Trends in Immunology* 2005. **26**: 637-643.

260. **Amara,A., Lorthioir,O., Valenzuela,A., Magerus,A., Thelen,M., Montes,M., Virelizier,J.L., Delepierre,M., Baleux,F., Lortat-Jacob,H., and renzana-Seisdedos,F.,** Stromal cell-derived factor-1 alpha associates with heparan sulfates through the first beta-strand of the chemokine. *J.Biol.Chem.* 1999. **274**: 23916-23925.

261. **Scapini,P., Bazzoni,F., and Cassatella,M.A.,** Regulation of B-cell-activating factor (BAFF)/B lymphocyte stimulator (BLyS) expression in human neutrophils. *Immunology Letters* 2008. **116**: 1-6.

262. **Ramanujam,M., Wang,X., Huang,W., Liu,Z., Schiffer,L., Tao,H., Frank,D., Rice,J., Diamond,B., Yu,K.O., Porcelli,S., and Davidson,A.,** Similarities and differences between selective and nonselective BAFF blockade in murine SLE. *Journal of Clinical Investigation* 2006. **116**: 724-734.

263. **Wu,H.L., Chen,G., Wyburn,K.R., Yin,J.L., Bertolino,P., Eris,J.M., Alexander,S.I., Sharland,A.F., and Chadban,S.J.,** TLR4 activation mediates kidney ischemia/reperfusion injury. *Journal of Clinical Investigation* 2007. **117**: 2847-2859.

264. **Manz,R.A., Hauser,A.E., Hiepe,F., and Radbruch,A.,** Maintenance of serum antibody levels. *Annual Review of Immunology* 2005. **23**: 367-386.

265. **Burman,A., Haworth,O., Hardie,D.L., Amft,E.N., Siewert,C., Jackson,D.G., Salmon,M., and Buckley,C.D.,** A chemokine-dependent stromal induction mechanism for aberrant lymphocyte accumulation and compromised lymphatic return in rheumatoid arthritis. *Journal of Immunology* 2005. **174**: 1693-1700.

266. **Janatpour,M.J., Hudak,S., Sathe,M., Sedgwick,J.D., and McEvoy,L.M.,** Tumor Necrosis Factor-dependent Segmental Control of MIG Expression by High Endothelial Venules in Inflamed Lymph Nodes Regulates Monocyte Recruitment. *J.Exp.Med.* 2001. **194**: 1375-1384.

267. **GomezChiarri,M., Ortiz,A., GonzalezCuadrado,S., Seron,D., Emancipator,S.N., Hamilton,T.A., Barat,A., Plaza,J.J., Gonzalez,E., and Egido,J.,** Interferon-inducible protein-10 is highly expressed in rats with experimental nephrosis. *American Journal of Pathology* 1996. **148**: 301-311.

268. **Culton,D.A., Nicholas,M.W., Bunch,D.O., Zhen,Q.L., Kepler,T.B., Dooley,M.A., Mohan,C., Nachman,P.H., and Clarke,S.H.,** Similar CD19 dysregulation in two autoantibody-associated autoimmune diseases suggests a shared mechanism of B-cell tolerance loss. *Journal of Clinical Immunology* 2007. **27**: 53-68.

269. **Nicholas,M.W., Dooley,M.A., Hogan,S.L., Anolik,J., Looney,J., Sanz,I., and Clarke,S.H.,** A novel subset of memory B cells is enriched in autoreactivity and correlates with adverse outcomes in SLE. *Clinical Immunology* 2008. **126**: 189-201.

270. **Parsonage,G., Filer,A.D., Haworth,O., Nash,G.B., Rainger,G.E., Salmon,M., and Buckley,C.D.,** A stromal address code defined by fibroblasts. *Trends in Immunology* 2005. **26**: 150-156.

271. **Togel,F., Isaac,J., Hu,Z.M., Weiss,K., and Westenfelder,C.,** Renal SDF-1 signals mobilization and homing of CXCR4-positive cells to the kidney after ischemic injury. *Kidney International* 2005. **67**: 1772-1784.

272. **Balabanian,K., Couderc,J., Bouchet-Delbos,L., Amara,A., Berrebi,D., Foussat,A., Baleux,F., Portier,A., Durand-Gasselin,I., Coffman,R.L., Galanaud,P., Peuchmaur,M., and Emilie,D.,** Role of the chemokine stromal cell-derived factor 1 in autoantibody production and nephritis in murine lupus. *Journal of Immunology* 2003. **170**: 3392-3400.

273. **Desgeorges,A., Gabay,C., Silacci,P., Novick,D., RouxLombard,P., Grau,G., Dayer,J.M., Vischer,T., and Guerne,P.A.,** Concentrations and origins of soluble interleukin 6 receptor-alpha in serum and synovial fluid. *Journal of Rheumatology* 1997. **24**: 1510-1516.

274. **Malide,D., Russo,P., and Bendayan,M.,** Presence of Tumor-Necrosis-Factor-Alpha and Interleukin-6 in Renal Mesangial Cells of Lupus Nephritis Patients. *Human Pathology* 1995. **26**: 558-564.

275. **Tesar,V., Masek,Z., Rychlik,I., Merta,M., Bartunkova,J., Stejskalova,A., Zabka,J., Janatkova,I., Fucikova,T., Dostal,C., and Becvar,R.,** Cytokines and adhesion molecules in renal vasculitis and lupus nephritis. *Nephrol.Dial.Transplant.* 1998. **13**: 1662-1667.

276. **Tan,S.M., Xu,D., Roschke,V., Perry,J.W., Arkfeld,D.G., Ehresmann,G.R., Migone,T.S., Hilbert,D.A., and Stohl,W.,** Local production of B lymphocyte stimulator protein and APRIL in arthritic joints of patients with inflammatory arthritis. *Arthritis and Rheumatism* 2003. **48**: 982-992.

277. **Cheema,G.S., Roschke,V., Hilbert,D.A., and Stohl,W.,** Elevated serum B lymphocyte stimulator levels in patients with systemic immune-based rheumatic diseases. *Arthritis and Rheumatism* 2001. **44**: 1313-1319.

278. **Krumbholz,M., Theil,D., Derfuss,T., Rosenwald,A., Schrader,F., Monoranu,C.M., Kalled,S.L., Hess,D.M., Serafini,B., Aloisi,F., Wekerle,H., Hohlfeld,R., and Meinl,E.,** BAFF is produced by astrocytes and up-regulated in multiple sclerosis lesions and primary central nervous system lymphoma. *Journal of Experimental Medicine* 2005. **201**: 195-200.

279. **Krumbholz,M., Specks,U., Wick,M., Kalled,S.L., Jenne,D., and Meinl,E.,** BAFF is elevated in serum of patients with Wegener's granulomatosis. *Journal of Autoimmunity* 2005. **25**: 298-302.

280. **Zhang,J., Roschke,V., Baker,K.P., Wang,Z., Alarcon,G.S., Fessler,B.J., Bastian,H., Kimberly,R.P., and Zhou,T.,** Cutting edge: A role for B lymphocyte stimulator in systemic lupus erythematosus. *Journal of Immunology* 2001. **166**: 6-10.

281. **Petri,M., Stohl,W., Chatham,W., Mccune,W.J., Chevrier,M., Ryel,J., Recta,V., Zhong,J., and Freimuth,W.,** Association of plasma B lymphocyte stimulator levels and disease activity in systemic lupus erythematosus. *Arthritis and Rheumatism* 2008. **58**: 2453-2459.

282. **Cambridge,G., Isenberg,D.A., Edwards,J.C.W., Leandro,M.J., Migone,T.S., Teodorescu,M., and Stohl,W.,** B cell depletion therapy in systemic lupus erythaematosus: relationships among serum B lymphocyte stimulator levels, autoantibody profile and clinical response. *Ann Rheum Dis* 2008. **67**: 1011-1016.

283. **Arbuckle,M.R., McClain,M.T., Rubertone,M.V., Scofield,R.H., Dennis,G.J., James,J.A., and Harley,J.B.,** Development of autoantibodies before the clinical onset of systemic lupus erythematosus. *New England Journal of Medicine* 2003. **349**: 1526-1533.

284. **Baker,K.P., Edwards,B.M., Main,S.H., Choi,G.H., Wager,R.E., Halpern,W.G., Lappin,P.B., Riccobene,T., Abramian,D., Sekut,L., Sturm,B., Poortman,C., Minter,R.R., Dobson,C.L., Williams,E., Carmen,S., Smith,R., Roschke,V., Hilbert,D.M., Vaughan,T.J., and Albert,V.R.,** Generation and characterization of LymphoStat-B, a human monoclonal antibody that antagonizes the bioactivities of B lymphocyte stimulator. *Arthritis and Rheumatism* 2003. **48**: 3253-3265.